IDA DOCUMENT D-1189

SDIO WORKSHOP ON PIEZOELECTRIC CERAMIC ACTUATORS FOR SPACE APPLICATIONS

Janet Sater

June 1992

Prepared for
Strategic Defense Initiative Organization

INSTITUTE FOR DEFENSE ANALYSES
1801 N. Beauregard Street, Alexandria, Virginia 22311-1772

IDA Log No. HQ 92-41982

DEFINITIONS

IDA publishes the following documents to report the results of its work.

Reports

Reports are the most authoritative and most carefully considered products IDA publishes. They normally embody results of major projects which (a) have a direct bearing on decisions affecting major programs, (b) address issues of significant concern to the Executive Branch, the Congress and/or the public, or (c) address issues that have significant economic implications. IDA Reports are reviewed by outside panels of experts to ensure their high quality and relevance to the problems studied, and they are released by the President of IDA.

Group Reports

Group Reports record the findings and results of IDA established working groups and panels composed of senior individuals addressing major issues which otherwise would be the subject of an IDA Report. IDA Group Reports are reviewed by the senior individuals responsible for the project and others as selected by IDA to ensure their high quality and relevance to the problems studied, and are released by the President of IDA.

Papers

Papers, also authoritative and carefully considered products of IDA, address studies that are narrower in scope than those covered in Reports. IDA Papers are reviewed to ensure that they meet the high standards expected of refereed papers in professional journals or formal Agency reports.

Documents

IDA Documents are used for the convenience of the sponsors or the analysts (a) to record substantive work done in quick reaction studies, (b) to record the proceedings of conferences and meetings, (c) to make available preliminary and tentative results of analyses, (d) to record data developed in the course of an investigation, or (e) to forward information that is essentially unanalyzed and unevaluated. The review of IDA Documents is suited to their content and intended use.

The work reported in this document was conducted under contract MDA 903 89 C 0003 for the Department of Defense. The publication of this IDA document does not indicate endorsement by the Department of Defense, nor should the contents be construed as reflecting the official position of that Agency.

REPORT DOCUMENTATION PAGE

Form Approved
OMB No. 0704-0188

1. AGENCY USE ONLY *(Leave blank)*	2. REPORT DATE	3. REPORT TYPE AND DATES COVERED
	June 1992	Final--January - May 1992

4. TITLE AND SUBTITLE

SDIO Workshop on Piezoelectric Ceramic Actuators for Space Applications

5. FUNDING NUMBERS

C - MDA 903 89 C 0003

T - T-R2-597.09

6. AUTHOR(S)

Janet Sater

7. PERFORMING ORGANIZATION NAME(S) AND ADDRESS(ES)

Institute for Defense Analyses
1801 N. Beauregard St.
Alexandria, VA 22311-1772

8. PERFORMING ORGANIZATION REPORT NUMBER

IDA Document D-1189

9. SPONSORING/MONITORING AGENCY NAME(S) AND ADDRESS(ES)

SDIO/TNI
The Pentagon, Room 1E167
Washington, DC 20301

10. SPONSORING/MONITORING AGENCY REPORT NUMBER

11. SUPPLEMENTARY NOTES

12a. DISTRIBUTION/AVAILABILITY STATEMENT

Approved for public release; distribution unlimited.

12b. DISTRIBUTION CODE

13. ABSTRACT ***(Maximum 200 words)***

Lt. Col. Michael Obal of the SDIO Materials & Structures Office sponsored this workshop on piezoceramic actuators for space applications. Its purpose was threefold: to promote communications among the appropriate groups; to focus and prioritize issues for near-term improvements in actuator performance; and to identify and suggest research plans to obtain such improvements. Presentations were given by representatives from each of three invited groups: end users/designers; materials researchers; and materials/device manufacturers. Issues identified in the workshop seemed to fall into three major categories: (1) piezoceramic material performance limitations; (2) distribution of properties of vendor-supplied materials; and (3) actuator applications. Performance limitation issues include, for example, d_{31} vs. d_{33} performance, displacement/volt, fatigue life at high strains, and tensile strain-to-failure. Property distribution issues include composition, capacitance, and surface finish. Actuator application issues include ceramic material/actuator fabrication, material handling, application of electrodes to actuator, and post-composite fabrication actuator performance.

14. SUBJECT TERMS

piezoelectric materials, actuators, piezoelectric ceramic actuators, piezoceramic actuators, PZT, PLZT, PMN, vibration suppression, vibration

15. NUMBER OF PAGES

283

16. PRICE CODE

17. SECURITY CLASSIFICATION OF REPORT	18. SECURITY CLASSIFICATION OF THIS PAGE	19. SECURITY CLASSIFICATION OF ABSTRACT	20. LIMITATION OF ABSTRACT
UNCLASSIFIED	UNCLASSIFIED	UNCLASSIFIED	SAR

IDA DOCUMENT D-1189

SDIO WORKSHOP ON PIEZOELECTRIC CERAMIC ACTUATORS FOR SPACE APPLICATIONS

Janet Sater

June 1992

INSTITUTE FOR DEFENSE ANALYSES
Contract MDA 903 89 C 0003
Task T-R2-597.09

PREFACE

Lt.Col. Michael Obal of the Strategic Defense Initiative Organization, Materials and Structures Office, manages a wide variety of advanced technology programs addressing needs for various systems. Programs in the area of adaptive structures, particularly for space systems, have recently been initiated. Vibration suppression, one of the important program areas, is a key feature in improving the target tracking and hit-to-kill performance of the various systems. Results from some of the materials and structures vibration suppression projects led to a desire to bring together the device end users, the materials researchers, and the materials/device manufacturers for discussion. The agenda was put together by Lt.Col. Michael Obal, Dr. Fred Kahn (NRL), and Dr. Janet M. Sater (IDA) to address the identified issues.

The workshop was hosted by IDA on February 25, 1992. IDA was requested under SDIO Task T-R2-597.09 to participate in the workshop and to prepare a proceedings to document the content of the workshop. This effort was subsequently carried out by Dr. Janet Sater with input from Lt.Col. Michael Obal and Dr. Fred Kahn.

CONTENTS

GLOSSARY

ACESA	Advanced Composites with Embedded Sensors and Actuators
ACTEX	Advanced Control Technology Experiment
Ag	silver
AMASS	Advanced Materials Application to Space Structures
ASTREX	Advanced Space Structures Technology Research Experiments
BT	barium-titanate
FACT	Fast Acting Control Thruster
Gr/Ep	graphite/epoxy
Gr/TP	graphite/thermoplastic
Hz	hertz
IRAD	internal research and development
J	joules
JPL	Jet Propulsion Laboratory
K	degrees Kelvin
kHz	kilohertz
m	meters
M&S	Materials and Structures
μm	microns
mil	thousandths of an inch
mm	millimeters
MV	million volts
N	newtons

NDE	nondestructive evaluation
NUWC	Naval Undersea Warfare Center
ONR	Office of Naval Research
Pt	platinum
PLZT	lead-lanthanum-zirconate-titanate
PMN	lead-magnesium-niobate
psi	pounds per square inch
PT	lead titanate
PVDF	poly vinylidene fluoride
PZT	lead-zirconate-titanate
RT	room temperature
SDIO	Strategic Defense Initiative Organization
SMA	shape memory alloys
SPICE	Space Integrated Controls Experiment
V	volts
W	watts

1. INTRODUCTION

Lt.Col. Michael Obal of the Strategic Defense Initiative Organization, Materials and Structures Office, manages a wide variety of advanced technology programs. Programs in the area of adaptive structures, particularly for space systems, have recently been initiated (Appendix A, pp. A-1 to A-10). These programs are beginning to address solutions for potential difficulties resulting from the following: absence of scheduled maintenance; limited or no ability to assess performance capability after time in orbit; and limited ability to adjust performance capability. Potential benefits of the adaptive structures technology include on-orbit system health monitoring and reporting, threat attack warning and assessment, and improved target tracking and hit-to-kill performance.

Vibration suppression is a key feature in improving the target tracking and hit-to-kill performance of the SDIO space systems (Appendix A, pp. A-3 to A-4). One of the early materials and structures (M&S) efforts in the area of vibration suppression was the Advanced Composites with Embedded Sensors and Actuators program (ACESA). In the course of this program a number of issues associated with the use of piezoelectric ceramic devices for both sensors and actuators were identified. Results from ACESA coupled with those from other programs led to a workshop that brought together the device end users, the materials researchers, and the materials/device manufacturers.

This workshop was held at the Institute for Defense Analyses on February 25, 1992. An agenda and list of attendees can be found in Appendix B. Copies of charts used by each briefer can be found in Appendixes C through F. The format of this document follows the organization of the agenda.

Lt.Col. Michael Obal, Program Manager, opened the meeting by describing the overall M&S Adaptive Structures program. This also provided an introduction to the

workshop. The focus of the workshop, piezoelectric ceramic[1] materials for space-based actuators, was emphasized (Appendix C). Issues associated with these materials and devices that have been identified by the spacecraft/end user community were briefly discussed. These include, among others, the following:

1. Inherent piezoceramic material performance limitations such as fatigue life at high strains;
2. Noted spreads/distributions in properties of vendor-supplied materials such as capacitance and piezoelectric activity composition as well as geometric tolerances; and
3. Device fabrication-related difficulties such as material handling, electrical connections, and electrical insulation.

Objectives of the workshop were clearly defined:

1. To enhance communication between space-based actuator users and the materials research and the materials/device manufacturing communities;
2. To focus and prioritize issues for near-term improvements in actuator performance; and
3. To identify and suggest research plans to obtain such improvements.

Dr. Fred Kahn reiterated these objectives, stating that information exchange (particularly of unmet needs) among the participants was critical. More productive collaboration could be expected as a result.

The remainder of the report is divided into four chapters. The first three chapters correspond to the three groups represented at the workshop. The fourth chapter includes the final discussion and summary.

---

[1] Hereafter, "piezoelectric ceramic" is shortened to "piezoceramic."

2. SPACECRAFT DESIGNERS AND USERS OF PIEZOCERAMIC ACTUATORS

The spacecraft designer community was asked to cover five major topical areas, as follows:

1. The nature and design parameters of present actuator applications;
2. Identification of actuator issues experienced in past applications;
3. Spacecraft qualification requirements that the actuator would have to meet in order to be used in real systems, including ambient and life requirements;
4. Current and predicted actuator performance and reliability requirements, based on structural design or on the number of cycles required at design or maximum actuator strain levels; and
5. Quantification of the "value added" to various space surveillance and interceptor systems via implementation of advanced actuator materials and configurations.

Briefing charts used by each of the speakers in this session can be found in Appendix D.

A. DR. ALLEN BRONOWICKI (TRW)

TRW has been a significant participant in several SDIO programs[1] involving the embedding of piezoelectric actuators in composites: Advanced Composites with Embedded Sensors and Actuators (ACESA), Advanced Control Technology Experiment (ACTEX), and Advanced Materials Application to Space Structures (AMASS). The ACESA struts, 16 feet long, contain 24 sensors and 12 actuators each. The ACTEX tripod struts are shorter and contain 8 sensors and 4 actuators each. For ACTEX, an adaptive structures flight experiment, it is believed that the space environment may affect long-term performance of these devices. The environments of concern include the temperature range from –250 °F to +250 °F and the associated thermal cycling, as well as radiation.

---

[1] Refer to Appendix A, pages A-3 to A-4, for a description of these programs.

Dr. Bronowicki summarized the results of validation tests of Navy Type I and Type II lead-zirconate-titanate (PZT) actuators for ACESA and AMASS (Appendix D, p. D-3). Type 1 (PZT-4) actuators have a low intrinsic hysteresis and good stiffness match to the graphite fibers in a composite but Type II (PZT-5A) actuators have a higher free strain. Hysteresis in the Type II was reduced dramatically after it had been embedded in graphite/epoxy (Gr/Ep). The tensile strain-to-failure[2] of the Type I in Gr/Ep at room temperature (RT) was ~600 micro-strain (μ-strain). For the Type II in the same material it was 2,000 to 2,500 μ-strain. However, in graphite/thermoplastic (Gr/TP) composites, the Type II could only withstand 500 to 1,000 tensile μ-strain. Compressive strain-to-failure was above 8,000 μ-strain. Fatigue did not appear to affect stiffness. As long as μ-strains during fatigue cycles were kept below 600 for the Type I in Gr/Ep and 1,500 for the Type II in Gr/Ep no actuation losses were observed. Thermal cycling, however, resulted in 10 to 30 percent reductions in actuation strain. This is believed to be due to high stresses resulting from thermal expansion mismatch. When asked if the actuator was debonding or actually breaking, Dr. Bronowicki replied that cracks were observed in the piezoceramic. He indicated that the dynamic transfer functions were found to be quite insensitive to temperature, though the Type II were more sensitive to temperature than the Type I. Additional results can be found in the paper "Mechanical Validation of Smart Structures," pages D-7 to D-10.

Figures of merit were also described (p. D-4): strain coefficient (d_{31}) or charge/stress coefficient ($d_{31}\sigma_1$), lateral stress coefficient[3] ($Y^E_{11}d_{31}$) or charge/strain coefficient[4] ($Y^E_{11}d_{31}\epsilon_1$), and the planar coupling coefficient[5] (κ_p). The lateral stress coefficient is constant for most PZT piezoceramics at ~10 N/V–m. It is desirable that $Y^E_{11}d_{31}$ be flat with temperature. TRW would like manufacturers to measure the lateral stress coefficient and/or the charge/strain coefficient. Vernitron measures κ_p, which differs from the charge/strain coefficient by the square root of the dielectric constant.

TRW has come up with a preliminary specification for PZT actuators and/or sensors. Dr. Bronowicki solicited verbal or written suggestions from workshop attendees

---

2 Failure is defined as "irrecoverable degradation in actuation constant Ed_{31}." Ed_{31} is a material property that is used to optimize both sensing and actuation.

3 This is an indicator of ability to actuate against a stiff structure. A larger number is better.

4 This is an indicator of ability to sense lateral strain using a charge amplifier.

5 This is similar to the lateral stress coefficient and is a measure of conversion efficiency between electrical and mechanical energy.

for improvements in the specification (p. D-5, pp. D-11 to D-15). Basic requirements for Type I and Type II include the following:

1. Piezoceramic wafer thicknesses ≤0.02 inches with length and width controlled within +/–0.02 in.;
2. Electrode thickness = 0.0002 in. of nickel;
3. Wafers capable of withstanding 2 psi loads on a flat surface;[6]
4. Measured capacitance for each wafer within 5 percent of lot mean;[7]
5. Lateral stress output coefficient at RT ($Y_{11}d_{31}$) ≥ 10 N/V-m;[8] and
6. Planar coupling coefficient[9] (nominal at RT, κ_p) ≥ 0.55 with a variation in nominal κ_p within +/– 10 percent of RT value over a temperature range of –125 °C to +125 °C.

Dr. Bronowicki also presented a "wish list" for PZT materials and devices (p. D-6): thinner, multilayer wafers (~2.5 mils thickness per layer); cylindrically curved wafers at ~2.5 mils thickness per layer;[10] wafers that operate in the d_{33} mode rather than the d_{31} mode; wafers that operate in the d_{15} mode in the plane of the composite for torsion; and materials that have 10 times the stroke of PZTs with no loss of linearity or bandwidth and have 1,000 to 2,000 μ-strain actuation capability. One of the attendees indicated that Motorola has a proprietary method for slicing PZTs down to a thickness of 2.5 mils for a speaker application. These sliced wafers can be bent a significant amount, dependent somewhat on grain size. Actuation could be increased as much as 2.5 times by using the d_{33} mode rather than the d_{31} mode. This requires a thin stack[11] of PZTs in the plane of the composite, a very difficult manufacturing task. Hagood has developed a technique that uses alternating electrode fingers to approximate this type of behavior: the PZT thickness is 5 mils and the alternating electrodes are placed 30 mils apart.

---

6 Surface flatness appears to be a continuing problem.

7 Typically, there is a 10 percent variance in capacitance.

8 Measured values are typically 20 to 30 percent lower than the book value.

9 TRW would like to have this number measured for each lot. Low temperature sensitivity of this value is also desirable to ensure the gain margin.

10 The diameter of curvature is 1 in.

11 The thickness perpendicular to the stack is 5 mils. Each layer of the stack is 2.5 mils thick. See Appendix D, page D-6.

B. DR. DEAN JACOT (BOEING)

Boeing has been involved in a number of programs in the "Smart Structures" area for space. Included among these are embedding of piezoceramics in Gr/Ep composites, damping of aluminum via piezoceramics, ACESA (Phase 1), and embedding of piezoceramics for damping trusses, among others (p. D-17). Dr. Jacot described several of Boeing's efforts in more detail.

The ACESA program was addressing issues associated with precision pointing and jitter control of a 3-mirror-wide field of view optical system such as ASTREX (Advanced Space Structures Technology Research Experiments). Two types of beams, a low frequency and a high frequency, were investigated. Piezoceramics were selected for the actuators in the high frequency beam (p. D-19): G1195 type ceramics were used for the actuators which were embedded in Gr/Ep.

In some IRAD work Boeing is examining the use of piezoceramics for sensors and actuators (p. D-21). Twenty G1195[12] piezoceramic devices[13] were attached to each side of an aluminum square tube[14] with an epoxy adhesive. A relaxation behavior was noted over a relatively short period of time: the beam deflection per volt was less than expected. At first, this was believed to be due to inadequate curing of the epoxy adhesive. It was later attributed to local deformation of the tube wall. It was suggested that a bimorph actuator might help sidestep the surface damage problem. Dean Jacot pointed out, however, that such actuators probably wouldn't work in most structures.

He identified other problems that Boeing has experienced in working with these ceramic materials/devices. Cracking has been observed in devices embedded and cured in composites. Attachment of leads to the devices has been difficult. Initially, round wires were used which led to cracks in the piezoceramics. Now Boeing uses a flat wire attached with a silver epoxy, even though the control authority is less. In some cases the full force of the device cannot be obtained, probably due to incomplete curing of the epoxy. He emphasized that the load-carrying capability of the ceramic needed to be matched to the load-carrying capability of the composite as closely as possible.

---

12 G1195 materials are similar to the Navy Type II materials, PZT-5A.

13 The dimensions were as follows: 0.6 in. × 1.55 in. × 0.01 in. thick. The gap between devices was 0.25 in. (along the length, as near as I can tell).

14 The dimensions were as follows: ~5 feet long × 3 in. × 3 in. × 0.125 in. thick.

C. DR. BEN WADA (JPL)

Dr. Ben Wada discussed JPL's interests in piezoelectric actuators for dynamic and static control such as might be of interest for large truss structures or for attainment of micron level surface accuracies for large mirrors. Accuracy is the key since loads are low.

JPL's active truss member concept includes a high voltage piezoelectric motor.[15] The motor consists of a stack of cylindrical rings of piezoceramic/silver/epoxy/Sn/Cu/Sn/epoxy/Ag/piezoceramic combinations (p. D-26). Basic characteristics of the current active member are as follows (p. D-27): a maximum operating voltage of 1000 V with a normal bias voltage of 500 V; ceramic wafer thicknesses of 1 mm (39.4 mils); displacement of 63.4 μm (2.5 mils) at 1 Hz; a force of 505 N (114 lb) at 1 Hz; hysteresis of 16 percent at 1 Hz; and power of 3.77 W for 25 Hz at maximum voltage. The maximum stroke is about 50 μm. In actuality, what JPL thought they were getting from the manufacturer (non-U.S.) and what they got were not the same. Several of the motors failed and were disassembled to determine why. Vertical and horizontal cracks as well as voids were observed in the stacks. It was not clear if these flaws existed before the device was tested, i.e., if they were manufacturing defects. The wafers were specified to be 1 mm thick but measurements showed that they were 0.5 mm thick. The specific composition was also unknown.

An alternate design that uses piezoceramic discs without holes has also been investigated.[16] The piezoelectric stack consists of 66 wafers, each 16 mm diameter × 0.8 mm thick. The maximum stroke at 150 V is 45 μm and the maximum load is ~200 lb. The displacement per volt of the in-line actuators was found to depend on frequency. It is not yet known if the frequency dependency is related to the specific material or is a result of the structural dynamics. The actuators also elongate over time: peak-to-peak displacement increases over months (p. D-33).

Piezoelectric strip actuators are used in deformable composite reflectors[17] for static control, the requirements for which are more stringent than for dynamic control. The PZT-5H actuator strips are 3 in. × 0.5 in. × 0.039 in. thick. The strain level is 2 μm/in. at 500 V at an operating temperature of 200 K; both tensile and compressive strains are

---

15 The dimensions of the motor are 70 mm long × 15 mm outer diameter, 7 mm inner diameter.

16 See the attached paper, page D-41, for more detailed information on the reflector support structure using the in-line actuator.

17 The radius of curvature is 7.6 meters.

important. Space environmental factors such as radiation, atomic oxygen, and temperature as well as operational loads were mentioned as potential concerns. Dr. Wada indicated that JPL would like to be able to maintain the desired shape by applying a voltage periodically rather than continuously. What they are looking for is a hysteretic actuator. Some general lifetimes of these devices in space were predicted using a safety factor of four (p. D-37): for a random loading cycle, 0 to 50 °C, the device should be able to withstand 360,000 cycles; for a sine wave loading cycle, same temperatures, ~135,000 cycles are required. For a ground calibration test, using a compressive preloaded condition and low vibration levels at 100 K to 323 K, 20 million cycles are necessary. For space operation using the same vibration levels and a preloaded condition, the number of cycles for Mode 1 is 1.2 million, for Mode 2, 61,000. Apparently these devices have not been particularly reliable in application so far.

Dr. Wada identified a number of technical areas that need to be addressed for both the dynamic and static control devices. Issues for both include understanding fracture mechanics, strength properties and load-carrying capabilities, temperature limitations, flexibility in bending, bonds and interfaces, reliability, and heat output. Additional issues associated with static control include creep, stability, frequency, hysteresis, aging, and load effects on the piezoceramic/interface bonds; stroke capabilities;[18] application of continuous power; and d_{13} coupling.

Dr. Wada concluded by stating that there was value added, though this value was not quantified: performance goals could be met; reliance on analysis could be less; reliability of the system would be improved; overall system design and possibly ground validation tests could be simplified. Whether or not the use of these actuators will be cost effective remains to be seen.

D. DR. JOHN BREAKWELL (LOCKHEED)

Dr. Breakwell discussed the Space Integrated Controls Experiment program (SPICE). SPICE is a precision optical structure consisting of the following: a large, segmented primary mirror; a 250-strut bulkhead truss structure supporting the mirror; and a tripod secondary mirror support system (p. D-51). This experiment is directed toward

---

[18] JPL is interested in actuators with longer strokes from 45 to 1000 μm or inchworm-type actuators that are <1 in. diameter and 3 to 6 in. long.

addressing line-of-sight pointing stability for the SDIO directed energy weapon systems of the future.

Requirements (p. D-54) for the proof mass actuators currently being developed/ used for SPICE include a peak force capability of 60 N, a peak-to-peak stroke-proof mass product of 8.2 kg-cm, power of <30 W, and a frequency range of up to 500 Hz.

The V-struts being used for SPICE contain viscoelastic damping material. These struts have been tested at low frequency (≤55 Hz) to determine complex stiffness as a continuous function of frequency. Control system performance has also been evaluated. A global high authority control/low authority control/passive damping combination is believed to provide the best performance: attenuation of 100 to 1 can be achieved (p. D-57).

In conclusion, Dr. Breakwell indicated that precise design and modelling of the actuator devices were needed. Determination of interactions of these devices with other parts of the structure/system will also be critical. He stated that the major point was that there is an established procedure in order for a prime contractor to use these devices.

E. MR. RICHARD ALEXIUS (MARTIN MARIETTA-ORLANDO)

The Fast Acting Control Thruster program (FACT) was presented by Mr. Richard Alexius. The overall objective of this effort is to analyze, design, fabricate, and test a lightweight, ultrafast, linearly proportional thruster for various Army/SDI applications. The device, illustrated on page D-61, contains an electrostrictive[19] material stack. An elastomer is used with large and small pistons to amplify the motion (p. D-63): the output motion is directly proportional to the piston area ratio while the output force is inversely proportional to it. The stack has a 5-to-1 length over diameter ratio. Tests show (p. D-68) that with a 50-lb input load and an input-to-output amplification of 1-to-10 , the output load is 5 lb. A 96 percent motion conversion is obtained but the stack does not return to its original position: 0.0025 in. are lost after the first stroke. Apparently there is a friction problem with the motion amplifier and a compliance problem with the ceramic stack.[20] The compliance problem is being addressed via lapping stack ends so that they are smooth, flat, and perpendicular to the thruster bore mold line. Larger diameter stacks are also being investigated to reduce the effect of bending. Ben Wada indicated that JPL utilized mechanical fixtures at the ends of their actuator to avoid a similar bending problem.

---

19 The electrostrictor material that has been tested in the device is 100AVX 6-8.

20 Eight out of 10 stacks have failed due to stack bending.

When questioned about the processing of the ceramics, Mr. Alexius stated that they were cold-isostatically pressed to 30 ksi before firing at 1200 °C; the wafers were not hot-isostatically pressed after firing. The electrodes run along the sides of the actuator stack. Even though cracks have been observed at the tabs the stress concentration is believed to be low. According to Mr. Alexius, the disbond between the electrode and the ceramic is a limiting factor. The actuators have been cycled up to 0.5 billion cycles to failure without load but have not yet been fatigue tested under load.

F. DR. ROBERT GLASER (JPL)

JPL is examining the application of piezoceramics for cryocooler vibration isolation applications. The flight configuration illustrated on page D-73 is the actual size of the cryocooler to be flown. More typical piezoceramic actuators are being evaluated to damp the rest of the cryocooler, to prevent the cold finger from moving. These actuators (p. D-74) are of the Physik P-842.10 Low Voltage Piezo Translator type,[21] about 1.5 in. long. Specific capabilities of the devices include an operating voltage of −20 V to +120 V; expansions from −3 μm to 18 μm; a compressive preload of ~67 lb; operating temperature −20 °C to +80 °C; maximum pulling and pushing forces of ~67 lb and 180 lb, respectively; a stiffness of 314 ksi; and a capacitance of 1.8 μF.[22] The preload conditions are critical for launch. It is believed that low temperature operations should be limited; keep in mind that the particular spacecraft conditions are −50 °C to +50 °C. Capacitance is a key property for power requirements. Dr. Glaser mentioned that these actuators are always one-sided and need to be centered.

Piezoceramics in the form of an applique are being considered for the cold finger: the ceramic wraps around the cold finger; its action is out of phase with the movement of the cold finger. The Vernitron PZT-5H material (p. D-75) is being used as the applique for high d_{31} motion. One of the objectives is to minimize the height as well as thickness of the ceramic applique/sleeve. Minimization of power requirements to 1 W is also desired. Some optimization studies were run; results showing trade-offs among height, thickness, power,[23] and voltage can be found on page D-76. For lower values of voltage (<200 V) and power (<0.2 W) the height is larger (≥1.5 in.). For higher values of voltage (>400 V) and power (>0.5 W) the height is low (<0.8 in.). The applique material apparently exhibits

---

21 Physik is the name of the company that produces the devices.

22 JPL is using 0 to +28 V, 0μm to 4.2 μm expansion, zero lb pulling force; 52 lb pushing force.

23 The power is observed to increase almost linearly up to the limit of 1 W.

marginal behavior at the temperatures at which it is to be used. The ceramic is also brittle and difficult to handle. Dr. Glaser indicated that the diamond saw is probably causing cracks in the ceramic.

He also discussed the launch environment that these devices must withstand (p. D-77). The three worst cases are maximum dynamic pressures, before thrust termination, and during thrust tail-off. The longitudinal g-forces seem to be much more severe than lateral g-forces for these conditions. Two tests are of interest for simulating dynamic loading conditions: sinusoidal vibration tests and random vibration tests. The sinusoidal vibration test is not critical for this particular application since it is outside the limits.[24] The random vibration test, on the other hand, is critical; it covers the frequency range from 30 to 2000 Hz.

To conclude, Dr. Glaser stated that lead time from Vernitron for the materials was a problem. This difficulty has been attributed mainly to changing of designs by JPL after the order is placed. He believed JPL would buy more ceramics from Vernitron if delivery was more prompt. The difficulty of performing development work on the actual materials was mentioned as a problem. He also indicated that JPL desired larger preloads on the actuators and the inclusion of flexures with the actuators. Low power flight power supplies were identified as another area of concern.

G. DR. VIJAY VARADAN (PENN STATE)

The final speaker in this session was Dr. Vijay Varadan from Penn State. He discussed some processing techniques for making these devices and embedding them in composites. The process illustrated on page D-80[25] is a semiautomated manufacturing system concept. High purity ceramic powders can be produced by a sol-gel process or conventional powders can be calcined using a microwave process. This calcination process results in the formation of small, fine, uniform particles. Powders[26] are characterized by grain size and purity. Organics are added to the powder (produced by either method) and ball-milled for 24 hours; viscosity is measured during this step. The ceramic wafers are produced via a tape casting process. For process control purposes, tape thickness and dielectric properties are measured, nonintrusively. The tape can then be cut into blanks,

---

[24] The system is designed to be stiff at 300 Hz; the maximum frequency in the sinusoidal test is 100 Hz. Note that the cryocooler itself is driven at 60 Hz.

[25] Additional descriptions of the processes can be found on pages D-81 to D-83.

[26] The piezoceramic material of interest is PZT-5H.

metallized (for electrodes)[27], and hot-pressed. The final sequence is device fabrication and firing and sintering. The organic binders are removed during firing; sintering can be done via the conventional process or by a microwave process. Microwave sintering reduced the time for sintering from days to about 45 minutes. In an attempt to better understand how to control the process Dr. Varadan and his students have measured the dielectric constant of the ceramic in the green state and the fired state; at this time the relationship between the two values appears to be somewhat tenuous.

The piezoelectric chiral materials developed at Penn State were briefly mentioned. These materials are capable of larger displacements than conventional materials. Dr. Varadan indicated that processing is very critical for obtaining the desired properties. The chiral elements are electroded, though if they are all the same individual elements will not be electroded. These materials are useful for compliant surfaces or "smart skins."

Microwave processing can also be used to cure the composite in which the actuators are embedded (pp. D-84 to D-88). The microwave has no effect on the behavior of the actuator: heating of the ceramic is avoided by focussing power at the interface and applying pressure, as in an autoclave. Microwave processing is also suitable for repair of composite structures.

Dr. Varadan has developed a portable applicator microwave processing system for large area joining as well as a taper applicator for strip joining. The applicator is of a travelling wave type that bonds each layer separately. Bonds made by microwave processing have been tested in bending and appear to be very strong. The crack is initially at the joint but grows away from it on further bending.

---

[27] The electrode material is platinum.

3. PIEZOELECTRIC MATERIALS RESEARCHERS AND ACTUATOR EXPERTS

Five major topical areas were addressed by this group:

1. Currently available materials and performance trade-offs, both for production-qualified materials and limited quantity pilot-scale materials;
2. Developmental materials with promising characteristics;
3. Proposed or predicted actuator materials performance parameters and the corresponding rationale;
4. Proposed and available multiphase actuator configurations, composites, and motion amplifiers; and
5. Expected failure mechanisms of actuator materials and potential methods to maximize and estimate their reliability.

Briefing charts used by each of the speakers in this session can be found in Appendix E.

A. DR. ERIC CROSS (PENN STATE)

Dr. Cross began by describing several types of actuators such as shape memory alloys (SMAs), piezoelectrics, electrostrictors, contractile polymers, and muscles (p. E-2). The nature of the process by which actuation occurs and the specific phenomena associated with that process were also identified. For example, in the piezoelectric ceramics the nature of the process is electro-mechanical transduction; the phenomenon utilized is ferroelectricity in a poled ceramic or in a polymer. Achievable strain levels vary widely: the contractile polymers and muscles can achieve strain levels on the order of 0.5, with SMAs at 0.1, and piezoelectrics and electrostrictors at 0.002.

The relationship of piezoelectricity and electrostriction to the strain tensor were discussed to help focus on the achievement of high strain actuators. The polarization-related piezoelectric constants, b_{mij}, and the polarization-related electrostrictive constants, Q_{mnij}, are reasonably constant over a range of temperatures. Dr. Cross stated, however, that there is no known solid with high enough values of b or Q and breakdown to allow induction by an external field of electric polarization values adequate to generate 1 percent

strain. He indicated that values of spontaneous polarizations, on the other hand, can be large enough to generate spontaneous strains up to 15 percent in ferroelectric crystals. There are two options for control of spontaneous strain: (1) phase changes from a non-polar to a ferroelectric state, and (2) domain changes in ferroelectric crystals that reorient the spontaneous strain. Dr. Cross also indicated that, only if the electric polarization terms (P_mP_n) are homogeneous through the solid, large values of strain can theoretically be induced at zero stress without breaking it.

Various mechanisms for changing polarization to control electrostrictive strain were discussed in order of increasing induced polarization:

1. Homogeneous polarization of a paraelectric phase--These materials exhibit "dreadful" performance due to extreme temperature sensitivity; the zero strain state is stable.
2. Induced polarization in a relaxor ferroelectric (conventional electrostrictor)--These materials do not exhibit drift or aging behavior but are sensitive to temperature; the zero strain state is stable.
3. Induced polarization change in a poled ceramic (conventional piezoelectric)--The zero strain state is unstable due to aging changes of one of the polarization states.
4. Micro- to macrodomain poled relaxer--These materials exhibit hysteresis and are sensitive to temperature; the zero strain state is stable.
5. Field forced phase change--These materials exhibit hysteresis and are sensitive to temperature; the zero strain state can be stable or unstable depending on the system.
6. Field forced domain change--These materials exhibit hysteresis; the zero strain state is unstable.

Most of these materials can be operated using bias voltage to induce a larger d_{31}. There are problems with the bias field, however.

Dr. Cross next discussed the antiferroelectric to ferroelectric switching in the lead-lanthanum-zirconate-titanate (PLZT) materials. The polarization-applied field responses are shown on p. E-8 for compositions identified on page E-7. For these materials linearity of response is sacrificed for magnitude of strain: strain levels on the order of 0.5 percent can be achieved. In addition, switching between the two states can occur rapidly, <1 μsec if the applied field is large, on the order of kV/cm (pp. E-11-E-12). There are however, a number of factors that affect the performance of these materials: specific composition,

ambient temperature surface preparation, grain size, porosity, and electrodes. The figure on page E-13 illustrates the importance of surface preparation: the samples with rough surfaces show a significant degradation in polarization with an increasing number of switching cycles; the degradation in polarization for the polished samples is noticeably less. According to Dr. Cross, up to 10^9 cycles of fatigue can be achieved with these materials if one is careful in their preparation.

Microdomain to macrodomain switching was the final subject for discussion in this presentation (pp. E-14-E-23). This happens in spin glass materials that are transparent and capable of achieving large polarizations though they are sensitive to temperature (p. E-16). The material is fine grained with grain sizes on the order of microns.[1] The switching is essentially a volume fraction effect: the polarization is changed by controlling the volume fraction of microdomains being changed, which also controls the proportional strains. It is possible to achieve ~0.5 percent strain. A deliberate hysteretic response, such as would be desirable for static control applications, is also achievable. The same factors that affect domain reversal also apply to microdomain/macrodomain switching. For example (p. E-21), a conventionally sintered PLZT exhibits a 40 percent decrease in normalized polarization with an increasing number of cycles while a hot-pressed PLZT exhibits almost no change. As another example (p. E-20), an 80 percent degradation is observed in hot-pressed PLZT with a conventionally prepared surface compared to a clean surface. Dr. Cross indicated that stress concentrations in the ceramics at the electrodes are a factor and can be reduced with careful preparation.

B. DR. STEPHEN WINZER (MARTIN MARIETTA)

Dr. Winzer discussed the advantages and disadvantages of electrostrictive materials and multilayer actuators. The performance of the electrostrictors are significantly dependent on temperature,[2] field, and frequency; the phase transition and capacitive properties are also issues (p. E-26). These materials do, however, exhibit high energy densities; large force, high modulus and high strain (up to 0.2 percent) capabilities; low losses, fast response times; and low hysteresis. Issues associated with the multilayer actuators include the size, weight, and power requirements for the drive electronics;

---

1 The scale for polarization is on the order of nanometers.

2 It was mentioned that, in the PMN-type materials (lead-magnesium-niobate), for a temperature range of 40 °C, a 20 percent drop in strain capability is observed. For other, unidentified materials a smaller temperature range results in a 100 percent drop in strain capability.

fabrication; cost; reliability; fatigue; accessibility; coupling method (attach or embed); and compatibility. Dr. Winzer also suggested that it would be desirable to vary the thickness of the individual actuators in a stack. The multilayer devices are, however, flexible in design and can operate over a wide range of drive voltages.

Martin Marietta has been involved in the development of the lead-magnesium-niobate (PMN) type electrostrictive materials. A total of 75 compositions of PMN with lead-titanate (PT) and barium-titanate (BT) have been examined.[3] Both weak-field (T_{max}) and high-field (strain) behavior are predictable. In terms of weak-field behavior, T_{max} increases linearly with log frequency; increasing the PT content results in an increase in the slope of the frequency dependence (p. E-28).

Actuator fabrication techniques were also described by Dr. Winzer. The approach is similar to that used by commercial manufacturers of multilayer devices. The actuator layers are 20-25 μm thick; electrode materials are Pt and Ag,[4] a stripline electrode runs along the side of the stack with internal electrodes between the layers; operating voltages are ~25 V; and the field in the ceramic is 1 MV/m. Conventional ceramic powder and tapecasting processes are used to make the individual wafers. The actuators are then cut, electroded, layered, and co-fired. One of the workshop attendees asked if it would be possible to make a multilayer actuator then cut it so that the d_{33} poles are the poles that provide the actuation. Dr. Winzer indicated that it might be possible as long as the pieces held together during the cutting step: adhesion between the electrode and ceramic was believed to be the difficulty. Dr. Winzer worked on the development of the FACT actuator.

He concluded by stating that electrostrictive materials and actuators were applicable to space systems. Issues still to be addressed include the temperature dependence; field, and frequency dependence of T_c; fatigue analysis and identification of failure modes in both materials and devices; and miniaturization of the actuator drive electronics.

C. DR. GENE HAERTLING (CLEMSON)

Dr. Haertling provided an excellent overview of the limitations of piezoelectric and electrostrictive materials. The charts on pages E-35 to E-38 contain a significant amount of information; only selected highlights will be presented here. Properties and associated

---

[3] These materials can exhibit either an electrostrictive or a piezoelectric response. The piezoelectric response is observed below T_c.

[4] There is a difficulty with internal Ag electrodes: the silver can react with lead during firing.

phenomena for the PLZT ferroelectric ceramics were discussed first Dielectric, optical, and electrical resistivity properties are singular properties; the others, such as piezoelectric or electrostrictive properties, are interactive. Singular phenomena include, for example, photoconductivity (dielectric) and space charge effects (electrical resistivity). Interactive phenomena include photovoltaic (piezoelectric) or photostrictive (electrostrictive) effects.

A comprehensive list of 18 factors that determine performance of these materials is provided on page E-36. Included among these are composition, microstructure, aging, fatigue, and creep. Typical ranges for properties of various materials are shown on page E-37. Dr. Haertling emphasized the minimization of the tan δ value. He also indicated that the less complex compositions exhibited greater stability in terms of their properties. Common defects include domain bending which affects toughness; water enhances crack propagation; the combination of humidity and voltage degrades both the material and the electrodes such that grain separation can occur.

Dr. Haertling also presented some limiting values for selected factors that affect performance of these materials (p. E-38). He emphasized that the listed values are not those that would be received from a manufacturer; they are, in fact, more optimistic though achievable. For example, the best property reproducibility that can be achieved is thought to be +3 percent; a manufacturer might guarantee 10 percent. Note that the electric field breakdown values are for the hot isostatically pressed material.

D. DR. ROBERT NEWNHAM (PENN STATE)

Dr. Robert Newnham first considered the mechanisms by which electromechanical transducers operate--piezoelectricity, electrostriction, domain changes, or phase changes--and the associated strain versus electric field response of each (p. E-40). A variety of composite actuator components such as piezoresistors or varistors were briefly described. A number of examples of composite materials for these devices were also shown (p. E-42): for instance, rods in a matrix (1-3) or spheres in a matrix (0-3). Work at Penn State funded by ONR has emphasized connectivity patterns and sensors. The illustration on p. E-43 shows how compliance can be controlled by using a sensor and multilayer actuator combination: the sensor detects stress and the feedback amplifier reduces the actuator height and changes its elastic modulus.

One specific application was highlighted. Toyota uses piezoelectric sensors and actuators to electronically modulate an automobile suspension response (pp. E-44 to E-45):

a five-layer piezoelectric sensor located on the piston rod of the shock absorber detects road surface roughness within 2 msec; with a high voltage from the electronic control unit an 88-layer piezoelectric actuator produces a 50-μm displacement on the oil system (5 msec); the small displacement is hydraulically amplified to 2 mm, changing the shock absorber damping force in <16 msec. Several other applications were also mentioned (p. E-46).

Dr. Newnham spent some time comparing and contrasting actuator designs: multilayer stacks with large forces and small displacements; bimorph benders with small forces and big displacements; and the moonie disks with intermediate forces and displacements. The moonie actuators[5] consist of a piezoceramic disk sandwiched between two shaped metal electrodes, each having a flat, moon-shaped cavity at the sandwich/ceramic surface. Cavity size is a critical parameter (p. E-50): increasing the cavity size increases the hydrostatic piezoelectric charge coefficient, d_h; for a given cavity size, increasing pressure up to about 1000 psi has virtually no effect on d_h. The particular choice of metal for the electrodes is important since the metal does most of the straining during actuation. The stress state of the metal electrode and/or the ceramic will also be of concern. The bond between the metal electrode and the ceramic disk is another critical feature. Several types of bonds including polymers, solder, and solder with metal screens have been investigated. Apparently, these moonie PZT actuators offer a factor of about 5 improvement in performance/displacement over the multilayer stack actuators (at 1000 V, p. E-51). Moonie actuators fabricated from PMN-PT electrostrictive materials exhibit a factor of 10 improvement in performance over conventional PMN (at 1000 V, p. E-53). The d_{33} coefficient for the moonie actuators is a factor of 10 higher than that of PZT. Dr. Newnham indicated that PMN moonie actuators stacked to a length of 6 in. have achieved a 3-mm displacement.

E. MR. FRANK A. TITO (NUWC)

Mr. Tito began his review of high power transducers by discussing limitations of sonar projectors: media limits such as cavitation;[6] physical limits of the radiated sound that influence the projector size; and internal projector limits such as electrical, mechanical, or thermal factors. The schematic on page E-58 illustrates the relationship of radiated power

---

5 The approximate size is ~1 cm diameter, 2 to 3 mm thick.

6 Cavitation occurs when acoustic pressure exceeds fluid static pressure. The cavitation threshold increases with increasing depth, frequency (particularly above 10-15 kHz), or shorter pulses (< 0.005 sec).

versus frequency: at low frequency levels the applied field can limit the performance; at higher frequencies, stress is the limiting factor.

A number of devices were discussed in more detail (pp. E-62-E-77): hydroacoustic projectors, moving coil projectors, flexural bender bar projectors, flexural disk projector, Class IV flextensional projectors, and ring projectors. Common features include relatively large sizes and weights and high power requirements. These transducers operate over a wide range of frequencies--from a few Hz to over 100 kHz. For example, the flexural bender bar projector (p. E-69) is 5.75 in. long and weighs 15 lb; its frequency range is 1300 to 1800 Hz. The Class IV flextensional projector (p. E-73) has dimensions of 24 in. × 11 in. (elliptical) × 34 in. high and weighs 1150 lb; its frequency range is 450 to 600 Hz. A variety of materials have been utilized for these devices including PZT, PVDF piezoelectric polymers, PMN electrostrictives, and rare earth magneto-strictives. The energy density (as measured by $0.5Y_{33}S^2_{max}$, p. E-78) for the rare earth magnetostrictives at liquid nitrogen temperatures is 50 kJ/m^3, significantly higher than for the other materials: PVDF materials--110 J/m^3, PZT4 materials--826 J/m^3, and PMN materials--12.6 kJ/m^3. To conclude, Mr. Tito stated that size, reliability, cost, and the power-related source level were important considerations when examining new materials for these devices.

4. MATERIALS AND DEVICE MANUFACTURERS

This group was requested to address three major topical areas, as follows:

1. Producibility and repeatability issues in the manufacture of PZT materials and actuators;
2. Availability and associated constraints of processing equipment and testing facilities as necessary for production-quantity materials and devices; and
3. Estimated costs of setting up such facilities, if necessary.

Briefing charts used by each of the speakers in this session can be found in Appendix F.

A. MR. BARRY KOEPKE (ALLIANT TECHSYSTEMS)

Mr. Koepke discussed a possible approach to manufacturing PZT materials with improved and reproducible electro-mechanical properties, mechanical integrity, and microstructure. The proposed process would be an adaptation of a chemical precursor powder production technique currently used to produce transparent PLZT. Expected benefits include consistent, reproducible powder production; control of powder chemistry; homogeneous green density and dopant distribution; and a high quality sintered product. There are difficulties associated with the typical mixed oxide powder production process illustrated on page F-3: incomplete reaction and heterogeneous phase distribution due to relatively large starting powders;[1] inhomogeneous dispersion of dopants; formation of hard agglomerates due to high calcination temperatures (~900 °C);[2] and requirement for hot pressing to obtain high quality material.[3] Another issue is the binder: binders that burn cleanly are desired to prevent contamination; minimal binder concentration is needed for easier burnout.

---

1 The composition, morphology, and particle size distribution of these starting powders are critical. Morphology and size distribution, in particular, affect powder flow and packing. Alliant Techsystems is interested in using smaller starting powders for faster sintering.

2 Agglomerates can lead to the formation of internal flaws as a result of differential shrinkage.

3 Alliant Techsystems would like to eliminate the hot pressing step by decreasing the powder size via the chemical precursor process. On the other hand, for the tapecasting process a slightly larger particle size is desired for proper dispersion.

Time and cost are the main differences between the conventional process and the proposed chemical precursor process, illustrated on page F-5. With the chemical process one can obtain a uniform phase distribution; a homogeneous dopant distribution; lower calcination temperatures leading to smaller agglomerates;[4] and finer particle sizes. The chemical process may allow for better control of sintered grain size, lower sintering temperatures, and smaller flaws. The most typical flaws are voids. It was pointed out by a member of the group that while voids can stop cracks they are more likely to initiate them. Flaws are typically examined by inspecting fracture surfaces. Mr. Koepke concluded by stating that the chemical precursor process appeared to be the best choice for manufacturing actuator ceramics with repeatable and controllable properties, improved mechanical integrity, and improved microstructures. He proposed a joint Alliant Techsystems/Sandia program for optimizing this technology and indicated that the necessary facilities were already in place.

B. MR. CRAIG NEAR (VERNITRON PIEZOELECTRIC DIVISION)

Mr. Near discussed issues associated with development and manufacturing of high performance PZT materials. Reproducibility and reliability were identified as critical material performance issues. He began by presenting data on various properties[5] of high-power (hard) and high-strain (soft) PZT materials[6] (p. F-9): K, κ_p, d_{33}, and Q_m. Lot-to-lot variations were estimated to be +/– 5 percent for K, a few percent for κ_p, and +/– 8 percent for d_{33}; variations for Q_m are difficult to determine. The question of aging was raised. Mr. Near indicated that for the high-power/hard materials the degradation in properties was less than 5 percent per decade.

Stability of the new hard materials is being examined in terms of applied field, temperature, pressure, and frequency. Many of these new materials contain multiple components that are very interactive; compositions are, therefore, somewhat complicated. The observed improvements in the performance of these materials have been, so far, only due to formulation; additional improvements are expected with changes in processing, etc. Other manufacturing issues (p. F-11) include rheology control in various process steps,

---

4 Mr. Koepke indicated that Alliant Techsystems could increase the strength of these materials by 25 percent by eliminating agglomerates.

5 Properties are measured on disks of material.

6 The new PZT-5K material is a developmental material with a T_c of about 160 °C. Vernitron is attempting to obtain a d_{33} value of 1000 in this material.

selection of binder materials and ZrO_2 sources,[7] and the sintering environment and temperature control.

Some discussion was generated on multilayer actuator stacks. While Vernitron has not really made thin, hard materials for the multilayer stacks, Mr. Near also indicated that, though the domain wall phenomena of the soft materials was not well understood, Vernitron knows how to make multilayer stacks from soft PZT. For example, Vernitron makes a 12-layer, PZT-5H actuator that operates in the 0 to 400 V range; hysteresis is 7 percent at 50 V/mil.[8] However, the device must be operated below 1 kHz. Maximum displacements are on the order of ~4 μm. Mr. Near believed that hard actuator materials should be used for space applications since the soft materials will depole under continuous load levels and since the operational frequencies for the soft materials were limited. Multi-element arrays were mentioned as being useful for generating spatial displacements in optical applications such as deformable mirrors.

Development issues include not only formulation of compositions, but also selection of a chemical processing approach; control of the sintering environment and temperature;[9] and testing in realistic environments. Costs of powders produced by different chemical processes vary widely (p. F-13):[10] powder produced via hydrothermal synthesis, costs $8/lb; other powder costs are $20-30/lb for aqueous co-precipitation, $15/lb for thermal co-precipitation, and $18/lb for sol-gel.[11] The hydrothermal process appears to be most attractive in terms of material quality (p. F-14). Chemical processing can result in improved performance. For example, increases in K, κ_p, and d_{33} are noted for a PZT-5H material derived from special powder processing and special firing procedures (p. F-16). Variations in measurements of a specific material among vendors were identified as a problem, specifically. Data for a PZT-8M material tested using the DOD-1376A high field test approach show significant differences when tested by several groups, though all data are within the specification limits.

---

7 The quality of the PZT materials is especially sensitive to the ZrO_2 source.

8 Vernitron has fabricated 25-layer actuators. In the fabrication of 100-layer actuators parallelism of the layers is a problem. Vernitron uses a roll compaction process to help eliminate nonuniform thicknesses.

9 Data on p. F-15 indicate the importance of sintering pressure and temperature on various properties of PZT-4S1 and PZT-5K.

10 Particle sizes typically range from 200 A to microns with purity levels ranging from 99.5 percent to 99.9 percent.

11 The sol-gel process is considered by Mr. Near to be an R&D process.

Estimated costs for new facilities were also provided: a hydrothermal plant would cost ~$1.7 million; part manufacturing equipment costs are ~$1.5 million; special firing equipment costs are ~$250 thousand; testing equipment would cost ~$500 thousand.

C. MR. MELVIN MAIN (EDO CORPORATION)

Edo Corporation is capable of producing large numbers of piezoelectric ceramic devices. New materials development activities include large geometry products, high volume products, and extensions of performance of Terfenol-D, PZT, and PMN. The objective of Mr. Main's presentation was to address performance of piezoceramic devices in space, in particular at cryogenic temperatures.

The DOD-STD-1376(A)SH test geometry was utilized; the procedure was the American National Standard C83.24-1962. Data were collected from 5 K to 300 K on several PZT materials including Type I (EC-64), Type II (EC-65), Type III (EC-67 or -69), and Type V (EC-70). Graphs on pages F-27-F-33 show the relationships between various properties[12] and temperature. For example, values for d_{33} for all materials tested converge at ~50 K while values for d_{31} appear to converge at ~150 K. Results showing the percent change in a property compared to that at ambient conditions (295 K) are summarized in tables on pages F-34 and F-35. As an example, the percent change in d_{33} at 100 K is –34 percent, at 5 K, –61 percent.

Mr. Main stated that DOD-STD ceramics would not produce high strains at space temperatures and would perform poorly relative to their performance under ambient conditions. The devices would then operate over narrower bandwidths, at lower strains, and with lower efficiencies. He did not believe that changing the ZrO_2:TiO_2 ratio of the PZT materials would result in dramatic improvements in their performance at cryogenic temperatures. Alternative materials warranting development were PLZT and strontium titanate.

D. DR. JOHN GALVANI (AVX CERAMICS)

AVX Ceramics is a manufacturer of both multilayer capacitors and actuators. Dr. Galvani compared the capacitor and actuator manufacturing processes (p. F-38). AVX's capacitor production capacity is 15 million/day with costs for each on the order of pennies; actuator capacity, however, is less, on the order of hundreds/day with costs in the

---

[12] Properties include d_{33}, d_{31}, κ_p, κ_{33}, κ_{31}, Q_m, and K_{33}^T.

range of tens of dollars. Devices are presently fabricated according to specifications provided by prime contractors. Actuator materials are purchased from Vernitron, Channel Industries, or others.[13] Actuator electrode materials are platinum. Actuators, designed to operate at 150 V, contain as many as 500 layers, 125 of which are active. Limitations include the minimum thickness of the ceramic that can be obtained and firing shrinkage (p. F-39) with respect to the electrode. Burn-out times for the actuators are quite long, 60 to 170 hours, compared to those for the capacitors, 0 to 4 hours.

Electrode adhesion/bond strength influences the performance of the multilayer actuators. Dr. Galvani mentioned several different electroding techniques (pp. F-40 to F-41). To prevent the occurence of unpoled, highly stressed regions, electrodes are often applied over the full ceramic surfaces. External "pick-up" paths are then insulated from opposite polarity edges by a Japanese-developed electrophoretic deposition technique using a glass/epoxy material. Alternatively, a "loose pack" approach uses a porous ceramic and is designed to relieve these stresses: the porous ceramic is located between the ceramic layers some distance in from the edge. The diffuse electrode is a functionally gradient material: ceramic particles are deposited with Pt such that the volume fraction of ceramic particles varies across the cross-section; this requires multiple printing, usually 3 to 5 times.

E. MR. LESLIE BOWEN (MATERIALS SYSTEMS)

Materials Systems, Inc., manufactures piezoelectric composites and composite actuators as well as actuator assemblies. The company is also investigating alternative ceramic processing technologies such as injection molding and device prototyping. The injection molding process (p. F-44) is attractive since it allows complex shapes to be easily fabricated: PZT powders are ball-milled, mixed with an organic binder, and placed in a mold; burnout[14] in a controlled atmosphere, air flash, and sintering follow.

Mr. Bowen observed that there were several approaches for enhancing the displacement performance of piezoelectric actuators: high-strain materials; strain amplification via compound actuator designs; and multiple actuator assemblies. Of these the compound actuator assemblies were thought to be most likely for success, though high-strain materials and device designs were also claimed to be in the development stage.

---

[13] Actuator materials are PZT and PMN.

[14] This step removes carbon and binder residues.

He felt the actuators needed to be designed with respect to system goals, manufacturability, and cost.

Examples of compound actuator assemblies include piezoceramic/polymer composites and flextensional strain amplifiers (moonie actuators). Potential issues with the composites include the development of high-strain piezoceramics, processing of ceramic/metal/polymer interfaces, and fabrication of complex shapes. Alignment, joining, packaging, and testing will be important during assembly. The 1-3 piezoceramic/polymer composites consist of PZT rods embedded in a polymer, perpendicular to the electrode surface (p. F-47). Issues associated with the use of these composite materials include handling of large quantities of PZT rods or fibers and assembly of the composites; cost and application and integration into a real system. Injection molding has been selected to form the ceramics to net-shape. The ceramic preform would look something like a comb (p. F-48).

There are a few issues that need to be resolved for the flextensional strain amplifiers as well (p. F-49). Included among these are alignment and reproducibility of alignment during assembly; joining, particularly with reference to the device life; design and reliability of multiple actuator assemblies; and cost. Currently, Materials Systems is using manual assembly for pilot-scale quantities of prototype devices. According to Mr. Bowen, the devices would be redesigned for full-scale production to simplify joining and alignment.

5. DISCUSSION

The purpose of the discussion was to explore potential near-term improvements in PZT actuator performance. A number of research areas providing opportunities for such improvements were identified throughout the meeting. These are listed as follows: d_{31} vs. d_{33} performance; displacement/volt; power requirements; fatigue life at high strains; tensile strain-to-failure; aging behavior and hysteresis; temperature/environmental effects; ceramic material/actuator fabrication; surface finish; dimensions and available shapes; material handling; electrode materials and their application to the actuator; post-composite fabrication actuator performance; and actuator-structure interfaces. Due to the difficulty of addressing all of these items in detail, the discussion was focused somewhat using several questions as starting points for additional comments. [1]

A. MATERIAL IMPROVEMENTS

Lt.Col. Obal inquired if the available PZT materials could be improved. He believed that the community was coming up against theoretical limits in some cases. Dr. Newnham indicated that this was probably true for the hard PZT materials though it may not apply to the soft materials. Dr. Fred Kahn then asked what was specifically meant by improvement. The general consensus appeared to be that strain performance of the hard materials needed to be improved. Dr. Cross stated that the hardening mechanism of these materials is diffusion-controlled: if domain walls can be moved it may be possible to increase their strain capabilities.

Dr. Galvani indicated that the operating window for these actuators needed better definition: required strain levels and temperature ranges, as well as voltage/power limitations. Dr. Bronowicki stated that actuators used in the ACESA composite struts operated in the range of +/–400 V. TRW is interested in having 2-mil thick Type II actuators that can operate in the +/–50 V range for the small SDI interceptors. He then remarked that interceptors in the homing stage will be operating at their maximum

---

[1] Note that often there were several conversations occurring at the same time. This chapter contains the best information available from the author's notes.

performance level for about 100 sec; frequencies will be on the order of hundreds of hertz.[2] The operating conditions for SDI surveillance systems will be quite different. TRW would like to have actuators that operate at 10-12 V/mil for these systems. One of the workshop attendees said that force levels rather than strain should be the requirement for designing the actuators. In fact, it will probably be a trade-off between voltage and current. Dr. Bronowicki also indicated that the d_{33} mode of operation was preferred to the d_{31} mode currently used. The d_{15} mode may also be of interest since it has the largest coefficient. The ability of the material/device to withstand a large number of cycles and, if cracked, to continue to operate is important.

When questioned about loading on actuators, all the space system users agreed that the devices were used in tension. The manufacturers then indicated that this was not a good idea: for structural reliability these active devices should be kept in compression.

The idea of reinforcing the ceramics with whiskers was discussed. While the toughness of the material can be doubled from 0.6 to 1.2 MPa $m^{-1/2}$ there is a loss in piezoelectric properties, particularly in d_{33}. In addition, careful processing is required. The flaw size cannot be controlled: the initial flaw size is larger and, therefore, the material is weaker from the start. Dr. Tuttle from Sandia indicated that the critical parameters limiting the performance of these ceramic materials (with and without reinforcement) were flaw size and fracture toughness.

The particular aging rate of the materials is also of concern. Such information would be obtained from qualification testing. According to Dr. Pohanka, aging rates are included as part of the specifications for Navy transducers. In some cases, the Navy requirements are very stringent and push the quality of the materials.

B. MANUFACTURING PROCESS IMPROVEMENTS

A number of manufacturing issues were raised during the discussion. Lt.Col. Obal commented that there was usually a willingness on the part of the buyer of advanced systems to pay more for parts, etc., if what was needed could be obtained. This is particularly true for space systems where the value of improvement (to the system) is high.

In terms of material handling most agreed that improvements in current manufacturing methods as well as development of new technology such as tape casting

---

[2] Compare this to the few hertz expected for the large, floppy space structures in which NASA has an interest.

were in progress. It was believed that much more was possible. There are now only a limited number of people capable of producing PZT material via tapecasting. Dr. Tuttle also stated that the tapecasting process was still in the development stage. He did think that a chemical processing approach could significantly improve material yields over the conventional oxide mixing approach: a conventional oxide mixing approach was said by Dr. Tuttle to have a yield of about 10 percent while yields for the chemical approach are over 95 percent. Such a process would address material reproducibility issues but not reliability. Others would disagree with this assessment. Dr. Tuttle indicated that device reliability would be expected to increase if chemically processed materials were utilized. However, one of the other attendees mentioned that chemical processing was not necessary to eliminate aggregates in calcining: it could be done by screening, for instance.[3]

Several of the attendees indicated that problems are induced in the actuator ceramics prior to assembly. Surface and subsurface cracks introduced by machining, for example, can grow, eventually causing catastrophic failure. Some end users mentioned that for actuator layers 5 mils thick planar materials could not be obtained from vendors. Others felt that this was not a problem.

Mr. Main believed that the limitation was transducer design, not material. Mr. Tito stated that material was a problem 8 to 15 years ago. He indicated that vendor data (book values) are used to design the actuators. However, what usually happens is that pieces are ordered from the vendors, and properties which often do not agree with the book values are measured. Apparently, when a large number of layers are used in a device the variability in properties becomes less noticeable.

The microwave processing technology was thought to be an interesting possibility for implementing these devices into composites.

C. TESTING, NONDESTRUCTIVE EVALUATION (NDE)

Reliability of these devices, clearly an issue, is somewhat related to availability. One person mentioned the difficulty of obtaining adequate data on device performance to determine statistical limits because of limited availability.

The issues associated with qualification testing were discussed briefly. For space systems, "shake and bake" tests are required: these are basically vibration and thermal cycling tests. The need to be sure that qualification testing of the devices is not in the

---

[3] This was thought to be a cost issue.

region where permanent damage occurs was emphasized. Dr. Galvani stated that there is no good way of testing the devices under various loading conditions: AVX tests for voids and delaminations between the layers; proof tests[4] can only be performed at low levels so that damage is not induced.

Dr. Bronowicki discussed TRW's experience in measuring electrical characteristics before and after loading of actuators: capacitance measurements were within 4 percent of the expected value. Values for Ed_{31} were at least as good as the book value, sometimes even better. Cracks, however, were observed between the Ni-plated electrodes and the PZT; the PZT itself was cracked. It was pointed out that these cracks can close up during actuation. According to Dr. Bronowicki, for a system designer to accept this technology, data from a flight experiment such as ACTEX would be necessary. In addition, vibration testing in a thermal chamber would also be desirable. He suggested that efforts similar to those currently in progress in the SDIO M&S program be continued. The utility of a standard procurement specification with appropriate inspection techniques was highlighted.

[4] Some of the devices are tested in tension.

APPENDIX A

ADAPTIVE STRUCTURES PROGRAMS FOR THE STRATEGIC DEFENSE INITIATIVE ORGANIZATION

ADAPTIVE STRUCTURES PROGRAMS FOR THE STRATEGIC DEFENSE INITIATIVE ORGANIZATION

Lt.Col. Michael Obal*
The Pentagon
Washington, DC

Dr. Janet M. Sater*
Institute for Defense Analyses
Alexandria, Virginia

Abstract

In the currently envisioned architecture none of the Strategic Defense System (SDS) elements to be deployed will receive scheduled maintenance. Assessments of performance capability due to changes caused by the uncertain effects of environments will be difficult, at best. In addition, the system will have limited ability to adjust in order to maintain its required performance levels. The Materials and Structures Office of the Strategic Defense Initiative Organization (SDIO) has begun to address solutions to these potential difficulties via an adaptive structures technology program that combines health and environment monitoring with static and dynamic structural control. Conceivable system benefits include on-orbit system health monitoring and reporting, threat attack warning and assessment, and improved target tracking and hit-to-kill performance.

Introduction

The Strategic Defense Initiative Organization (SDIO) has undergone a dramatic change in its mission architecture. The system envisioned during the early years was concerned with the destruction of a substantial portion of a massive Soviet attack involving thousands of nuclear re-entry vehicles. Its purpose was to provide sufficient uncertainty to Soviet forces to enhance deterrence. The goal of the new architecture, Global Protection Against Limited Strikes (GPALS), is to prevent from one to, perhaps, hundreds of attacking missiles from reaching their target. This architecture may, however, have difficulty achieving its performance goal than the previously designed systems. The GPALS systems are to be designed to allow no "leakers - no penetration of US/allies air space by attacking missiles. With the proliferation of nuclear and missile technologies the threat against the US and its allies is of particular concern.

To attain this goal the elements that constitute the GPALS architecture must meet performance and reliability constraints much beyond those of current military weapon systems. The elements must be able to react quickly and perform optimally after remaining dormant for an extended period of time. Two critical components of the GPALS architecture consist of space-based autonomous surveillance and defensive elements. None of these elements will receive scheduled maintenance. Assessments of performance capability due to changes caused by the uncertain effects of natural environmental aging and man-made threats will be difficult, at best. In addition, the system will have limited ability to adjust critical structural components in order to maintain its required performance levels. A solution to these potential difficulties is adaptive structures technology that combines health and environmental monitoring with threat attack warning and assessment capabilities and static and dynamic structural control.

Several different concepts for "Adaptive Structures" may be found in the open literature and in the structures community at large [1-6, for example]. The Strategic Defense Initiative Organization Materials and Structures (SDIO M&S) Program has proposed an alternative concept illustrated in Figure 1. Different types of sensors, either embedded in or attached to certain structures, are used to measure specific environmental features and to perform various subsystem diagnostics. These real-time passive devices can provide several functions such as structural health monitoring for identification, status, and propagation of cracks; threat detection measurements; natural environment measurements including radiation, atomic oxygen, loads, dynamic and static states, and thermal states; and monitoring of system states. The sensory information obtained from measurements and subsystem diagnostics is then processed and can be stored on-site or telemetered to another location. This information can also be utilized for static and dynamic structural control[a] via appropriate feedback loops using active structures containing actuators. The actuator devices can be static such as for shape control or dynamic such as for vibration suppression; acoustic and propulsion devices may also be used. Applications of this technology are only now becoming achievable as a result of developments in microprocessors and miniature sensors. Conceivable benefits include on-orbit system health monitoring and reporting and threat attack warning and assessment via a combination of sensory structures and information processing, and improved target tracking and hit-to-kill performance using a combination of sensory and active structures with information processing.

Although adaptive structures offer some very attractive features for these complex, autonomous systems there are many issues to be resolved. For sensory structures questions remain on sensor attachment methods; their durability in natural and threat environments; the number of sensors required[b] sensor placement and any associated constraints; choice of analog or digital output; general sensor performance; and effects of electromagnetic interactions. Information processing issues include selection of local and/or global control approaches; development of degradation protocol, and selection of a numerical/classical, symbolic/rule-based, or a neural network control theory approach. Issues for active structures include active material performance[c]; type of active device; methods for energy coupling; device durability in natural and threat environments; device placement and any associated constraints; and power requirements. And, finally, in order for system designers to accept this technology, it must be

---

* Members AIAA

a Other properties of the system might also be controlled by such feedback loops: thermal properties, optical properties, electromagnetic properties, etc. [5]

b A large number of low sophistication sensors or a few smart sensors could be utilized.

c This includes, for example, the ability of piezoceramic materials to withstand high strains over many cycles.

least intrusive to the design in terms of weight, power, and reliability. These issues are being addressed to some degree by the SDIO M&S Program as well as by other researchers.

M&S Adaptive Structures Programs

The M&S program intends to leverage outside research whenever possible. However, in order to provide the most appropriate adaptive structures technologies for the Strategic Defense Systems M&S efforts are currently focusing on the application of adaptive structures technology to provide SDS space elements: on-orbit system health monitoring and reporting and threat attack warning and assessment via a combination of sensory structures and information processing; improved target tracking and hit-to-kill performance via a combination of sensory and active structures with information processing. A M&S program chart showing points of contact and areas of research can be found in Table I. The general approach is through ground-based demonstrations leading to generic structural space experiments as appropriate. Examples of some of these programs follow.

Sensory Structures

Four areas M&S is currently focusing on in this area are real-time assessments of the state of (1) critical moving mechanical assemblies (MMAs) and momentum transfer devices; (2) micrometeoroids and debris (MM&D) identification; (3) real-time evaluation of critical materials deterioration and spacecraft contamination; and (4) threat attack warning and assessment.

Moving mechanical assemblies and momentum transfer devices are mission critical components on many DoD space assets: if the device fails the system cannot perform its mission. Examples are illustrated in Table 2. Wright Laboratories has initiated a M&S program to develop a health monitoring system for MMAs to help address potential failure problems. An example of a smart tribomechanism is illustrated in Figure 2. Major segments of the program include the following: (1) identification of vibration and torque signal signatures[d] for bearing structural mechanism and lubricant failures; (2) use of embedded or attached sensors to identify changes in acoustic or thermal signatures of the device; (3) development of an on-board control system to enable corrective action such as activation of adaptable bearing preload or of exercise protocol for fretting suppression; and (4) analyses of actual and predicted signatures to determine the expected remaining life of the device. This technology, applicable to any space assets having MMAs, would provide on-orbit capabilities to control or alter performance to extend system life.

One of SDIO's concerns for SDS elements is the degrading effect of MM&D or kinetic energy weapons (KEW) attack over time on critical sensor structures. To provide real-time assessment of these impacts, NRL is chartered to investigate technologies for impact detection, location identification, and damage assessment sensor systems. These sensor systems will be demonstrated via extensive ground and/or flight testing. M&S is leveraging ongoing work for DARPA on application of such sensor systems in submarine hulls for damage detection and analysis. The general approach is to detect, locate, and assess local structural damage and to determine the remaining structural performance capability. The operational requirements and specific environments need to be defined in order to select appropriate sensors and devices and locations, thereof. Acoustic emission and optical methods are being examined. Typical sensors may consist of piezoelectrics, capacitance-type sensors, and fiber optics.[e] A proposed acoustic emission technique uses a passive plate wave approach that recognizes source orientation effects and the true nature of the waveform as a function of structural geometry. Several types of fiber optic sensors are also being considered in a two-phase program: in Phase 1, speckle modulation and multiplexed interferometric arrays (shown in Figure 3) to detect occurrence of impact and location; and in Phase 2, distributed strain rosettes to detect deformation. The sensors, to be located on critical areas of the spacecraft, are also expected to be least intrusive to the system in terms of power and weight. This technology is applicable to a broad range of systems; examples are BP and BE optical sensor, antenna, heat exchanger, and solar array surfaces.

To actively determine the health of critical optical coatings and other materials and assess spacecraft self-contamination in the orbiting environment, M&S is developing the Space Active Modular Materials Experiments (SAMMES) program. The SAMMES modules, located on a generic spacecraft, and the system configuration are illustrated in Figure 4. Though not the original goal of this program, an additional benefit of SAMMES may be the capability to provide spacecraft with lightweight, low power, modular avionics for active health monitoring of mission critical materials. Recent findings from the Long Duration Exposure Facility (LDEF) suggest that contamination may pose serious problems for SDIO-like sensor systems. SAMMES may also offer the potential for active monitoring of contamination.

To field a fleet of surveillance and space-based interceptors or high value directed energy weapon (DEW) platforms will require continuous knowledge of the threat environment. Potential kill mechanisms range from the subtle (i.e., damage to parts of an electronic system from microwaves) to the direct (i.e., major structural damage from a nuclear explosion or a high-power laser). The external surface of the space asset provides an opportunity to embed or attach sensors that can identify and measure the threat. An additional benefit will be the ability to distinguish between system failures caused by natural or man-made environments. The M&S Program has initiated a program to develop a "Smart Skin": a prototype, light weight, low power sensor skin. These sensors will be able to measure radio frequency (RF), laser, and nuclear energy deposition on the satellite. These sensors include conformal antennae for RF detection, coated pyroelectric films for laser detection (Figure 5), and fiber optics for nuclear detection. The sensors and initial signal conditioning are embedded or attached to the spacecraft skin which provides thermal and space environment protection for the devices. Information from the skin is provided to on-orbit or ground-based systems that would identify the source of the energy and its damage capability. Since some of these sensors do require

[d] These signature outputs are to be correlated with specific failure mechanisms. Under another M&S tribology program Lockheed is correlating torque signals with failure mechanisms of super-dense MoS_2-coated bearings.

[e] Fiber optics have advantages that include light weight, immunity from electro-magnetic interactions, electrical passivity, low power consumption, minimal leads in and out, and no direct current drift or bias offset. Disadvantages depend on the specific sensor type and may include inadequate sensitivity, requirement for integrated measurement over the whole fiber length, complex signal processing, fabrication of many reflective splices, requirement for multiple wavelength light sources, temperature sensitivity, and the need for high speed electronics.

surface mounting, the skin itself must not interfere with the thermal balance of the spacecraft or require an excessive amount of surface area. A variety of materials have been examined for the skin structure. Combinations of advanced thermoplastics with shuttle tile ceramics appear promising for structural rigidity and thermal balance features. The advantage of real-time threat detection and assessment is the ability to provide critical information for the SDS fleet "user" to enhance survivability of those elements. This technology would be applicable to all US and Allied space assets.

Sensory/Active Structures

SDS elements require extreme tracking capabilities to meet mission performance goals. Sensor jitter from structural response seriously degrades this capability. Active and passive vibration suppression technologies provide a method of adaptable jitter control. Vibration control using piezoelectric devices as sensing and actuating elements has been in development for at least two decades. B.K. Wada's overview [5] of adaptive structures identifies research efforts undertaken in the early 1980's. This research has been significantly extended by industry and academia to the point where integration into fielded systems is more appropriate.

The ACESA (Advanced Composites with Embedded Sensors and Actuators) program was an early M&S initiative into the sensory/active structures arena. Overall goals for the program included design, fabrication, testing, and evaluation of composite components containing embedded sensors, actuators, and microprocessors. A number of parameters important in the selection of the sensors and actuators were identified: accuracy, dynamic range, frequency response, linearity, noise rejection, health monitoring capability, networking, device cost, survivability in natural and threat environments, technology readiness, embedding capability, and material processing conditions. A number of sensors and actuators, among which are fiber optics for sensors and shape memory alloys (SMAs) and piezoelectric ceramics for both sensors and actuators, were examined in light of the above parameters. The ability to use relatively simple drive electronics combined with other beneficial properties[f] led to the selection of piezoelectric ceramics for both sensors and actuators.

Some difficulties with embedding these and other devices into the composites were noted [7, 8]: fiber optic breakage, piezoelectric ceramic electrical insulation and cracking[g], mandrel thermal expansion, longitudinal mandrel bowing, and electrical insulation of shape memory alloy devices. Additional issues included mechanics of the device/structure interface during compression or tension, miniaturization for weight and power management, and central vs. distributed analog-to-digital (A/D) processing. Generally, though, characterization tests verified that the sensitivities and dynamic ranges of the sensors and actuators met the requirements derived from the system studies. The active structural control tests showed that the devices promoted significant damping and very short settling times. Good agreement was obtained between control simulations and experiments. Additional work is still needed, however, to address other issues such as active material development to obtain better actuator performance/watt, sensor and actuator placement, miniaturization of circuits and power conditioning, advanced control theory for adaptable control, neural network development for the "intelligent" aspects, and survivability in the space and threat environment.

Forward, Swigert, and Obal[9] completed one of the first successful demonstrations of the application of surface-mounted piezoceramic sensors and actuators for vibration control in a SDIO-like directed energy weapon system - the AF Airborne Laser Laboratory. A substantial amount of jitter reduction on a cavity resonator mirror was achieved with the combination of a passive tuned mass damper and an active rate feedback vibration control network that included piezoceramic devices. Unfortunately, the state of the technology at that time led to excessive high voltage power requirements. ACESA demonstrated an order of magnitude improvement in both actuator coupling and power requirements.

To meet current SDIO system power constraints using active vibration control, the performance of these active materials must be improved in order to obtain greater strains for a given input electrical load. To that end a task has been initiated at the Naval Research Laboratory (NRL) to improve toughness and durability of piezoelectric and electrostrictive actuator materials in order to obtain larger deflections, possibly up to 10 times that of conventional materials. The M&S Program is also looking for significant improvements in the number of cycles these materials can withstand under high/maximum strain conditions to address reliability concerns. Improvements in material reproducibility and manufacturing quality are also desired: i.e., it is difficult to obtain lead zirconate-lead titanate (PZT) materials having small variances in performance parameters from current vendors. Some interesting work is being done by Litton Optical Systems in conjunction with The Pennsylvania State University on the development of discrete multi-layer actuators made from lead magnesium niobate doped with lead titanate (PMN:PT)[10]. Results of their parametric studies showed a factor of ~3 improvement in achievable strain as well as improvements in material reproducibility and manufacturing yield. Included in the NRL task are specific research studies on methods to eliminate extrinsic voltage breakdown; the use of compositional chemistry, i.e., doped barium-containing PZT, to increase strain performance; and development of composite piezoelectric and electrostrictive materials containing whiskers or fibers to improve strength and toughness and to obtain higher c/a ratios. Methods for integrating these piezoelectric devices[h] into different actuator design configurations are also being investigated. Improved actuator materials would be applicable over a broad range of structural systems to provide better energy coupling.

Recognizing that the option of embedded sensors and actuators will not be permitted for all structures,[i] a concept

---

[f] Piezoceramic sensor materials such as lead zirconate-lead titanate (PZT) exhibit low temperature and radiation sensitivity and high strain sensitivity. As sensors they have a large dynamic range and a frequency range exceeding the kHz level. In terms of actuation PZT devices have a quick response time coupled with high efficiency and a potentially large force authority.

[g] One solution to this difficulty was to encapsulate the PZT device with fiberglass or kevlar/epoxy prior to placement within the structure. This step is particularly crucial if the device is to be embedded into a graphite-reinforced composite since the fibers are conductive and will ground the high voltage circuits necessary to power the device.

[h] The Japanese are transitioning advanced piezoelectric devices into a number of commercial products, i.e., autofocus mechanisms for cameras, curtain pullers, aerators for fish tanks, laser printer heads, etc.

[i] For example, sensors and actuators may not be able to endure severe composite component manufacturing processes. Or, vibration problems may not have been anticipated or identified during the design process thus requiring a retrofitted solution.

for a space-durable modular patch is being developed. The patch integrates the sensor, actuator, controller, and power conditioning electronics into a single package that can be bonded to the structure and interfaced directly with the power system. An individual patch could exhibit local vibrational control or could work in concert with other patches in a global manner. Naturally, the patch must be space-durable and engineered in such a manner as to provide optimized coupling between the actuator and the structure. Expected benefits include significantly reduced control system weight and volume and, potentially, increased damping. This technology could be used to retrofit structural components for which embedding such devices is not an option: systems that undergo severe composite manufacturing process conditions or existing systems having vibration problems.

Such active vibration suppression concepts will be demonstrated on the Advanced Materials Application to Space Structures (AMASS) program. This program includes studies on dynamic decoupling of solar array support structure during rapid motions. Figure 6 is an illustration of the concept. Solar arrays, utilized on a number of existing satellites, are expected to be used for several SDI systems.

As mentioned previously, sensor jitter continues to be an issue with the advanced SDS assets. One of the greatest sources of sensor jitter, given a quiescent spacecraft, is the cryocooler itself[11, 12]. A project was initiated by M&S with JPL to address this difficult problem. A PZT device is being used to isolate the motion of a cryocooler cold finger on an existing, advanced Stirling cryocooler. JPL expects to demonstrate a factor of 2 to 5 reduction in transmitted vibratory forces in the 0 to 200 Hz range. Such a cryocooler system is expected to be flown on a UK satellite in FY93 to obtain space durability data in a high radiation environment. The technology is applicable to extremely small cryocooler systems intended for BP or BE where cryocooler-induced vibrations couple to the focal plane array sensor and lead to increased jitter.

To provide adaptive control of the sensor critical structures, the state of the plant must be known at all times. The M&S program is pursuing demonstrations of system and parameter identification (ID) technologies to meet this requirement. To address this issue researchers at the Jet Propulsion Laboratory (JPL)[13] have been examining methods for system ID of open and closed loop structural systems in space using active members on ground test articles. Experiments were performed on a cantilever truss structures. Their results indicate that active members can be used as an excitation source for on-orbit system identification for both closed and open loop systems. The active members provide a modal excitation source to aid in identification of low amplitude dynamic characteristics that are important in large, precision space structures. The difficulty of simulating on-orbit conditions on the ground for system/structural identification is well known. M&S is cooperating with the Phillips Laboratory in advancing such investigations via the Inexpensive Flight Experiment (INFLEX) program. On-orbit system and parameter ID experiments will be carried out on this space test bed in FY95.

The Advanced Control Technology Experiment (ACTEX) will demonstrate many of the adaptive structures technologies being investigated by M&S for improved tracking and hit-to-kill performance in space. In fact, the technology developed by the ACESA program provides the basis for this experiment. A small, composite, sensor-mounting tripod (Figure 7) with numerous embedded PZT sensors and actuators and corresponding control avionics will perform various vibration suppression and adaptive control experiments. Issues being examined include mechanics of piezoelectric device/structure interfaces, durability of the devices and structural materials in space, system identification of the structure, methods to change structural stiffness for re-identification, and miniaturization of power and control devices. Three years of on-orbit performance and space effects data are to be obtained via a space flight.

An ultra-fast (~1 msec), lightweight (~0.1 lb), linearly proportional control thruster (10 lb maximum force) called the Fast Acting Control Thruster (FACT), is being developed to improve vehicle attitude control for various SDS elements. The device, 0.625 inches (diameter) by 2.5 inches (length), consists of a piezoelectric/electrostrictive actuator, an elastomeric motion amplifier, and a cold gas, high force-gain valve. It is illustrated in Figure 8. A number of issues are being addressed in this program: active material hysteresis, general performance, and fatigue limits; active material stack design and manufacturing; motion amplification device performance; throat position determination and feedback; and reductions in size, weight and power requirements of drive electronics.

Transfer of an innovative spacecraft technology such as adaptive structures into developing spacecraft is the last step in the maturation of a technology and can be a formidable challenge. Spacecraft designers are justifiably cautious in accepting a new technology without flight heritage. Therefore, M&S has initiated plans for a program called TechSat. Its purpose is to provide an on-orbit, multi-discipline experiment platform for testing and validating promising technologies important to SDI space assets. An initial list of candidate experiments for TechSat includes several adaptive structure demonstrations that build on advances described elsewhere in this paper.

System advantages obtained from use of adaptive structures technologies are expected to include increased agility, pointing precision, stability, and shape/alignment control, all of which contribute to enhanced target tracking and hit-to-kill performance. These technologies would be applicable to a number of SDI systems such as BP, BE, Ground-Based Interceptor (GBI), E^2I, THAAD, and Neutral Particle Beam (NPB).

Summary

A number of potentially significant benefits for SDS elements using adaptive structures technologies have been identified: on-orbit system health monitoring and reporting, threat attack warning and assessment, improved target tracking and hit-to-kill performance. The current M&S programs were basically selected and initiated during FY91. Communication and coordination with the SDS program elements (BP, BE, etc.) is a continuing effort. All the M&S programs have planned intermediate ground demonstrations to assess their progress since many technical issues still need to be resolved. Additionally, all of the adaptive structures technologies developed under the M&S program must satisfy the necessary space and threat durability requirements as well as provide minimum weight, power, and reliability concerns for the system. Though some elements of adaptive structures technology are ready for demonstration there are issues that remain to be addressed. The SDIO M&S Program is leveraging existing efforts in and coordinating with other U.S. government programs and agencies to address some of the most important concerns.

References

1. "Fiber Optic Smart Skins and Structures," August 1990. Marketing Research Review via NewsNet, based on International Resources Development, Report 772.

2. Rogers, C.A., E.S. Chen, and A.F. Findeis. 1988. "International Workshop on Intelligent Materials." *ONRASIA Scientific Information Bulletin*, 14 (3): 23-33.

3. Ahmad, Iqbal. 1990. "U.S.-Japan Workshop on Smart/Intelligent Materials and Systems."*ONRASIA Scientific Information Bulletin*, 15 (4): 67-75.

4. Brown, A.S. March 1990. "Materials Get Smarter." *Aerospace America* ,30-36.

5. Wada, B.K., J.L. Fanson, and E.F. Crawley. April 1990. "Adaptive Structures." *Journal of Intelligent Material Systems and Structures*, 1 (1): 157-174.

6. Wada, B.K. May-June 1990. "Adaptive Structures: An Overview." *Journal of Spacecraft and Rockets*, 27 (3): 330-337.

7. Ikegami, R., D.G. Wilson, and I.H. Laakso. June 1990. "Advanced Composites With Embedded Sensors and Actuators (ACESA)," Boeing Final Report, Contract F04611-88-C-0053, 111 pages.

8. Bronowicki, A.J., T.L. Mendenhall, and R.M. Manning. April 1990. "Advanced Composites With Embedded Sensors and Actuators (ACESA)," TRW Final Report, Contract F04611-88-C-0054, 162 pages.

9. Forward, R.L., C.J. Swigert, and M.Obal. May 1983. "Electronic Damping of a Large Optical Bench." *The Shock and Vibration Bulletin, Part 4 Damping and Machinery Dynamics*, Bulletin 53,: 51-61.

10. Wheeler, C.E. and B.G Pazol. 1991. "Multilayer Electrodisplacive Actuators." *Ceramic Bulletin*, 70 (1): 117-119.

11. Ludwigsen, J., "Vibration Suppression of Cryogenically Cooled Sensor Systems," white paper, Nichols Research Corporation - Albuquerque, April 25, 1991, 5 pages.

12. Ludwigsen, J., "Cryocooler Vibration Effects on Sensor Performance," white paper, Nichols Research Corporation - Albuquerque, September 18, 1991, 5 pages.

13. Kuo, C.P., G-S Chen, P. Pham, and B.K. Wada. April 2-4, 1990. "On-Orbit System Identification Using Active Members," 31st AIAA/ASME/ASCE/AHS/ASC Structures, Structural Dynamics and Materials Conference, AIAA-90-1129-CP: 2306-2316.

Table 1. Materials and Structures Adaptive Structures Program Organization FY92

	Programs	Points Of Contact	Phone No.
Sensory Structures With Information Processing	**F1504 (Air Force)**		
	Health Monitoring of Moving Mechanical Assemblies	Mr. Karl Mecklenburg	513-255-2465
	N1504 (Navy)		
	Sensor Development for Micrometoroid/Debris Identification	Dr. Robert Badaliance	202-767-6380
	S1504 (SDIO)		
	Space Environmental Effects and Contamination Sensor Developments	Lt.Col. Michael Obal	703-693-1663
	E1504 (Department of Energy)		
	Sensory Structures	Dr. Mark Hodgson	505-667-6772
Sensory/Active Structures With Information Processing	**F1504 (Air Force)**		
	Passive Damping Application Technology	Dr. Alok Das	805-275-5412
	Vibration Suppression for Cryocoolers	Mr. Paul Lindquist	513-255-6622
	Advanced Materials Applications for Space Structures (AMASS)		
	Advanced Composites with Embedded Sensors and Actuators (ACESA)		
	Advanced Control Technology Experiment (ACTEX)		
	Modular Control Patch		
	High Frequency Passive Damping Strut Development		
	Optional PZT Passive Damping		
	Autonomous System Identification		
	Adaptive Structural Control		
	A1504 (Army)		
	Adaptive Thermal Isolator	Mr. Doug Ennis	205-955-1494
	Fast Acting Control Thruster		
	N1504 (Navy)		
	Large Deflection Ceramics for Actuators	Dr. Manfred Kahn	202-767-2216
	S1504 (SDIO)		
	System Identification Flight Experiment (INFLEX)	Dr. Fred Hadaegh	818-354-8777
	TechSat	Lt.Col. Michael Obal	703-693-1663

Table 2. A History of Tribology Problems in Space and Spacecraft System Impacts

Program	Tribological System	Problem	Impact
DMSP	OLS Sensor Launch Clamp	Seizure on Launch Pad	Single Point Failure, Prohibit Launch
NAV/GPS	Reaction Wheels (4/Satellite)	Torque/Temperature Runaway, Pointing Errors	Lubricant Loss and Starvation
Skylab	CMG Bearing	Failure	Premature Mission Failure
CDP	CMG Bearing	Failure	Loss of Mission
CDP	ATP Harmonic Drive	Excessive Wear	Degraded Mission, Possible Failure
CDP	Large CMGs (4/Satellite)	Runaway Torque, Cage Fracture, Lubricant Breakdown During Test	Life Test Failures @ ≤1/2 Life, Lubricant Starvation, Cage Instability Using Active Oiler
DSCS, CDP	Slip Ring	Excessive Noise	Communication Antenna Pointing Mission Compromised
Galileo	High Gain Antenna	Sticking of Antenna Rib Pins Due to Dry Lubricant Loss	Unfurled Antenna, Crippled Mission

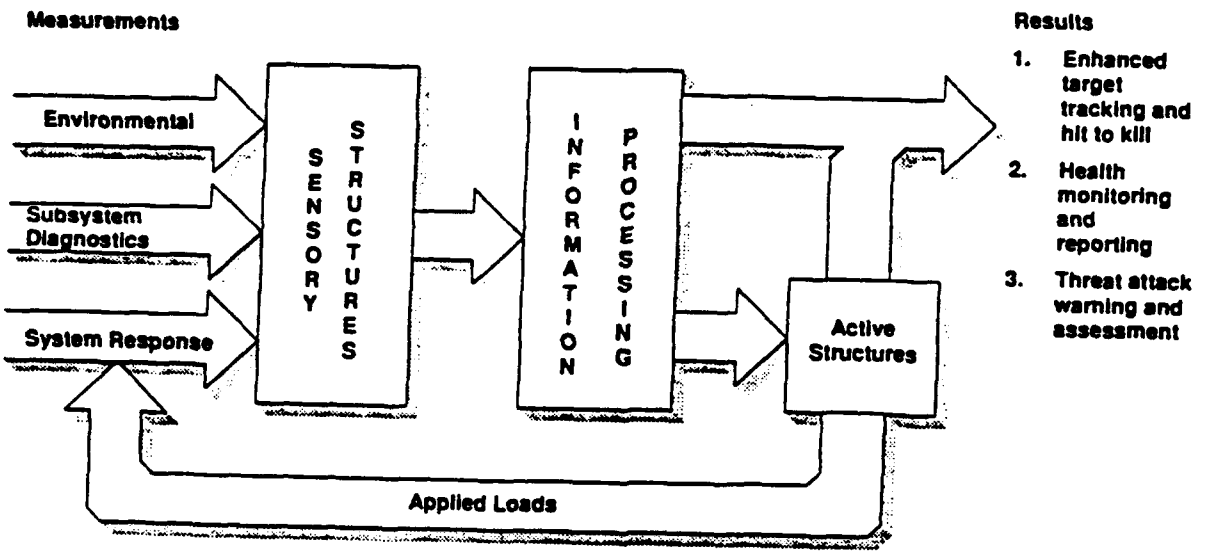

Figure 1. SDIO Proposed Concept for Adaptive Structures

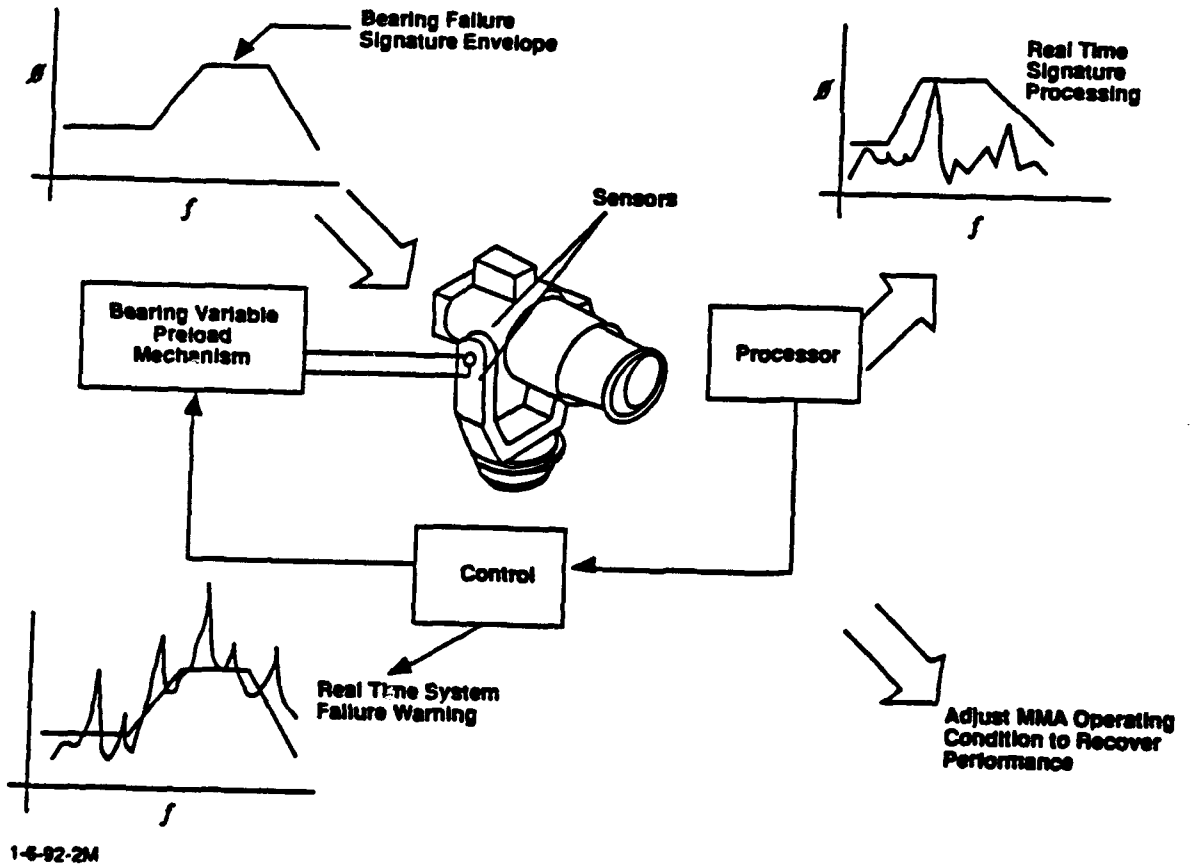

Figure 2. Schematic of Smart Tribomechanism

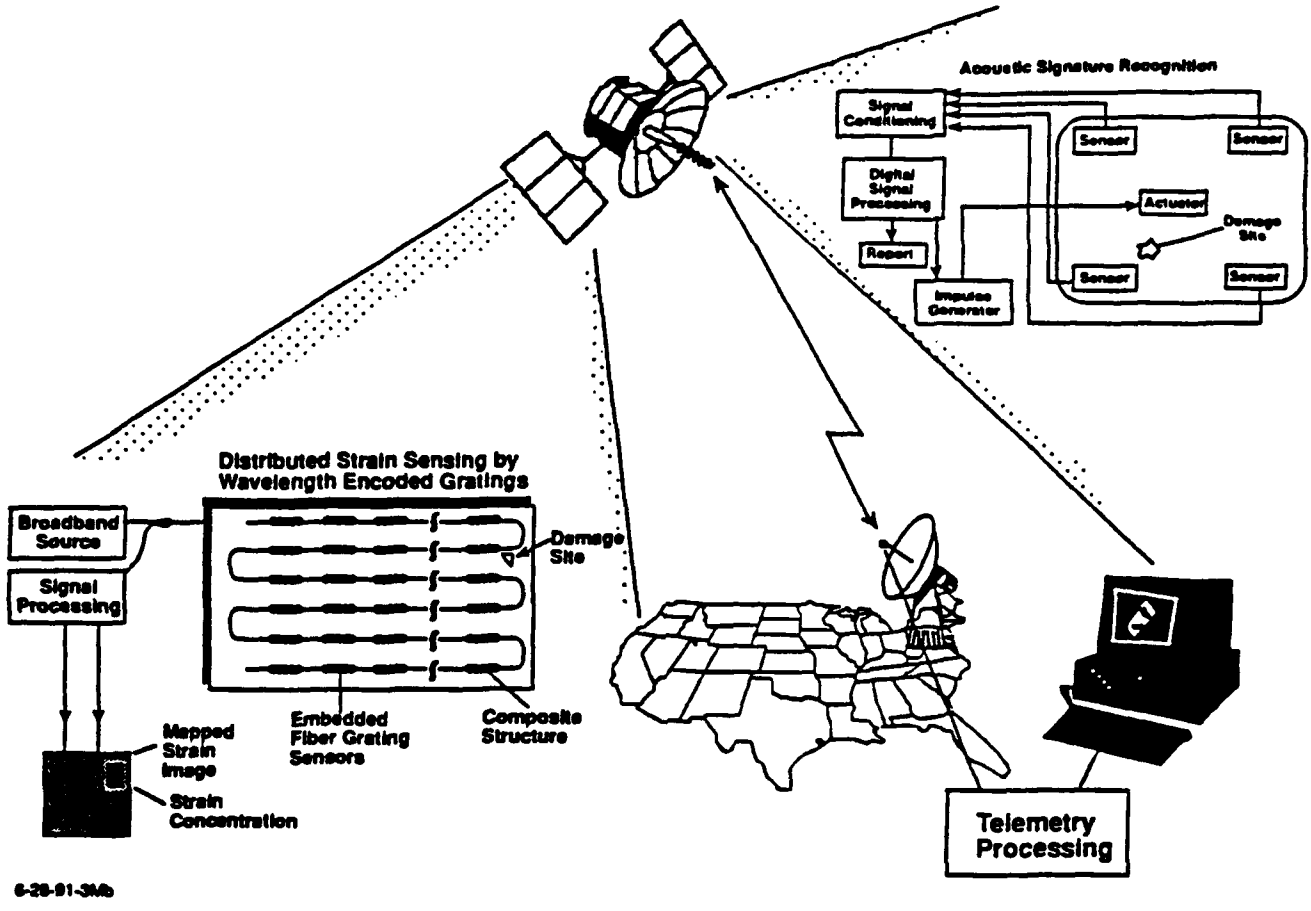

Figure 3. Micrometeorite Impact Detection and Damage Assessment

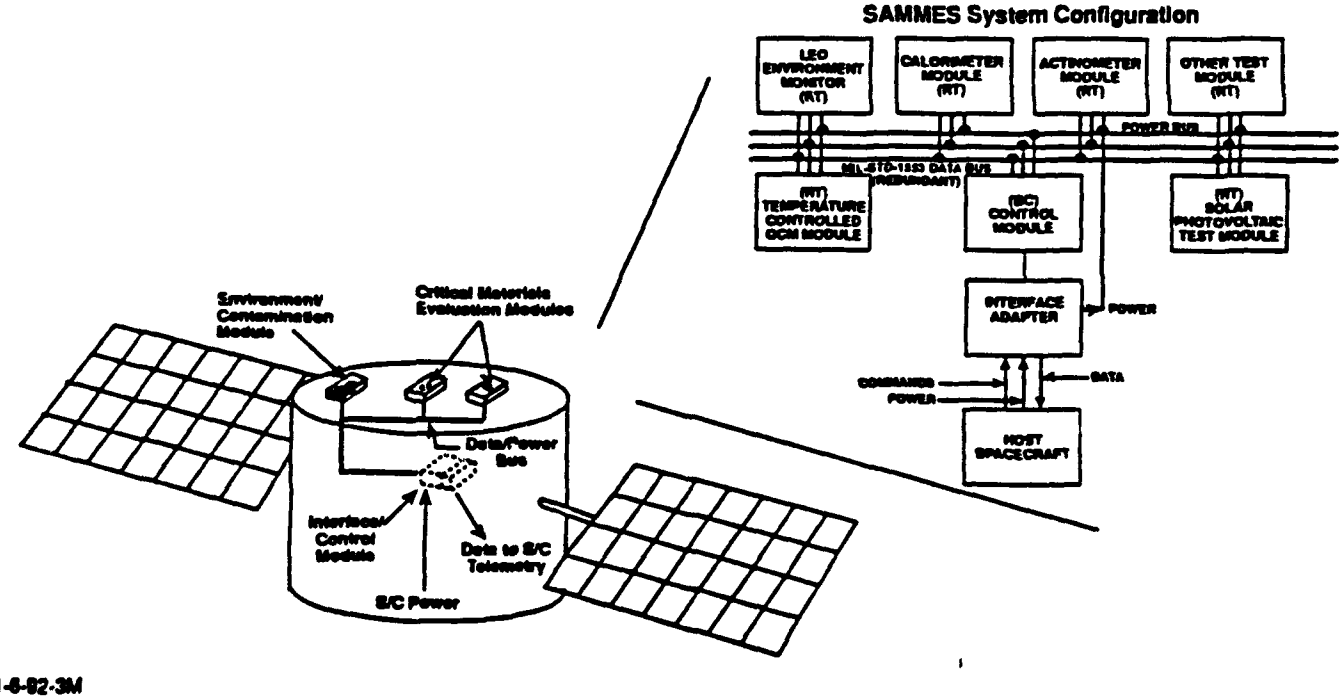

Figure 4. Schematic of Critical Materials Health and System Contamination Monitoring Concept (SAMMES)

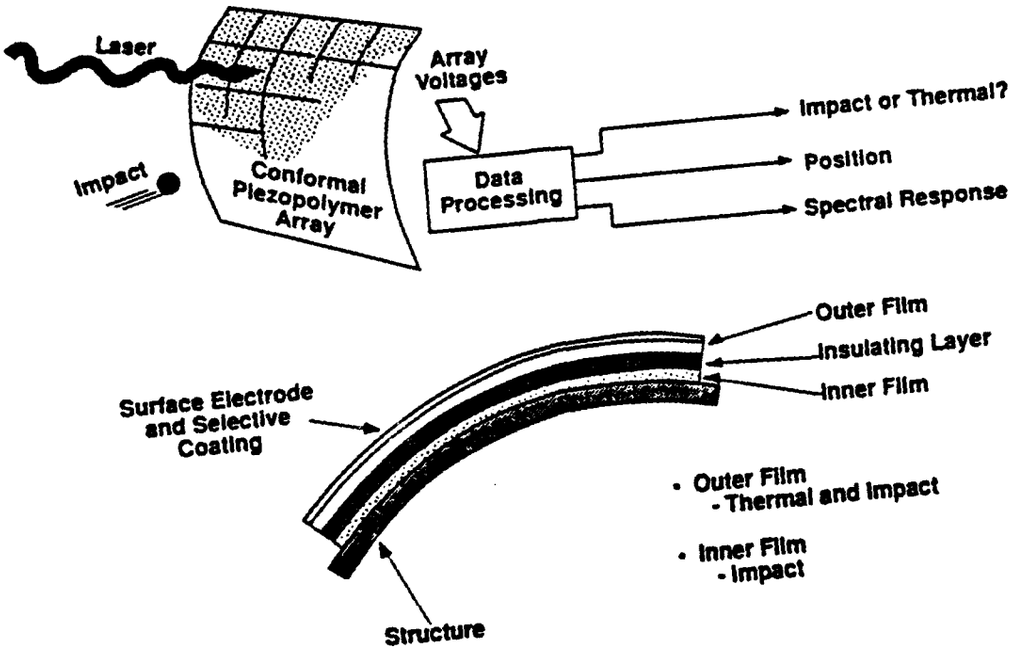

Figure 5. Schematic of Polymer Laser Sensor Skin.

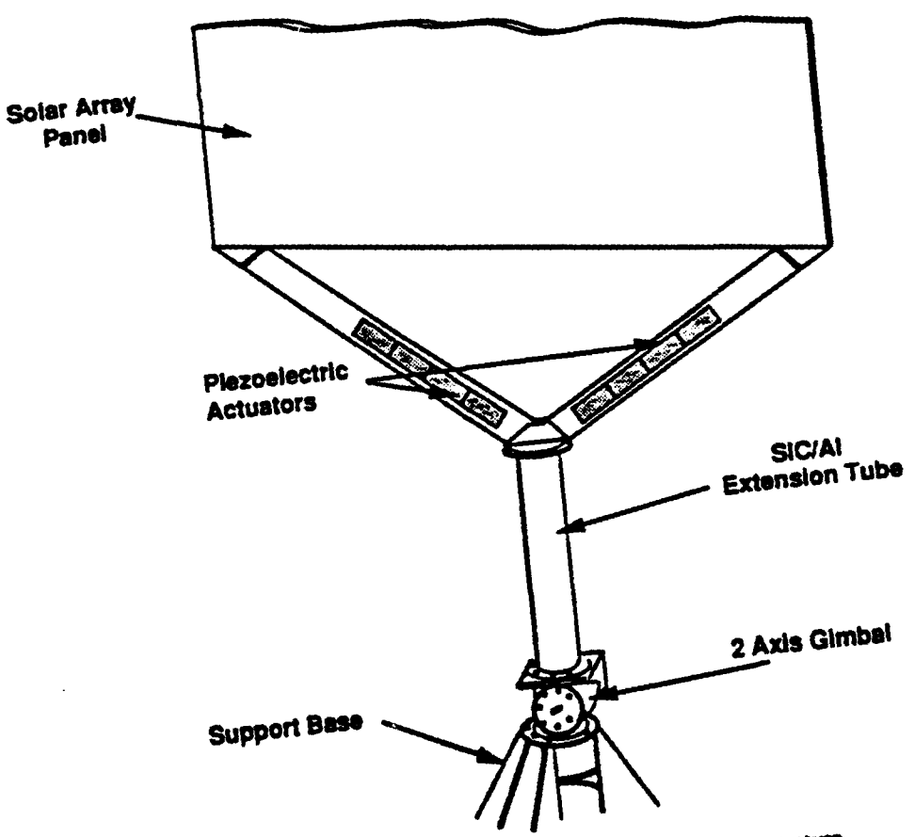

Figure 6. Schematic of AMASS Solar Array Structure

6-29-91-1M

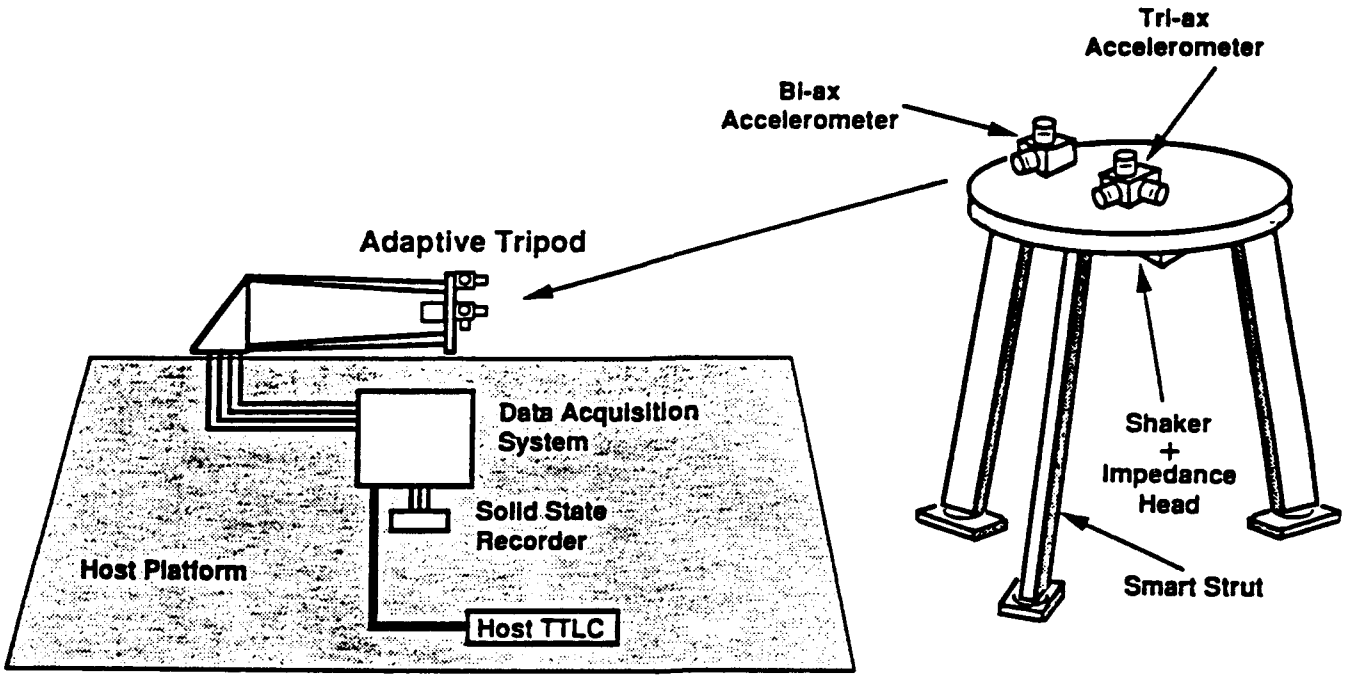

Figure 7. Schematic of Advanced Control Technology Experiment (ACTEX)

6-28-91-2M

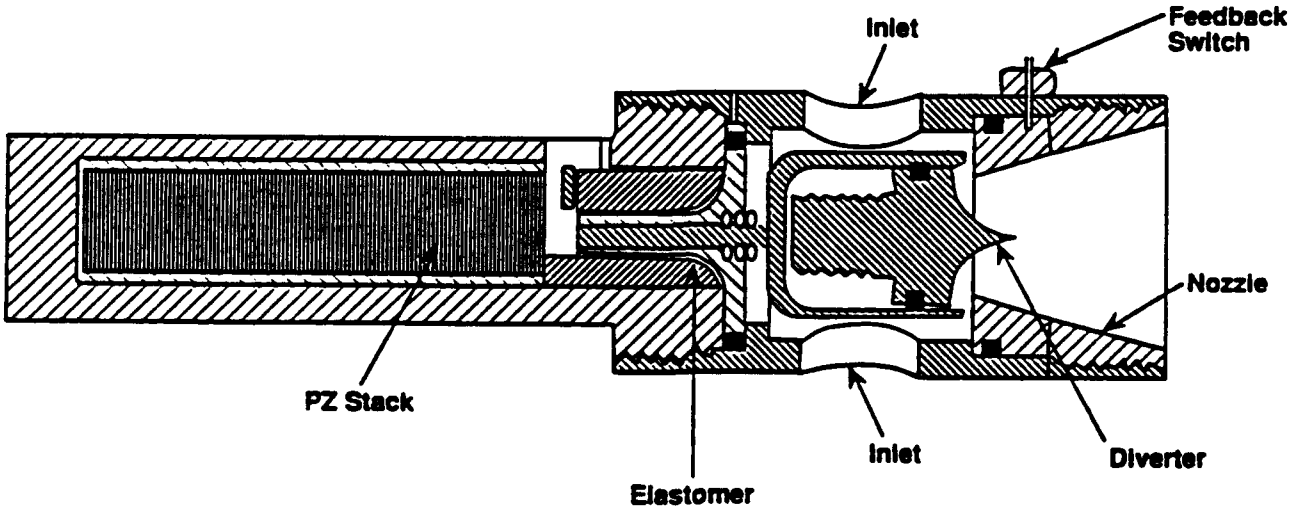

Figure 8. Schematic of Fast Acting Control Thruster.

1-6-92-5M

APPENDIX B

WORKSHOP AGENDA AND LIST OF ATTENDEES

Workshop Agenda[1]

Institute for Defense Analyses
2001 N. Beauregard Street
Rooms 121-123

7:55 am	Welcome	J.M. Sater, IDA
8:00	Introduction	Lt.Col. M. Obal, SDIO
8:10	Meeting Objectives	M. Kahn, NRL
	I. Piezoceramic Actuator Application Designers and Users	
8:15	ACESA, ACTEX Experiments	A. Bronowicki, TRW
8:30	Piezocontrol Benefits	D. Jacot, Boeing
8:45	JPL In-Line Truss Actuator Experience	B. Wada, JPL
9:00	DEW Space System Applications	J. Breakwell, Lockheed
9:15	Fast-Acting Control Thruster	R.C. Alexius, Martin Marietta
9:30	Cryocooler Vibration Isolation	R. Glaser, JPL
9:45	Application of Piezoelectric Materials to Mechanical Response Control	V. Varadan, Penn State
10:00	Break	
	II. Piezoceramic Materials/Actuator Researchers/Experts	
10:15	Practical High Strain Materials	E. Cross, Penn State
10:30	Design of Space-Qualified Actuator Materials	S. Winzer, Martin Marietta
10:45	Intrinsic Limitations of High Drive Piezoelectric Materials	G. Haertling, Clemson
11:00	Actuator Configurations	R. Newnham, Penn State
11:15	High Power Transducer Design	F. Tito, NUWC
11:30	Actuator Testing and Reliability	E. Cross, R. Newnham, Penn State
11:45	Composite Materials	M. Kahn, NRL
12:00	Lunch	

[1] Speakers, please limit the number of briefing charts for presentation to 5 or 6. Plan for a 10 minute briefing to allow 5 minutes for questions and discussion. Additional charts may be provided to attendees or used as backup and during the discussion period. You may also bring samples, etc.

III. Materials/Device Manufacturers:

1:00 pm	Bulk Powder Processing - Impacts on Reproducibility and Reliability	B. Koepke, Alliant Techsystems
1:15	Manufacturing Issues with High Performance PZT Materials	C. Near, Vernitron Piezoelectric Div.
1:30	DoD STD 1376 (A) SH Ceramics Types I, II, III, V at Cryogenic Temperatures	M. Main, EDO Corp.
1:45	Manufacturing Constraints of Co-Fired Multi-Layer Actuators	J. Galvani, AVX Ceramics
2:00	Tooling Up to Make Actuator Assemblies	L. Bowen, Materials Systems
2:15	Break	
2:30	Discussion and Closing Remarks	All

List of Attendees

Speakers:
J.M. Sater, IDA
Lt.Col. M. Obal, SDIO
A. Bronowicki, TRW
D. Jacot, Boeing
B. Wada, JPL
J. Breakwell, Lockheed
R.C. Alexius, Martin Marietta
R. Glaser, JPL
V. Varadan, Penn State
E. Cross, Penn State
S. Winzer, Martin Marietta
G. Haertling, Clemson
R. Newnham, Penn State
R. Tito, NUWC
M. Kahn, NRL
B. Koepke, Alliant Techsystems
C. Near, J. Gray, Vernitron Piezoelectric Div. of Morgan Matroc
M. Main, EDO Corp.
J. Galvani, AVX Ceramics
L. Bowen, Materials Systems

Guests:
S. Griffin, PL
W. Smith, R. Pohanka, ONR
B. Tuttle, Sandia
G. Horner, NASA-Langley

APPENDIX C

ADVANCED PIEZOELECTRIC CERAMIC ACTUATOR MATERIALS FOR SPACE APPLICATIONS

Workshop
on
Advanced Piezoelectric Ceramic Actuator Materials
for
Space Applications

Lt.Col. Michael Obal, SDIO
Dr. Manfred Kahn, NRL
Dr. Janet M. Sater, IDA

Institute for Defense Analyses
February 25, 1992

Issues

- Piezoceramic material performance limitations
  - Displacement/V
  - Fatigue life at high strains
- Distribution of properties of vendor-supplied materials
  - Capacitance
  - Surface finish
  - Dimensions
  - Compositions
  - d_{31} measurements
- Actuator applications
  - Material handling
  - Electrical connections
  - Electrical insulation
  - Post-composite fabrication actuator performance
  - Actuator/structure interface

Meeting Objectives

- Enhance communication between space-based actuator users and piezoceramic research and manufacturing communities

  Description of technical issues
  Current actuator performance specifications

- Focus and prioritize issues for near-term improvements in actuator performance

- Identify and suggest research roadmap to obtain gains in near-term improvements in actuator performance

APPENDIX D

ACESA, ACTEX AND AMASS PZT MATERIAL NEEDS

ACESA, ACTEX & AMASS
PZT Material Needs

Contributors:

Allen J. Bronowicki	**ACESA Program Manager**
Lt. Steve Griffin	**ACESA Project Officer**
Roy Schubert	**ACTEX Program Manager**

TRW Materials Engineering Department (all programs)

ACESA & AMASS Validation Test Summary

- Hysteresis in Type I is intrinsically low
  Hysteresis in Type II reduced drastically by embedding in Graphite/Epoxy
- Failure defined as irrecoverable degradation in actuation constant Ed_{31}
- Peak-peak def'n of Ed_{31} greater than tangent def'n at higher voltages.
- Tensile Strain to Failure
  Type II/Gr/Ep at 2,000 - 2,500 micro-strain
  Type I/Gr/Ep at 600 micro-strain
  Type II/Gr/Thermoplastic at 500-1000 micro-strain
- Compressive Strain to Failure above 8,000 micro-strain
- Fatigue has little effect on stiffness.
- No actuation loss in Type II/Ep below 1,500 micro-strain fatigue
  No actuation loss in Type I/Ep below 600 micro-strain fatigue
- Thermal cycling caused 10-30% drop in actuation
- Ability to track temperature dependence of vendor dielectric data excellent after embedding, fatiguing and thermal cycling.
- Dynamic transfer functions remarkably insensitive to temperature.
  - Charge Amp less temperature sensitive than Voltage Follower since it does not depend on sensor capacitance.
  - Charge Amp not sensitive to shorts in sensors at high temperature.
  - Type I less sensitive to temperature than Type II.
  - Temperature dependence of actuator/sensor feedforward Vs/Va correlates well with coupling factor K_p.

PZT Actuation Comparison

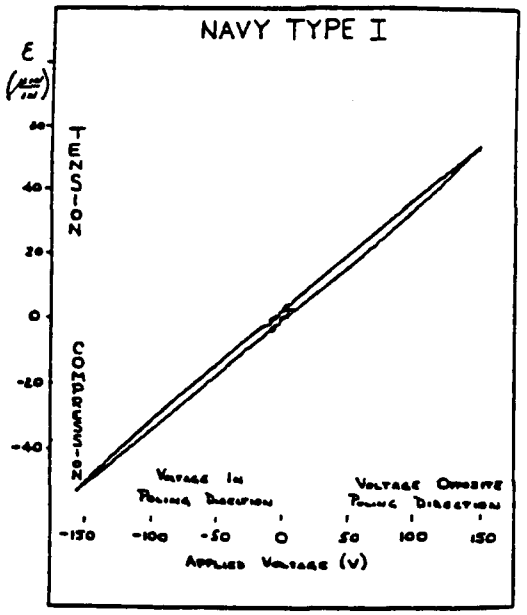

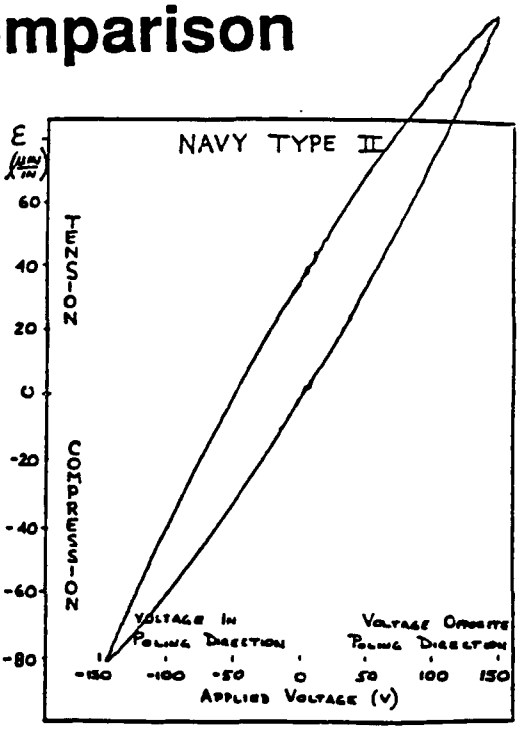

Free PZTs

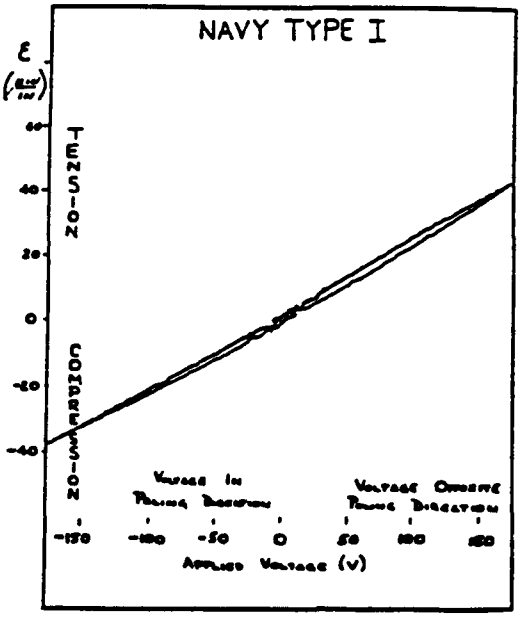

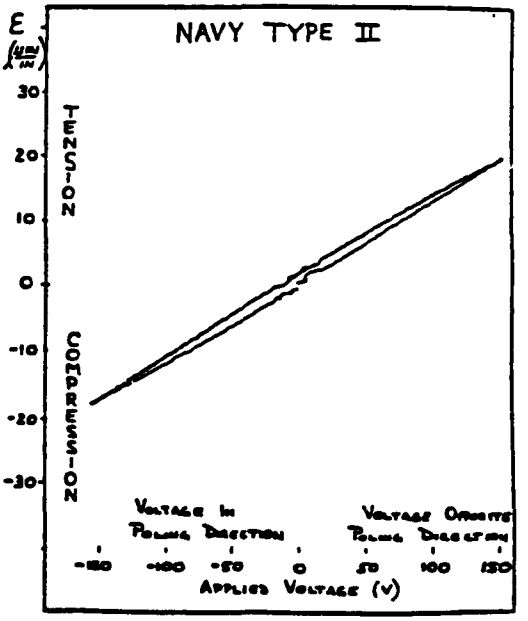

PZTs Embedded in Graphite/Epoxy

Type I has lower intrinsic hysteresis & better stiffness match to graphite.

Type II has higher free strain. Embedding decreases hysteresis.

Figures of Merit

d_{31} : Strain Coefficient (m/m)/(V/m) = m/V : $\varepsilon_1 = d_{31}\ V/t$

or Charge/Stress Coefficient (C/m2)/(N/m2) = C/N : $Q/A = d_{31}\,\sigma_1$

$Y^E_{11}\,d_{31}$: Lateral Stress Coefficient (N/m2)/(V/m) = N/V-m : $\sigma_1 = Y^E_{11}\,d_{31}\,V/t$

Indicator of ability to actuate against a stiff structure.

Y^E = Short Circuit Modulus

$S^E_{11} = 1/Y^E_{11}$

or Charge/Strain Coefficient (C/m2)/(m/m) = C/N : $Q/A = Y^E_{11}\,d_{31}\,\varepsilon_1$

Indicator of ability to sense lateral strain using a charge amplifier.

Feedforward from actuator to sensor ~ $(Y^E_{11}\,d_{31})^2$ important for active damping.
Y11d31 is roughly constant for most PZTs at 10 N/V-m. Want this flat with Temp.

k_p = Planar Coupling Coefficient : Unitless : Easily measured. Similar to Y11d31
measure of conversion efficiency between mechanical and electrical energy.

$$k_p = \sqrt{\frac{2d_{31}^2}{\varepsilon_{33}^T\left(S_{11}^E + S_{12}^E\right)}}$$

$$\frac{V_s}{V_a} \sim (Yd_{31})^2$$

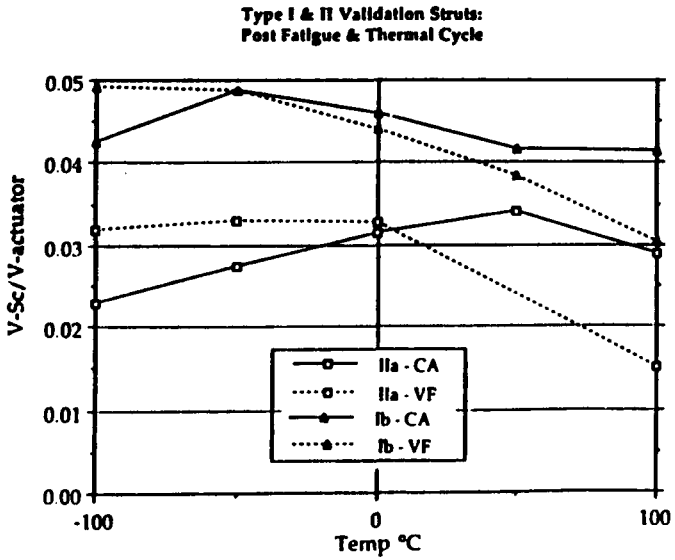

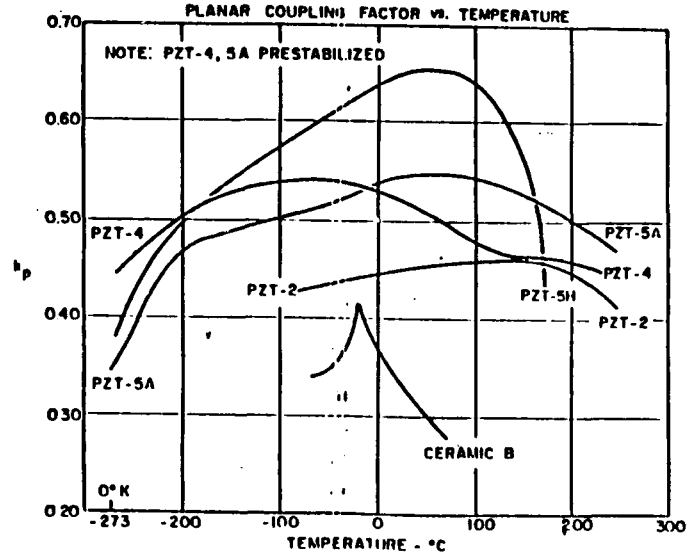

Summary of PZT Specification

1. Navy Type I (PZT4) and Type II (PZT5A) wafers .020" or thinner
2. Electrode Thickness = .0002" Nickel
3. Waviness of PZT Unacceptable; Each wafer must withstand 2 psi load on flat surface.
4. Thickness after electroding with ± 10% of nominal for each wafer
5. Length and Width controlled within ±0.020" for each wafer
6. Capacitance: Measured C of each wafer within 5% of mean for lot.
   Mean C of lot within 5% of nominal C = $K_{33}\,\varepsilon_o\,A / t$
7. Lateral Stress Output Coefficient: Used for Qualification of Material
   The larger this number the better one can actuate and sense.
   (Vernitron quotes 10 N/(V-m) for Type I and 10.4 for Type II)

   Nominal Room Temp $Y_{11}d_{31}$ <u>at least 10</u> N/(V-m)

8. Planar Coupling Coefficient: Used for Qualification of Material
   Desire Low Temperature Sensitivity in this Value to ensure Gain Margin.
   Would be nice if this number could be measured for each lot.

   Nominal R.T. K_p <u>at least 0.55</u>

   Variation of Nominal K_p <u>within ±10%</u> of R. T. value over range ±125° C.

PZT Wish List

1. Desire Thinner PZTs, multi-layer if possible.
   At 20 Volt/mil max field for Type II and 50 Volts available, only 2.5 mil PZTs are needed.

2. Desire cylindrically curved PZTs at thicknesses as above

3. If used in a d_{33} mode one could get 3 times as much actuation as in d_{31} mode.
   This requires a thin stack in the plane of the composite.

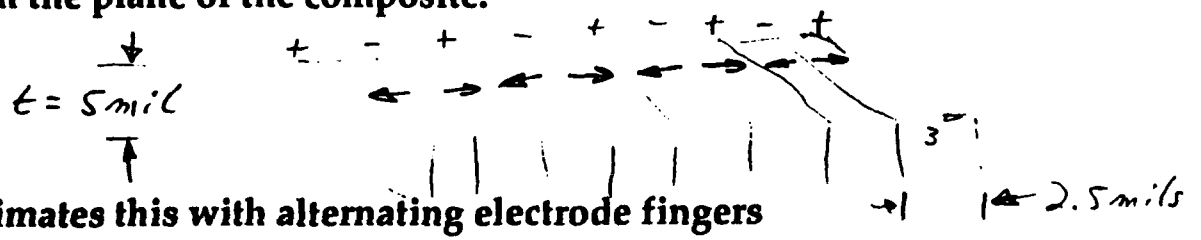

Haygood's method approximates this with alternating electrode fingers

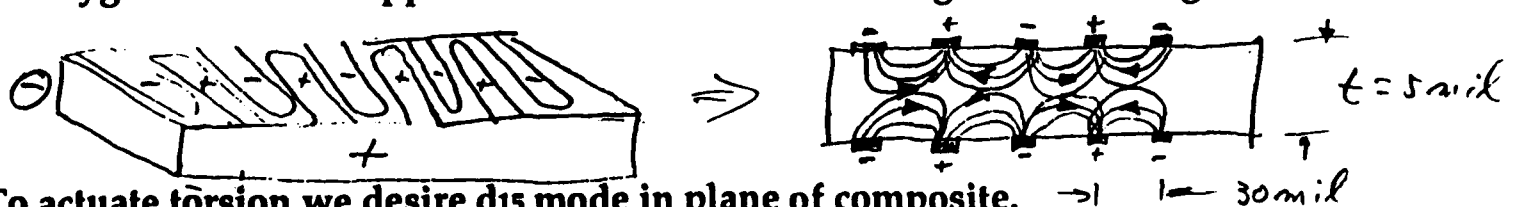

4. To actuate torsion we desire d_{15} mode in plane of composite.

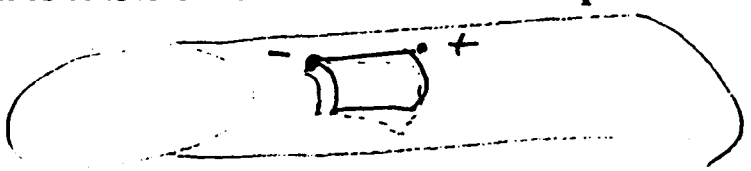

5. Numerous commercial applications open up if a material having roughly 10 times the stroke of PZTs with no loss of linearity or bandwidth. Need 1-2,000 micro-strain actuation capability. TRW ower steering hydraulic valve actuator would be one example.

Mechanical Validation of Smart Structures

Allen Bronowicki, Robert Betros & Ted Nye†
and
Lori McIntyre, Lee Miller & George Dvorsky‡

TRW Space & Defense
1 Space Park, R4/1074
Redondo Beach, California 90278
(310) 813-9124

ABSTRACT: TRW is developing smart strut technology for application to spacecraft vibration and shape control on a number of contract and internally funded research programs. Performance verification of lightweight composite structures with embedded piezoceramic sensors and actuators in the harsh spacecraft environment is a key requirement. Graphite epoxy, graphite polycyanate and graphite thermoplastic members have been fabricated with thin lead zirconate-titanate (PZT) actuator and sensor wafers embedded in the composite layup. These members have then been subjected to tension and compression loading, hundreds of cycles of fatigue loading at levels indicative of launch loads, and thermal cycling tests at temperatures found in the hard vacuum of space. Results of the testing are promising.

1. INTRODUCTION:

TRW has been performing mechanical validation testing of smart composite members under the Advanced Composites with Embedded Sensors and Actuators (ACESA) program, and the Advanced Materials for Application to Space Structures (AMASS) program, run by the AF Phillips Lab and Wright Lab respectively. The goal is to determine static limit load and fatigue allowables, and to determine the effect of temperature cycling on endurance and performance of these members.

2. STATIC ACTUATION EVALUATION:

The PZT d_{31} coefficient relates strain to field, and is a major determinant of actuation and sensing capability in actively damped composites. Two standard Navy PZT compositions, Types I and II, were evaluated. The strain limits of the encapsulated wafers in the lateral 1-direction were tested to determine the applied strain level at which point actuation losses occur.

2.1 COUPON DESCRIPTION: 7.5 mil thick PZTs were encapsulated in an insulating medium prior to embeddment in either a graphite/epoxy or a graphite/thermoplastic (Radel© - polyarylsulfone) laminate.

The graphite composite lay-up was designed to provide a modulus similar to the PZT's (10 Msi) being tested. Strain gauges were applied to the exterior of the completed coupons, and the coupon strain was recorded as a function of applied voltage. An example of one of the generated plots can be seen in Figure 1.

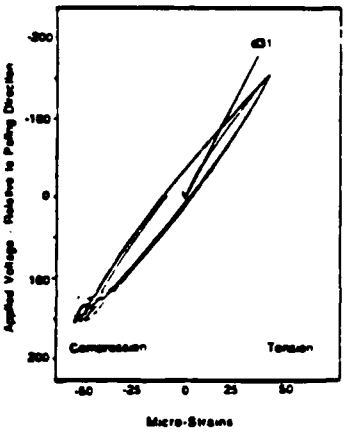

Figure 1. Initial Actuation Response of Navy Type II PZT Encapsulated in Thermoset.

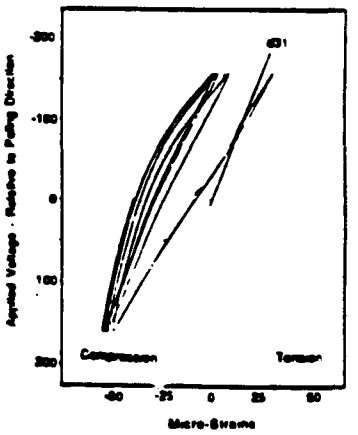

Figure 2. Actuation Response of Navy Type II PZT Encapsulated in Thermoset After 4000 μ-Strain Tensile Load Conditioning.

† Dynamics Department
‡ Materials Engineering Department

Each specimen was loaded in tension to a specified strain level. The specimens were unloaded and the actuation curves were replotted. The loading cycles were then repeated at higher strain levels until significant degradation in actuation properties were noted. The loss in actuation can be seen by comparing the initial actuation curve seen in Figure 1 to the actuation curve of the same specimen after a 4000 μ-strain applied load, shown in Figure 2.

2.2 Actuation Definition: Most piezoelectric drivers employ PZTs in the d33 mode to apply axial point loads to structures. More recent smart structure applications employ the d_{31} mode since thin wafers can apply loads in parallel to thin composite structures. The d_{31} value is determined by measuring the strain-voltage relation in the coupon and deriving the PZT coefficient using the relation:

$$\varepsilon_1 = d_{31}\,(V/t_p)\,(E_{1p}t_p) \,/\, (E_{1p}t_p + E_{1c}t_c)$$

where the subscripts p and c indicate PZT and composite properties, respectively. When the composite stiffness is significantly greater than the PZT's, the product of PZT lateral modulus (E_{1p}) and piezoelectric coefficient is more accurately determined. The material constant E_1d_{31} represents lateral stress generated per unit field, and is the best measure of ability to actuate force on a composite smart structure.

The d_{31} value presently quoted by most vendors is the initial or low voltage response of the wafer (note Reference). Actual d_{31} responses are not linear, and increase as the applied voltage increases. The value of E_1d_{31} can be computed using peak strain and voltage levels, or by using the initial tangent response. Figure 3 shows a plot of E_1d_{31} calculated using peak to peak and tangent actuation values. The bottom response curve (marked as 0) is the actuation determined using the initial/tangent actuation portion of the coupon strain vs. voltage plots. The 50, 100, and 150 Volt peak to peak actuation plots are located above the tangent curve.

2.3 Definition of Strain to Failure: Static tests were initially performed on the ACESA program and a tentative definition of failure was determined to be 600 and 1,500 μ-strains for Types I and II, respectively. These definitions were later redefined on the AMASS prgram. This data, shown in Figure 3, illustrates that the peak to peak actuation values decrease more than the tangent actuation value when stressed beyond 2500 μ-strains for Type II.

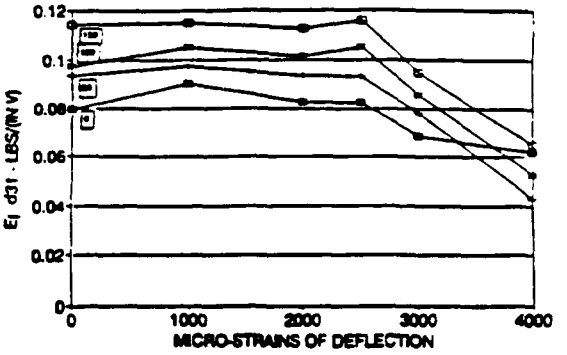

Figure 3. Computed E_1d_{31} as a Function of Applied Strain At Various Peak Voltage Levels for Navy Type II in Thermoset.

2.4 Gr/Ep vs. Gr/Tp: Prior efforts were made to encapsulate the Navy type II PZTs into graphite/PEEK composites. The high processing temperature of the PEEK thermoplastic (+700° F) depoled the PZTs resulting in a loss in actuation capability. Additional thermoplastic encapsulation studies were performed using a lower processing temperature thermoplastic (Radel at 550° F).

Figure 4 shows that the applied strain limit of the thermoplastic encapsulated Navy type II PZTs is significantly less (500 to 1000 μ-strains) than that of the graphite/epoxy encapsulated wafers. Internal thermal stresses, caused by the higher processing temperature of the graphite/Radel composite, are considered the cause of the reduced strain limit.

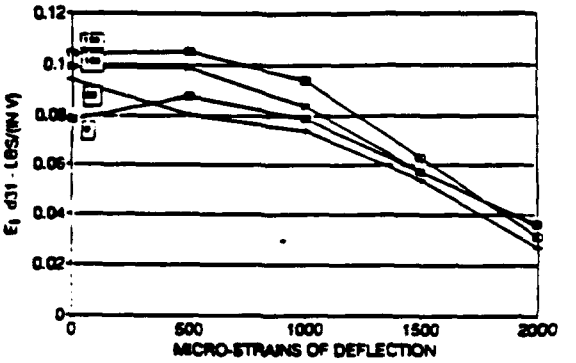

Figure 4. Computed E_1d_{31} as a Function of Applied Strain for Navy Type II in Thermoplastic.

3. DYNAMIC COUPON EVALUATION:

Following definition of static failure strains in the ACESA program, a set of four dynamic validation coupons were fabricated and subjected to fatigue and thermal cycling. The coupons were flat-sided tubes roughly 1/2 inches deep, 2 inches wide and 50 inches long. The layup had ten 0° plies and 5 sets of ±60° plies of T300 graphite epoxy. Type I actuator and sensor wafers were 10 mils thick, and Type II actuator wafers were 15 mils thick with sensors at 7.5 mils. Wafers were poled so as to actuate and sense bending motions. Actuators were 12.5 inches long and were located near the base of the cantilever beam. Sensors were 1.25 inches long. A nearly colocated sensor was located just below the actuator, and a colocated sensor was in the middle of the actuator region.

3.1 Fatigue and Thermal Cycle Testing:

Tensile fatigue loads were applied to the first two struts (I-a & II-a) at 60% of limit as defined by ACESA testing. The lack of measurable damage led to the higher loading schedule on struts I-b and II-b shown in Table 1. Schedule b) is representative of cyclic tests used for Space Shuttle fracture control. Thermal analysis indicated that passive thermal control could maintain the temperature of a strut exposed in space within the range ±100° C. Following fatigue loading, the struts were subjected to 12 temperature cycles from -100° to +100° C.

Table 1. Fatigue Loading Schedules

Type - Schedule	Load lb	Strain μ-ε	% of limit	# of cycles
I-a	1,500	360	60%	100
I-b	2,500	600	100%	10
	2,000	480	80%	50
	1,500	360	60%	800
II-a	4,200	900	60%	100
II-b	7,000	1,500	100%	10
	5,600	1,200	80%	50
	4,200	900	60%	800

It was found that the fatigue loads reduced 1st and 2nd Mode frequencies an average of 1.2% and the thermal cycling reduced frequencies an additional 0.5%. This loss in stiffness could be due to a combination of PZT and matrix cracking, fiber breakage and end fitting bond deterioration. Capacitance of actuators and sensors was found to degrade an average of 1% due to the fatigue loads, and an additional 1% due to thermal cycling.

Actuator/sensor feedforward is a measure of the actuator's ability to transfer load to the composite and of the ability of the sensor to produce a charge proportional to laminate deformation. The first three fatigue loading schedules were found to actually enhance actuator/sensor feedforward by 1-10% in all cases. Perhaps this is due to degraded stiffness of the laminate being pushed upon. Schedule II-b, which was the only one producing strains at 1,500 μ-ε, caused a deterioration of at least 12% in feedforward. Thermal cycling was found to be universally damaging to feedforward, degrading actuator/sensor transmissibility an additional 10-30% over that caused by mechanical fatigue loads.

In summary, we feel that repeated tensile mechanical loads on active graphite members is probably not a concern if strain is kept below 1,500 μ-ε, and compressive loads are of almost no concern. Repeated thermal excursions over a wide range may cause an accumulation of damage, which warrants further investigation for space structures subject to thousands of cycles over a lifetime.

3.2 Thermal Testing:

Capacitance and dynamic transfer functions between actuator and sensor were measured in a thermal chamber at the completion of the thermal cycle testing.

Capacitance of the embedded sensors and actuators was found to correlate very well with published vendor data. Figure 5 shows a plot of normalized actuator capacitance for Type I and II struts, along with normalized vendor dielectric constant data. It is apparent that embedding the PZTs does not have a significant effect on thermal variations in dielectric performance. The Type I ceramic appears to have a substantially lower temperature sensitivity, especially in the range ±50° C.

Invariance of the transfer functions over the operating temperature range is important to maintain active damping performance, and stability margins of the closed loop system. Figure 6 shows strut I'-a's nearly colocated sensor transfer function measured with a charge amplifier at the temperature extremes. The two curves are shifted vertically slightly with respect to each other, indicative of changes in feedforward gain. The second mode at +100° C shows passive damping due to softening at high temperature of the fiberglass support stand. The similarity in transfer functions

means that a suitably designed damping controller could operate without change over the temperature range. Figure 7 shows a comparison of feedforward gain from actuator to sensor for Navy Type I and II validation struts, using both voltage followers (VF) and charge amplifiers (CA). Type I appears to be slightly less temperature sensitive than Type II. The charge amplifiers give universally better performance than voltage followers. For a charge amp the sensor/actuator gain term is proportional to the material constants $(E_1 d_{31})^2$, and for a voltage follower gain is proportional to $(E_1 d_{31})^2/D$, where D is the dielectric coefficient. The non-appearance of dielectric constant in gain is believed to result in better temperature performance of the charge amp. It was also found that the charge amp was not sensitive to shorts which sometime developed on the sensors, since the charge amp removes strain-induced charge from the sensor before the short can bleed it off.

The material constant $E_1 d_{31}$ is seen to be a figure of merit for both sensing and actuation.

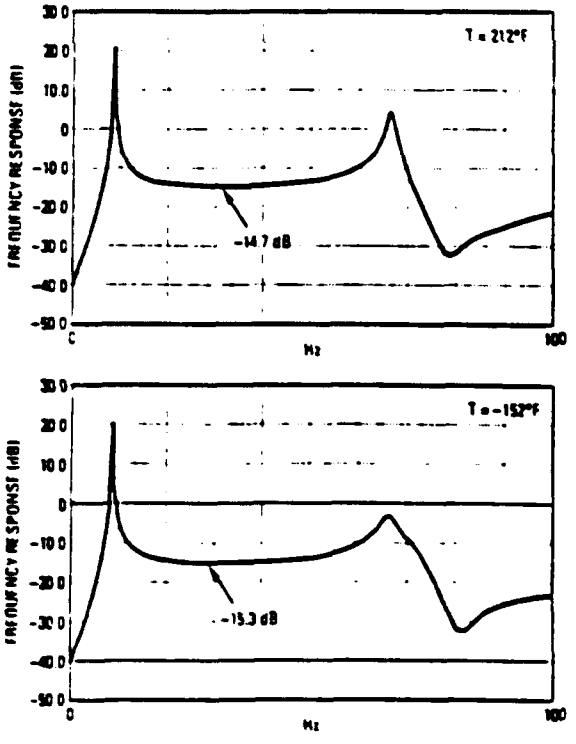

Figure 5. Nearly Colocated Sensor Transfer Functions for Strut IIa Using Charge Amp.

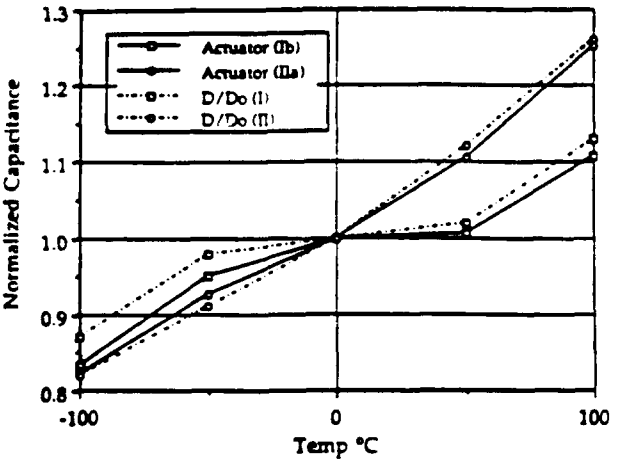

Figure 6. Variation of Actuator Capacitance for Struts I-b and II-a Compared to Vendor Dielectric Data (courtesy Vernitron).

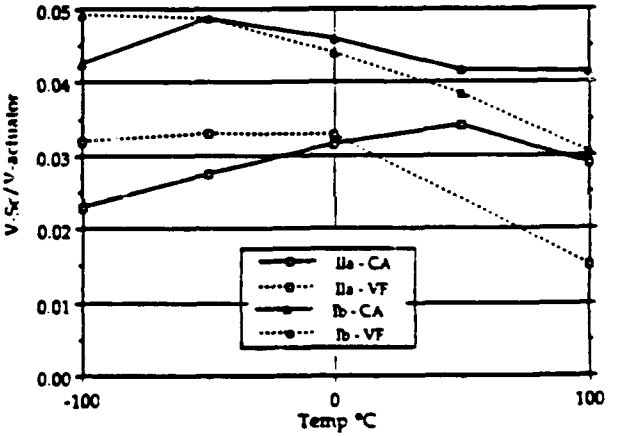

Figure 7. Variation of Feedforward from Actuator to Colocated Sensor for Struts I-b and II-a, Using Charge Amps and Voltage Followers.

REFERENCE: Berlincourt, D. "Current Developments in Piezoelectric Applications of Ferroelectronics," Ferroelectronics Vol. 10, pp 111-119, Gordon and Breach, 1976.

ACKNOWLEDGEMENT: We would like to thank the Air Force, and especially Lt. Steve Griffin, the ACESA technical monitor, and Dr. Wayne Yuen, the AMASS technical monitor, for their encouragement and helpful suggestions.

TRW

Preliminary Specification
Piezoelectric Ceramics
Type I and Type II
February, 1992

1 SCOPE

1.1 Scope

This specification establishes the requirements for thin (less than 20 mil thickness) lead zirconate titanate (PZT) piezoelectric wafers for use as actuators and sensors embedded in or bonded onto composite structures. Maximum encapsulation processing temperature is 180 C. Service temperature range is +,- 125 C.

1.2 Classification

The requirements provide for use of piezoelectric ceramic compositions specified as follows:

Navy Type I- "Hard" piezoelectric lead zirconate titanate ceramic composition

Navy Type II- "Soft" piezoelectric lead zirconate titanate ceramic composition

2 APPLICABLE DOCUMENTS

The following documents form a part of this specification to the extent specified herein. Unless otherwise indicated, the issue in effect on the date of procurement placement shall apply. Later issues of these documents may be used at the option of the supplier providing no degradation of the product ensues. Mandatory use of later documents shall be negotiated between the buyer and the supplier.

SPECIFICATIONS

TRW Space and Defense Sector

STANDARDS

Military
Mil Standard Specification of DOD Spec 1376A

Drawings

3 REQUIREMENTS

3.1 Electrode

Outer electrode composition is to be nickel deposited with a nominal thickness of 0.0002". Silver can be utilized between the

PZT substrate and the nickel coating.

Electrode placement is to be negotiated with supplier during ordering. Positive polarity is to be clearly identified on each part.

3.2 Poling and Poling Date

The positive electrode is to be marked on each wafer with a round dot or a plus "+". Poling date for each lot of material is to be indicated on the packing slip and on the packing container.

3.3 Dimensional Tolerances

3.3.1 Warpage/flatness

Waviness- Some manufacturing processes can result in a waviness or ruffled part. Unacceptable.

Flatness- A loaded flatness without cracking is acceptable. Apply weight to impart a 1-2 psi loading evenly over the surface of the PZT coupon.

3.3.2 Thickness

Thickness is to measure within +,- 10% of nominal. Thickness measurement is to be taken after electroding.

3.3.3 Length and Width

Length and width should measure within +,- .020".

3.4 Electrical Properties

3.4.1 Capacitance

Capacitance (C) is a function of thickness, surface area, and PZT composition/manufacturing process. Nominal capacitance is computed from the formula:

$$C_{nom} = K_{33}^{T} \epsilon_0 A / t$$

where K^{T}_{33} is the nominal dielectric constant, E_0 is the permittivity of free space, A is the nominal area, and t is the nominal thickness. Measured capacitance of each wafer should be within 5% of the mean for the lot. Mean capacitance of the wafers in the lot is to be within 5% of the nominal capacitance.

3.4.2 Lateral Stress Output Coefficient, $Y^{E}_{11} d_{31}$

The quantity, $Y^{E}_{11}d_{31}$, is a measure of the lateral stress output per unit applied field. This quantity, defined here as lateral stress output coefficient, is an indicator of the ability to actuate upon stiff substrate materials. The stress output coefficient is also a measure of charge generated per unit area for applied lateral strain. In this form it is an indicator of ability to sense lateral strains of a substrate material when measured by a charge amplifier.

The nominal value of the lateral stress output coefficient is to be greater than 10 Newtons per volt-meter, regardless of composition.

3.4.3 Planar Coupling Factor, K_p

The planar coupling factor, K_p, is a measure of the ability to transform electrical energy into lateral strain energy. It is strongly correlated with the lateral stress output coefficient defined in section 3.4.2 and is easily measured. The nominal value of K_p at room temperature should be 0.550 or greater, regardless of composition. Variation of nominal K_p over the temperature range +,- 125 C is to fall within +,- 10% of the room temperature value.

4 Quality Assurance

4.1 Acceptance

The supplier shall certify that each PZT shipped for acceptance conforms to the requirements of this specification and that all fabrication was accomplished in accordance with procedures, inspections, and other controls found acceptable at the time of qualification. Records of inspections, tests and other controls shall be available for examination by TRW for a period of one year.

4.2 Responsibility for Acceptance Testing

The supplier shall be responsible for the performance of all acceptance tests and inspections, and in process inspections specified herein.

4.3 Test Methods

Test method and sample size should be clearly identified.

5 PREPARATION FOR DELIVERY

5.1 Packaging

PZT ceramics are fragile and should be packaged in a manner that does not load the ceramic during shipment.

Each container is to be marked with the poling date of the

PZT ceramic along with its brand identification.

5.2 Marking

5.2.1 Individual

The positive pole of each PZT coupon is to be clearly marked with water-proof ink.

5.2.2 Shipping Items

Each shipping container shall be permanently and legibly marked with the following information which shall be visible without opening the container:

Part Number/Size
Material identification
Per this Specification Number
Type designation
Quantity
Electrode Material
Poling Date
Purchase Order Number
Manufacturer

Boeing
Defense &
Space Group
Engineering

Boeing Smart Structures

Dean Jacot
206-773-8629

* Smart Structures Involvement
* Contractual Studies
* IR&D Efforts
* Summary

Boeing
Defense &
Space Group
Engineering

Boeing Smart Structures Involvement

Flight

1987	1988	1989	1990	1991	1992

Fiber-optic sensors - IR&D

GREP beam - NiTinol damping - IR&D

Piezo embedding

Aluminum beam, piezo damping - IR&D

ACESA = Advanced Composites with Embedded Sensors and Actuators

ACESA Phase 1 contract

Piezo embedding
Truss damping - IR&D

Attached piezo/piezo - IR&D

Ongoing - IR&D

Space

Aircraft

Health monitoring - fiber-optic emphasis

.050.1 jacot 18feb92 sam

ACESA - Smart Structure Benefits

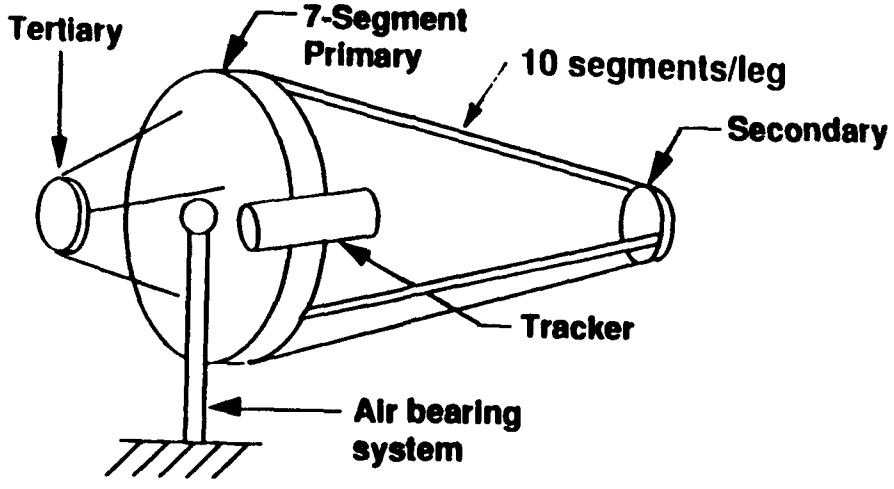

- ASTREX models 3-mirror-wide field of view optical system
- Optical beam control system does vernier pointing and jitter control

Simulated ASTREX doing 1-second RCS slew

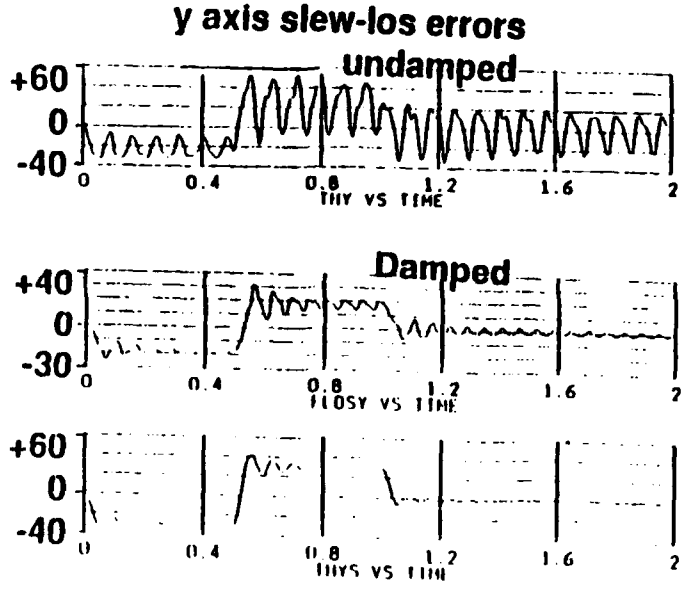

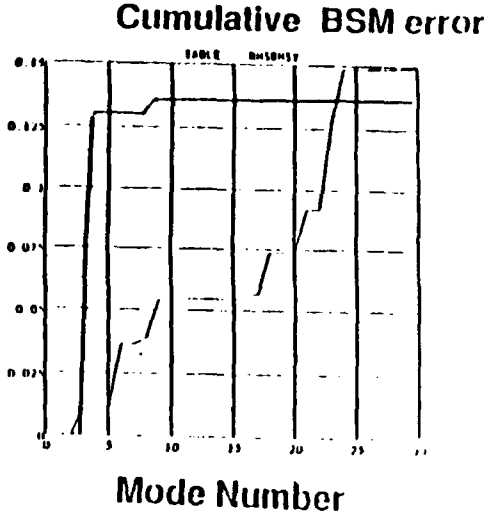

.051.3 jacot 20feb92 sam

Boeing ACESA Studies

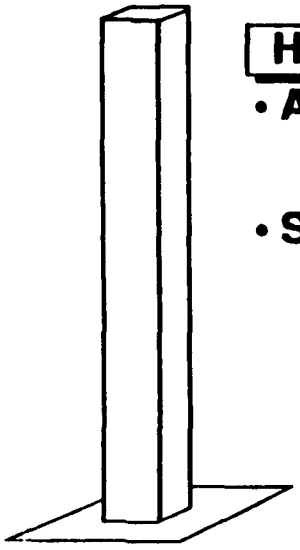

High-frequency beam

- Actuation
  - Piezo
    - (G1195 - embedded)
- Sensing
  - NiTinol
    - (attached/embedded)
  - Fiber Optic
    - (attached/embedded)

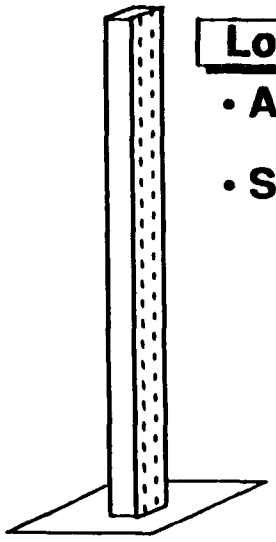

Low-frequency beam

- Actuation
  - NiTinol
- Sensing
  - NiTinol

Studied

- Embedding materials - Gr/Ep, Gr/BMI, Gr/PI/ Gr/PEEK/ Gr/PPs, MMC
- Sensors - Piezo, Fiber Optic, NiTinol , capacitive, acoustic, strain gauges
- Actuators - Piezo, NiTinol , electrostrictive, magnetostrictive
- Embedding techniques - Fabrication plan, process requirements

Proposed Phase 2

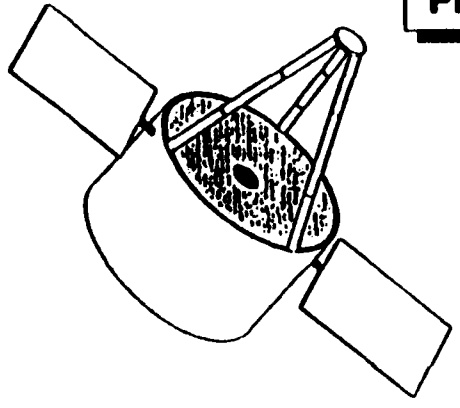

- High frequency
  - Piezo/Fiber Optic
  - (damping and shape)
- Low frequency
  - NiTinol/Fiber Optic
  - (damping and shape)

051.2 jacot 20feb92 sam

Dynamic Anomoly
Attached Smart Structures - 2

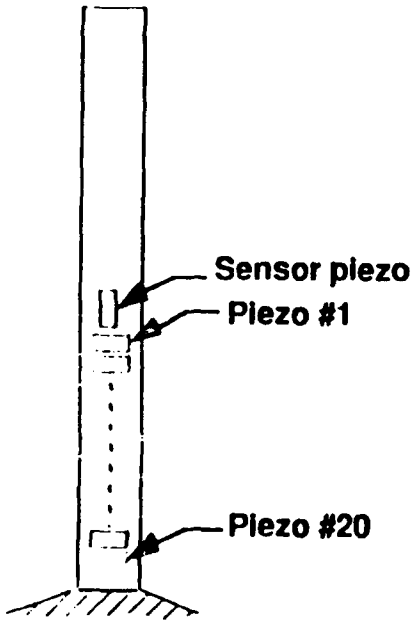

Theoretical response

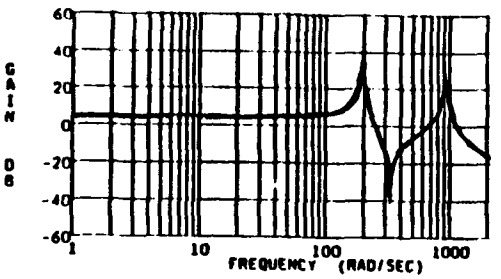

Actual response

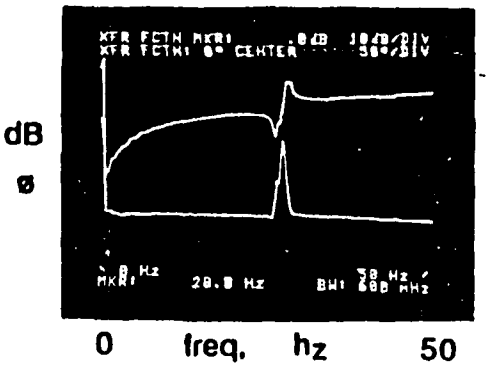

Sensing top piezo

- **Pursued several explanations**
  - **EMI, ground path, torsion, beam cross-coupling, defective piezos**
- **Finally deduced local deformation of tube wall**
  - **Phenomena destroys utility of collocated sensor**

- Did tests
  - sensing top piezo
  - actuating single piezo

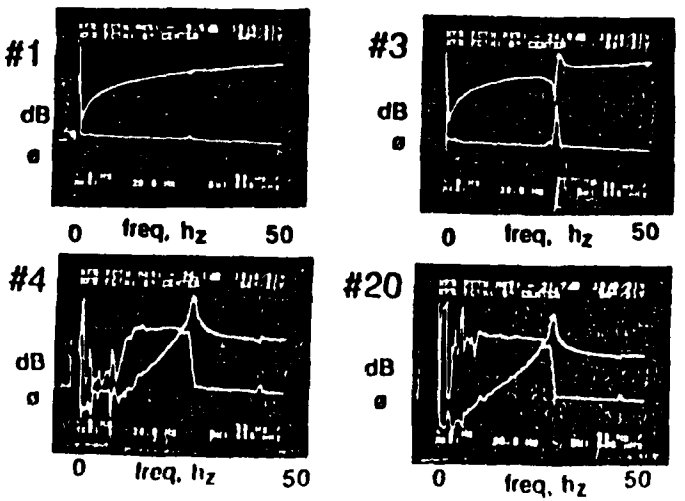

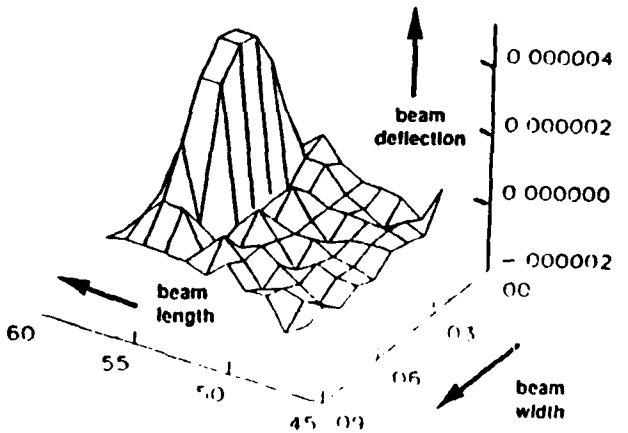

Skin Strain Phenomena

Attached Smart Structures - 1

Piezo sensing/piezo actuation

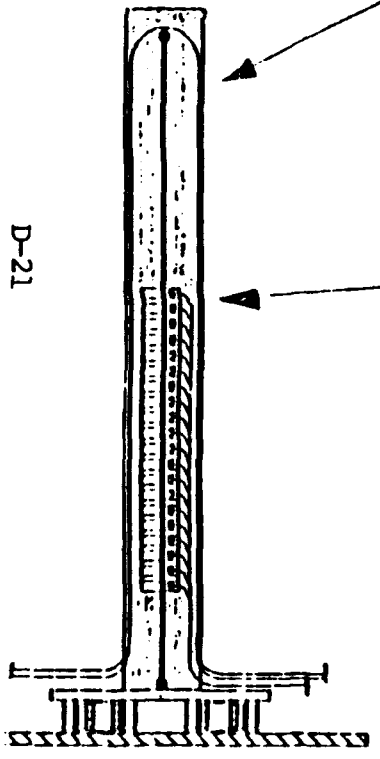

6061 Al beam

57" length, 3" x 3"
0.125 wall thickness

G1195 Piezoelectric
20 on each side
- 0.6" x 1.55" piezos
- 0.01" thick
- .25" gap

Undamped

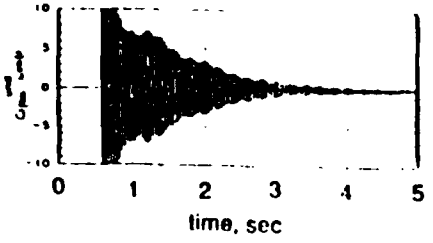

- Experimentally selected piezo phase
  - Damp first mode
  - Top piezo sensing
  - Required positive rate feedback

Actively Damped

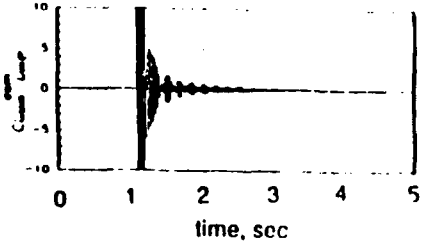

Unfiltered input & response

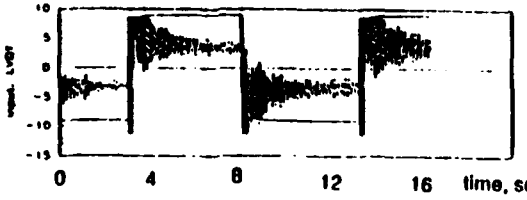

Filtered input & response

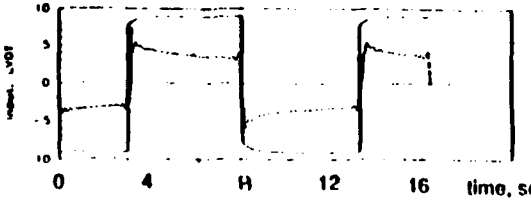

- Presently think relaxation is due to Epoxy adhesive
  - viscosity effect if inadequately cured
  - shows less beam deflection per volt than expected

.051.4 jacot 18feb92 sam

Piezo Material Experience

- Boeing has mostly used 10 mil G1195 piezoceramic material
  - Considerable effort on how to embed
- Demonstrated system advantages in:
  - Active damping
  - Vibration isolation
  - Shape control
- Potential materials research topics
  - Attachment adhesives/piezo interface
  - Piezo load capability - match to composite structure
  - Piezo fatigue/micro-cracking
  - Coating of thin piezo material on Gr fibers
  - Piezo material/electronics integration

Piezo Material Experience/ Summary

- Boeing has mostly used 10 mil G1195 piezoceramic material
  - Considerable effort on how to embed
- Demonstrated system advantages in:
  - Active damping
  - Vibration isolation
  - Shape control
- Potential materials research topics
  - Attachment adhesives/piezo interface
  - Piezo load capability - match to composite structure
  - Piezo fatigue/micro-cracking
  - Coating of thin piezo material on Gr fibers
  - Piezo material/electronics integration

JPL IN-LINE ACTUATOR EXPERIENCE

BEN K WADA

JET PROPULSION LABORATORY

FEBRUARY 25, 1992

INSTITUTE FOR DEFENSE ANALYSES
ALEXANDRIA, VA

WORKSHOP ON ADVANCED PIEZOELECTRIC ACTUATOR
MATERIALS FOR SPACE APPLICATIONS

OUTLINE

- APPLICATIONS
- ACUTATOR EXPERIENCES
- OPERATIONAL REQUIREMENTS
- TECHNOLOGY REQUIREMENTS/NEEDS
- VALUE ADDED

JPL

ACTIVE-MEMBER CONCEPT

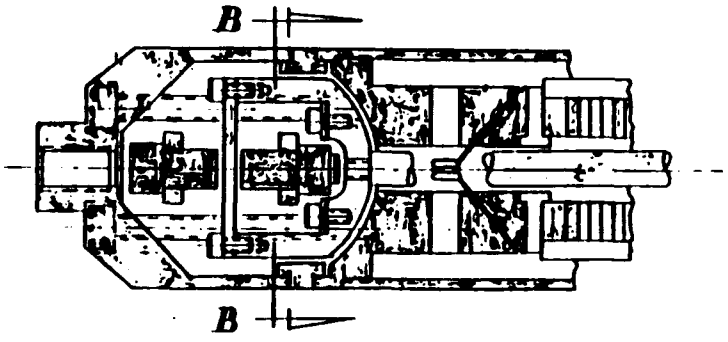

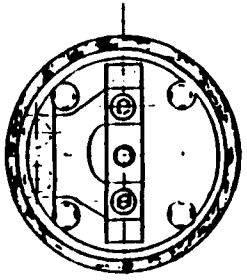

SECTION BB

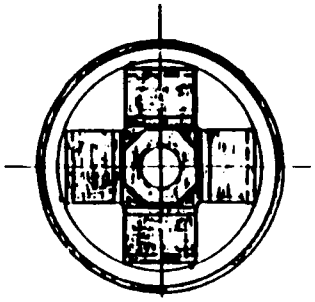

SECTION AA

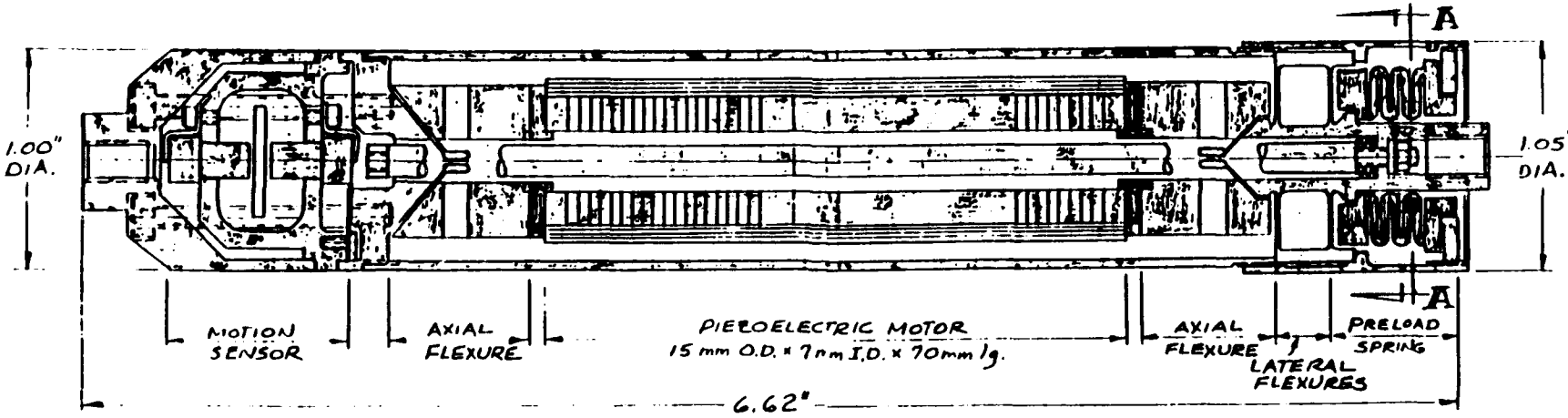

Current JPL Active Member Characteristics

Stiffness (short circuit)	14.6 N/μm (83.6 lb/mil)
Mass	240 g (0.53 lb)
Maximum Operating Voltage	1000 V
Normal Bias Voltage	500 V
Single Wafer Thickness	1.0 mm (39.4 mils)
Displacement (1 Hz)	63.4 μm (2.50 mils)
Force (1 Hz)	505 N (114 lb)
Hysteresis (1 Hz)	16.0 %
Capacitance (25 Hz)	0.6 μF
Current, rms (25 Hz)	33 mA
Power (25 Hz at Max Voltage)	3.77 W

Active Member Hysteresis

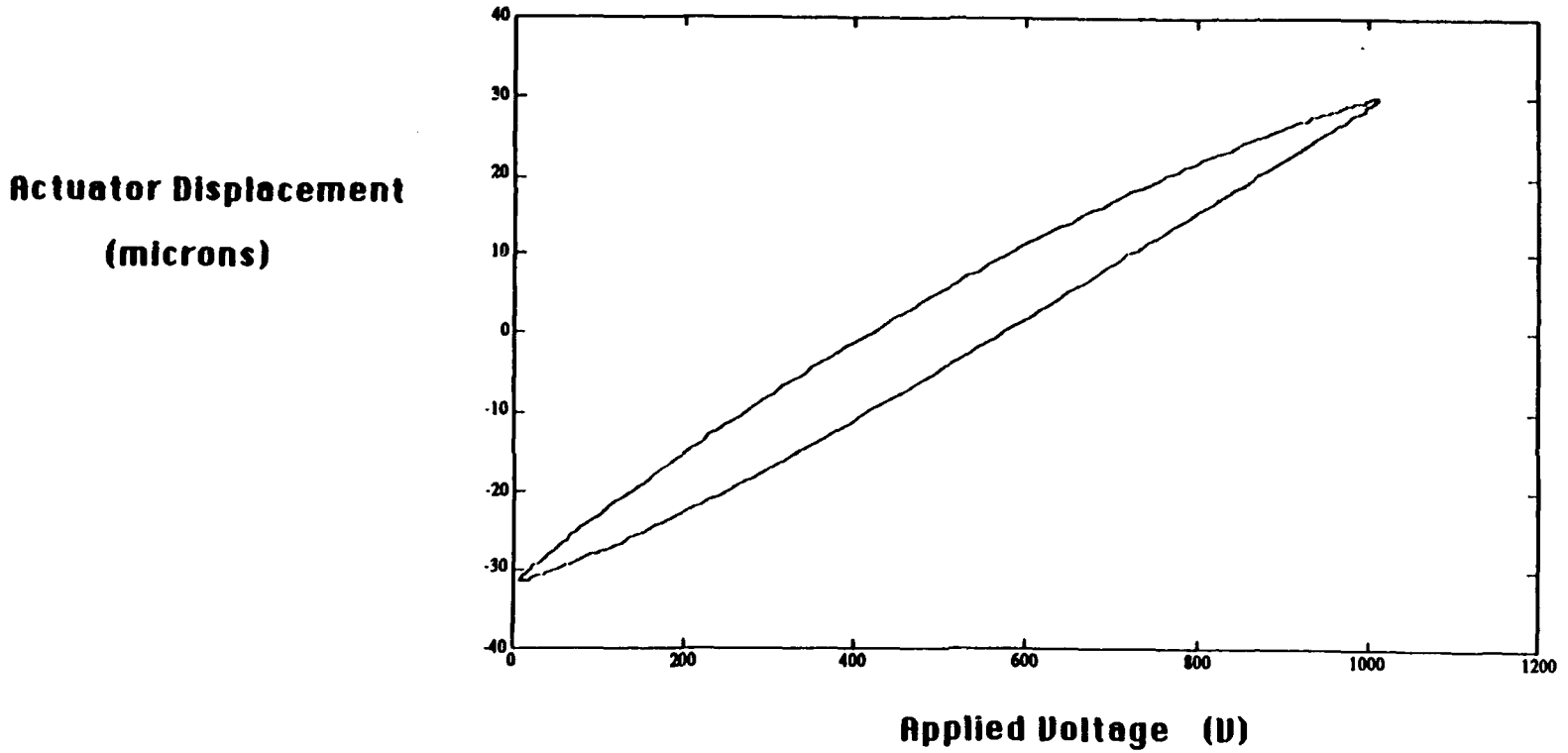

- displacement hysteresis loop width as high as 16% of the total stroke of the actuator

Architecture of Present High Voltage Piezo Motor

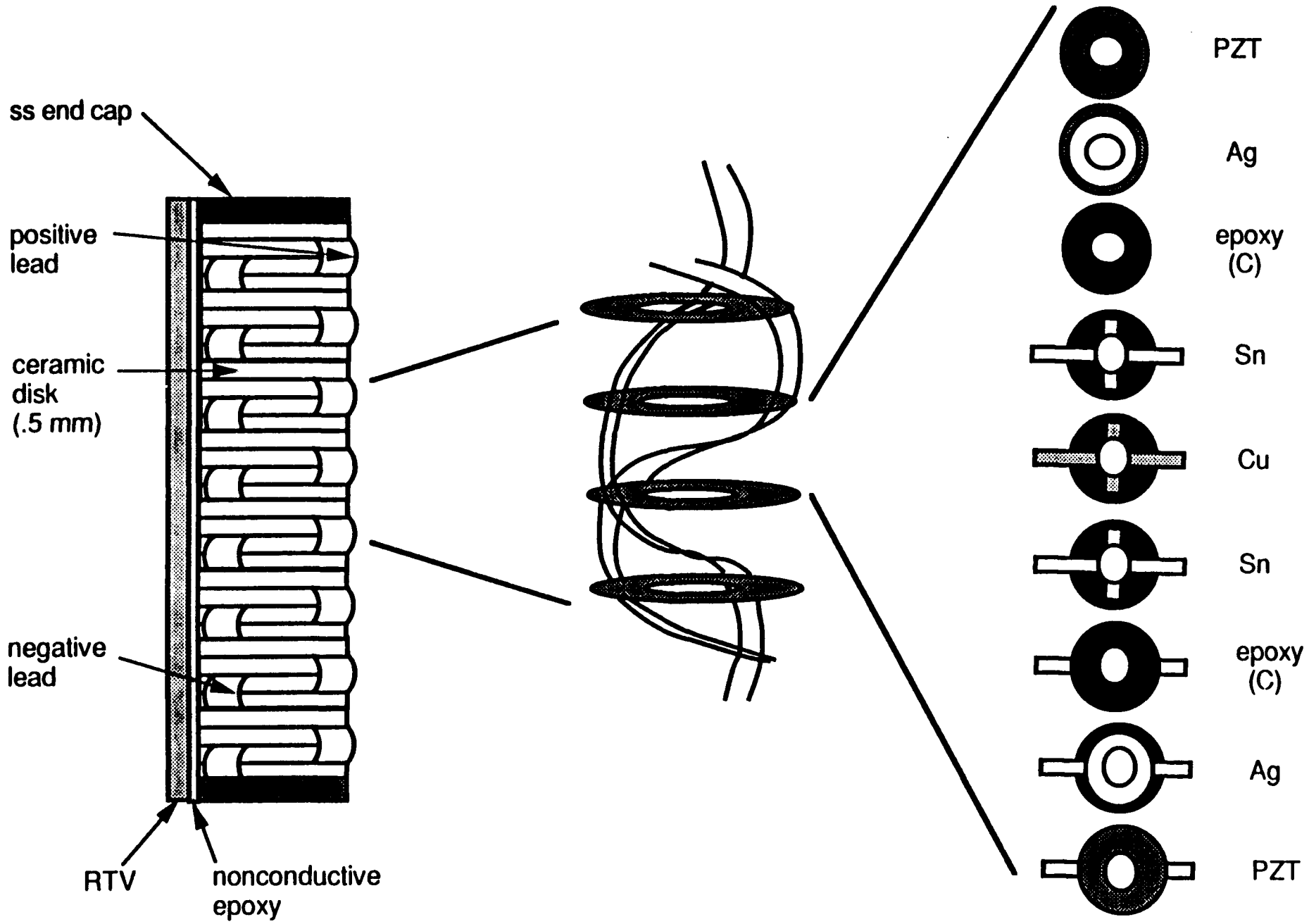

ACTUATOR FAILURE INVESTIGATION – ELECTRON-MICROGRAPHS OF PZT STACK

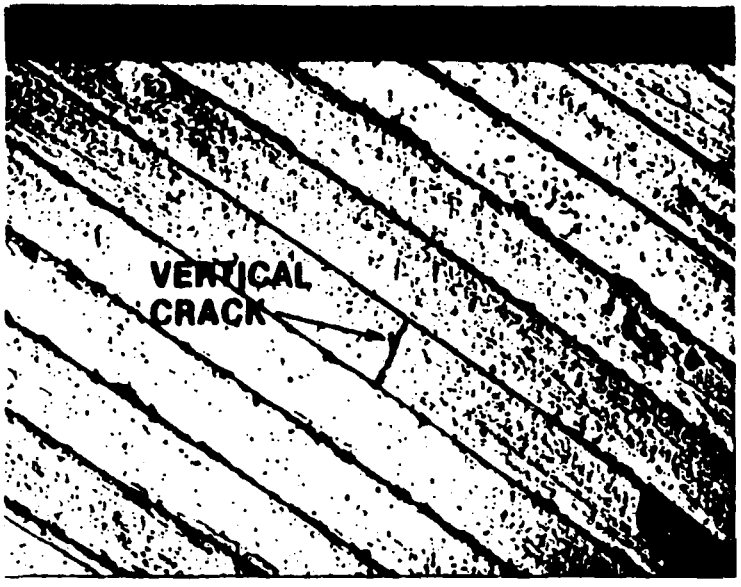

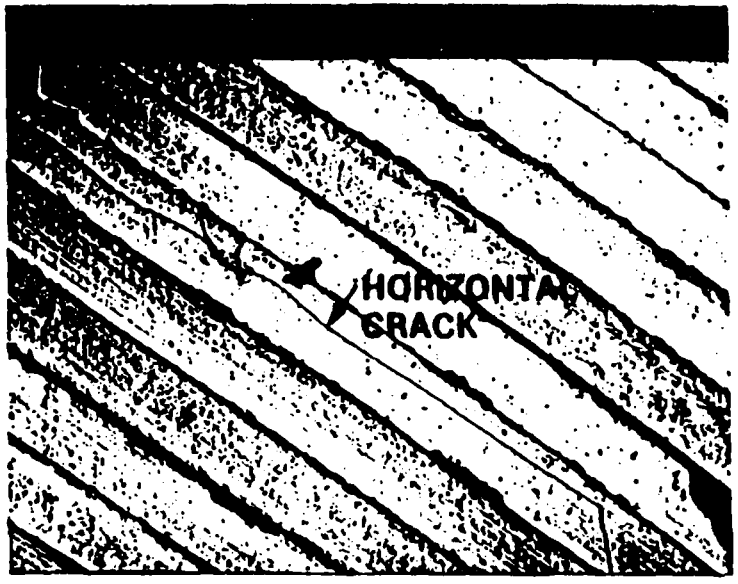

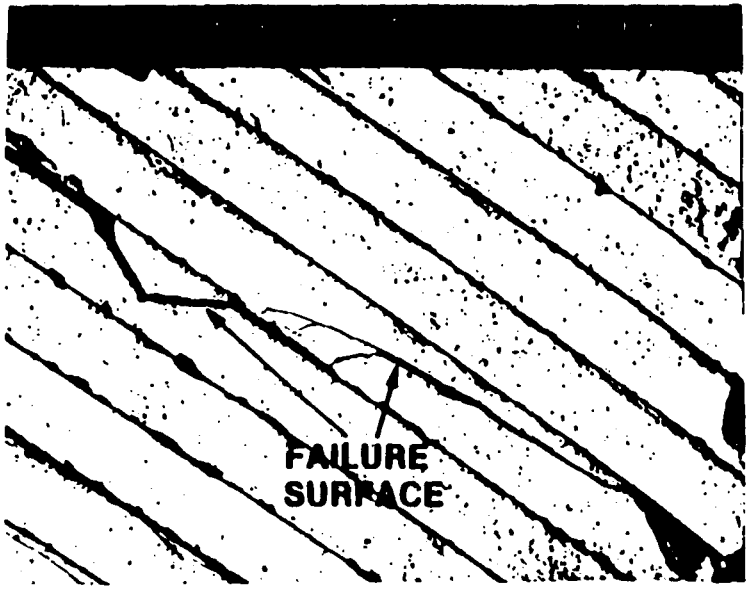

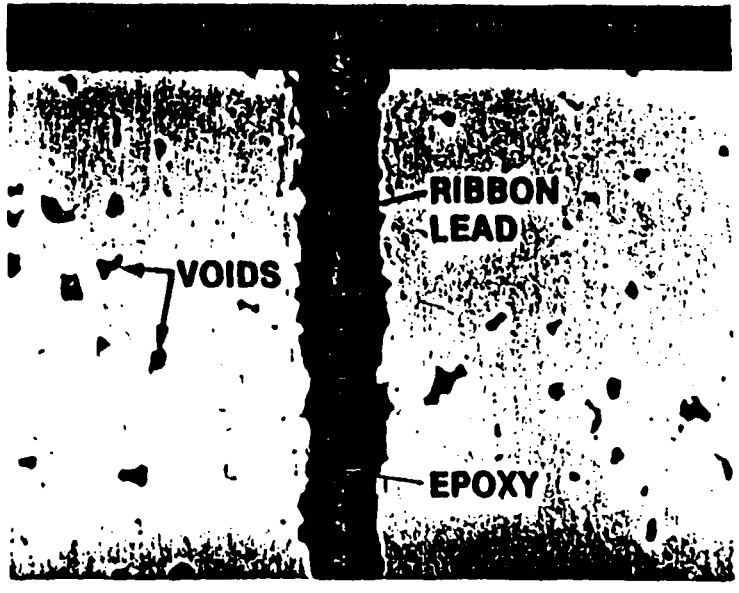

Summary of JPL Piezo Motor Failures

- Four failures - all with Kaman piezo motors and JPL custom hardware
- No failures with Kaman active struts which supposedly contain the same piezo motors
- Three failures occurred during closed loop operation, 1 during open loop operation
- Amplifiers used during failures :

failure #1 - Trek 613 (amp failed also)
failure #2 - Physik E-120/P-268
failure #3 - Trek 601
failure #4 - Trek 601

- Piezo motor from failure #1 was "repaired" by vendor
- 3 failures occurred at 500 v bias voltage and one occurred at 250 v bias voltage

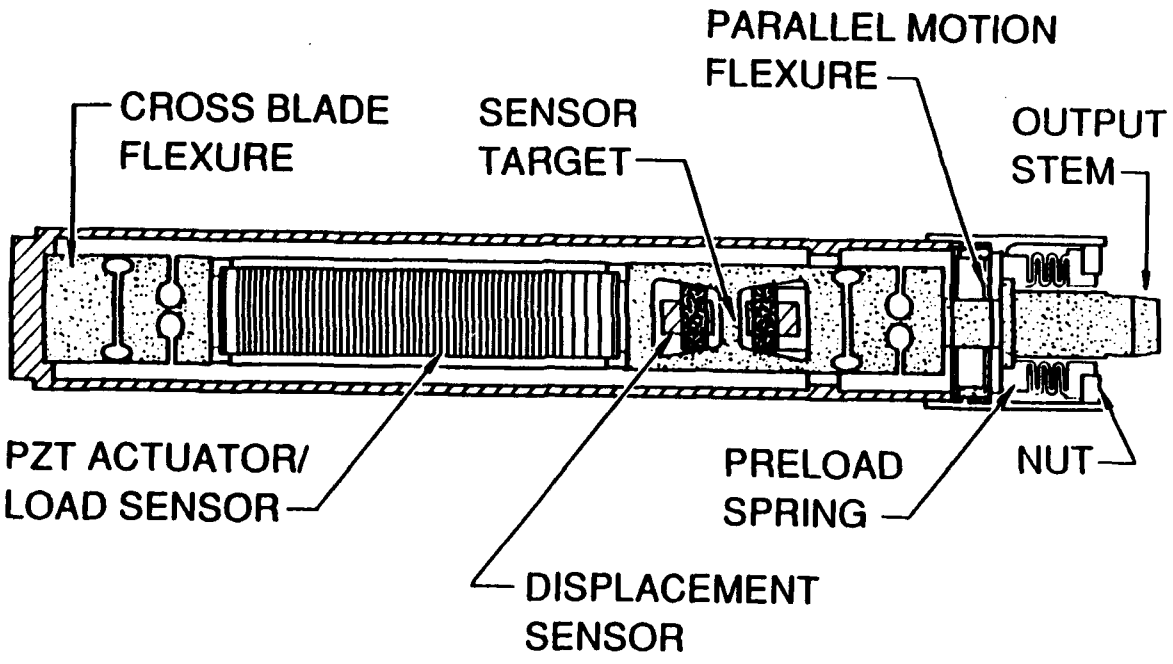

66 0.8mm thick wafers
16mm in diameter

Maximum Stroke at 150V = 45μm
Load (max) ≃ 200*

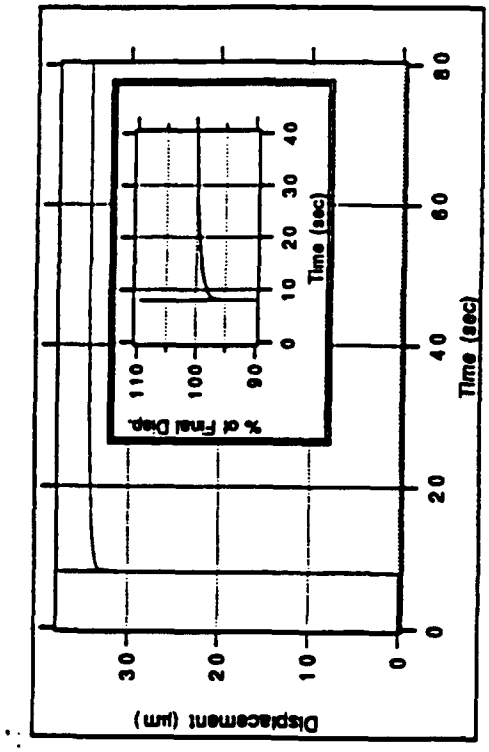
Displacement (µm)
Time (sec)
% of Final Disp.
Time (sec)

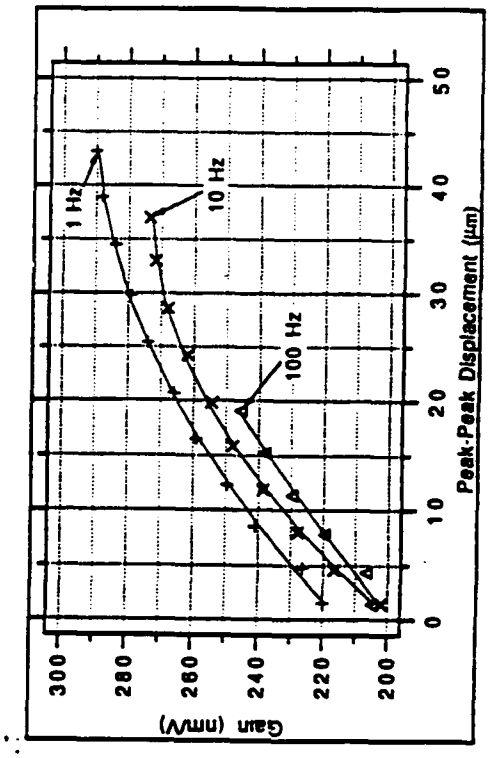
Gain (nm/V)
Peak-Peak Displacement (µm)
1 Hz
10 Hz
100 Hz

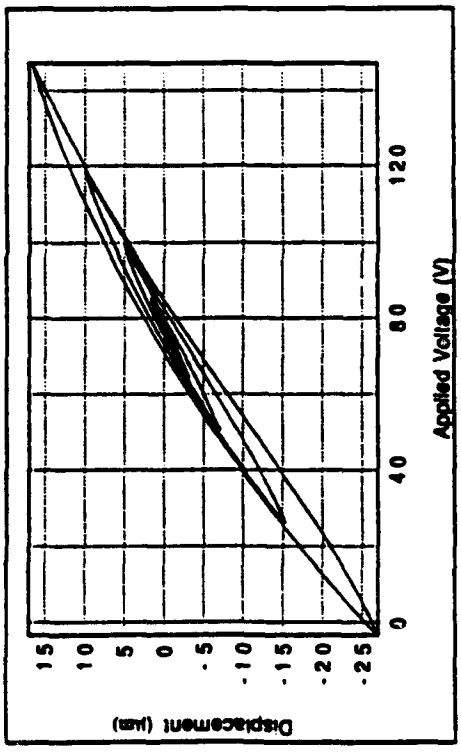
Displacement (µm)
Applied Voltage (V)

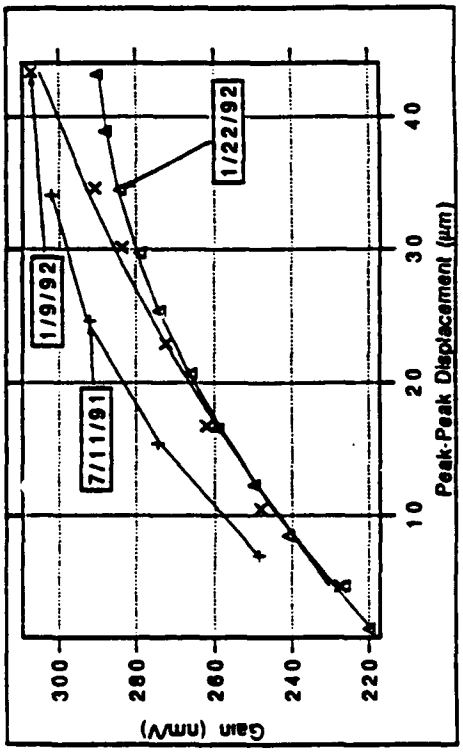
Gain (nm/V)
Peak-Peak Displacement (µm)
1/9/92
1/22/92
7/11/91

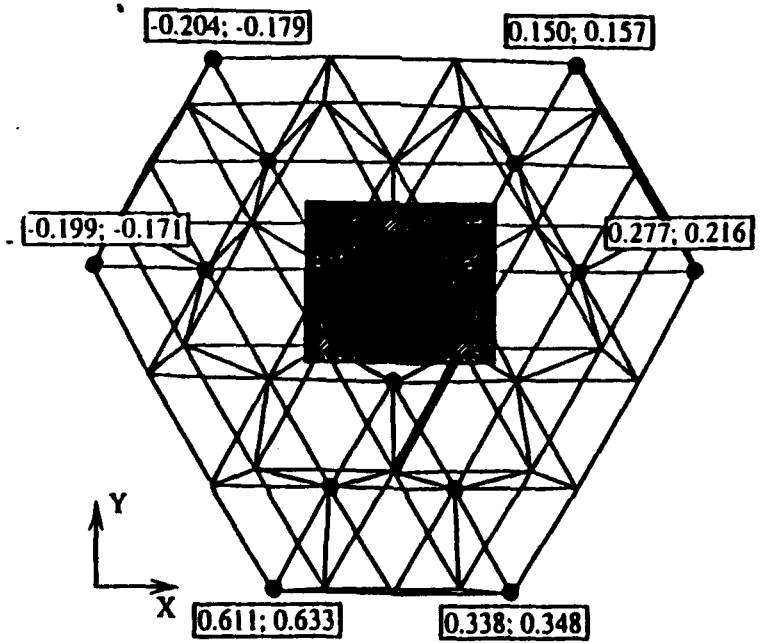

● - Support Point

● - LVDT Location

▬ - Active Member Location

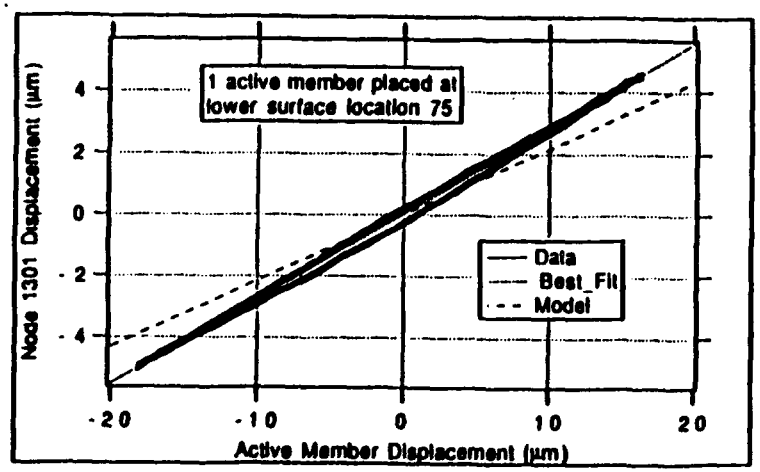

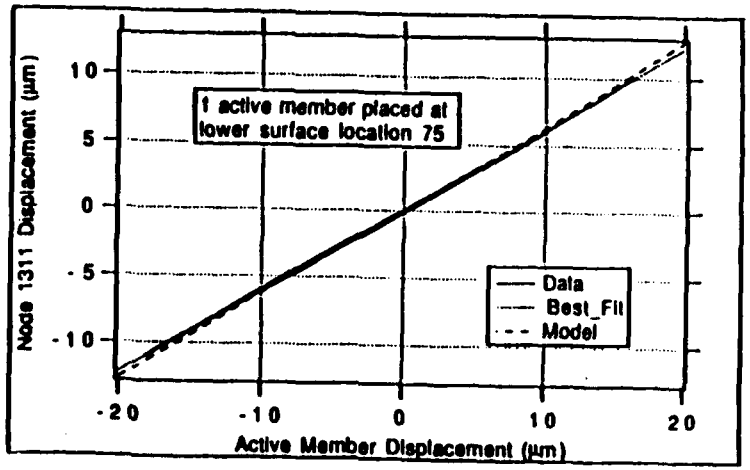

PIEZOELECTRIC STRIP ACTUATORS USED IN DEFORMABLE COMPOSITE REFLECTORS

- PIEZO ACTUATOR IS A 3" x 1/2" x .039" PZT-5H STRIP
- ACTUATORS ARE BONDED TO A SHPERICAL COMPOSITE REFLECTOR, ROC=7.6 M
- STRAIN LEVEL, 2 MICRONS PER INCH, AT 500 VOLTS
- OPERATING TEMPERATURE 200°K
- ACTUATORS EXPERENCE BOTH TENSIL AND COMPRESSIVE STRAIN

SPACE ENVIRONMENT

- SPACE AFFECTS
  - RADIATION
  - VACUUM
  - ATOMIC OXYGEN
- TEMPERATURE
- OPERATIONAL LOADS

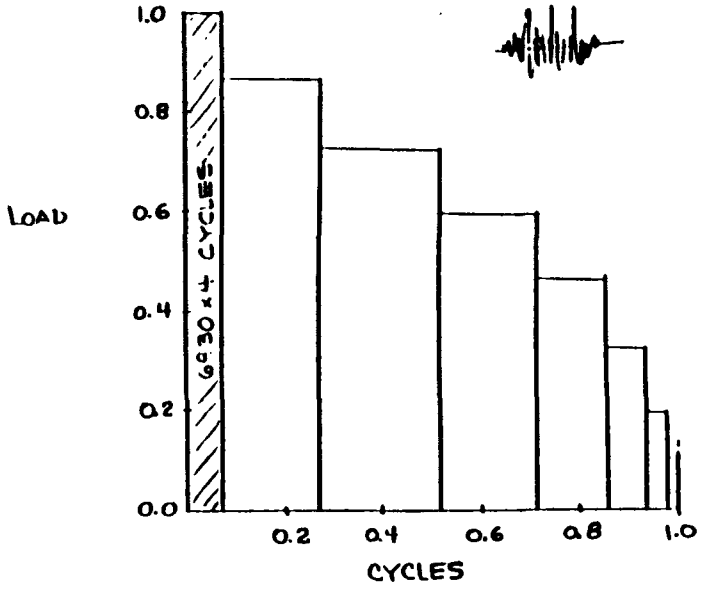

N(TOTAL) = 90,000 CYCLES x 4

RANDOM

(TEMP = 0-50°C)

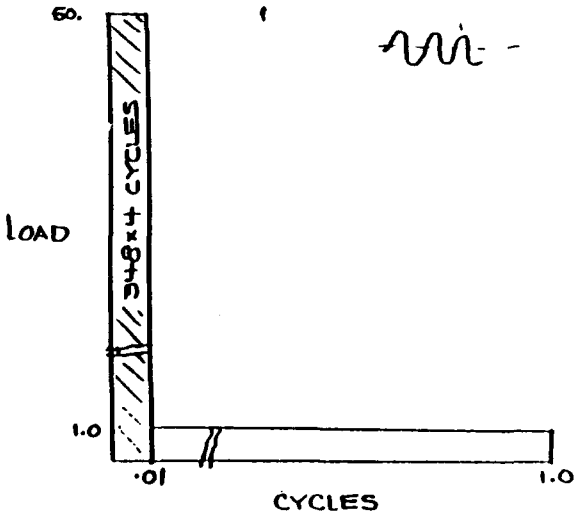

N(TOTAL) = 33,760 CYCLES x 4

SINE

(TEMP = 0-50°C)

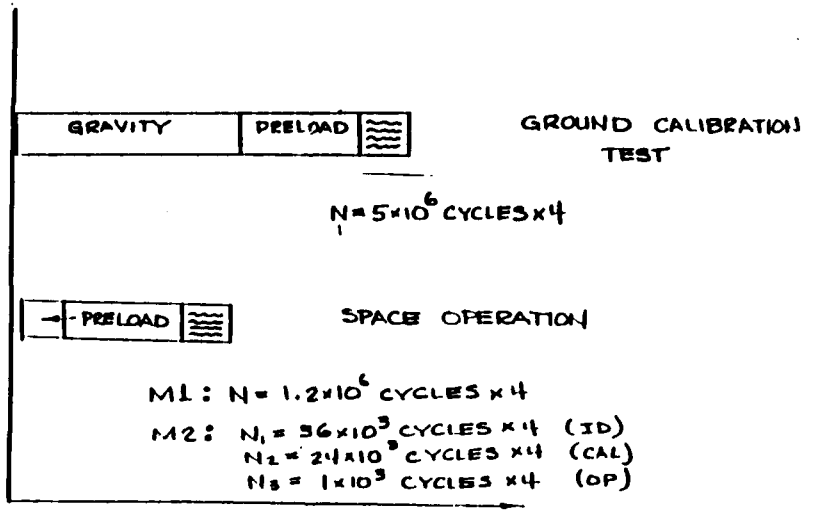

LOW LEVEL VIBRATION LEVELS

(TEMP = 100°K - 323°K)

TECHNOLOGY REQUIREMENTS/NEEDS

DYNAMIC:

- FRACTURE MECHNICS
  - NDE REQUIREMENTS/CAPABILITY
  - Kic, Kiic, Kiic, Kth
  - GEOMETRIC INSPECTION
  - RESIDUAL STRESSES
  - PREDICT GROWTH, FAILURE
- STRENGTH PROPERTIES
- PZTs FOR BROAD TEMPERATURE RANGES
  - OPERATIONAL
  - PRODUCTION (> Tc)
- FLEXIBILITY IN BENDING
- BONDS/INTERFACES
- HIGHER LOAD CAPACITY
- RELIABLE
- Low Heat Output

TECHNOLOGY REQUIREMENTS/NEEDS (CONT)

STATIC (MORE STRINGENT REQUIREMENTS):

IN ADDITION TO THE REQUIREMENTS FOR DYNAMIC LOADS,

- **CREEP, STABILITY, FREQUENCY, HYSTERESIS, AGING, F(LOAD) FOR PZT/INTERFACES/BONDS**
- **LONGER STROKE- (45-1000 microns) OR INCHWORM WITHIN 1.0" dia. AND 3"-6" LONG VOLUME**
- **SUSTAIN CHANGE IN POSITION WITHOUT POWER**
- **GREATER D13 COUPLING**

VALUE ADDED

- MEET PERFORMANCE GOALS
- LESS RELIANCE ON ANALYSIS
- RELIABILITY (ACTUATOR & SYSTEM)
- SIMPLICATION OF OVERALL SYSTEM DESIGN AND POSSIBLY GROUND VALIDATION TESTS
- COST EFFECTIVE ?

ACTIVE MEMBER VIBRATION CONTROL FOR A 4 METER PRIMARY REFLECTOR SUPPORT STRUCTURE

J. W. Umland* and G-S. Chen*
Jet Propulsion Laboratory
California Institute of Technology
Pasadena, California 91109

Abstract

The design and testing of a new low voltage piezoelectric active member with integrated load cell and displacement sensor is described. This active member is intended for micron level vibration and structural shape control of the Precision Segmented Reflector test-bed. The test-bed is an erectable 4 meter diameter backup support truss for a 2.4 meter focal length parabolic reflector. Active damping of the test-bed is then demonstrated using the newly developed active members. The control technique used is referred to as bridge feedback. With this technique the internal sensors are used in a local feedback loop to match the active member's input impedance to the structure's load impedance, which then maximizes vibrational energy dissipation. The active damping effectiveness is then evaluated from closed loop frequency responses.

1. Introduction

One major element of future space-borne astronomical installations will be a structural system with strict dimensional accuracy requirements. In the case of a diffraction limited telescope, the wavefront error will be on the order of $\lambda/10$, where λ represents the wavelength of interest. Based on this wavefront error, the surface error will be $\lambda/20$. Given a surface error budget of $\lambda/20$, approximately ninety percent of the surface error is allocated to the primary reflector. Therefore, the primary reflector's rms surface accuracy must be kept to within a fraction of the observing wavelength (e.g., 1/20 - 1/25) during the observing period. Therefore, for an infrared astronomy application, the structural accuracy requirements are on the order of a micron. Vibration arising from transient dynamic disturbances generated from on-board equipment or telescope operation is one potential source of reduced structural accuracy, and hence telescope performance.

At the Jet Propulsion Laboratory (JPL), the Precision Segmented Reflector (PSR) program has investigated an active structure approach to mechanical vibration suppression. The active structure uniqueness involves the use of structural components in which actuator, sensors and feedback control are integrated into an active member. Using this approach, previous investigations at JPL have successfully demonstrated an active damping concept for both a beam-like truss structure[1], and a more complex truss structure[2]. This technique has been shown to effectively damp structures that are truly free-free[3], as well as those that are rigidly[2] or softly attached to ground[1]. The active damping augmentation consists of maximizing vibration damping by matching the active member impedance to the structure's impedance.

The present paper extends these studies to a 4-meter diameter primary support structure of a 2.4 meter focal length parabolic segmented reflector. The objective of this work is to demonstrate active damping on this test-bed. The design and testing of an active member which utilizes a low voltage piezoelectric actuator, an integrated force sensor, and a simplified elastic deflection sensing scheme is described. Experiments are then performed to evaluate both the new active member, and the effectiveness of the control strategy. The active damping performance is evaluated by comparing the closed loop response to the open loop response. Damping performance is demonstrated using: (1) an individual active member and, (2) two active members operating simultaneously.

2. Test-bed Structure

The dynamic test-bed, shown in figure 1, is made of flight-like hardware consisting of 150 graphite/epoxy truss members and 300 erectable aluminum joints. The total weight of the structure is 86.4 kg. This structure was designed and fabricated at NASA's LaRC[4]. The geometry of this highly redundant construction is driven by the location of the nodes on the upper surface, which are determined based on the desired reflector panel locations. The nodes on the upper surface are then connected by members of the required length. The lower surface nodes are located by forming a tripod of equal length members whose base is determined by three adjacent nodes on the upper surface. The lower surface is then formed by connecting the nodes with members of suitable length. The stiffness of an individual core member is 19.5N/μm. The stiffness of the upper and lower surface members will vary according to member length. For the purposes of this investigation the structure is rigidly fixed at the three central nodes of the lower surface. A 1130 kg steel block is used as ground during testing.

---

*AIAA Member,
Dynamics Research Laboratory,
Applied Mechanics Technologies Section.

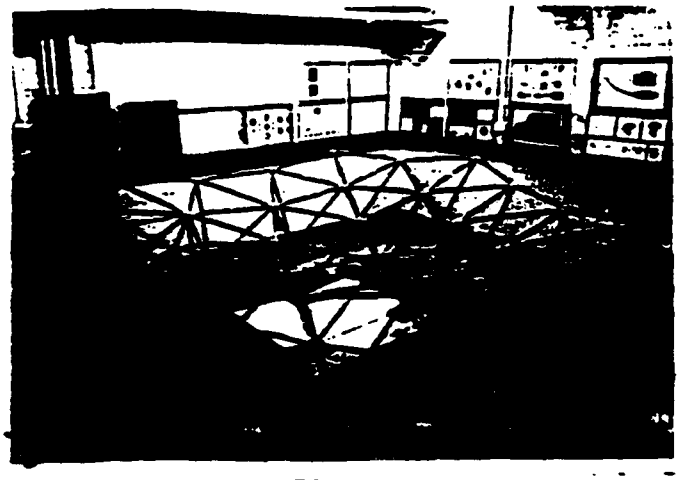

Figure 1: PSR TB structure

The structure's dynamic characteristics are detailed in table 1. Note that the first three modes can be described as a relative shearing of the upper surface with respect to the lower surface. The fourth mode is described as a breathing mode. As the aspect ratio, relating the support structure's diameter to thickness, is increased, as would be the case for the Large Deployable Reflector (LDR), these breathing modes would become more predominate. Therefore, it is desirable at the current test-bed phase of the PSR program to demonstrate an ability to control this type of mode.

Table 1: Test-bed dynamic characteristics.

Mode No.	Freq. (Hz) LaRC Data[4]	Freq. (Hz) JPL Data	Damping Ratio % JPL Data	Description
1	34.5	32.5	0.9	x Rocking and Shearing
2	35.6	33.4	0.9	y Rocking and Shearing
3	51.9	42.3	0.7	Twisting
4	57.3	56.0	1.8	Twisting and Shearing
5	78.1	75.8	3.3	1st z Breathing
6	96.6	93.4	1.1	z Saddle
7	97.3	97.6	1.5	z Saddle

3. Active Member Mechanical Design and Description

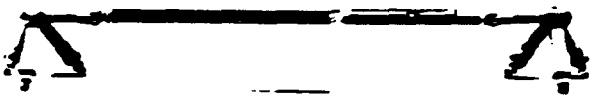

Figure 2: Erectable active damping member.

Two active members, whose major components consist of an integrated piezoelectric actuator and load sensor, a displacement sensor, and erectable joints, were fabricated, see figure 2. A detailed assembly drawing of the member is shown in figure 3. While these new active members are similar to those used in previous investigations[5,6], there are significant differences, namely: (1) a low voltage piezoelectric material is used, (2) the load sensor is integrated into the same package as the motor, and (3) the displacement sensing scheme is simplified.

The design challenge undertaken here was: to produce an active member whose performance was equal to or better than previous designs, was simpler, and placed less stringent requirements on external components. In the previous active member designs, a high voltage piezoelectric material was used. This actuator material produces a 63 micron displacement when 1000 V is applied. The ±31 micron operational dynamic range of these actuators was achieved by applying ±500V with a 500V bias voltage. Here, a low voltage piezoelectric material was chosen such that the operational range of the actuator was reduced to ±75V with a 75V bias voltage.

In both of the previous designs the piezoelectric stack was pre-loaded by a pre-load spring, such that the ceramic material never experienced a tensile stress. The more recent active member design[6], used a pre-load spring and parallel motion flexures to eliminate the 'stiction' observed in the active member[5] pre-loaded with a Belleville washer. Furthermore, crossblade flexures were incorporated into the

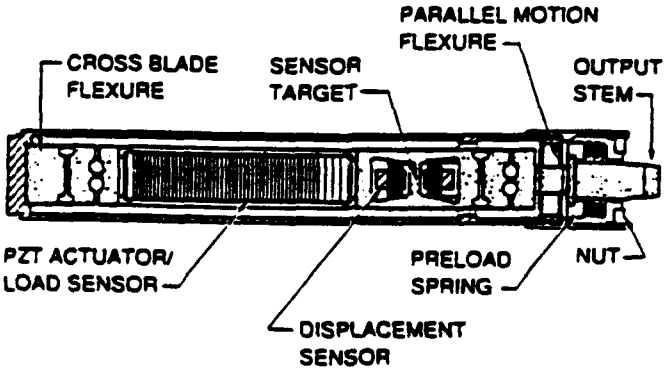

Figure 3: Assembly drawing of active member.

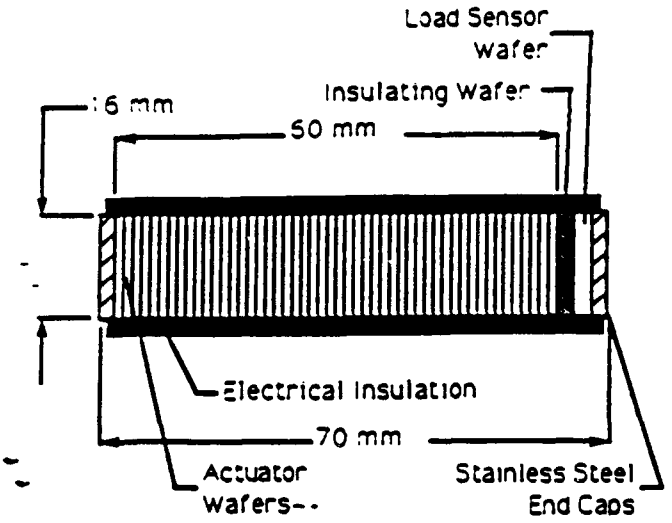

Figure 4: PZT stack drawing.

active member design[6], to isolate the actuator stack from bending moments. The flexure and preload spring design of the JPL active member[6] is also incorporated into this design.

The design of the piezoelectric stack is shown in detail in figure 4. The actuator is built up by stacking wafers 16mm in diameter and 0.8mm thick. The wafers are bonded together with an electrode placed between each wafer. The electrodes are wired in parallel, such that the voltage applied across an individual wafer produces an electric field in the appropriate direction for the wafer. The underlying mechanism of the piezoelectric actuator relies on the electromechanical coupling of the piezoelectric material. In other words, when an electric field is applied to the piezoelectric material a mechanical strain related to the field is created. This relationship tends to be nonlinear, and hysteretic.

Included in the same package as the motor is a single wafer of piezoelectric material that is used as a load sensor. The same piezoelectric material that is used for the actuator portion of the stack is used for the load cell. This wafer is electrically insulated from the actuator wafers. The operation of the load sensor relies on the converse of the piezoelectric effect, i. e. when a pressure is applied to the piezoelectric material an electric charge is produced across the material.

The parameters of the piezoelectric stack are listed in table 2. Note, that as expected the stack open circuited stiffness is 55% greater than the short circuited stiffness. It is generally expected that a PZT is roughly twice as stiff open circuited as short circuited[6]. Finally, stainless steel caps are bonded to the end of the stack, and RTV insulation is used on the outer surface.

Table 2: Piezoelectric stack parameters.

PZT wafer diameter (mfg data)	16mm
PZT wafer thickness (mfg data)	0.8mm
Number of PZT wafers in actuator (mfg data)	66
Number of PZT wafers in load sensor (mfg data)	1
g33 (mfg data)	0.023 Vm/N
d33 (mfg data)	530 pC/N
ε dielectric constant (mfg data)	2600 F/m
Stiffness, short circuit	64 N/μm
Stiffness, open circuit	99 N/μm
Capacitance, actuator	22 μF
Capacitance, load cell	3.5 nF

The displacement transducer is the same as used previously: a Kaman-7200 eddy current proximity sensor. In the previous designs[5,6], the motion sensor was referenced to the fixed end of the active member by a reference rod. The actuator stack was annular, so that the reference rod could be passed through. A different displacement measuring scheme was used here, where the motion sensor was mounted directly to the active member casing. The casing of the member is not in the load path, i. e. it does not deflect elastically, thus leaving the motion sensor fixed relative to the dead end (left end in figure 3) of the member. The motion sensor target is mounted on a yoke, which is an integral portion of the active member output stem.

The cross-blade flexure located at the live end (right end of figure 3) of the active member is an integral portion of the output stem. The live end of the assembly is supported laterally by a parallel motion flexure which consists of a pair of wide blade flexures. The cross-blade flexure, piezoceramic stack, and output stem are placed into the active member casing and held in place with an end cap. The end cap is mated to the active member casing by a lens-type screw thread. The desired compressive preload on the actuator assembly is then applied by a preload spring and nut.

A 140 lb compressive preload is applied to the active member by using an Instron machine. The preload nut is screwed into the active member end cap, such that it does not contact the preload spring. The assembly is then placed into the Instron machine. End fittings and ball bearings are used at both ends of the active member such that bending

moments are not applied. The active member is then compressively loaded until the Instron machine load cell indicates 140 lb has been applied. The preload nut is slowly tightened until the load cell reading just begins to drop. This indicates that the preload nut has just contacted the preload spring, and that the load on the Instron machine is being relieved. The external load is removed, and the active member assembly is completed.

4. Active Member Characterization and Calibration

The effectiveness of the active member, and the low voltage material can be evaluated based on a series of experiments. First, the active member sensors are calibrated. Secondly, the effective piezoelectric field relation of the active member is evaluated. The active member stiffness is measured.

For all tests where the actuator was driven, a Burleigh PZ-150 power amplifier was used. Unless it is otherwise indicated all the data was acquired using a Tektronix 2630 4-channel Fourier analyzer.

4.1.1 Displacement Sensor Calibration

The internal eddy current displacement sensor was calibrated once the active member was completely assembled. A Schaevitz LB-375 Linear Variable Differential Transformer (LVDT) was used as the reference measurement. The active member was fixtured such that it was horizontal, and its dead end was fixed. At the live end of the member the LVDT was brought into contact with the member. The LVDT was adjusted so that its axis was parallel to that of the active member. The internal displacement sensor was calibrated dynamically by driving the actuator with a 1Hz sinusoidal voltage. The signals from both the internal and external displacement sensors were then recorded simultaneously. The sensitivity of the internal displacement sensors were then determined to be 25.3μm/V. The eddy current displacement transducer displayed zero hysteresis with respect to the LVDT.

4.1.2 Load Cell Calibration

The internal load cell was calibrated before the active member was assembled. An Instrum 2606 charge amplifier was used as the signal conditioning for the load cell. This charge amplifier is AC coupled via a second order high pass filter that has a cut-off frequency of 0.5 Hz, and a damping ratio of 0.7.

The first calibration technique used is the standard load cell calibration method utilized by the JPL instrumentation section. The data was acquired using a digitizing voltmeter and transferred to a computer system for print out. The system was triggered manually by removing a jumper, thus enabling data acquisition. The load cell was calibrated by aligning the integrated stack vertically, and

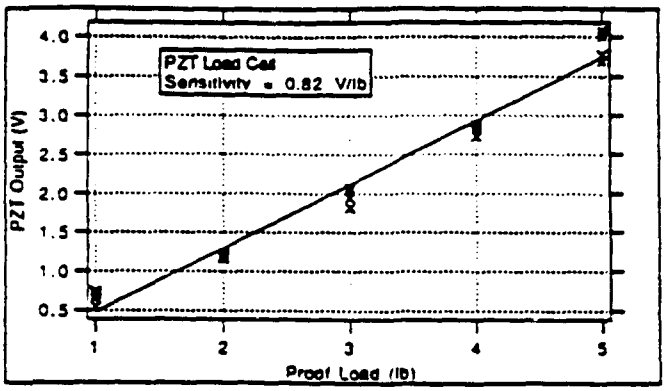

Figure 5: Dead weight load cell calibration curve.

applying a known dead weight load. Sufficient time was allowed to pass, such that the signal produced from the system was zero. The system was triggered, the dead weight was quickly removed and the resulting signal was recorded. The load cell sees the removal of the dead weight as an effective tensile load, and the peak value is correlated to the load removed. Unfortunately, for this system the AC coupling is relatively fast and this technique produces significant scatter in the results, see figure 5.

The load cell was also calibrated with an impact hammer. The stack was placed vertically on a rigid base, and the free end of the stack was tapped with a Dytran 4122 impact hammer. The signals from both the impact hammer, and the charge amplifier were then acquired with a Fourier analyzer and an averaged transfer function was calculated, see figure 6. The sensitivity of the load cell was then calculated based on the magnitude of the flat portion of the frequency response, from approximately 10 to 100 Hz. The effects of the electronic AC coupling are evident at low frequency, where it is observed that there is some amplification, and phase lead.

4.2.1 Hysteresis

The displacements produced by a 1 Hz sinusoidal voltage input to the actuator are shown in figure 7. As

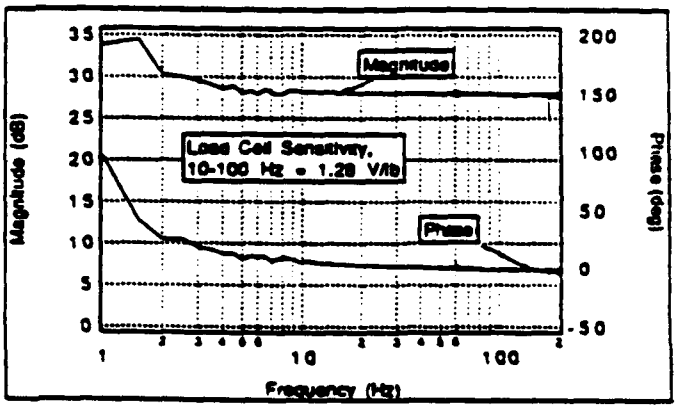

Figure 6: Dynamic load cell calibration.

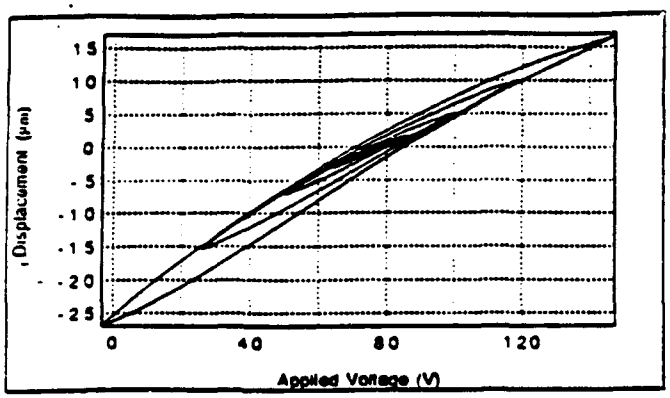

Figure 7: Active member hysteresis.

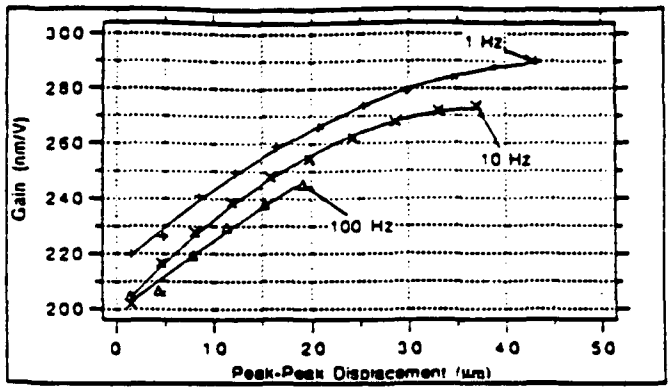

Figure 8: Active member gain.

expected the actuator displays some hysteresis. The plot in figure 6 shows four different hysteresis loops due to four different input voltages. A measure of the hysteresis present in each loop is defined as the aspect ratio of the loop. The aspect ratio of the loop is the maximum loop displacement width divided by the peak to peak displacement. The percent hysteresis present in the four loops is 8.8%, 10.2%, 11.3%, and 10.9%. These hysteresis values are stated in order of increasing peak to peak displacement. The hysteresis shown here is a reflection of the lossy dielectric coefficient of the PZT.

A nonlinearity, such as hysteresis, in an actuator can tend to be detrimental to the actuator's performance. For example, if the actuator is to be used as a displacement driver a control system that will eliminate the nonlinearity may be required for accurate and repeatable operation. In other words the hysteresis can produce residual displacements at DC.

4.2.2 Gain

The fundamental field strain relation of the PZT is also indicated in figure 7. That is, for a voltage applied to the piezoelectric material a proportional strain is induced. For larger peak to peak displacements the slope of the hysteresis loop increases. This implies that the material's piezoelectric coefficient increases with increasing displacement. An actuator gain can be defined as the ratio of the peak-to-peak displacement to the peak-to-peak applied voltage. The actuator gain has been calculated for the hysteresis loops of figure 7, as well as for several other driving frequencies. These results are indicated in figure 8. This data shows that the PZT gain increases with increasing amplitude, and decreases with increasing driving frequency.

The behavior of the PZT gain increasing with increasing displacement is somewhat analogous to a friction coefficient versus sliding velocity curve with a negative slope. In the case of the friction versus velocity curve, the faster the motion the less resistance there is to that motion. These two cases are analogous in the sense that they both have a destabilizing influence. The difficulty with an increasing gain, is that for control design an increase in gain reduces the stability margin.

An aging effect was also observed. The gain measurements were measured three separate times, for a 1 Hz sinusoidal input. A noticeable decrease in gain over time was observed, see figure 9. This can be detrimental to control system performance over time, since the system will tend to detune itself.

4.2.3 Step Response

A series of step response tests were performed on the active member. The step response shown in figure 10 is the displacement response of the active member given a 115 Volt step input. This plot shows the quick response capability of the PZT material along with its long term creep. There is some initial oscillation due the imperfect step produced by the function generator. The response reaches 95% of its final value due to the initial motion of the actuator. Approximately 25 seconds are required for the response to reach its final value. Qualitatively, this behavior was observed for the 33 micron response of figure 10, and for step responses down to 2 microns.

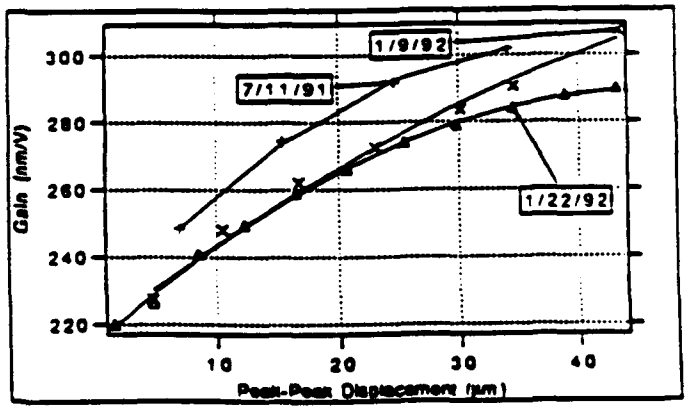

Figure 9: Active member gain aging.

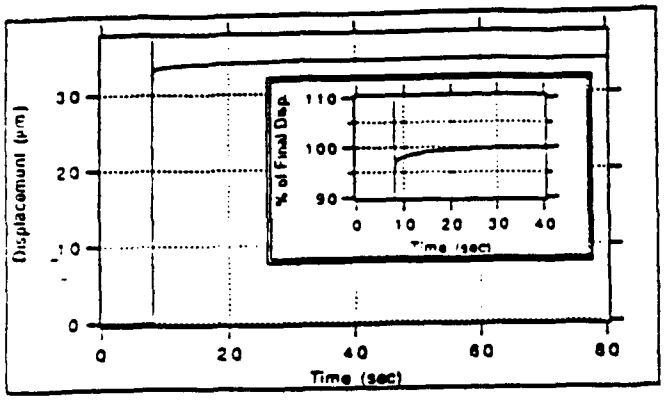

Figure 10: Active step response.

4.3 Active Member Stiffness

The active member stiffness was measured using the Instron machine and the same fixturing that was used during assembly. This test is static in nature, therefore the active member's AC coupled internal load cell is not used. Rather, the Instron machine load cell is used to measure the applied force. The internal displacement sensor is used to measure the resulting deflection. The average open circuit active member stiffness is 44.1 N/μm, and the average short circuit stiffness is 39.8 N/μm. The stiffness of the active member is different from the stiffness of the PZT stack because the stiffness of the crossblade flexures is in series with the stack. The preload spring is then in parallel with the stiffness of the PZT stack and flexures.

5. Active Damping Augmentation

The damping augmentation concept used, is described in this section. First the feedback control strategy and gain adjustment is summarized, then the active member placement problem is considered.

5.1 Feedback Control Law

The feedback control strategy used in this experiment is referred to as bridge feedback[1], where the active member's force and relative velocity signals are fed back locally. This control strategy is summarized in the block diagram shown in figure 11. The advantage of using bridge feedback is that the desired loop gain function and the active member's input impedance function are implemented without adverse interaction and conflicting requirements. This control strategy is then implemented as an analog circuit.

The gain tuning strategy used here is as follows. First the load impedance function is measured. This is done by driving the structure with the active member actuator, and measuring the transfer function between the displacement sensor and the load cell. This transfer function is then numerically differentiated to give an impedance. This impedance will be highly frequency dependent due to the dynamics of the structure. Secondly the open loop active member input impedance is measured. This is done by measuring the same transfer function as above, but with the structure being driven by an external disturbance. Typically, the active member open loop input impedance will be not frequency dependent and is usually an order of magnitude less than the average value of the load impedance. Although, the active member impedance will have a positive slope since an open loop active member is essentially a passive spring. This implies that the active member is stiffer than the structure. The feedback paths are then closed and the active member impedance is again measured. The feedback gains are adjusted until the active member impedance is approximately equal to the average value of the load impedance. The active member is electronically softened by this procedure.

5.2 Active Member Placement

An objective of this study is to demonstrate the ability to control the test-bed's first four modes. Since only two active member were available, it was decided to perform separate tests to control individually targeted modes. Given the small number of actuators and the experimental scenario, the active member placement is relatively straightforward. Based on engineering judgement it was decided to replace the two structural members that saw the highest percentage strain for the mode of interest with the active members. Since this is a structure with clamped boundary conditions, it was intuitively expected that the struts with high strain energy would be near the mounting points. Using this rationale the active member locations were chosen, and are shown in figure 12. Note, for each of the chosen locations one end of the active member is attached to ground. Secondly, the active member placement for the third mode is on the lower surface rather than at one of the core member locations, as is the case for modes one, two, and four.

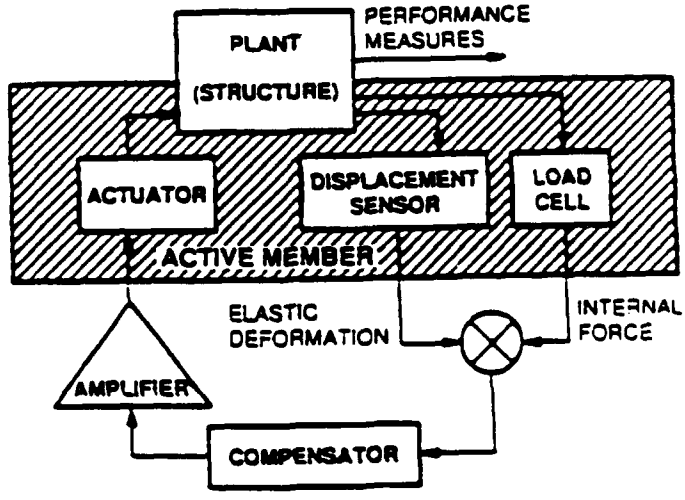

Figure 11: Bridge feedback control block diagram.

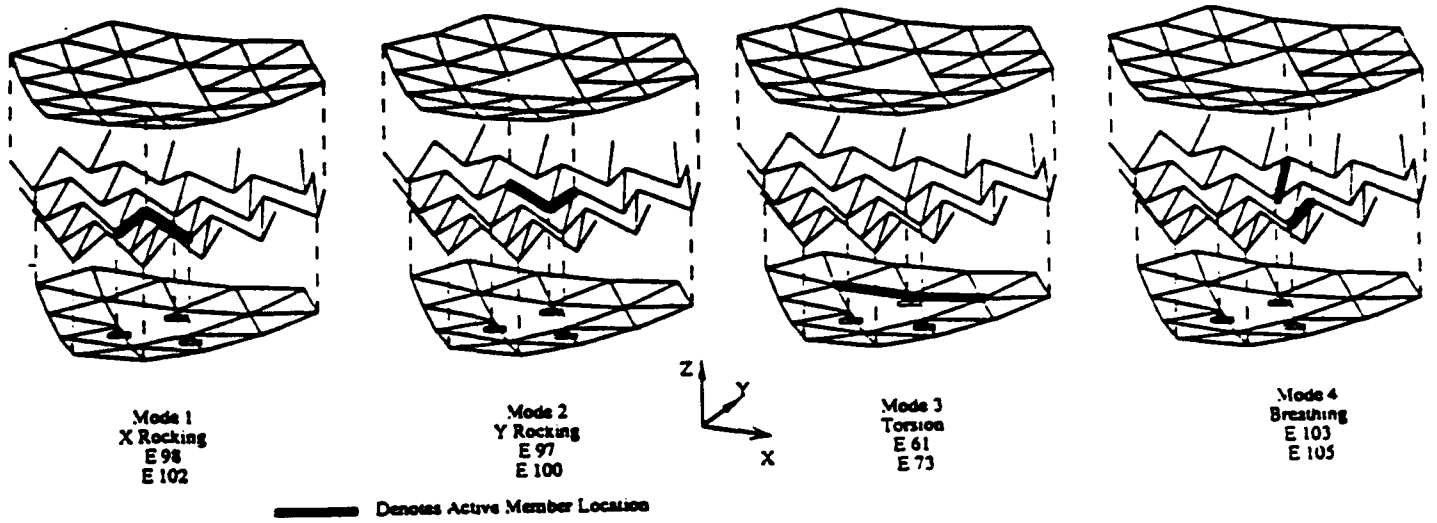

Figure 12: Active member placement.

6. Experimental Results

The test-bed structure was instrumented with twelve Sundstrand QA-1400 servo accelerometers, grouped into four triaxial sets. The accelerometers were AC coupled such that the constant acceleration due to gravity was removed from the vertically mounted accelerometers. The accelerometers were placed at four of the test-bed structure's upper surface outer corners, as shown in figure 13. Dead weights were placed at the remaining two upper surface outside corners to simulate the mass of an accelerometer set. A mini-shaker was used as an external disturbance source.

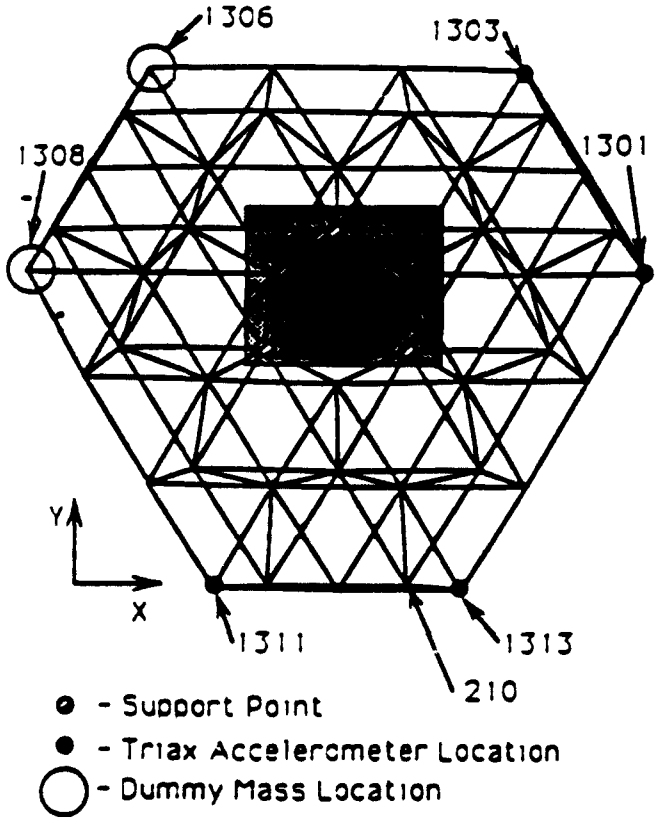

Figure 13: Experimental setup.

6.1 Test Procedure

All test data was taken in the form of transfer functions generated by a broadband random input signal. The active members were placed in the structure and the gains tuned according the technique described above. Transfer functions of the accelerometer response to the input force were taken with the active damping disabled, i. e. open loop, and enabled, i. e. closed loop.

6.2 Test Results

Initially, open loop response tests were performed on each feedback channel. Transfer functions were measured between the compensator inputs and the active member internal sensors. A negative stability margin was observed at approximately 2kHz on the force feedback loop given only modest gain levels. Normally, force feedback of an active member has 180 degrees of phase margin[2]. The negative stability margin was caused by the combination of three factors. First, the compensator rolls off at -4dB/octave with a phase change of approximately -30 degrees. Secondly, the power amplifier coupled with the capacitance of the actuator act as a second order system whose natural frequency is 900Hz and damping ratio is 0.7. The amplifier and actuator system produce a 180 degree phase change at 2 kHz. Finally, the active member internal force transducer observes an axial resonance at 2 kHz that has a high dynamic amplification. It is because of this axial resonance that a negative gain margin is observed.

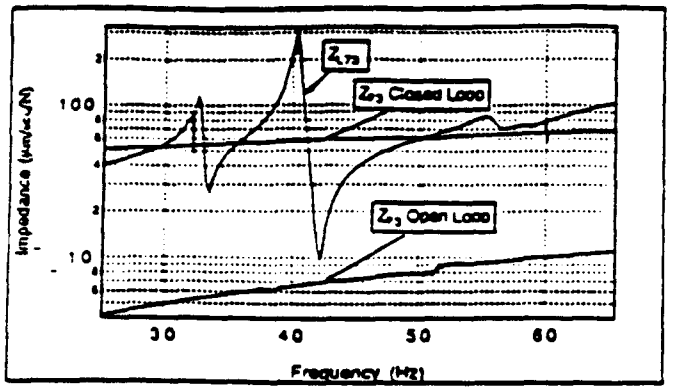

Figure 14: Active member and structure impedances.

This problem was solved by using an external load cell mounted at the tip of the active member. The load cell used is a PCB 208A02 ±100 lb load cell.

An example of the active member impedance matching to the load impedance is shown in figure 14. An active member was located at location number 73 which is on the lower surface of the structure to provide damping to the torsional mode. As expected, the load impedance, denoted in the figure as Z_{L73}, is frequency dependent, representing the dynamics of the structure. The open loop active member impedance, denoted as $Z_{73\ open\ loop}$, is roughly an order of magnitude less than the average value of the load impedance. Additionally, the active member impedance is gradually increasing with frequency. This indicates that the open loop active member is effectively a spring that is stiffer than the structure. The tuned closed loop active member impedance, denoted as $Z_{73\ closed\ loop}$ in figure 14, is approximately equal to the average value of the load impedance. The closed loop feedback gains were tuned via the procedure outlined above. The procedure takes only a few iterations until the active member impedance is "optimally" tuned.

The transfer functions shown in figure 15, show the

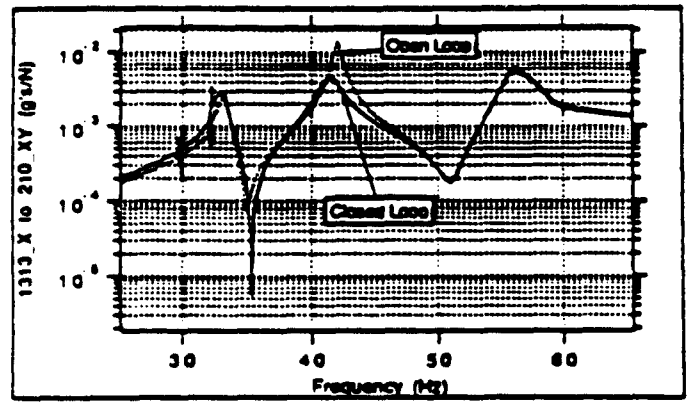

Figure 15: Open and closed loop structure frequency response functions using 1 active member.

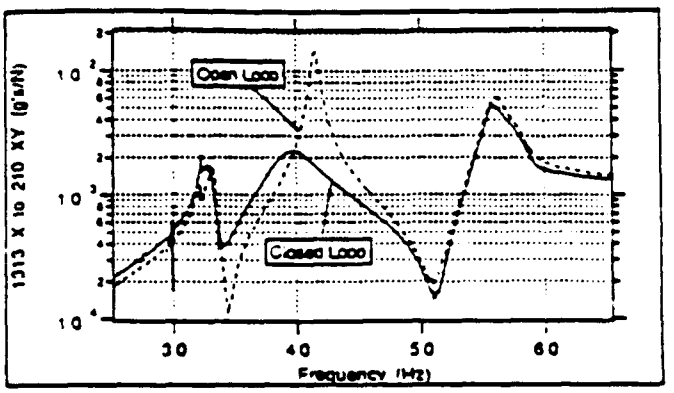

Figure 16: Open and closed loop structure frequency response functions using 2 active members.

accelerometer response at node 1313X due to an external driving force at node 210XY. In figure 15, the open loop response is compared to the closed loop response for one active member placed in the structure. The first twisting mode response amplitude, at 42Hz, is reduced by a factor of 3, while the amplitudes of the other modes shown remain relatively unchanged. A modal curve fitting technique was used to the modal natural frequencies and damping ratios. The damping ratio for the first torsional mode is improved from 0.7%, to 2.0%. Also note, that the frequency for this mode has reduced slightly, from 42.1 Hz to 41.6 Hz. Similarly, a comparison of the structures open and closed loop response using two active members is shown in figure 16. Here the response of the first torsional mode is reduced by a factor of 6. The damping ratio for this mode is increased from 0.7% to 5.2%, while the frequency has dropped from 42.1 Hz to 40.1 Hz.

The active members were then used to replace core members of the structure. The actuator placed to provide damping to the first two modes. Time domain data was acquired by performing a so called "twang" test. The TB was given a static deflection by hanging a 10 lb dead weight from node 210. The TB was then excited by suddenly cutting the string that held the weight, thereby imparting a

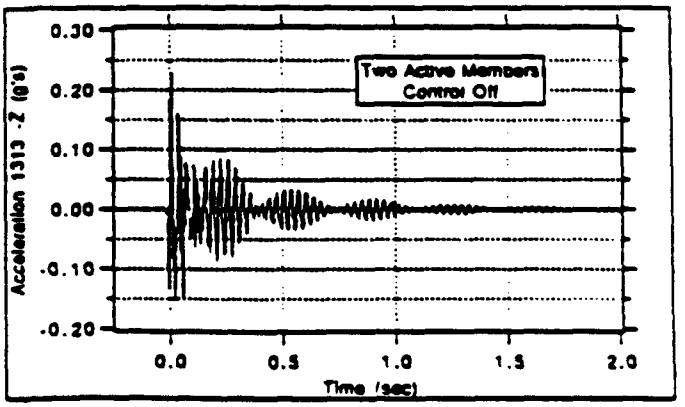

Figure 17: Time domain response, 2 active members placed in the TB core, control off.

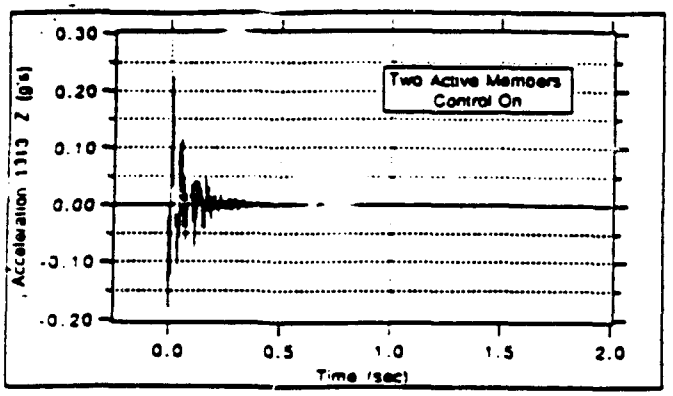

Figure 18: Time domain response, 2 active members placed in the TB core, control on.

step change in applied load. The open and closed loop acceleration response at node 1313 in the z direction is shown in figures 17 and 18, respectively. Note that with the control off, the response clearly shows a low frequency mode of approximately 32 Hz. It is also evident, because of the beating phenomenon, that there is a second mode that is of roughly the same frequency. These two modes are the TB's x and y rocking modes. The TB's settling time with the control turned off is greater than two seconds. When the control is turned on the settling time is less than a half a second and the low frequency modes are no longer evident.

7. Summary

In this paper the design and testing of a new low voltage active member was described. The maximum stroke of this active member was measured to be 45 microns, which is more than adequate for vibration damping applications in precision structures. The internal displacement sensing functioned as expected. The internal force sensor displayed an active member axial resonance that had a very high dynamic amplification. This resonance led to a closed loop stability problem. This problem was resolved by using an external load cell. The nature of the active member axial resonance, and compensating for it is a subject for future work.

Active modal damping was successfully demonstrated on a realistic dynamic test-bed. The low voltage active member, using only collocated force and displacement measurements, was dynamically softened by electronic feedback such that its impedance matched the load impedance. The benefit of impedance matching is that the vibrational energy dissipation is maximized. The advantage of bridge feedback control, given the large stability margins normally associated with force feedback, is that it is robust with respect to the uncertainty of the structure's dynamic characteristics.

8. Acknowledgements

The research described in this paper was performed at the Jet Propulsion Laboratory, California Institute of Technology, under a contract with the National Aeronautics and Space Administration, code RM. The authors gratefully acknowledge the assistance of the following: Chris Miller, John O'Brien, Andy Kissil, and the JPL Dynamics Laboratory.

9. References

[1] G-S. Chen and B. J. Lurie, "Bridge Feedback for Active Damping Augmentation," AIAA Paper 90-1243, *31st AIAA/ASME/ASCE/AHS/ASC Structures, Structural Dynamics, and Materials Conference*, Long Beach, CA, April 1990, also to appear *AIAA J. of Guidance, Dynamics, and Control*.

[2] J. L. Fanson, et al, "System Identification and Control of the JPL Active Structure," AIAA Paper 91-1231, *32nd AIAA/ASME/ASCE/AHS/ASC Structures, Structural Dynamics, and Materials Conference*, Baltimore, MD, April 1991.

[3] C. R. Lawrence, B. J. Lurie, G-S. Chen, and A. D. Swanson, "Active Member Vibration Control Experiment in a KC-135 Reduced Gravity Environment," *First US/Japan Conference on Adaptive Structures*, Maui, HA, November 1990.

[4] H. G. Bush, et al, "Design and Fabrication of an Erectable Truss for Precision Segmented Reflector Application," AIAA Paper 90-0999, *31st AIAA/ASME/ASCE/AHS/ASC Structures, Structural Dynamics, and Materials Conference*, Long Beach, CA, April 1990.

[5] Kaman Aerospace Corporation, "Constant Length Strut," United States Patent No. 4,742,261, May 3, 1988.

[6] E. H. Anderson, D. M. Moore, J. L Fanson, and M. A. Ealey, "Development of an Active Member Using Piezoelectric and Electrostrictive Actuation for Control of Precision Structures," AIAA Paper 90-1085, *31st AIAA/ASME/ASCE/AHS/ASC Structures, Structural Dynamics, and Materials Conference*, Long Beach, CA, April 1990.

Presentation to Workshop on Advanced Piezoelectric Actuator Materials

February 25, 1992

John Breakwell, Lockheed

SPICE TESTBED

Lockheed
Honeywell
CSA Engineering, Inc.
BOEING
Holmes & Narver

- The SPICE Testbed is a large precision optical structure
  - a large segmented primary mirror
  - a 250-strut bulkhead truss structure supporting primary mirror
  - a tripod secondary mirror support system

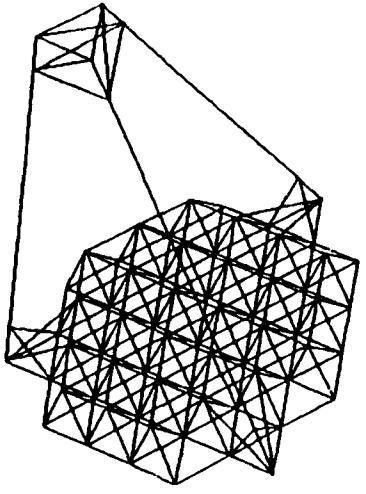

Finite Element Model

Finite Element Model Summary

No. of Nodes	357
No. of Elements	486
1st Tripod Bending Mode	8.88 Hz
Modes Below 100 Hz	62
Modes Below 200 Hz	105

SPICE4 FINITE ELEMENT MODEL

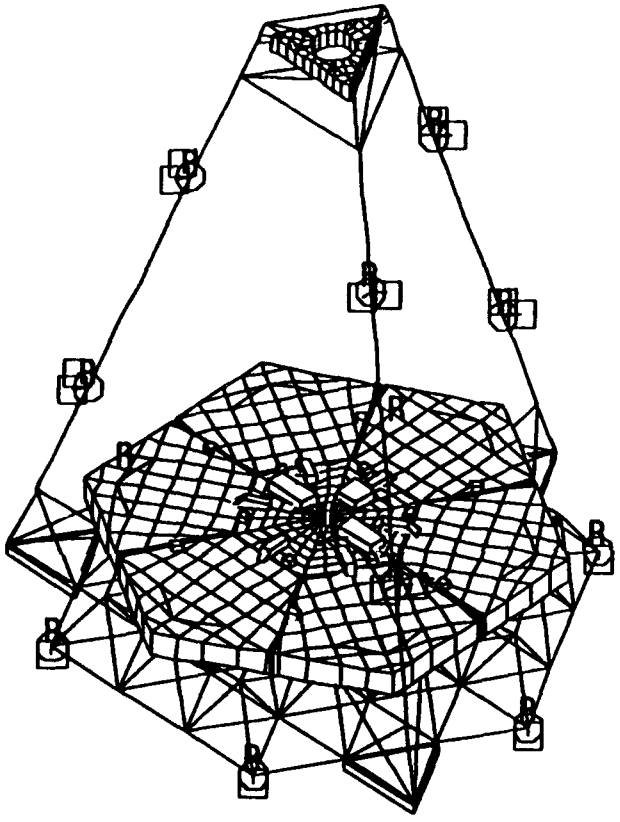

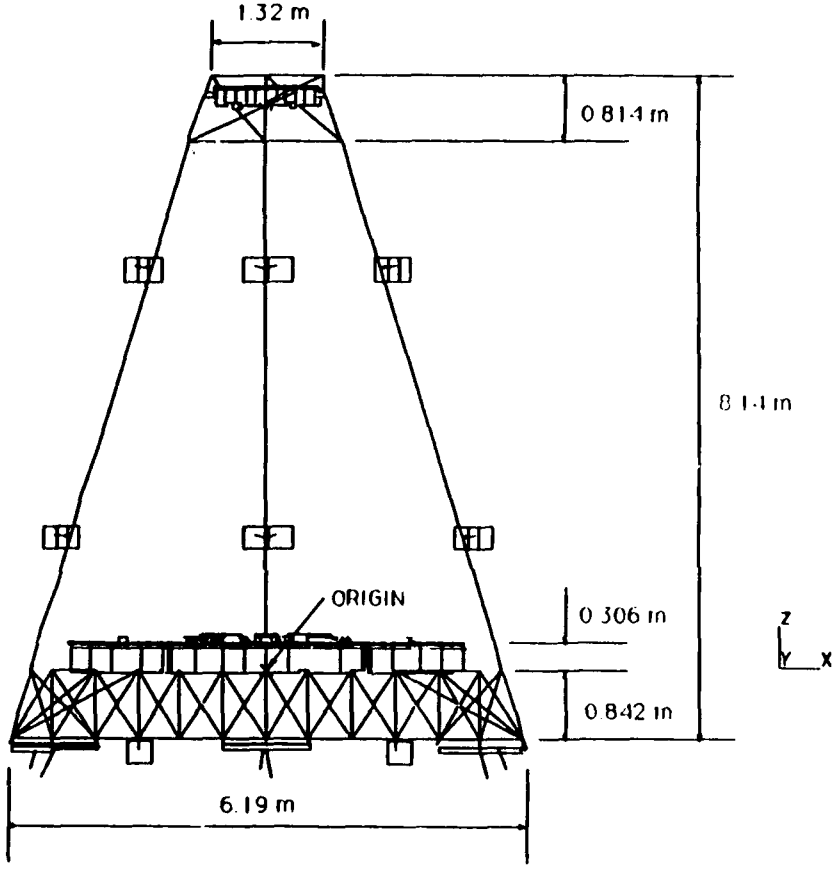

1568 NODES
3134 Elements
9410 Total Degrees of Freedom
7413 Dynamic Degrees of Freedom
Mass = 2840 kg (6260 lb)

CLOSED-LOOP SYSTEM MODEL

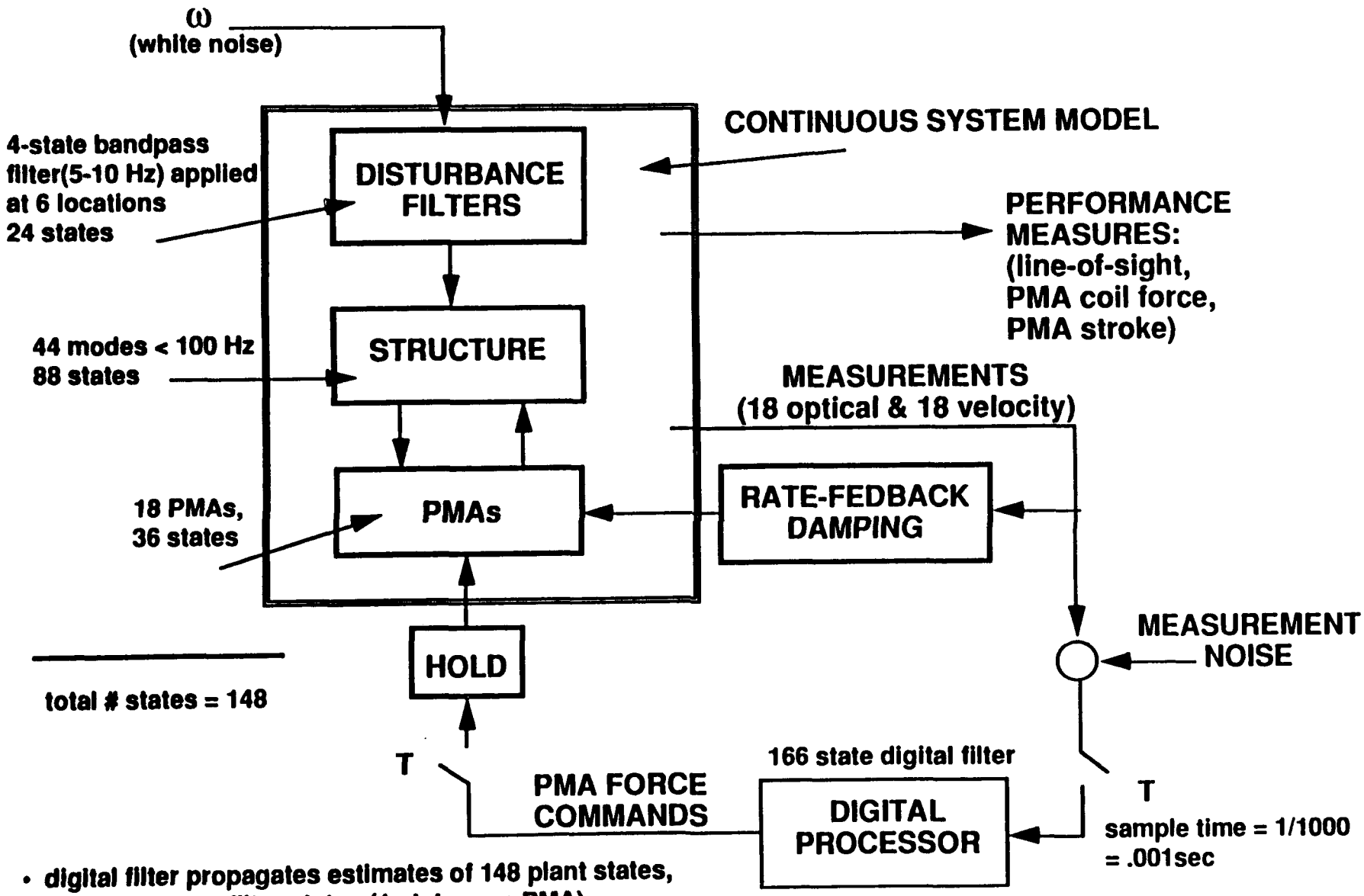

- digital filter propagates estimates of 148 plant states, plus 18 low-pass filter states (1 states per PMA)

- performance model contains 148 + 166 = 314 states

SPICE PMA Requirements

- Force (0 to peak) 60 N
- Stroke-proof mass product 8.2 kg-cm (peak to peak)
- 20 N_{rms} power < 30 W
- First mode in-axis < 5 Hz
- First mode cross axis > 150 Hz
- Frequency range 0 → 500 Hz

V-strut Design

- **Damping Mechanism - viscoelastic material**

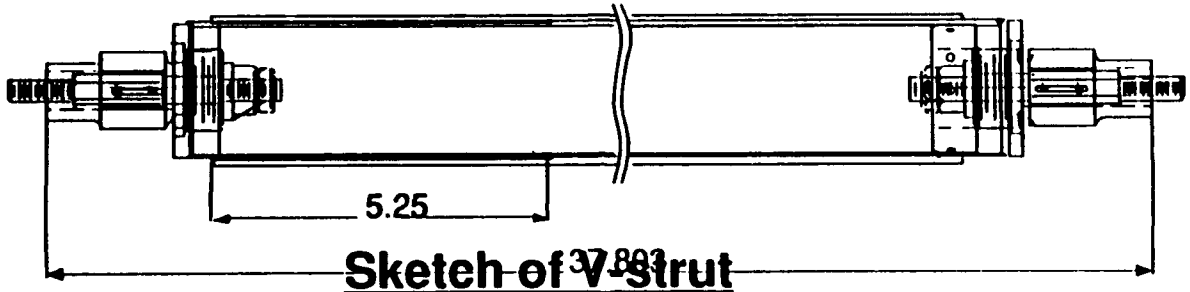

Sketch of V-strut

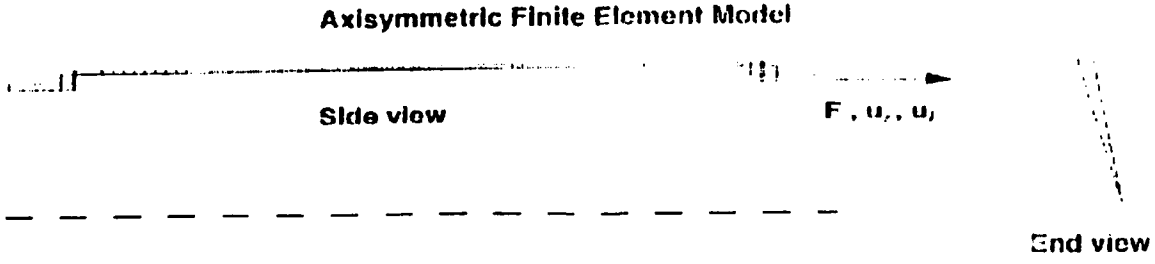

Model of V-strut

Direct Complex Stiffness Test

- **Low frequency test (1-55 Hz)**
- **Apparatus avoids resonance**
- **Random force input**
- **Complex stiffness as continuous function of frequency**

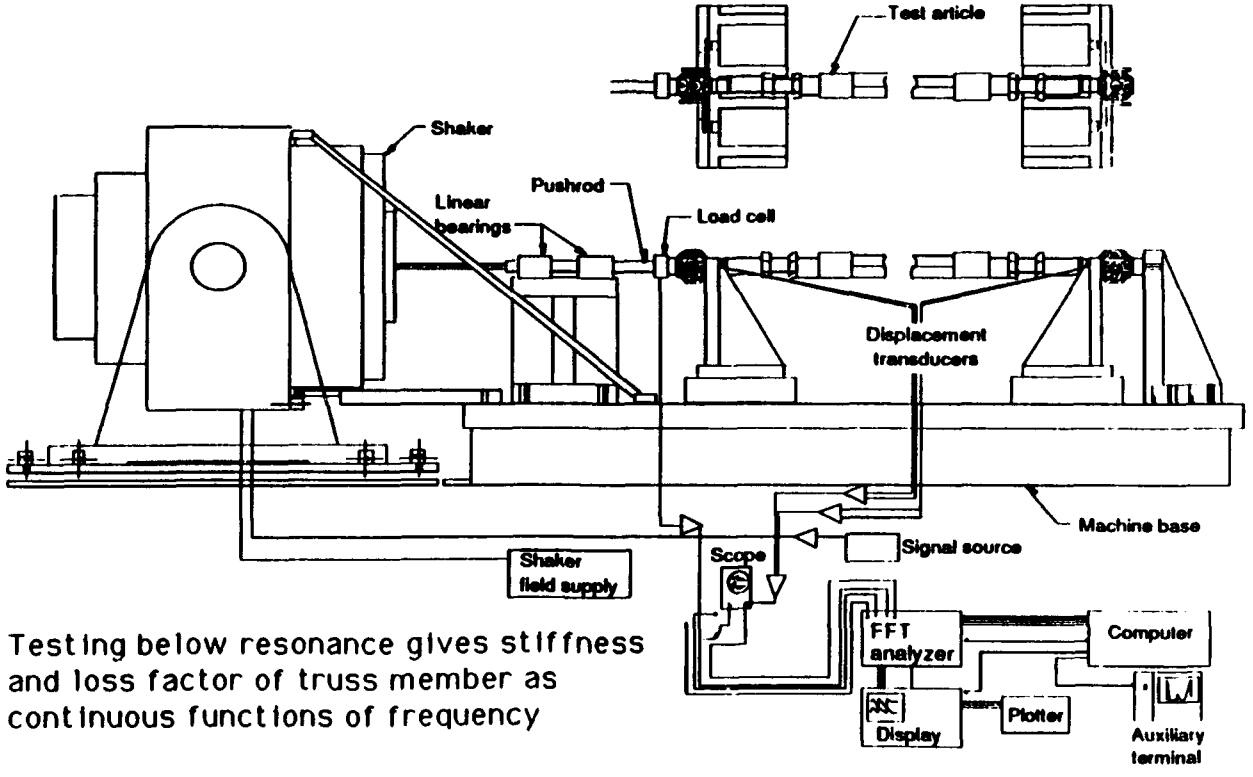

Testing below resonance gives stiffness and loss factor of truss member as continuous functions of frequency

CONTROL SYSTEM PERFORMANCE

5 LOW AUTHORITY CONTROL (LAC) - CO-LOCATED RATE FEEDBACK - DISSIPATES ENERGY IN TARGETED MODES - INHERENTLY STABLE.

4 HIGH AUTHORITY CONTROL (HAC) - HIGH PERFORMANCE OPTIMAL SYSTEM - NOT NECESSARILY DISSIPATIVE - REQUIRES GOOD MODEL OF THE SYSTEM.

3 PASSIVE ONLY - DISSIPATIVE.

2 HAC/LAC BLEND - PROVIDES MORE MARGINS FOR HAC - ALLOWS HIGHER PERFORMANCE.

1 HAC/LAC/PASSIVE BLEND - PROVIDES EVEN LARGER MARGINS FOR HAC - ALLOWS 100 TO 1 ATTENUATION.

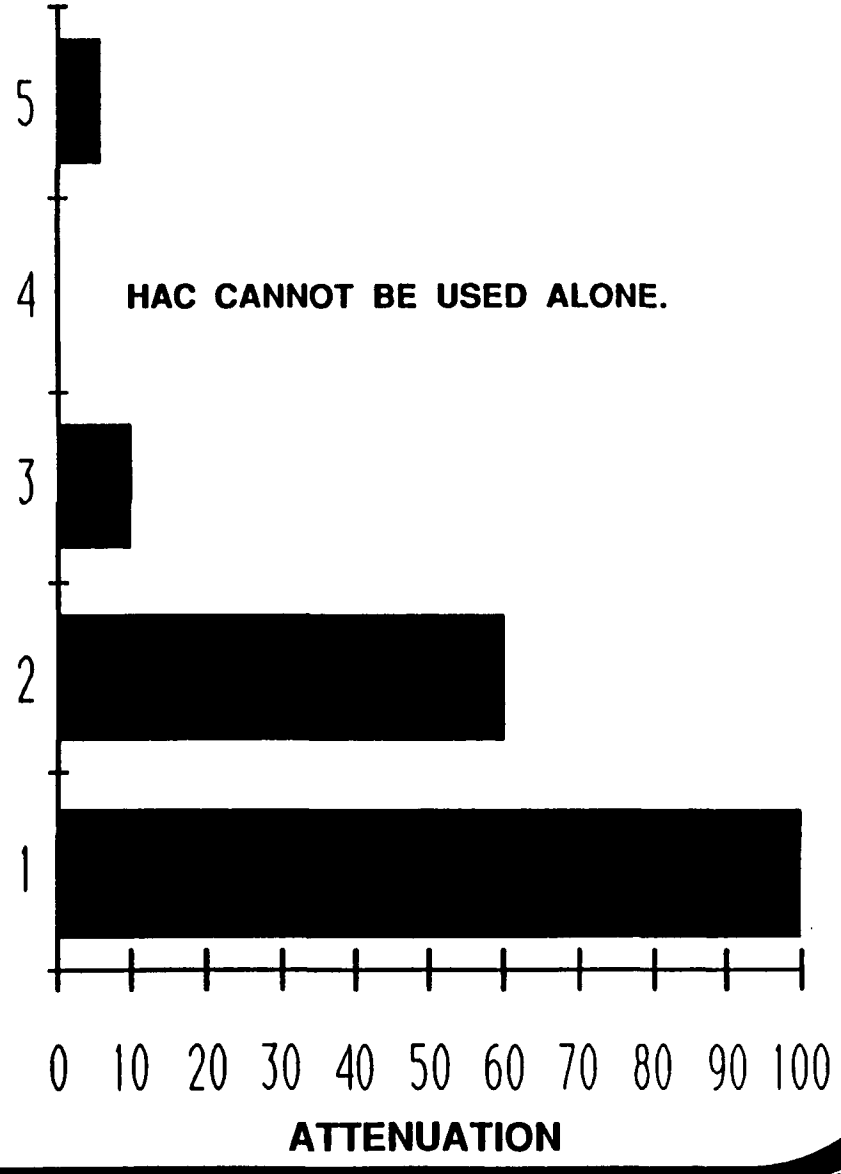

Conclusions

- Careful Flowdown of Actuator Requirements is Essential
    - Structural Model
    - Controls Design
    - Actuator Requirements
    - Actuator Developement
- Global Control Systems offer Much Higher Performance Payoffs

PROPULSION/POWER/ THERMAL MANAGEMENT

FAST ACTING CONTROL THRUSTER (FACT)

PROPULSION/POWER/THERMAL MANAGEMENT – FACT DEVELOPMENT PROGRAM – (U)

PROGRAM OBJECTIVE

ANALYZE, DESIGN, FABRICATE AND DEMOSTRATE A LIGHTWEIGHT FAST ACTING CONTROL THRUSTER (FACT) FOR SDC APPLICATIONS AND FOR THE DEVELOPMENT OF ADVANCED TECHNOLOGY CONCEPTS AND COMPONENTS.

TECHNOLOGY TASKS

- DEVELOP AN ULTRA FAST, LIGHTWEIGHT, INEXPENSIVE, LINEARLY PROPORTIONAL CONTROL THRUSTER
- DEVELOP A PROPORTIONAL, PRECISION HIGH FORCE-GAIN VALVE
- DEVELOP A SPECIFICALLY SIZED, BUT GENERICALLY ORIENTED, MOTION AMPLIFIER
- DEVELOP A STROKE OPTIMIZED ELECTROSTRICITIVE ACTUATOR STACK
- DEVELOP A THRUSTER REQUIRING VERY LOW INPUT ACTUATION FORCE TO MODULATE OUTPUT FORCE GENERATION

FAST ACTING CONTROL THRUSTER (FACT) CONCEPT

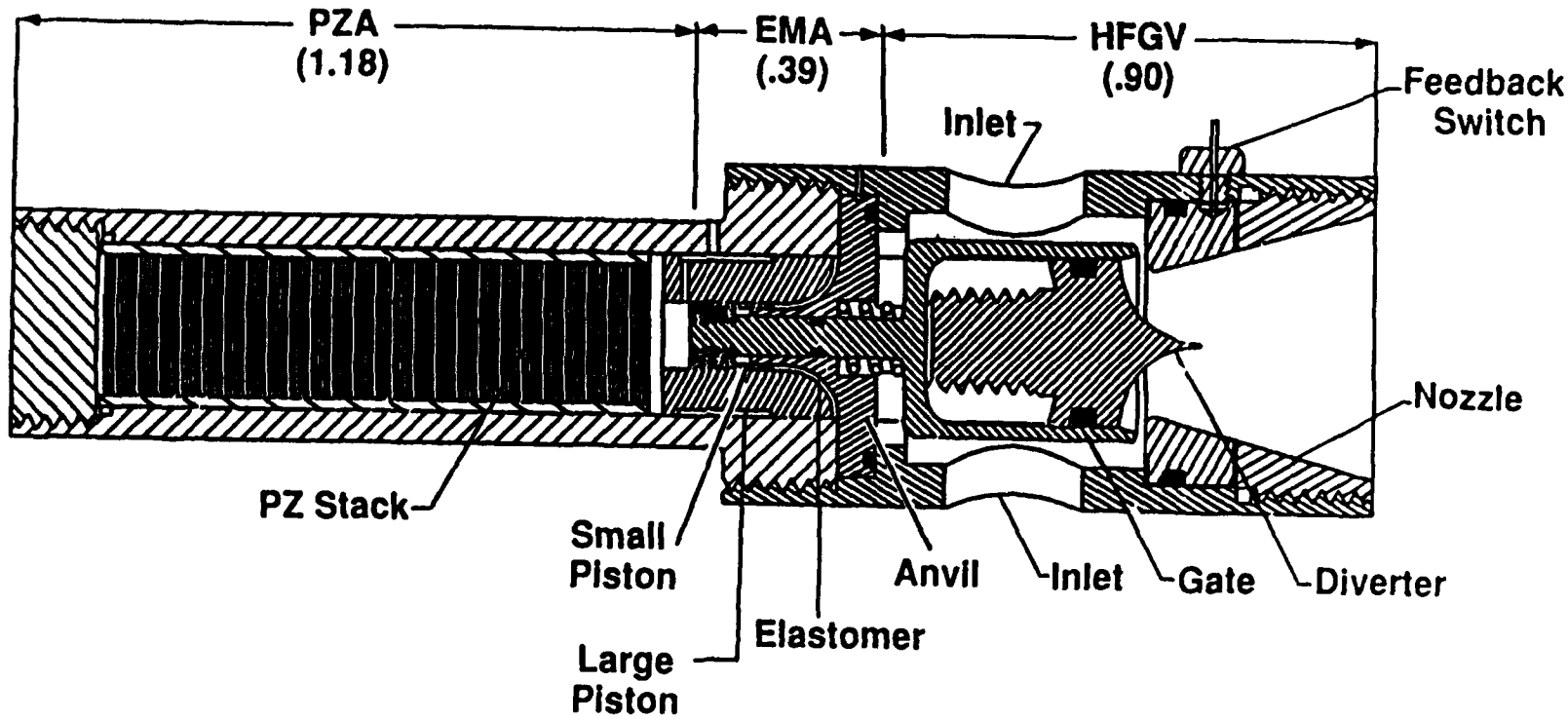

U.S. Patent No. 4,995,587

MS5049-01

FACT COMPONENT ASSEMBLY

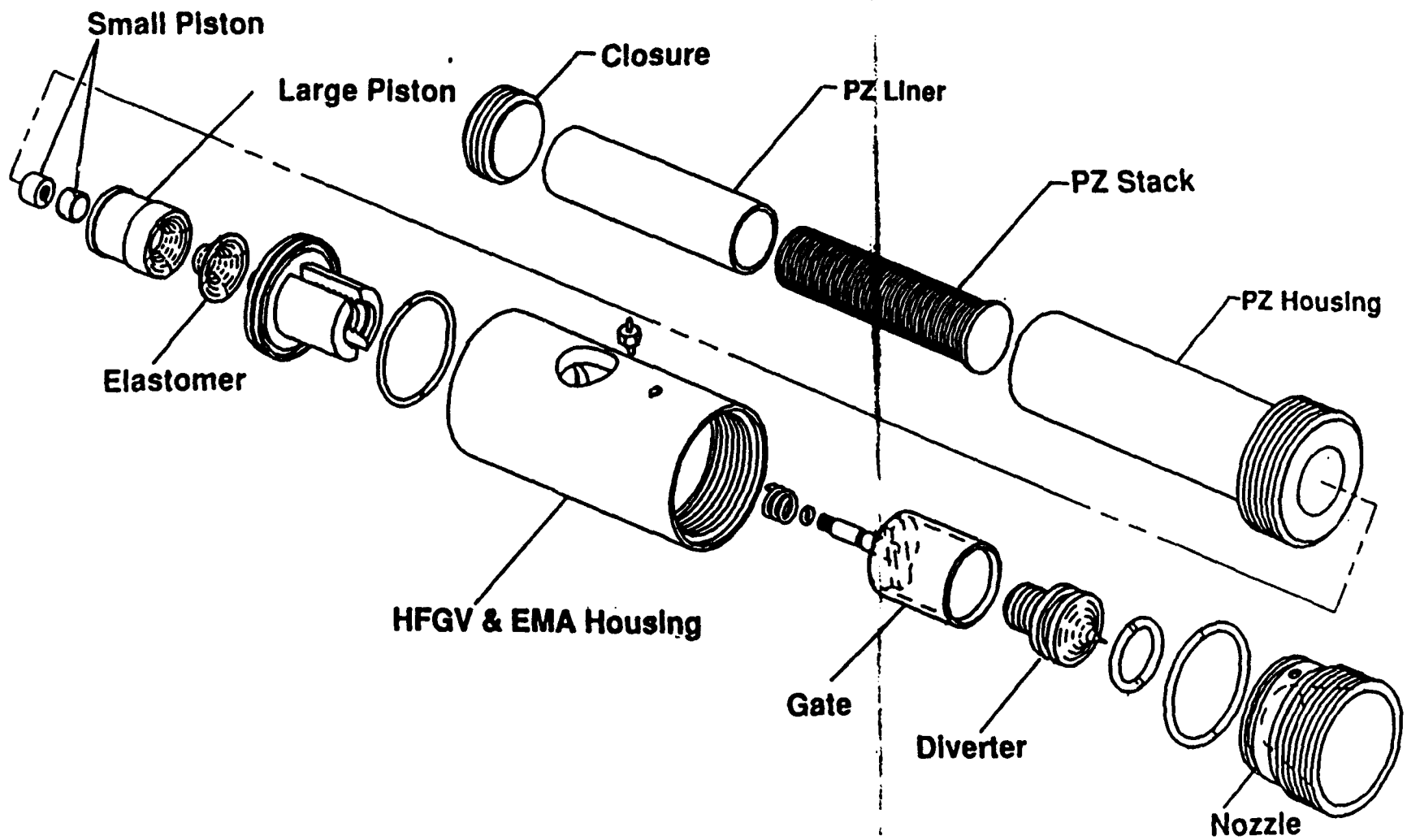

U.S. Patent No. 4,995,587

MS5049-02

PROPULSION/POWER/THERMAL MANAGEMENT – FACT VALVE ACTUATOR – (U)

ELASTOMERIC MOTION AMPLIFIER – PRINCIPLE PHYSICS

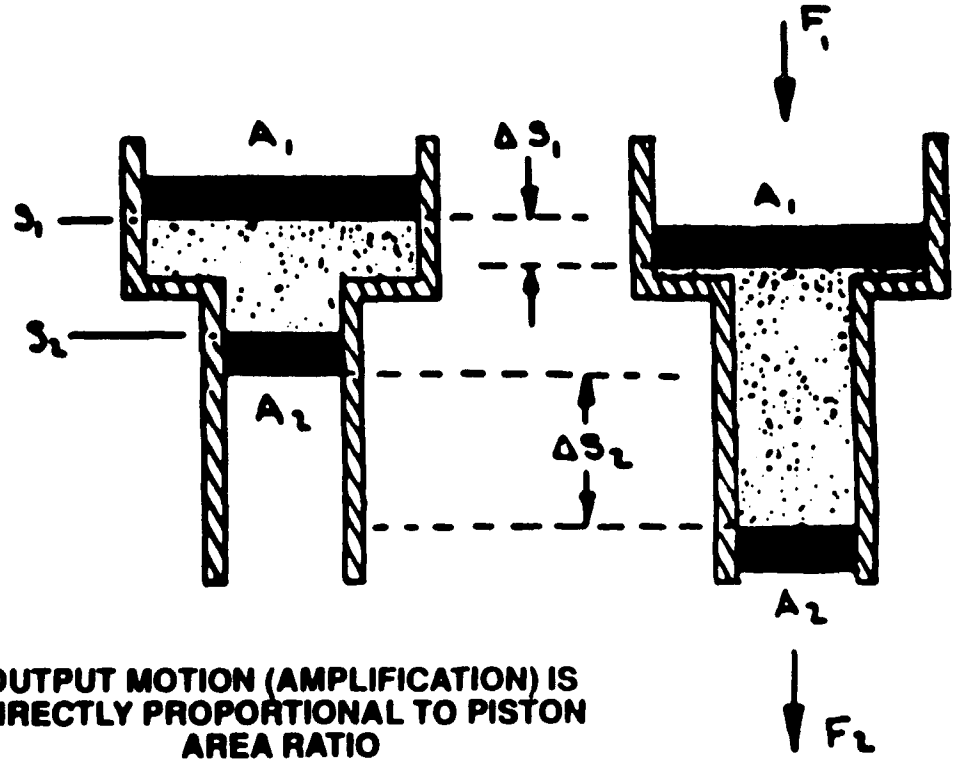

OUTPUT MOTION (AMPLIFICATION) IS DIRECTLY PROPORTIONAL TO PISTON AREA RATIO

OUTPUT FORCE (ATTENUATION) IS INVERSEELY PROPORTIONAL TO PISTON AREA RATIO

PROPULSION/POWER/THERMAL MANAGEMENT – ELASTOMER MOTION AMPLIFIER (EMA) – (U)

M-900302-28U (0183)

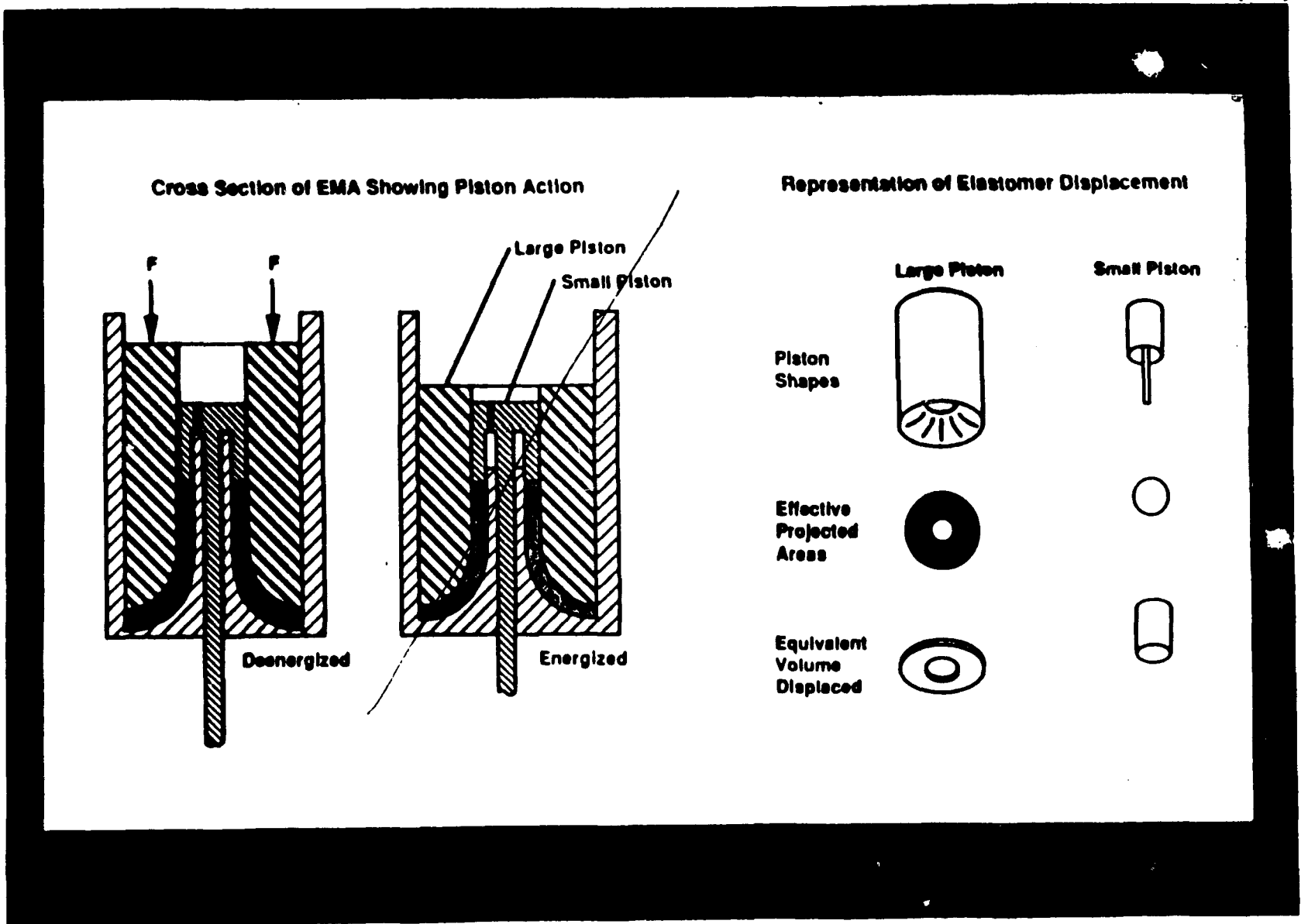

UNCLASSIFIED

EMA Development Testing

Test Setup

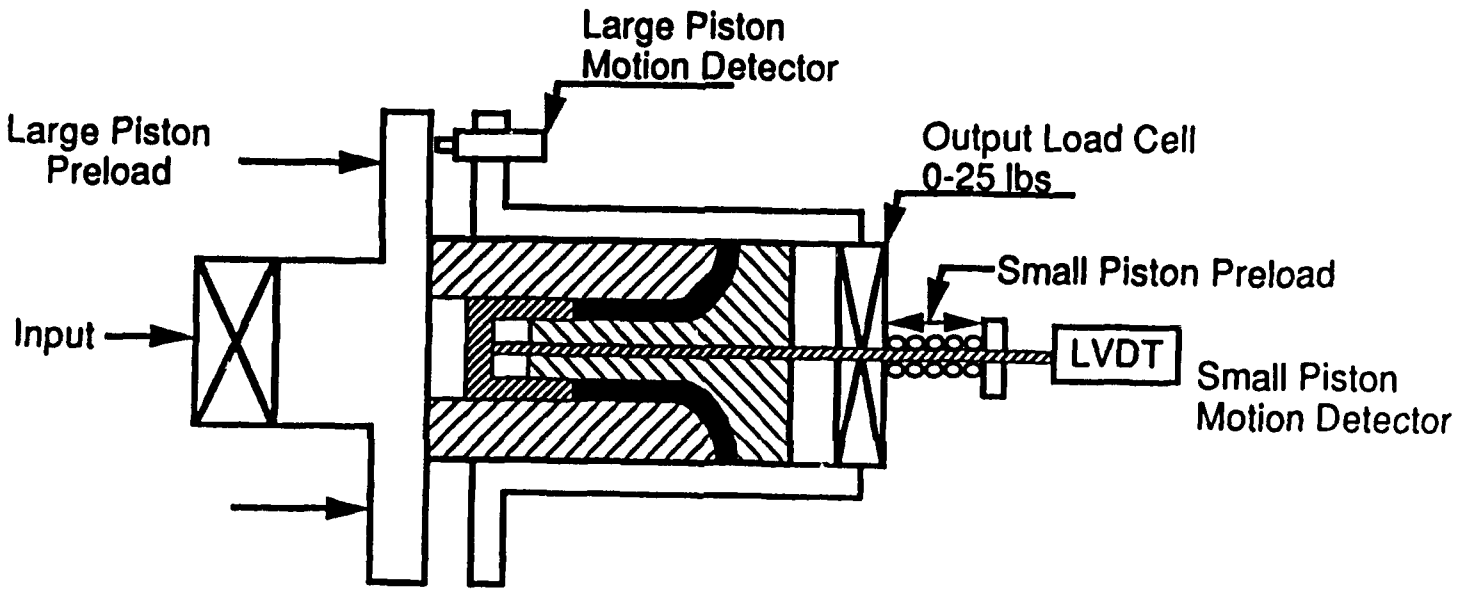

Input devices:

Screw Jack - Steady state compliance measurements
PZA - Dynamic inputs, thruster operational simulation

Test Objectives

- Conduct elastomer material performance evaluations
- Evaluate vacuum assembly effectiveness
- Determine preload/compliance/stroke requirements
- Acquire test data, define EMA dynamic response characteristics
- Conclude EMA final design configuration for FACT

C031-4050-03

SENSITIVE EQUIPMENT
DO NOT DISTURB

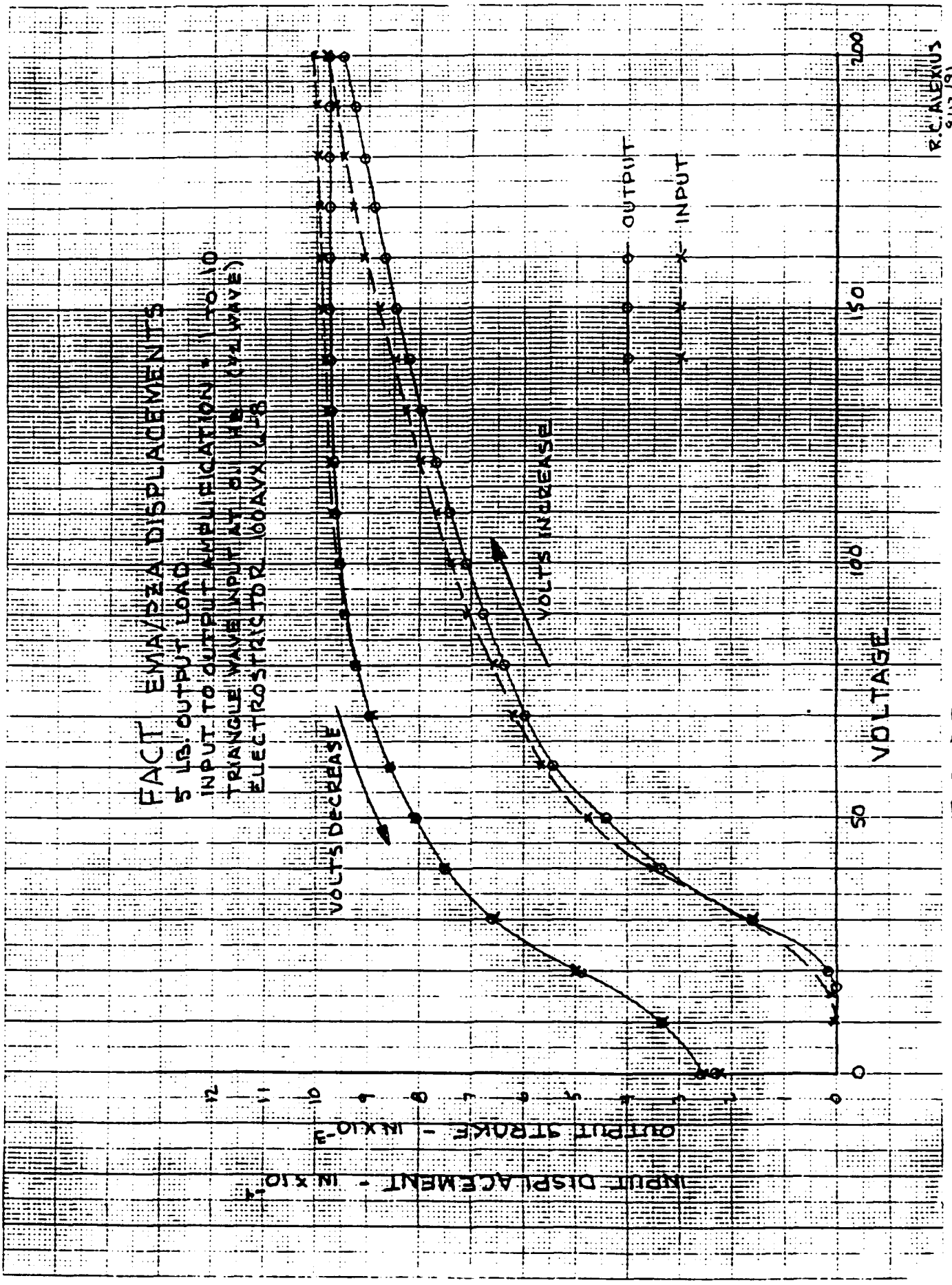
FACT EMA/PZA DISPLACEMENTS
5 LB. OUTPUT LOAD
INPUT TO OUTPUT AMPLIFICATION = 10 TO 10
TRIANGLE WAVE INPUT AT 5 Hz (1/2 WAVE)
ELECTROSTRICTOR 60 AVX JTB
VOLTS DECREASE
VOLTS INCREASE
OUTPUT
INPUT
INPUT DISPLACEMENT - IN x 10⁻³
OUTPUT STROKE - IN x 10⁻³
VOLTAGE
R.C.ALEXIUS
8/12/91

FIGURE 1

9/8R1
Amplifier
PZ test

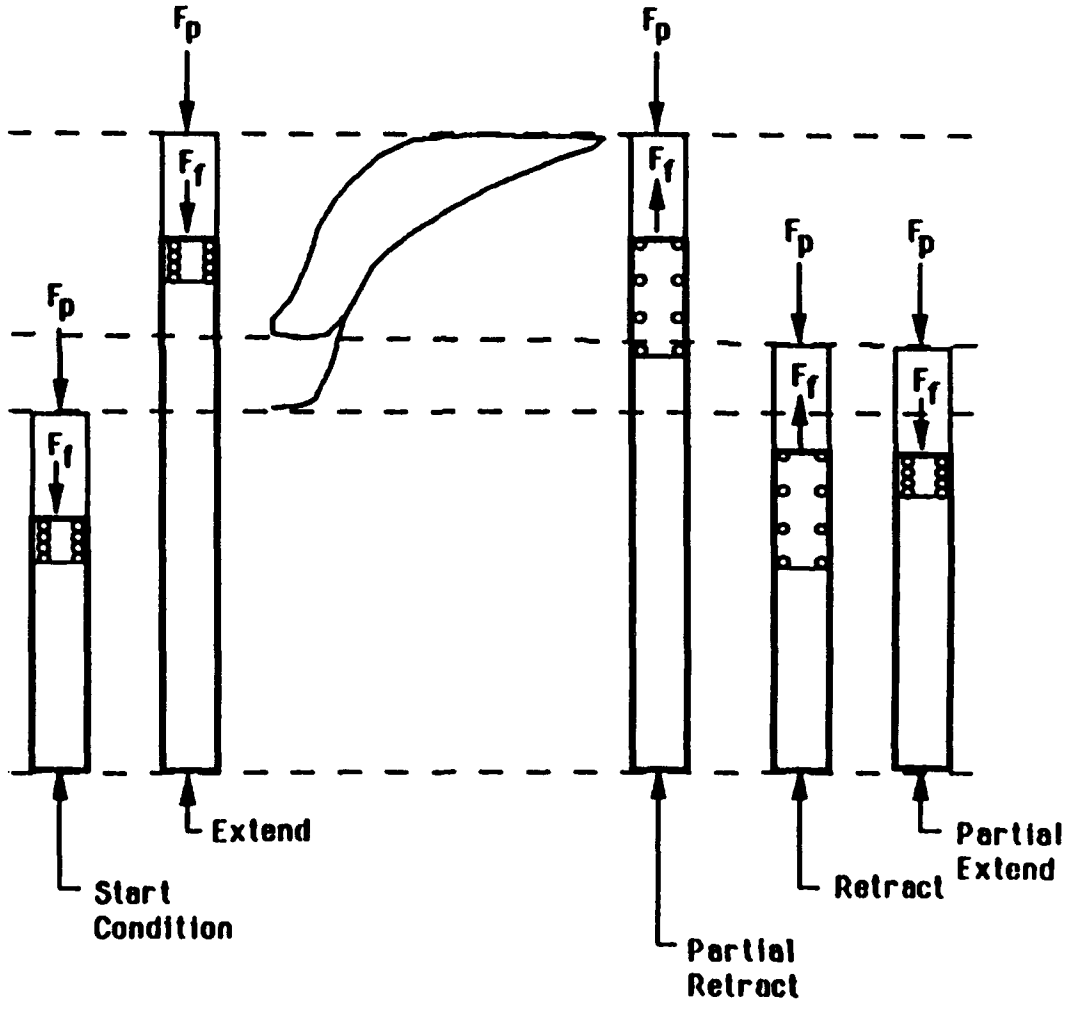
Fp
Ff
Fp
Ff
Fp
Ff
Fp
Ff
Fp
Ff
Start Condition
Extend
Partial Retract
Retract
Partial Extend

ANALYSIS AND TESTS SHOW THAT NON-RETURN TO ZERO AND STROKE LOSS ARE A FUNCTION OF PZA STACK COMPLIANCE AND EMA FRICTION.

- ACTIONS BEING TAKEN TO REDUCE PZA STACK COMPLIANCE:

  LAP STACK ENDS SMOOTH, FLAT AND PERPENDICULAR TO THE FACT BORE MOLD LINE

  TEST LARGER DIAMETER STACKS WITH REDUCED L/D AND LOWER UNIT STRESS

- ACTIONS BEING TAKEN TO MINIMIZE EMA FRICTION LOADING:

  SUBSTITUTE NON-ABRASIVE POLYURETHANE FOR CONAP MATERIAL

  TEFLON COAT PISTON AND ANVIL SLIDING SURFACES

  LOWER STP VISCOSITY BY DILUTION

CRYOCOOLER VIBRATION ISOLATION

JPL

Robert J. Glaser
(818) 354-5404
FTS 792-5404

Jet Propulsion Laboratory
4800 Oak Grove Dr MS157-316
Pasadena, California 91109

JPL

FLIGHT CONFIGURATION

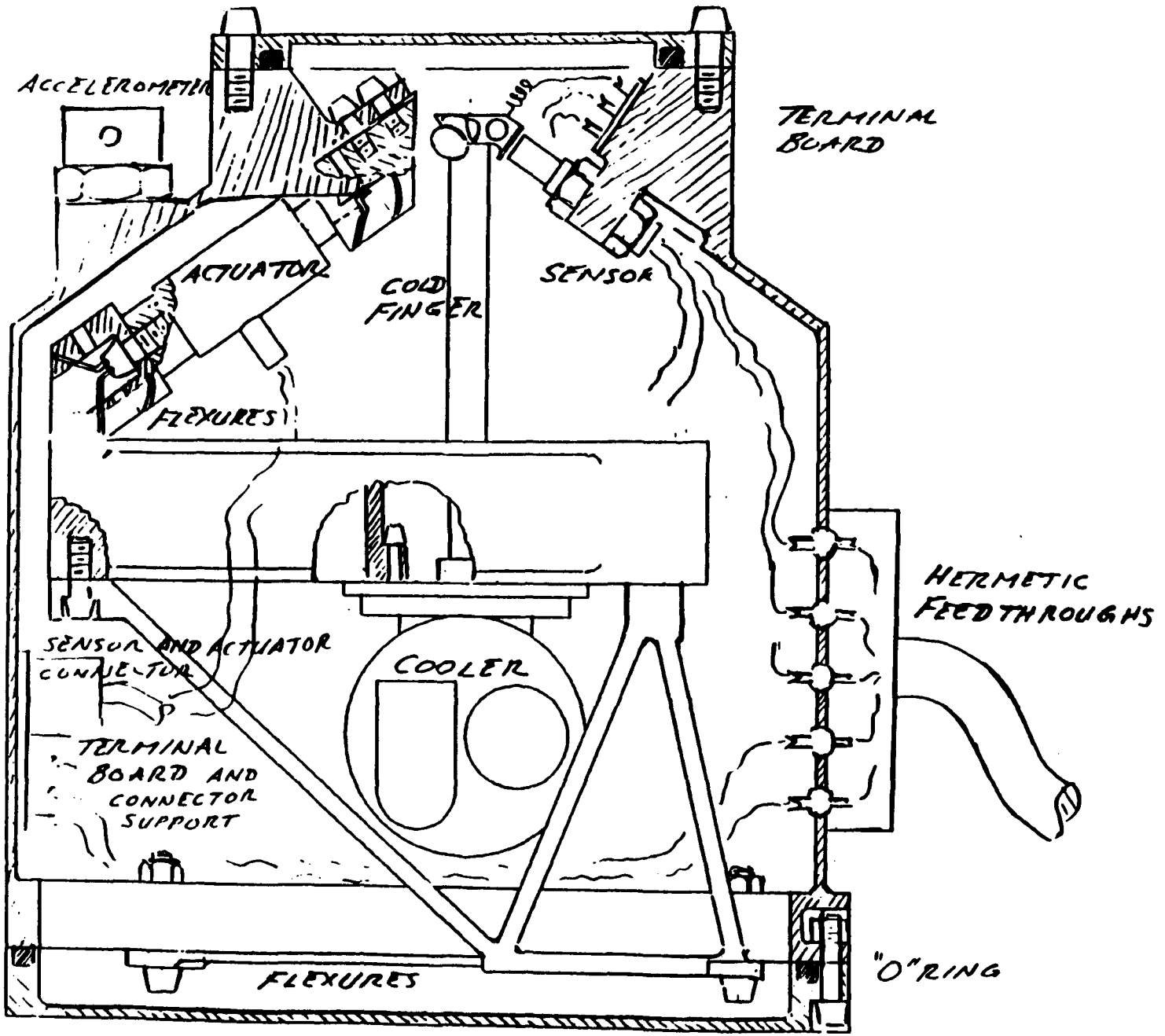

JPL

ACTUATORS

- **Physik P-842.10 Low Voltage Piezo Translator (LVPZ):**
  - Operating voltage -20 V to +120 V — We are operating 0 V to +28 V
  - Nominal expansion -3 μm to 18 μm — We are operating 0 μm to 4.2 μm
  - Preload 300 N (67.4 lb) — Critical for launch
  - Operating temperature -20 °C to +80 °C — Must limit low temperature operation Spacecraft between -50 °C to +50 °C
  - Poling temperature +80 °C
  - Maximum pushing force 800 N (180 lb) — We are operating 231 N (52 lb)
  - Maximum pulling force 300 N (67.4 lb) — We are operating 0 lb
  - Stiffness 55 N/μm (314,000 lb/in) — Flexures are much softer
  - Capacitance 1.8 μF — Key for power

- **Special Order:**
  - Vacuum holes and torr seal
  - Extreme temperature option
  - Lower screw thread is an M4

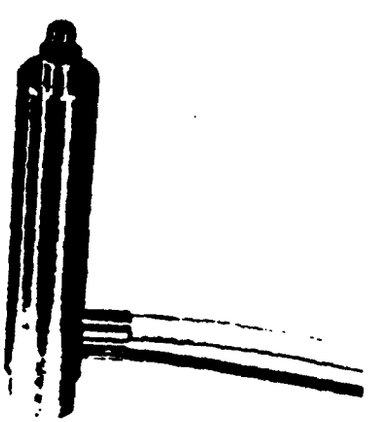

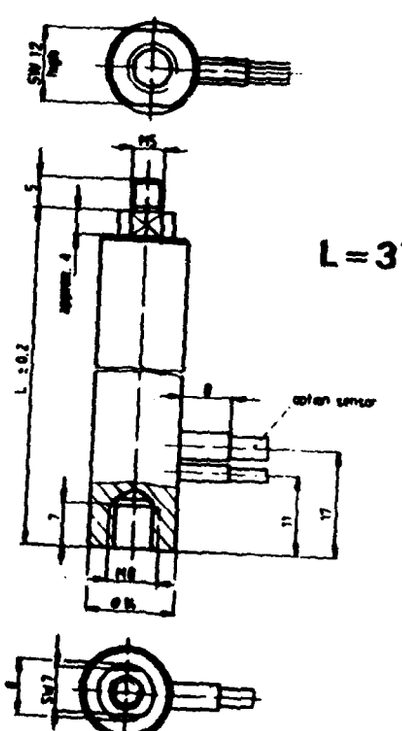

L = 37 mm (1.457 in)

APPLIQUE CERAMICS

- **Vernitron PZT-5H (Navy Type VI) for high d_{31} motion**

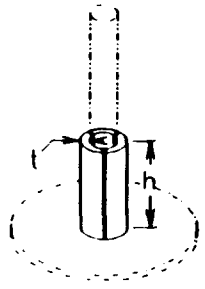

MIN h

Subject to:

1) *Power*(V,h,t): $\dfrac{C(h,t)\,V^2 f}{\eta(V)} \le P_{max}$

2) *PolingVoltage*(V,t): $V \le r\,p\,t$

3) *MinimumThickness*(t): $t \ge t_{min}$

4) *Displacement*(V,h,t): $d_{31}\dfrac{Vh}{t}\,g\,S(t) \ge x$

$$C(h,t) = 2K\epsilon_0\pi\frac{h}{\ln(OD/ID)} \approx 2K\epsilon_0\pi\frac{h}{t}R$$

$$\eta(V) \approx -.152\ln\frac{V}{3162} \qquad \begin{matrix}\eta(100) = .75\times.70 \\ \eta(1000) = .25\times.70\end{matrix}$$

$$S(t) = \frac{A_c E_c}{A_c E_c + A_s E_s} \approx \frac{E_c t}{E_c t + E_s w}$$

Design Parameters:
- h = height of the ceramic
- t = thickness of the ceramic
- V = voltage applied across the ceramic

Design objectives:
- P_{max} = power objective = 1.0 Watt
- x = displacement objective = 2.9527559×10^{-6} inches

Ceramic properties:
- d_{31} = piezo effect = 1.07874×10^{-8} inches/volt
- ϵ_0 = dielectric constant = 2.2479×10^{-13} farads/inch
- E_c = Young's modulus = 6.96×10^{6} psi
- K = dielectric ratio = 3400 (dimensionless)
- t_{min} = minimum thickness = 1.96853×10^{-2} inches

Cooler/Cold Finger:
- E_s = Young's modulus = 30×10^{6} psi
- f = frequency cooler operates at = 50 Hz
- R = radius of the cold finger = 0.125 inches
- w = wall thickness of cold finger = 0.004 inches

Processes:
- p = poling voltage ratio = 40×10^{3} volts/inch
- r = ratio of usable to poling voltage = 0.5 (dimensionless)
- g = displacement through the glue = 0.33333 (dimensionless)

JPL

OPTIMIZATION RESULTS

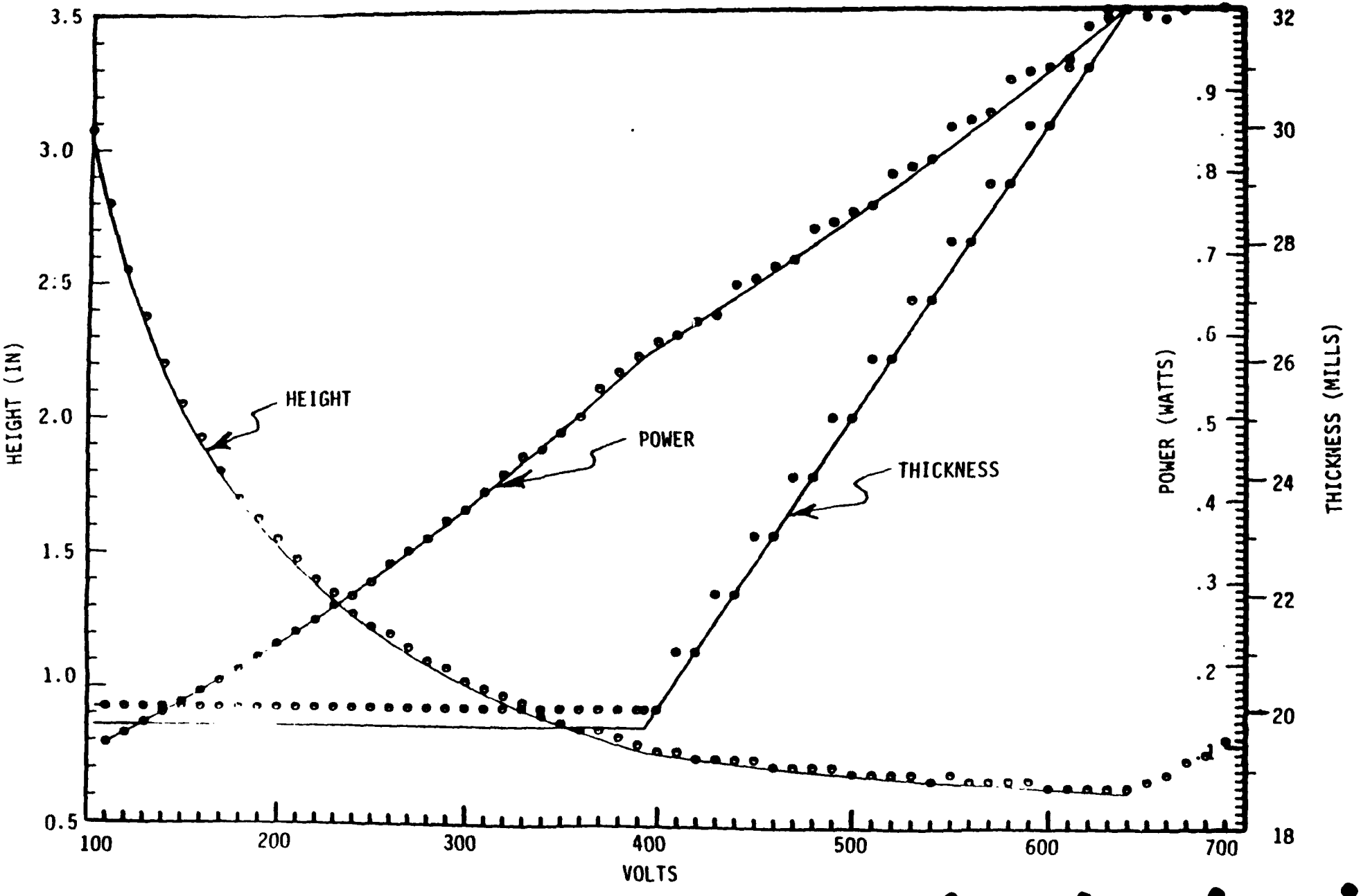

LAUNCH ENVIRONMENT

QUASI-STATIC LOADING

Worst three cases	Longitudinal	Lateral
Max Dynamic Pressure	-3g	±1.5g
Before Thrust Termination	-7g	±1g
During Thrust Tail Off	+2.5g	±1g
Safety Factors	1.25 ultimate	1.1 yield

DYNAMIC LOADING

Sinusoidal Vibration Test	Frequency range (Hz)	Qualification levels (0-peak)	Acceptance levels (0-peak)
Longitudinal	5-6 6-35 35-100	17.3mm 17.3mm 2.5g	10.4mm 2.25g 1.5g
Lateral	5-100	1g	0.8g
Sweep rate (Oct./min)		2 Oct./min	4 Oct./min

Random Vibration Test	Frequency range (Hz)	Density (g2/Hz)	RMS value (g)
Qualification Levels	30-150 150-700 700-2000	+6dB/Oct 0.2 -3dB/Oct	15.9
Acceptance Levels	30-150 150-700 700-2000	+6dB/Oct 0.1 -3dB/Oct	11.2

JPL

WISH LIST

- Lead time from Vernitron is a problem.
  - Flight project with an accelerated schedule.
  - Largely JPL's fault, the design changes after the order is placed.
  - Vernitron would sell JPL more ceramics if we got them sooner.
  - Very difficult to do any development work on the ceramics.
- Low-power flight power-supplies need work.
  - System is about 5% dissipative, should recover 90% of the power.
  - LC approach doesn't work when the coil needs to be >1 Henry.
  - Simulate a coil with operational amplifiers?
  - We need a less restrictive approach.
- Preload on the actuators never seems to be enough.
- Flexures don't come with the actuators.

Workshop on Advanced Piezoelectric Actuator materials for Space Applications, Arlington, VA ; Februarary 25, 1992

APPLICATION OF PIEZOELECTRIC MATERIALS TO MECHANICAL RESPONSE CONTROL

Vijay K. Varadan and Vasundara V. Varadan

Alumni Distinguished Professors of Engineering
Center for the Engineering of Electronic and Acoustic Materials

Pennsylvania State University, University Park, Pa

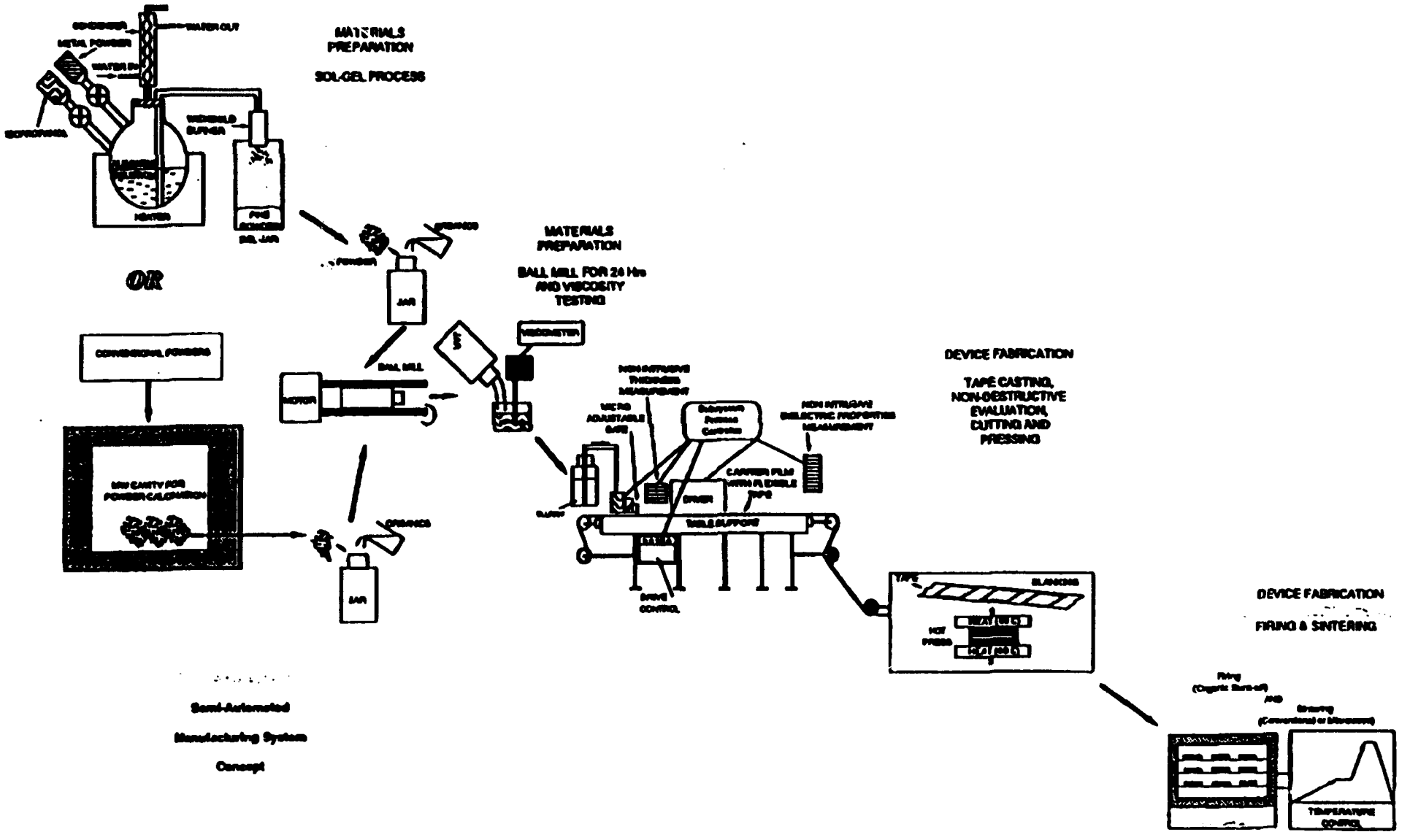

Semi-Automated Manufacturing System Concept

@ TAPE CASTING

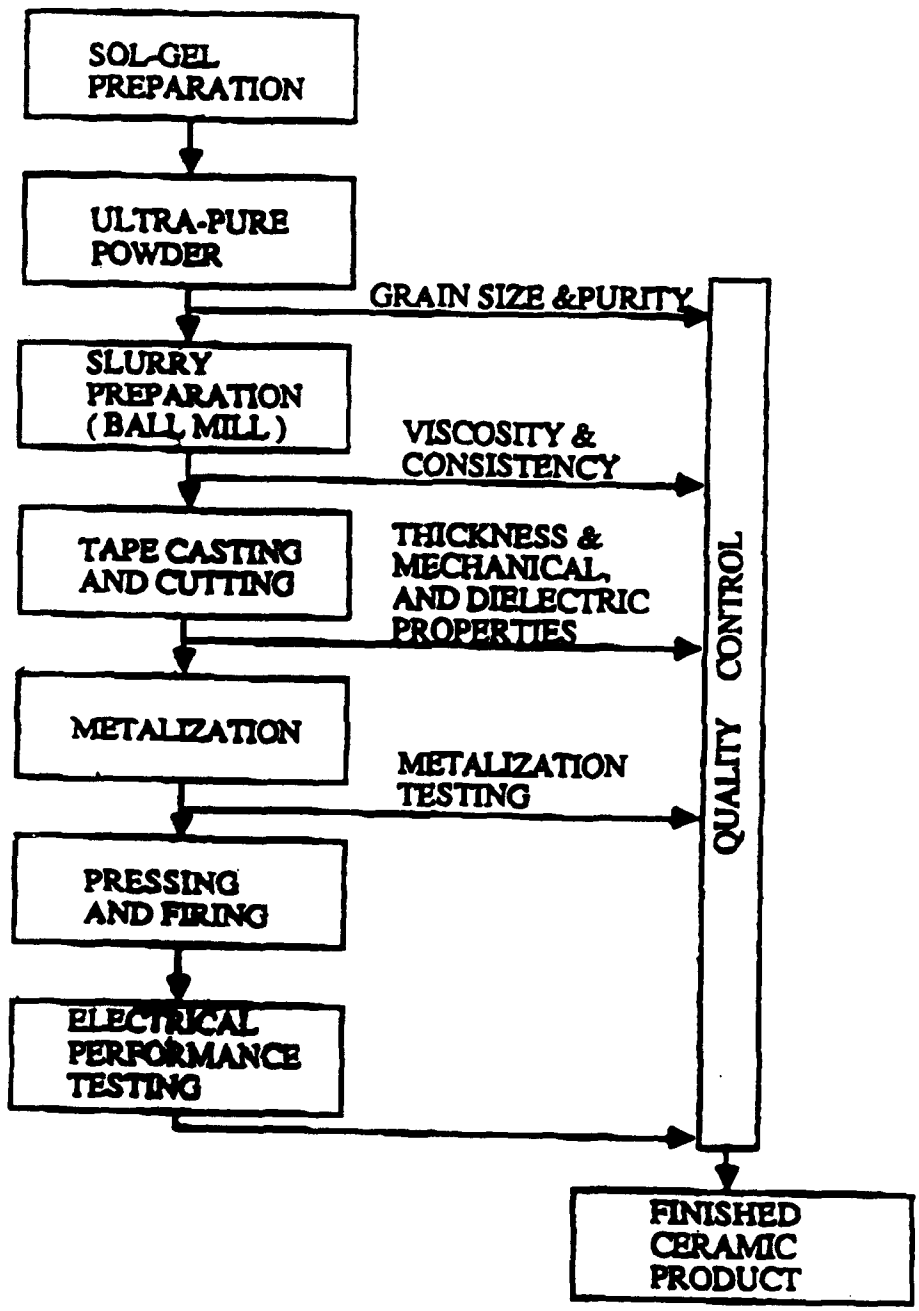

Starting powders

↓

Mix powders and binders

↓

Cast tape

↓

Cut

↓

Screen print electrodes

↓

Burn out binder

↓

Sinter

↓

Terminate

↓

Attach leads

↓

Encapsulate

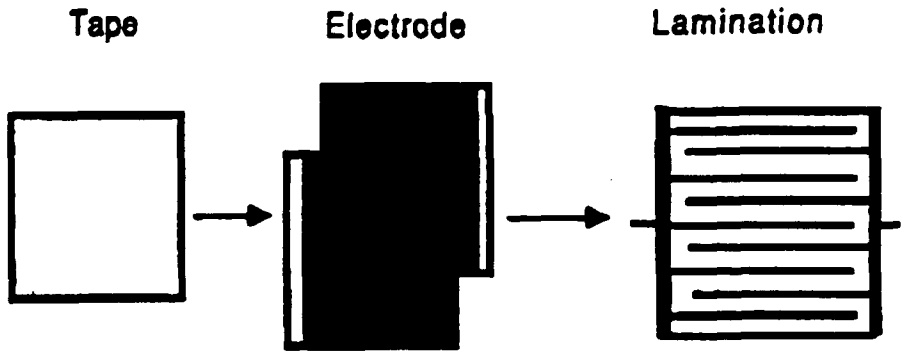

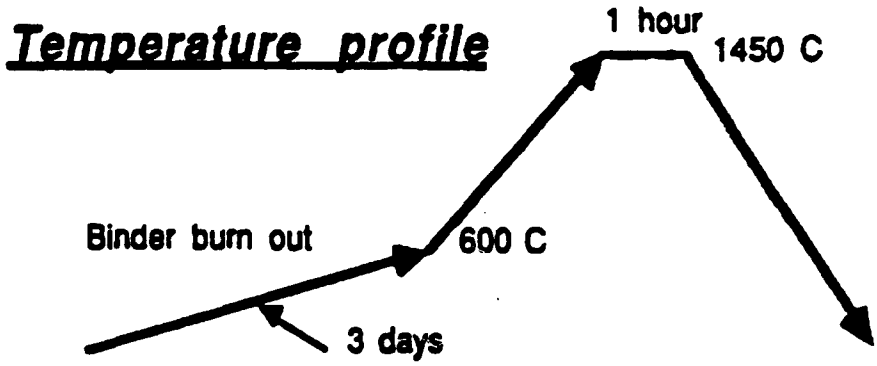

MW 40 - 45 min.

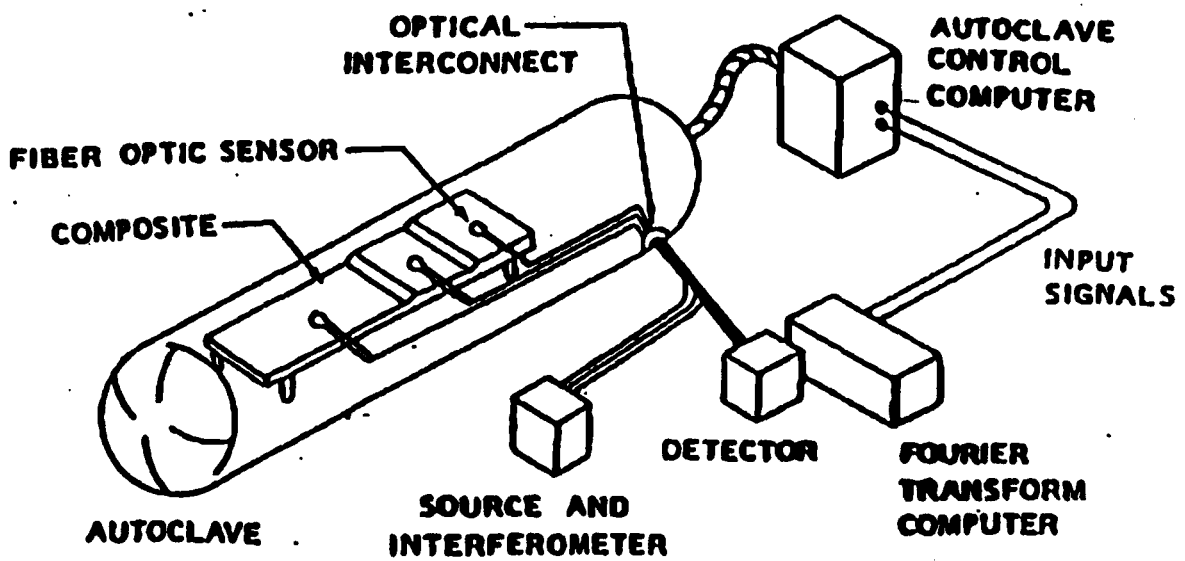
OPTICAL
INTERCONNECT
AUTOCLAVE
CONTROL
COMPUTER
FIBER OPTIC SENSOR
COMPOSITE
INPUT
SIGNALS
DETECTOR
FOURIER
TRANSFORM
COMPUTER
AUTOCLAVE
SOURCE AND
INTERFEROMETER

Figure 1: Setup for the Microwave Repair System

MICROWAVE REPAIR - SYSTEM FOR ADVANCED COMPOSITES:

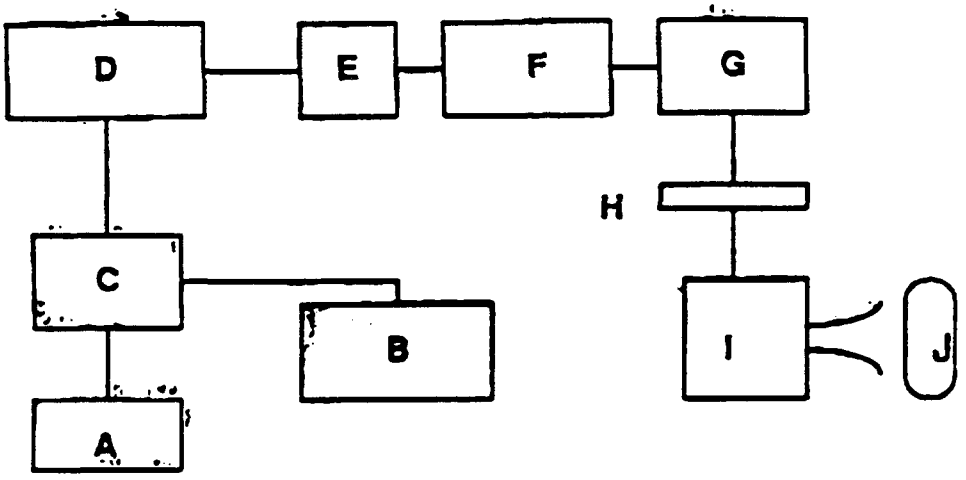

A.....D.C. Supply Source

B.....110 V A.C. Supply

C.....Power-Supply

D.....Microwave-Power Generator

E.....Ferrite Isolator

F.....Forward / Reflected Power Indicator

G.....Tuner

H.....Variable-Coupling Iris

I.....Applicator

J.....Material Under Process/Repair

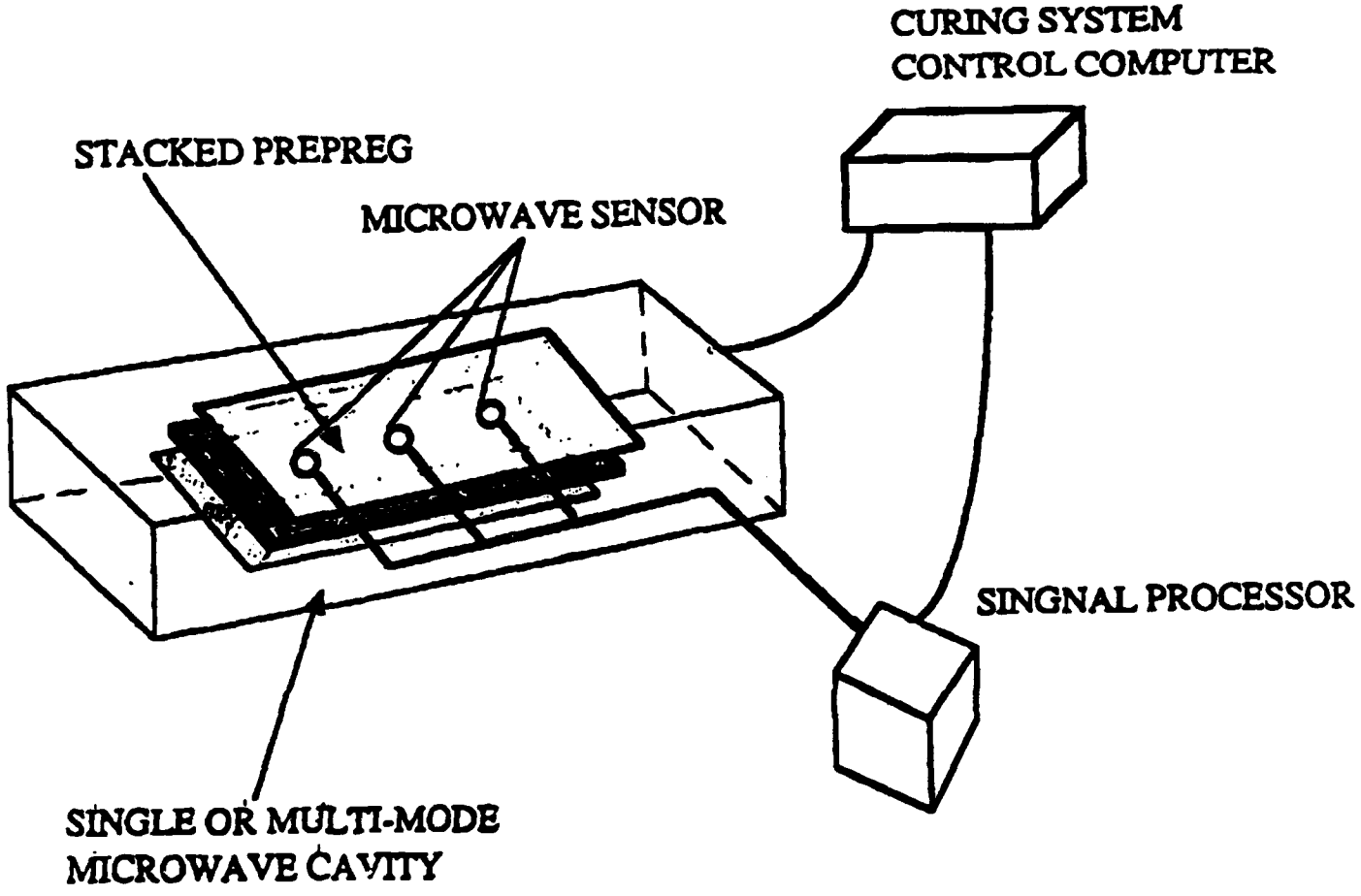
CURING SYSTEM
CONTROL COMPUTER
STACKED PREPREG
MICROWAVE SENSOR
SINGNAL PROCESSOR
SINGLE OR MULTI-MODE
MICROWAVE CAVITY

Portable Applicator

Large Area Joining

Advantages:

- Large Area Processing
- Product Dissassembly
- High Safety Constraints

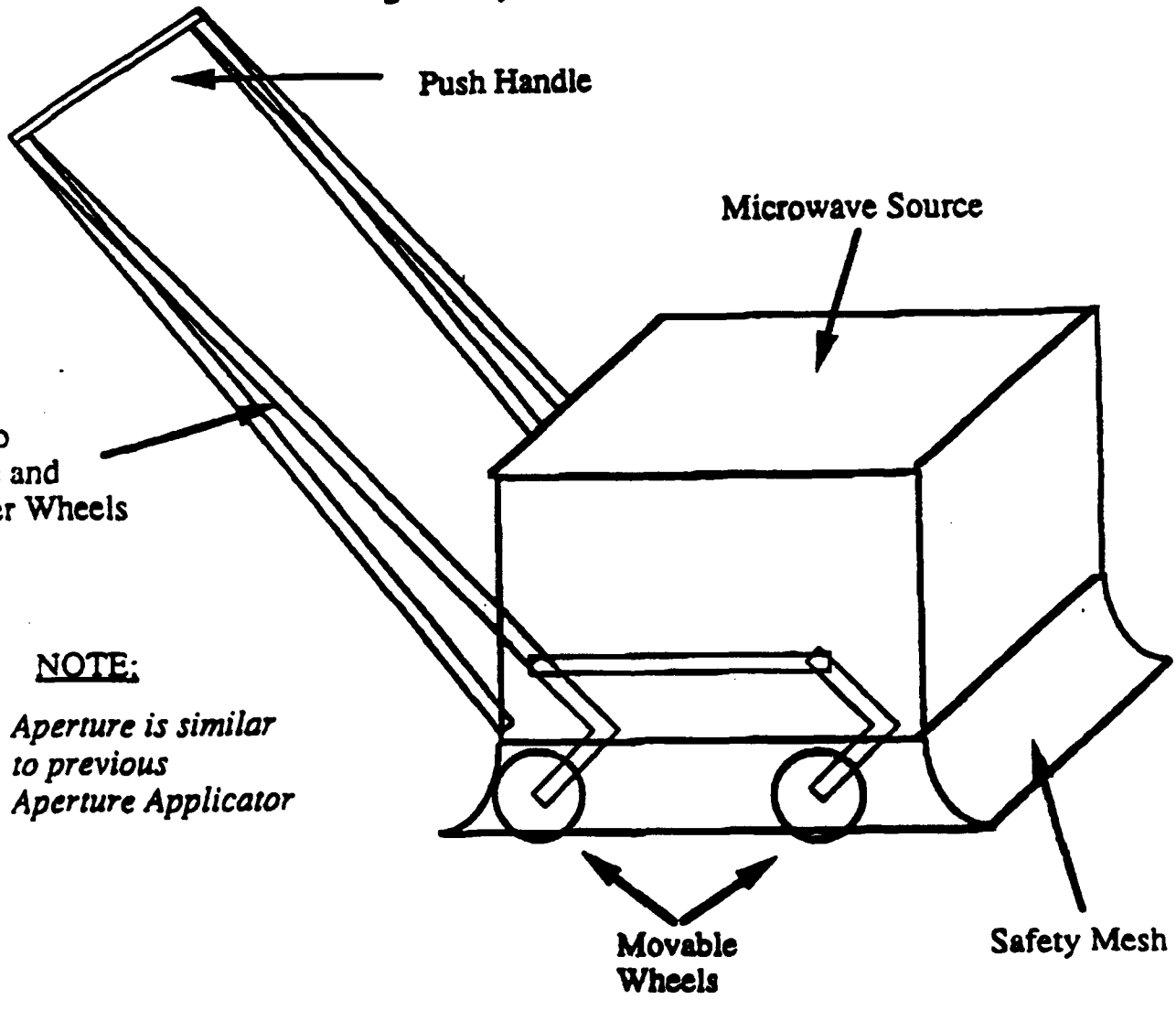

NOTE:

Aperture is similar to previous Aperture Applicator

Safety Devices: Movable Wheels for good sheet contact

Surrounding Mesh Protector

Automatic Shut-off when lifted from surface

Taper Applicator
Strip Joining

Advantages:
- High Field Concentration
- Fast Heating Rate
- Easy Material Handling

Taper Applicator with Supporting Equipment

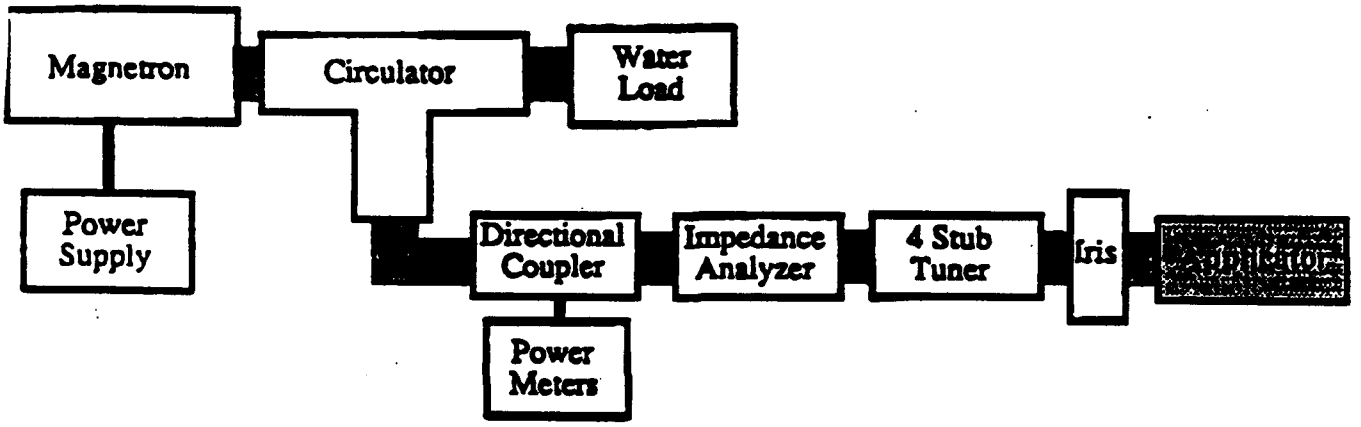

Enlargement of Taper Applicator

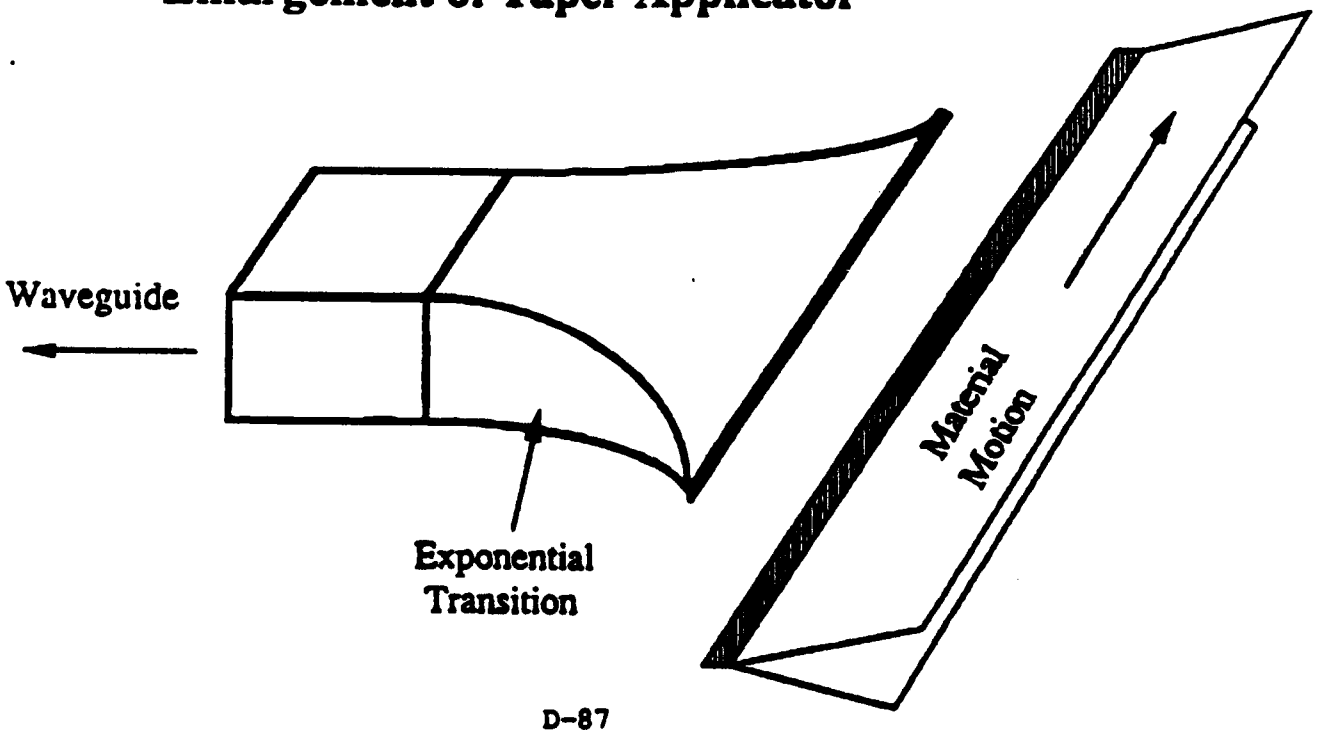

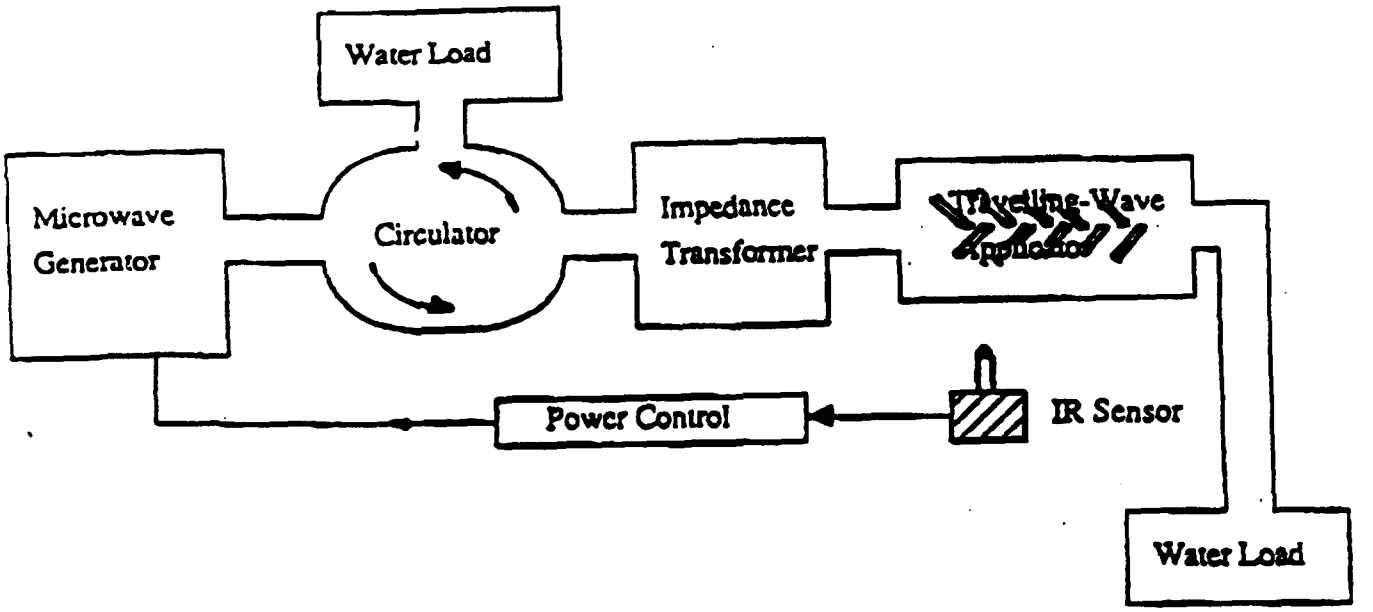

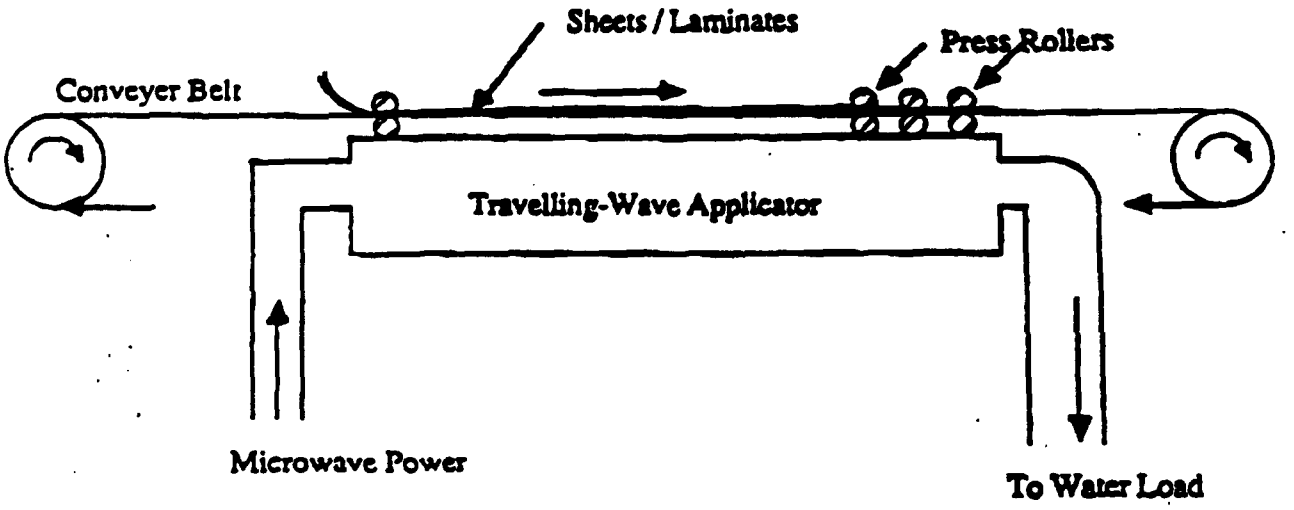

Microwave Heating and Joining/Sealing of Sheets / Laminates

Smart Skin

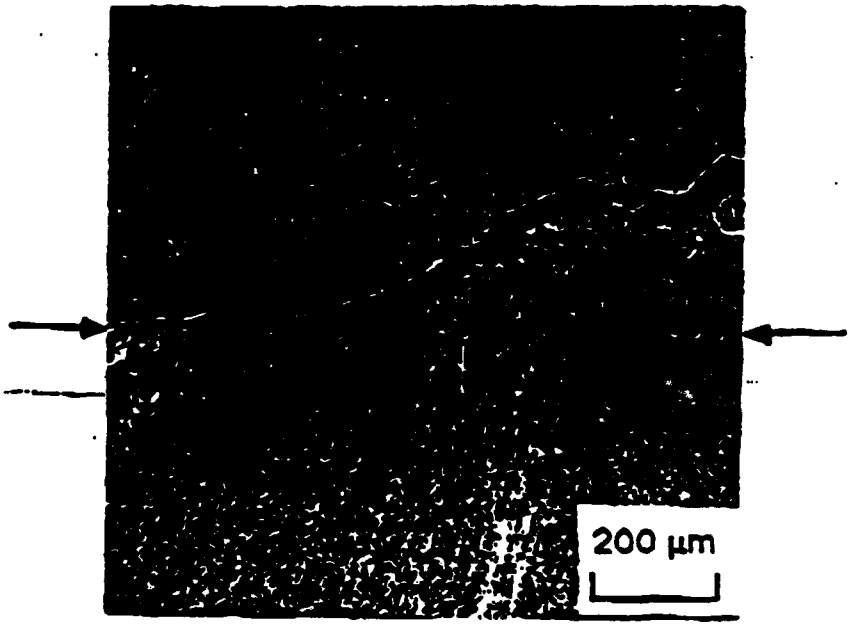
200 µm

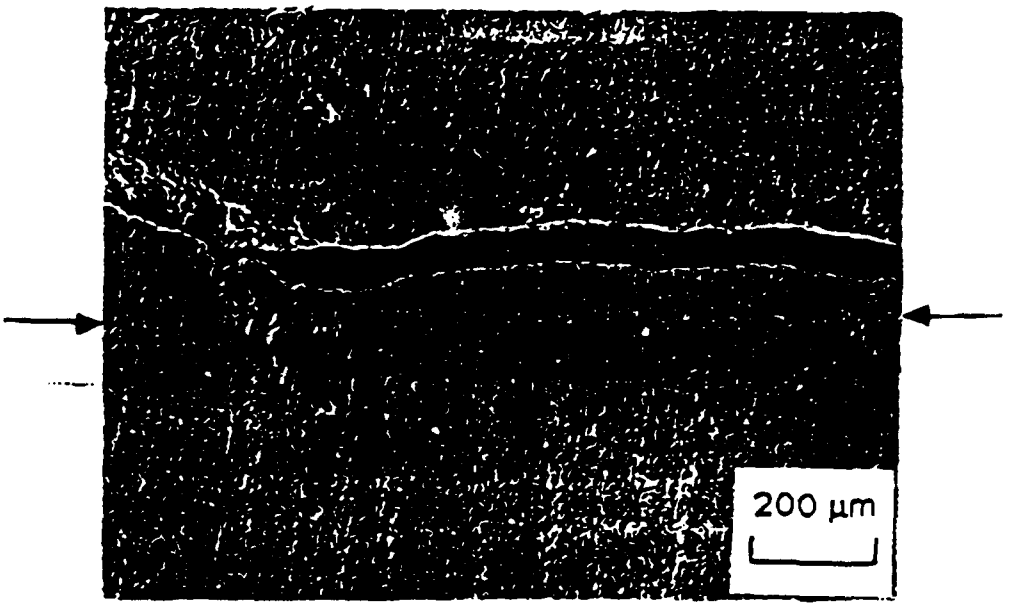
200 µm

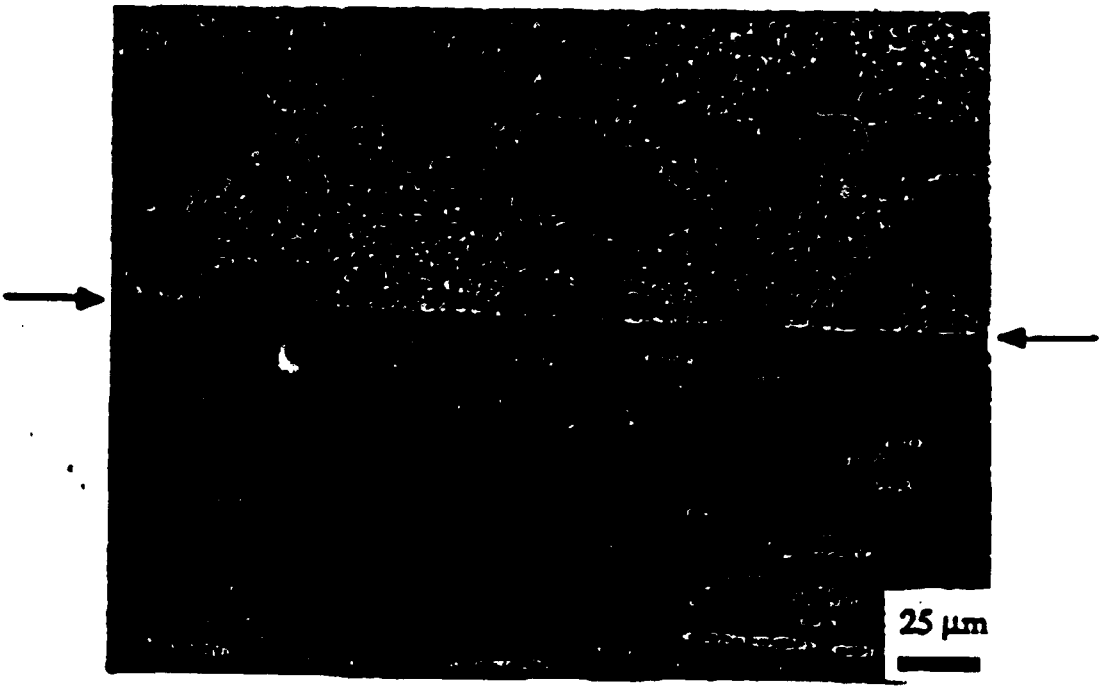
25 µm

APPENDIX E

HIGH STRAIN ACTUATORS

HIGH STRAIN ACTUATORS

SOLID STATE ACTUATORS

TYPE OF ACTUATOR	NATURE OF THE TRANSDUCTION	PHENOMENA EXPLOITED.
Shape Memory Alloys	Thermo-Mechanical	Ferroelastic Phase Change.
Piezoelectric	Electro-Mechanical Opto-Electro-Mechanic	Ferroelectricity in a poled ceramic or polymer.
Electrostriction	Electro-Mechanical	Incipient Ferroelectricity in a spin glass.
Contractile Polymers	Chemo-Mechanical Electro-Mechanical Thermo-Mechanical Opto-Mechanical	Differs in different types.
Muscle	Electro-Mechanical	Action potential pulses.

POLARIZATION CHANGE MECHANISMS USED TO CONTROL ELECTROSTRICTIVE STRAIN.

INDUCED POLARIZATION INCREASING

(a) Homogeneous polarization of a Paraelectric Phase

$E = 0 \quad \bar{P} = 0 \quad \sqrt{\overline{P^2}} = 0 \quad P \propto E.$
Stable zero strain state.

• (b) Induced polarization in a Relaxor ferroelectric

$E = 0 \quad \bar{P} = 0 \quad \sqrt{\overline{P^2}} \neq 0 \quad P \not\propto E$
Stable zero strain state.

Conventional Electrostrictor.

• (c) Induced Polarization change in Poled Ceramic

$E = 0 \quad \bar{P} = P_R \quad \sqrt{\overline{P^2}}_{ind} \simeq 0 \quad P_{ind} \propto E.$
Unstable zero strain state (Aging change of P_R).

Conventional Piezoelectric.

(d) Micro => Macrodomain Poled Relaxor

$E = 0 \quad \bar{P} = 0 \quad \sqrt{\overline{P^2}} \neq 0$ P vs E Hysteretic
Stable zero strain state

(e) Field forced Phase Change

$E = 0 \quad \bar{P} = 0 \quad \sqrt{\overline{P^2}} = 0$ P vs E Double Hysteretic
Stable or unstable depending on system

(f) Field Forced Domain Change

$E = 0 \quad \bar{P} = 0 \quad \sqrt{\overline{P^2}} \neq 0$ P vs E Hysteretic
Unstable zero strain state

THINKING BEHIND THE STUDY

The useable phenomena in the electrical control of the dimensions of an insulating solid are piezoelectricity and electrostriction.

$$x_{ij} = s_{ijkl}X_{kl} + b_{m\ ij}P_m + Q_{mnij}P_mP_n$$

where x_{ij} are the components of the strain tensor
X_{kl} are components of the stress tensor
P_mP_n are components of electric polarization
s_{ijkl} the elastic compliances
b_{mij} the polarization related piezoelectric constants
Q_{mnij} the polarization related electrostriction constants

1) No know solid has high enough values of b_{mij}, Q_{mnij} to permit the induction by external field of P_mP_n values sufficient to generate 1% strain.

2) In ferroelectric crystals values of spontaneous polarization P_s are large enough to give spontaneous strains up to 15%.

3) We must therefore either
a. explore phase changes which take us from a non-polar into a ferroelectric state $P = O$ to $P = P_s$;
b. explore domain changes in ferroelectric crystals which reorient the spontaneous strain.

4) From equation I if P_mP_n are homogeneous throughout the solid large values of strain x_{ij} may be induced at ZERO STRESS. Thus even in brittle solids, as with thermal expansion, large induced strains are theoretically possible without breaking the solid.

TOPICS OF STUDY AT PENN STATE MATERIALS RESEARCH LABORATORY

* Field Forced Switching from Antiferroelectric to Ferroelectric Phases in Lead Lanthanum Zirconate Titanate Stannate Ceramics

* Field Forced Microdomain to Macrodomain Switching in Compositions of Lead Lanthanum Zirconate Titanate Close to the Morphotropic Phase Boundary

* Field Force Paraelectric to Ferroelectric Switching in Single Crystal Barium Titanate

* Domain Switching in $BaTiO_3$ Single Crystals
  Single Field 90° Domain Switching
  Orthogonal Field 90° Domain Switching

* Switching of Lamellar Wedge Domains in $BaTiO_3$ Crystals to Produce Ultra-high Strain Bimorph Configuration

ANTIFERROELECTRIC to FERROELECTRIC SWITCHING.

TABLE 1: COMPOSITIONS AND REFERENCE NUMBERS

No	Composition
4	$Pb_{.97}La_{.02}(Zr_{.66}Ti_{.09}Sn_{.25})O_3$
5	$Pb_{.97}La_{.02}(Zr_{.53}Ti_{.12}Sn_{.35})O_3$
6	$Pb_{.97}La_{.02}(Zr_{.66}Ti_{.11}Sn_{.23})O_3$
7	$Pb_{.97}La_{.02}(Zr_{.66}Ti_{.105}Sn_{.235})O_3$
8	$Pb_{.97}La_{.02}(Zr_{.64}Ti_{.09}Sn_{.27})O_3$
9	$Pb_{.97}La_{.02}(Zr_{.64}Ti_{.11}Sn_{.25})O_3$
10	$Pb_{.97}La_{.02}(Zr_{.62}Ti_{.11}Sn_{.27})O_3$
11	$Pb_{.97}La_{.02}(Zr_{.68}Ti_{.09}Sn_{.23})O_3$
12	$Pb_{.97}La_{.02}(Zr_{.60}Ti_{.1}Sn_{.3})O_3$
13	$Pb_{.97}La_{.02}(Zr_{.575}Ti_{.1125}Sn_{.3125})O_3$
14	$Pb_{.97}La_{.02}(Zr_{.55}Ti_{.1}Sn_{.35})O_3$

T1
85
90
95
Sn
50
55
60
65
70
75
Zr
Fr
AT
#5
#13
#10
#9
#7
#6
#14
#12
#8
#4
#11

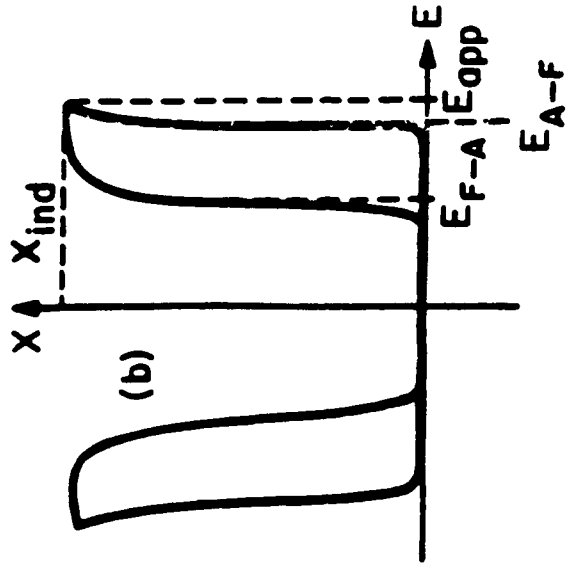
E
E_{app}
E_{A-F}
E_{F-A}
X_{ind}
X
(b)

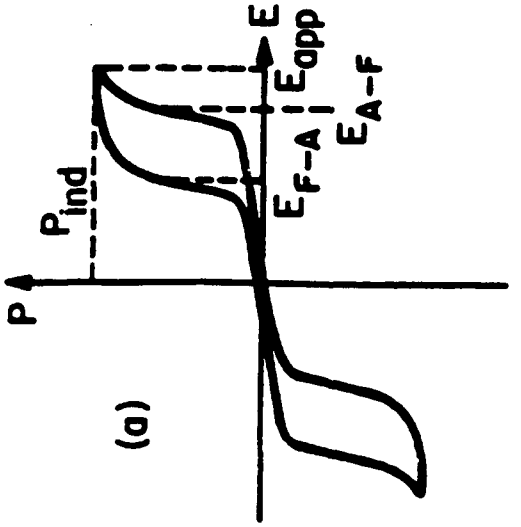
E
E_{app}
E_{A-F}
E_{F-A}
P_{ind}
P
(a)

Table II: Switching Data for Different Compositions

(a) Group 1 Compositions

No	P(uC/cm^2)	E_{A-F} (Kv/cm)	E_{app} (Kv/cm)	$x_{1(Ind)}$
5	30	30	35	0.18%
13	28	30	43	0.45%
10	36	28	60	0.5%
9	36	24	60	0.59%
7	36	22	58	0.52%
6	40	21	46	0.87%

(b) Group 2 Compositions

No	P (uC/cm^2)	E_{A-F} (Kv/cm)	E_{app} (Kv/cm)	$x_{1(Ind)}$
14	31	44	56	0.35%
12	32	49	59	0.42%
8	30.5	52	68	0.37%
4	43	50	75	0.55%
11	33	45	60	0.45%

Forward switching in composition #5

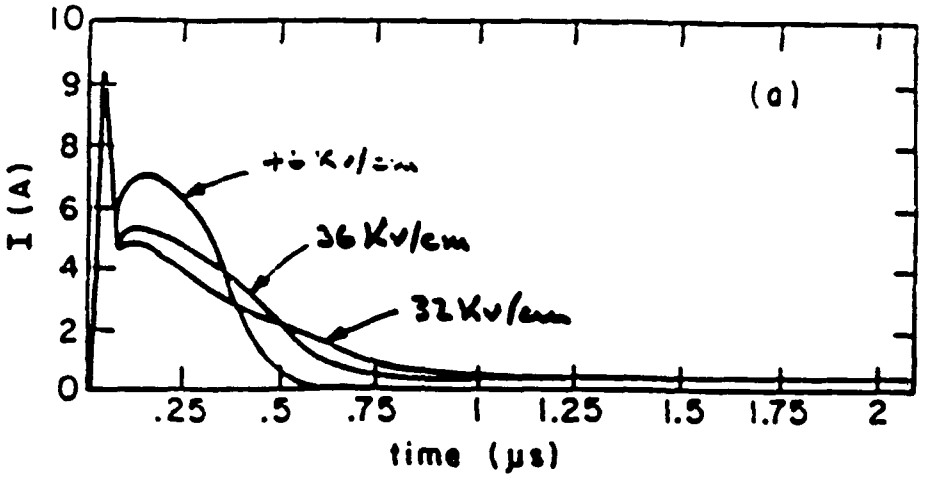

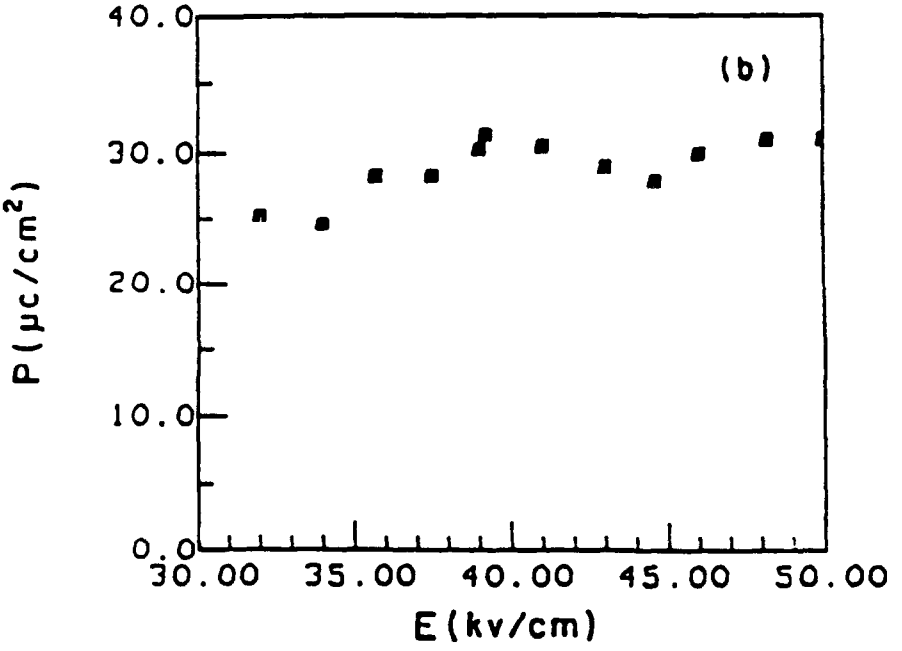

(a) A set of switching current -time curves under various applied fields
(b) charges obsorbed per unit sample area due to switching as a funcion of applied field for $Pb_{0.97}La_{0.02}(Zr_{0.66}Ti_{0.09}Sn_{0.25})O_3$ ceramic samples.

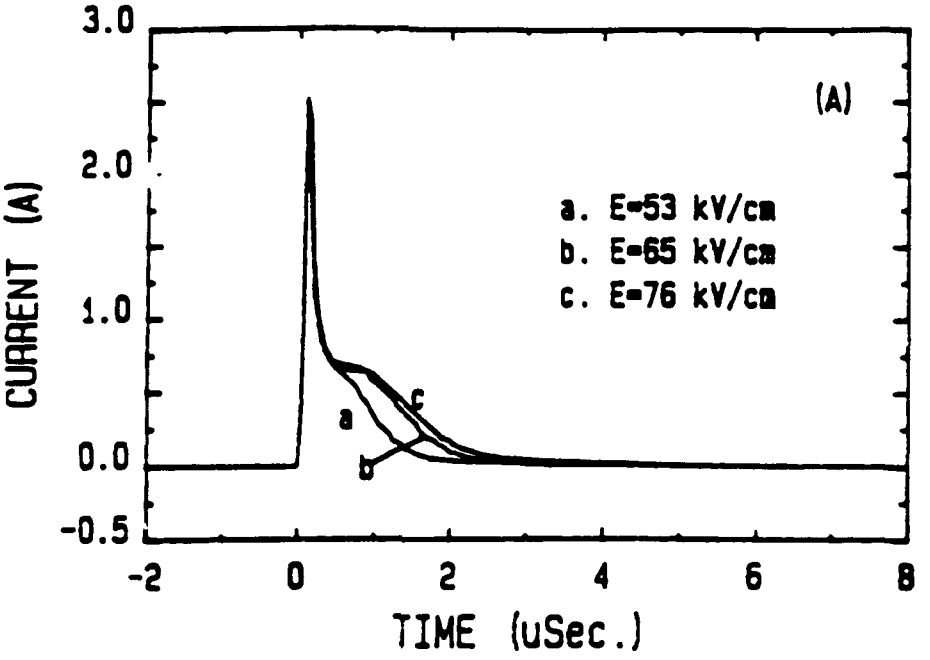

Backward Switching in composition #4, Field dependence

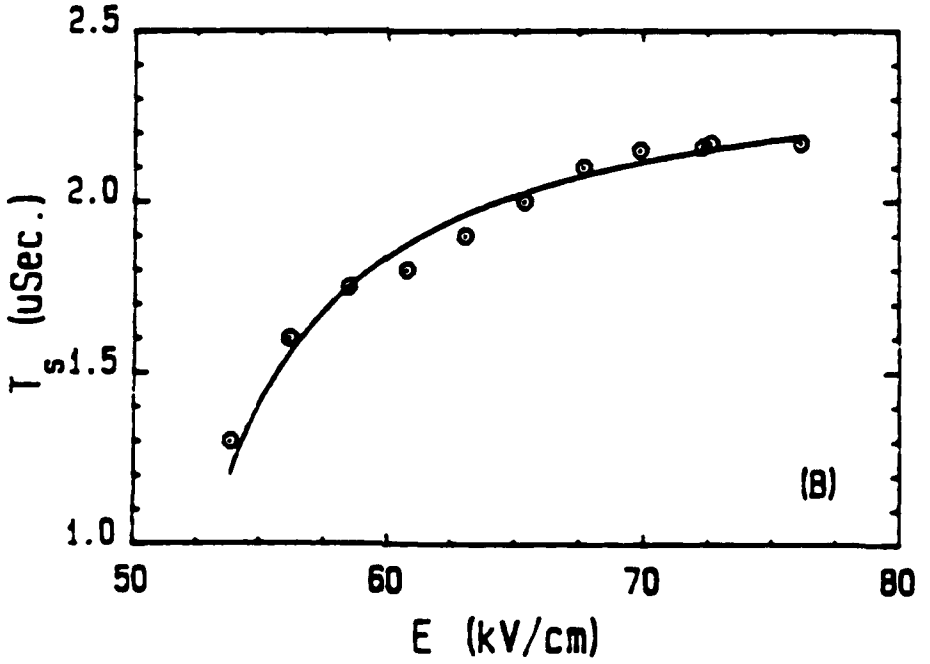

F-24

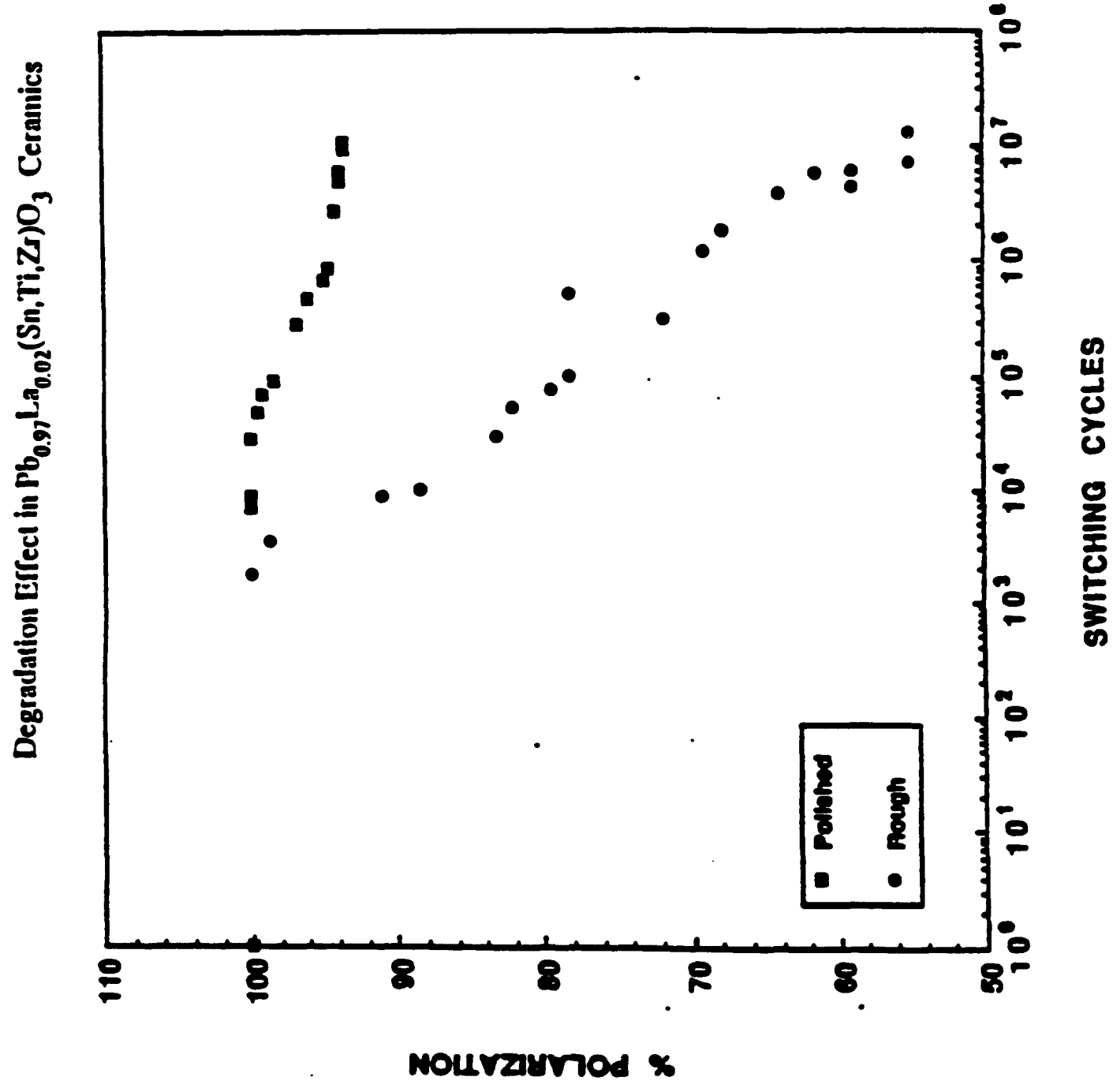
Degradation Effect in $Pb_{0.97}La_{0.02}(Sn,Ti,Zr)O_3$ Ceramics
% POLARIZATION
SWITCHING CYCLES
Polished
Rough
110
100
90
80
70
60
50
10^0
10^1
10^2
10^3
10^4
10^5
10^6
10^7
10^8

MICRODOMAIN to

MACRODOMAIN SWITCHING.

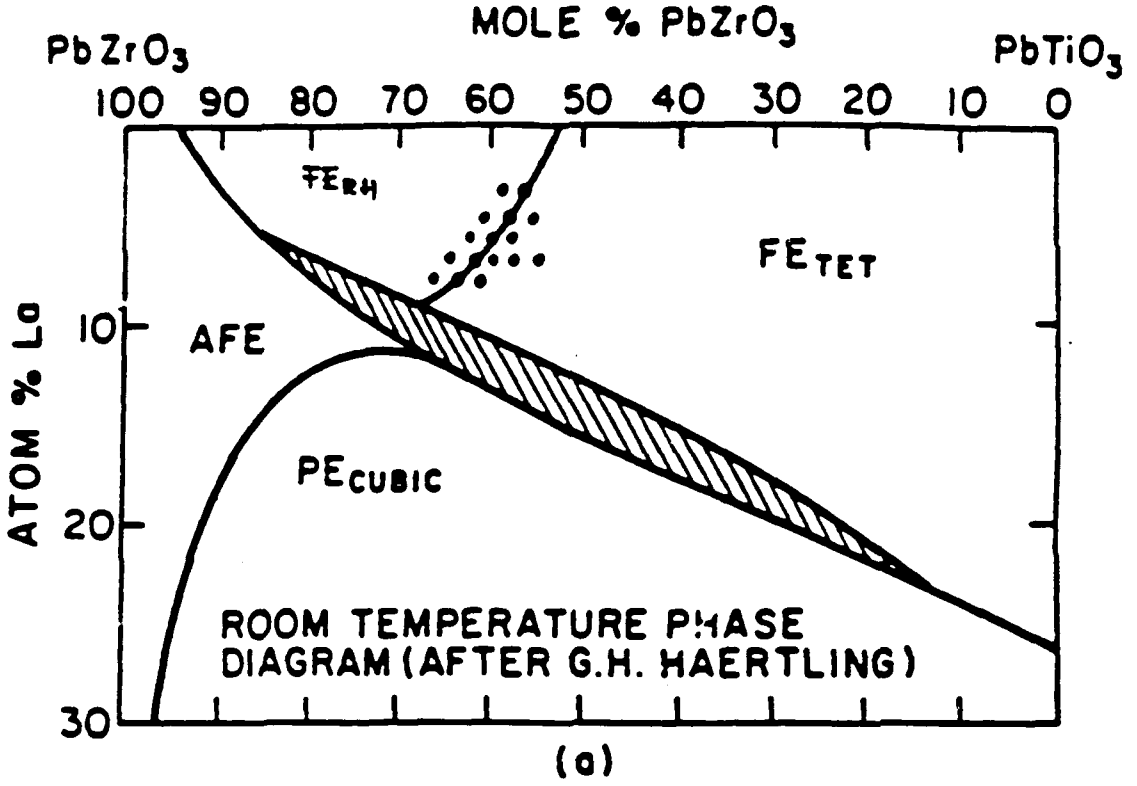
MOLE % PbZrO3
PbZrO3
PbTiO3
100 90 80 70 60 50 40 30 20 10 0
FERH
FETET
AFE
PECUBIC
ATOM % La
10
20
30
ROOM TEMPERATURE PHASE DIAGRAM (AFTER G.H. HAERTLING)
(a)

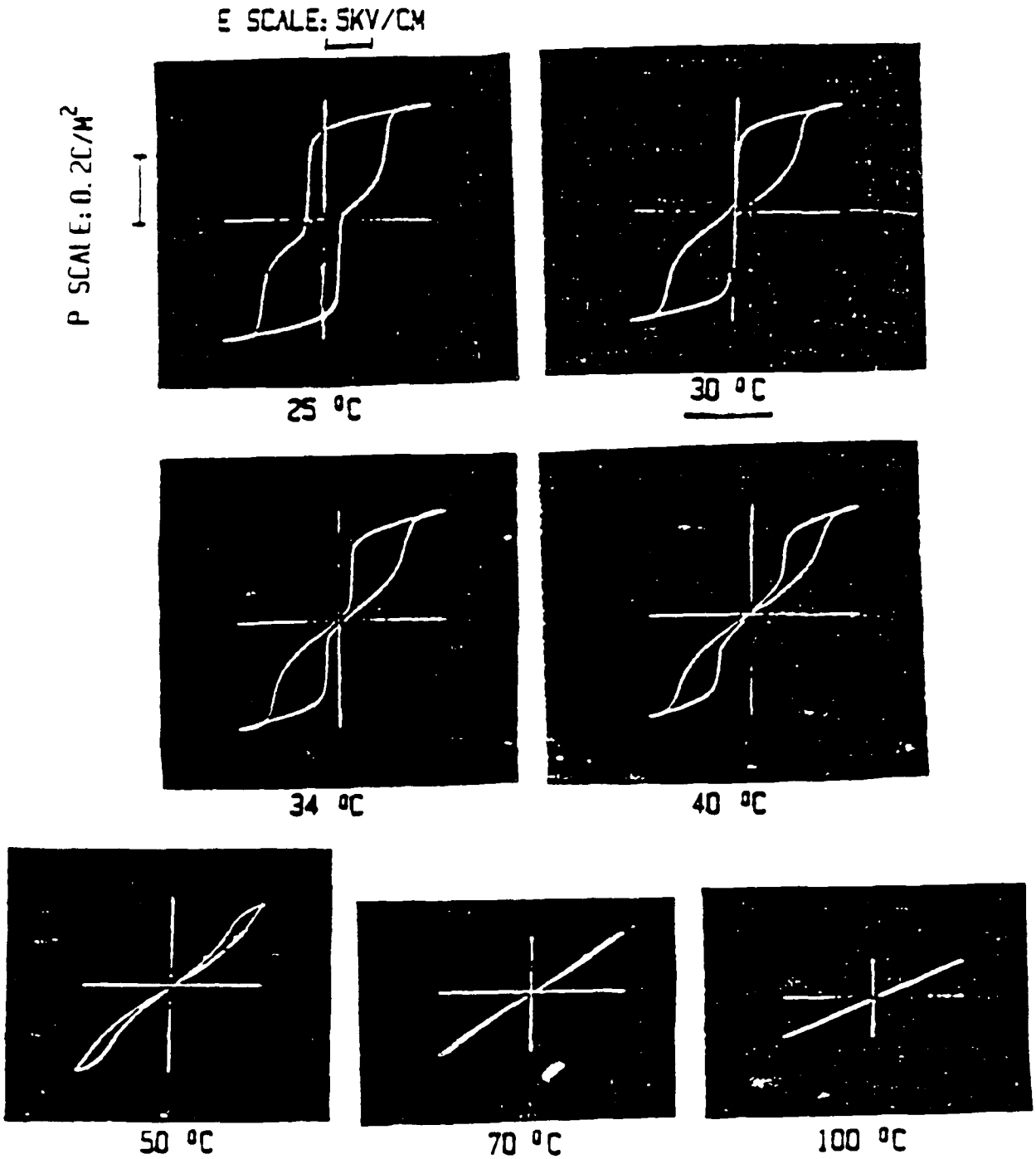
E SCALE: 5KV/CM
P SCALE: 0.2C/M²
25 °C
30 °C
34 °C
40 °C
50 °C
70 °C
100 °C

PLZT 8:70:30 TRANSVERSE STRAIN.

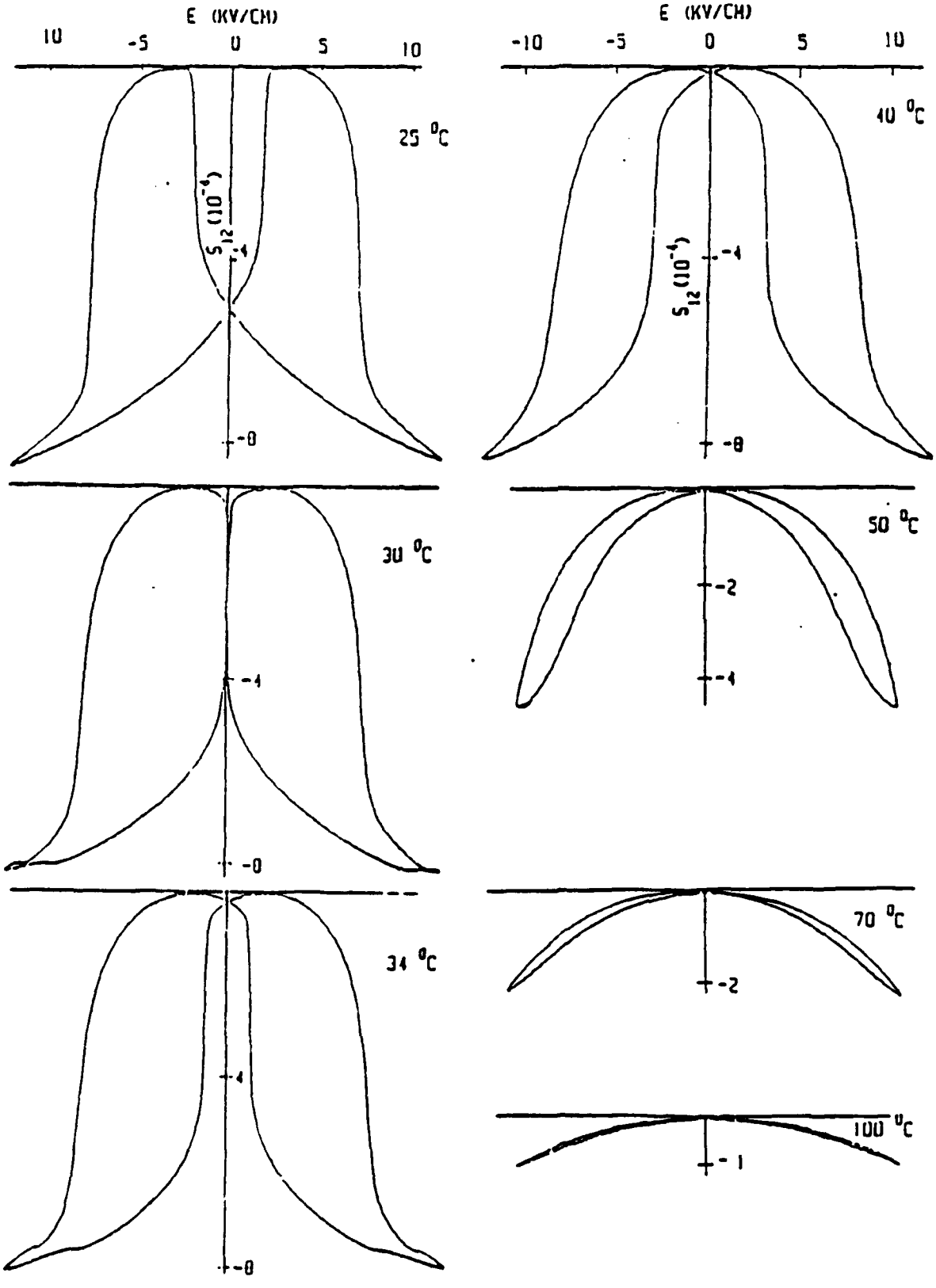

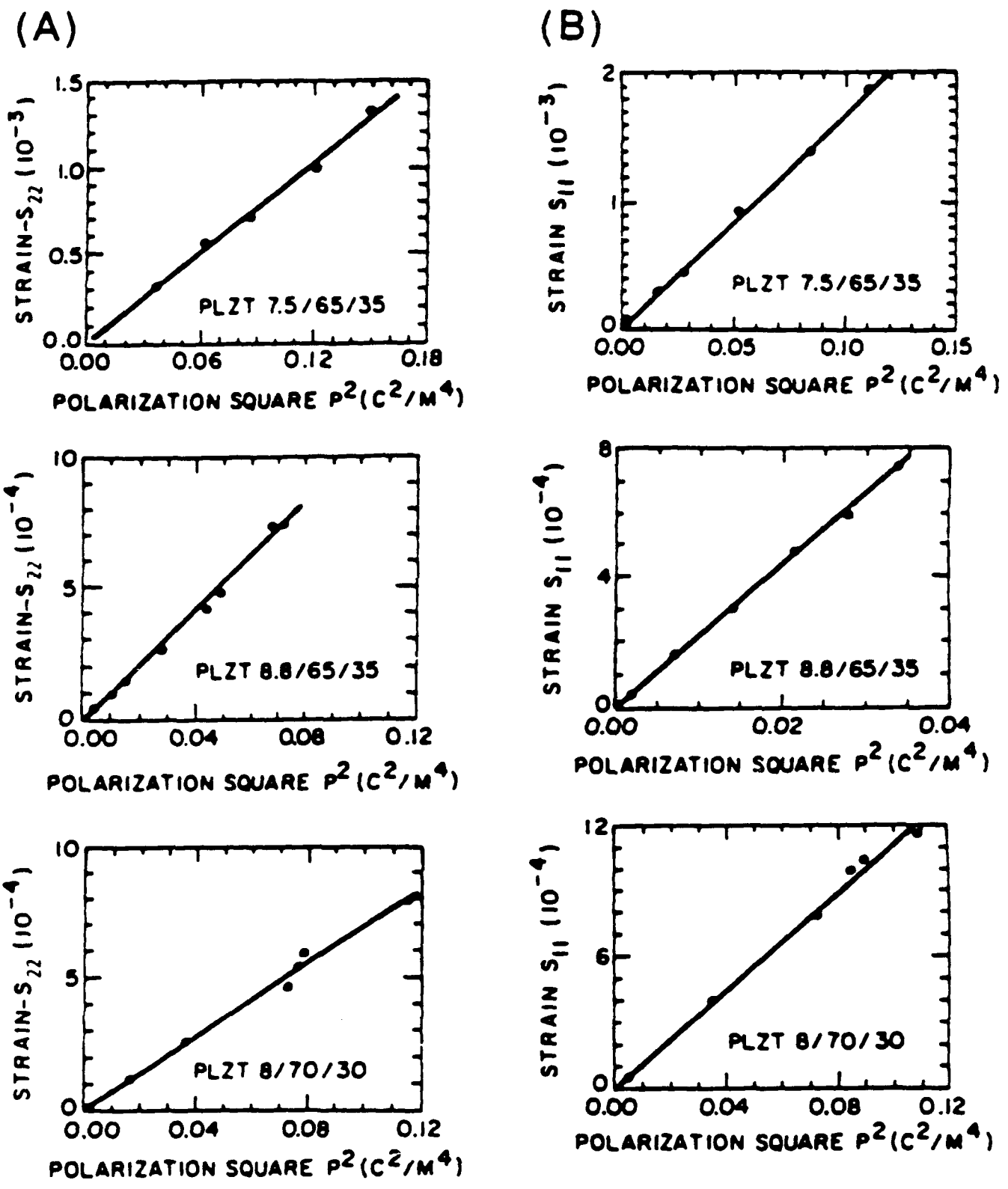

(*A*) transverse strain, S_{22}, and (*B*) longitudinal strain, S_{11}, vs square of polarization, *P*, in 7.5/65/35, 8.8/65/35, and 8/70/30 compositions at room temperature.

Table 5: Field induced strain and related dielectric data
for conventionally sintered PLZT ceramics

comp.	T_m(°C)	Km	K_{25}	Ec (kv/cm)	Pr (uc/cm^2)	$x_t(10^{-3})$	$x_l(10^{-3})$	x_{tr}/x_t
8/67/33	99	12000	5500	2.6	21	.81	2.5	.1
8/65/35 *	106	11350	4600	3.6	20	.82	2.3	.32
8/63/37	114	11300	4500	4.7	21	.76	1.9	.32
7/65/35	140	15000	3000	4.5	28.4	1	3.1	.7
7/62.5/37.5*	160	16000	2900	5	27.2	1.2	3.7	.64
7/60/40	172	17000	3000	6.3	26.2	1.2	3.8	.4
7/58/42	180	17300	2600	8	22	1.1	3.2	.39
7/56/44	190	17200	2200	10	22	.94	2.3	.4
6/62/38	196	19000	2100	5	31	1.45	4.1	.58
6/60/40 *	204	18000	2000	5.6	29.5	1.35	4.7	.57
6/58/42				7.45	29	1.32	3.9	.53
5/60/40	230	19000	1600	6.52	32	.79	4.2	.53
5/58.5/41.5*				6.41	34	1.24	4.5	.59
5/56/44				8.5	32.1	1.6	5.4	.56
4/57/43 *				7.47	35.2	1.26	3.0	.6
4/55/45				10	29.5	1.21	2.9	.55

* MPB compositions

T_m: Temp. of dielectric maximum

x_t: Transverse strain induced at 15kv/cm

K_m: Maximum dielectric constant

x_l: Longitudinal strain induced at 15kv/cm

K_{25}: Dielectric constant at 25°C

x_{tr}: Transverse remanent strain

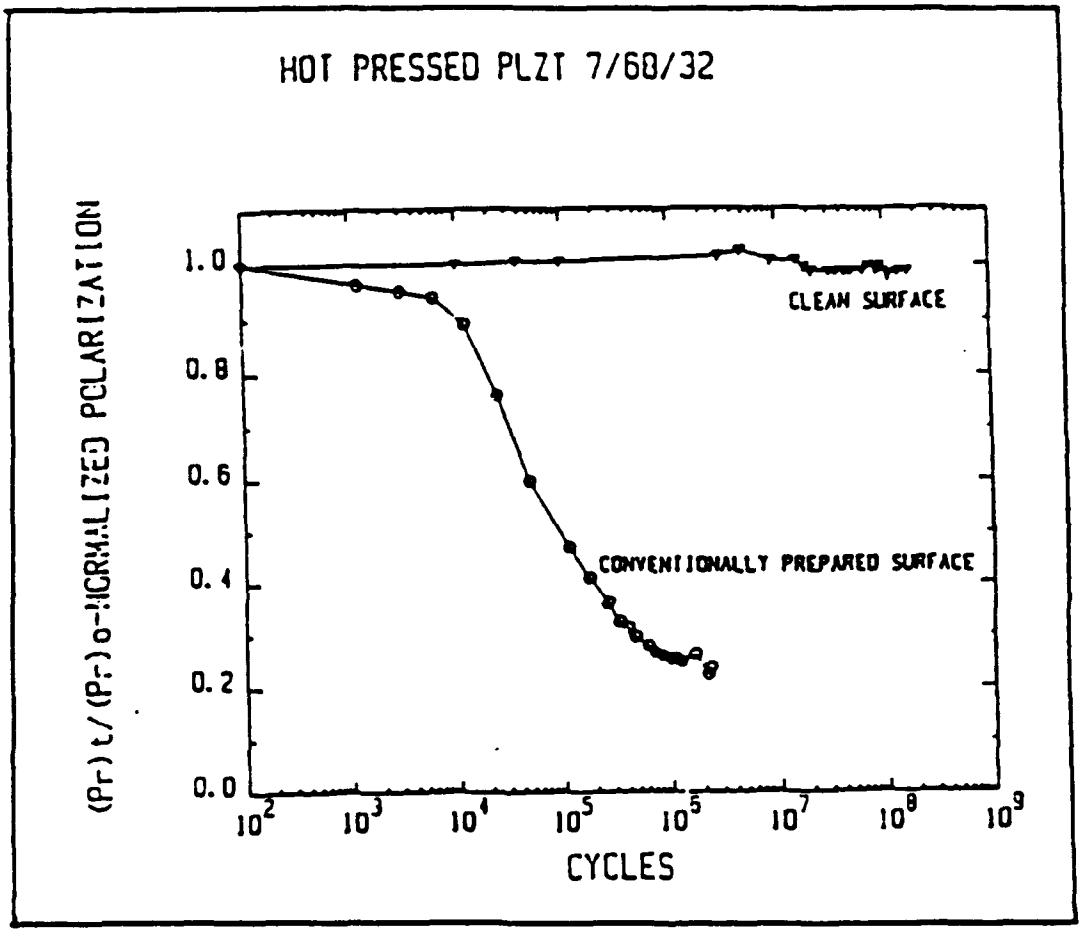
HOT PRESSED PLZT 7/60/32
(Pr)t/(Pr)o-NORMALIZED POLARIZATION
1.0
0.8
0.6
0.4
0.2
0.0
CLEAN SURFACE
CONVENTIONALLY PREPARED SURFACE
10^2
10^3
10^4
10^5
10^6
10^7
10^8
10^9
CYCLES

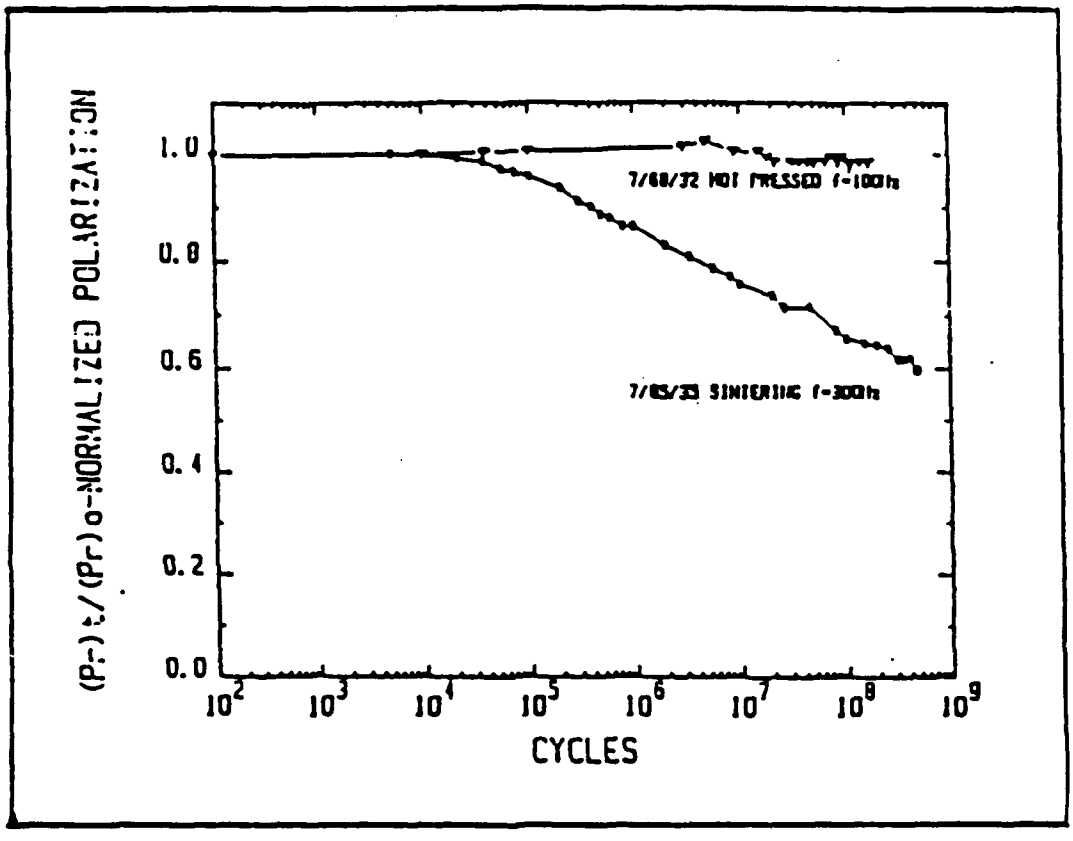
(Pr)t/(Pr)o-NORMALIZED POLARIZATION
1.0
0.8
0.6
0.4
0.2
0.0
10^2
10^3
10^4
10^5
10^6
10^7
10^8
10^9
CYCLES
7/68/32 HOT PRESSED f-100Hz

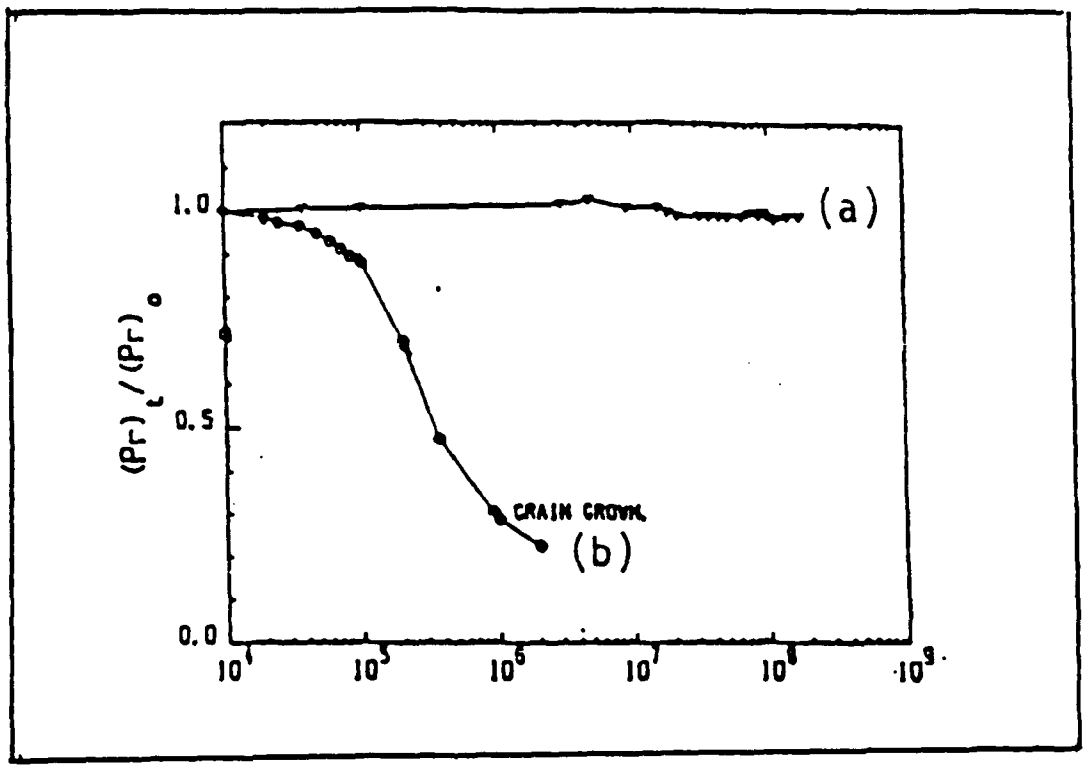
1.0
0.5
0.0
$(P_r)_t / (P_r)_o$
(a)
GRAIN GROWTH
(b)
10^4
10^5
10^6
10^7
10^8
10^9

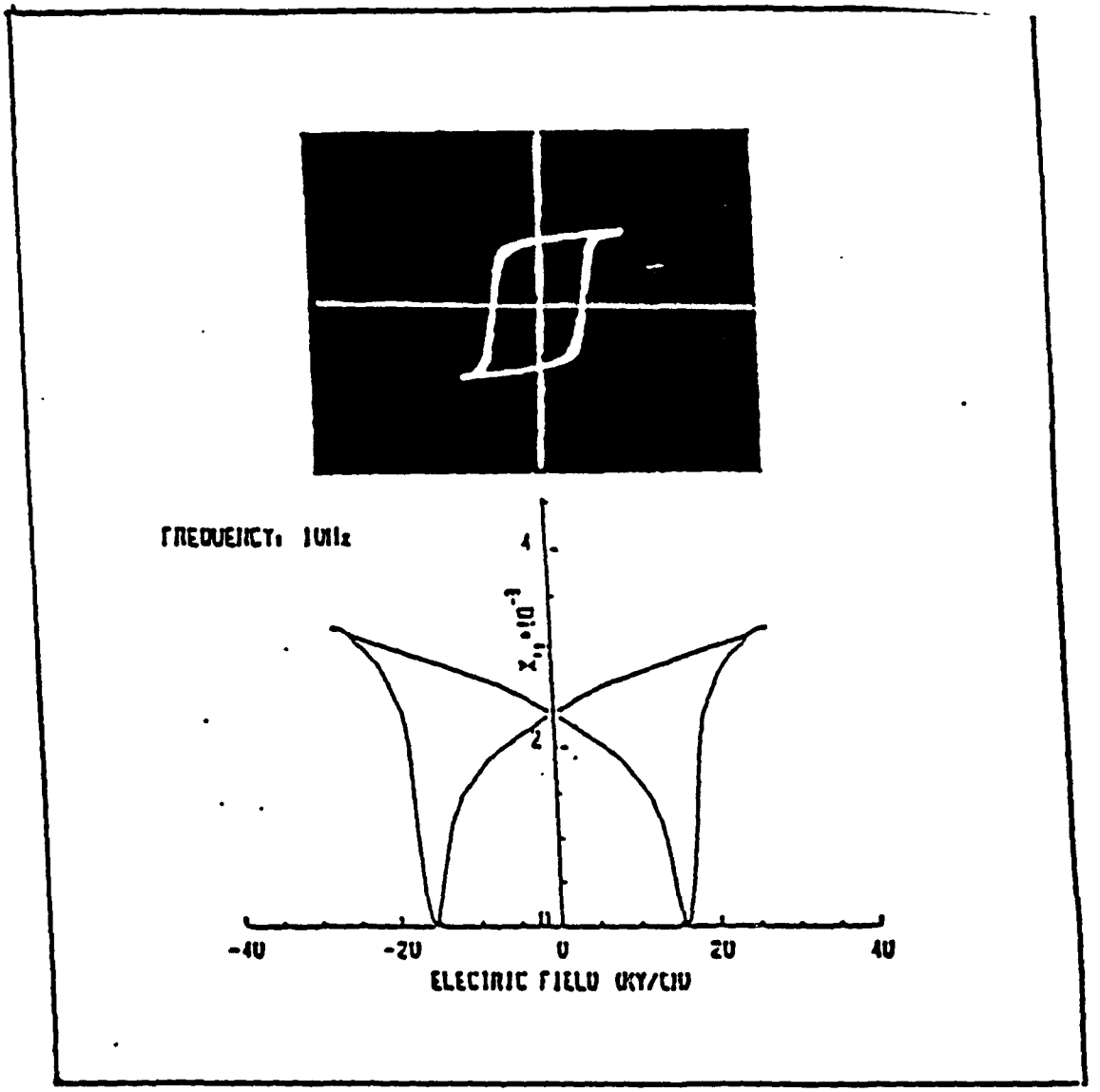

Low temperature polarization and strain cycles in a 9·5/65/35 PLZT. Frequency 10 Hz. Temperature -132°C. Cycling field 30 KV/cm.

DESIGN OF SPACE-QUALIFIED ACTUATOR MATERIALS

Workshop on Advanced Piezoelectric Actuator Materials for Space Applications

Institute for Defense Analyses
Alexandria, Virginia

February 25, 1992

by:

Dr. Stephen R. Winzer
Martin Marietta Laboratories

MARTIN MARIETTA
Martin Marietta Laboratories
1450 S. Rolling Road
Baltimore, Maryland 21227-3898
(410) 247-0700
(410) 247-4939 (facsimile)

PMN MATERIAL DEVELOPMENT PROGRAM

MARTIN MARIETTA

Historical Development

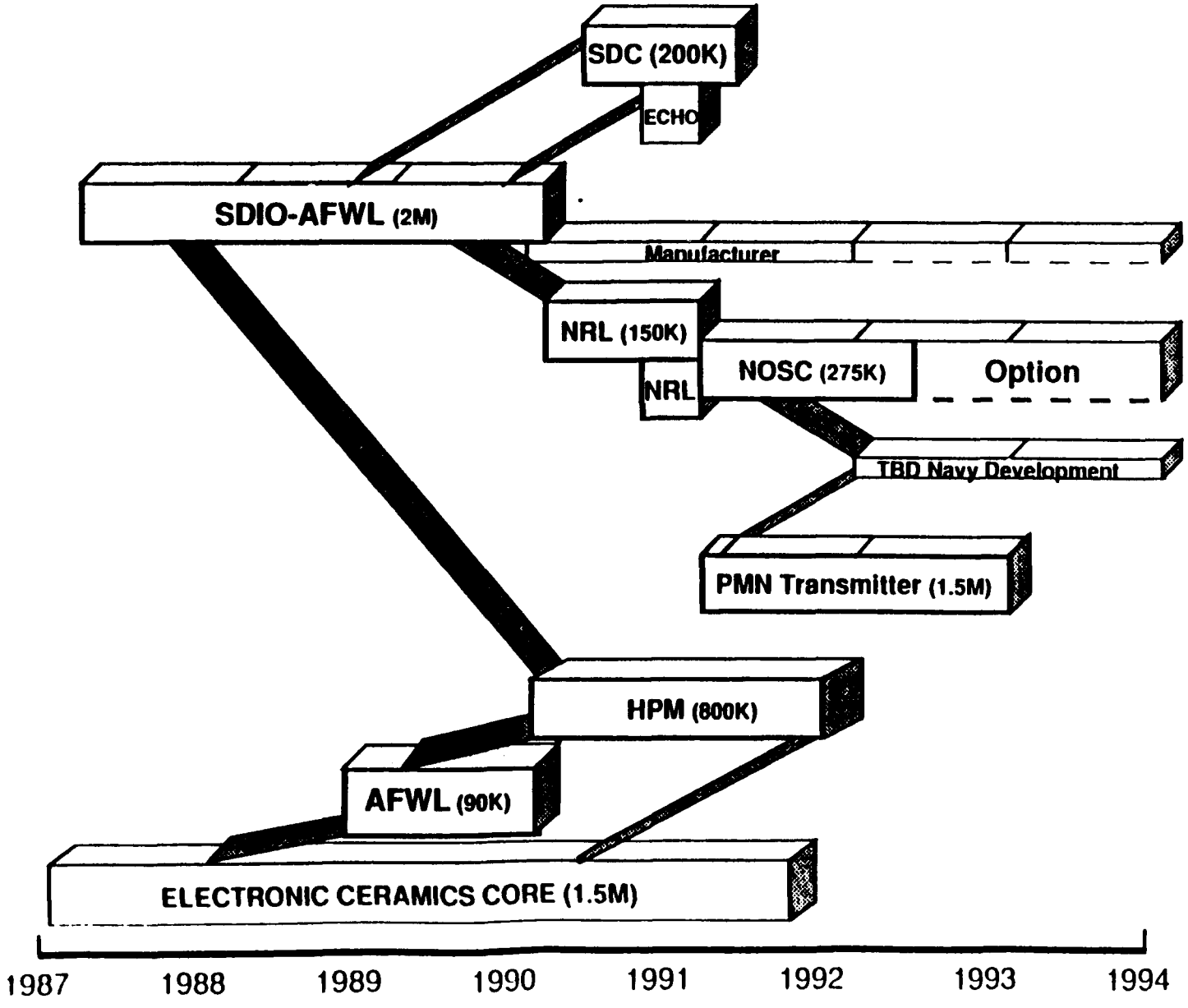

ELECTROSTRICTIVE ACTUATORS

MARTIN MARIETTA

Promise and Issues

	PROMISE	ISSUES
Electrostrictive Materials	High energy density High strain Low loss Fast response Low hysteresis Large force Temperature tolerant Radiation hard	Temperature dependence Field dependence Frequency dependence Transition to piezoelectric Capacitance
Multilayer Actuators	Flexible drive voltage Flexible design Manufacturable Reliable	Drive electronics Fabrication Cost Reliability Accessibility Embeddability Compatibility

PMN MATERIAL DEVELOPMENT PROGRAM

MARTIN MARIETTA

Properties

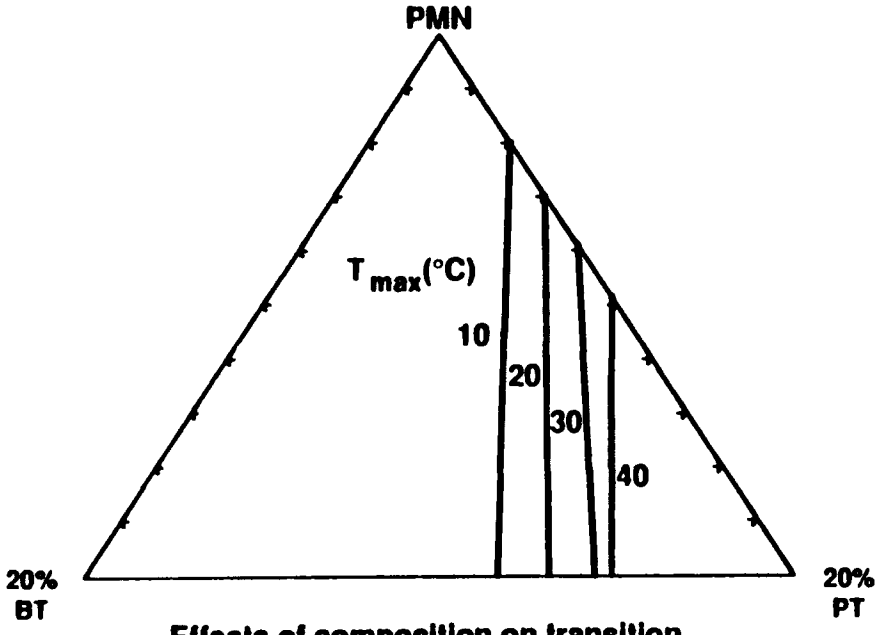

Effects of composition on transition temperature, PMN-PT-BT system

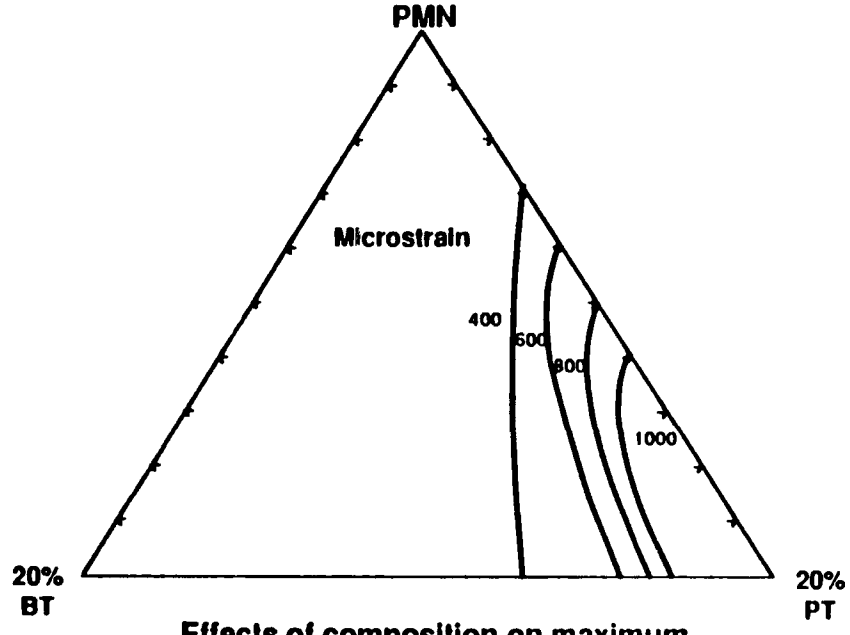

Effects of composition on maximum strain, PMN-PT-BT system

Based on 75 compositions:

- T_{max} (weak-field behavior) is predictable.
- Strain (high-field behavior) is predictable.

PMN MATERIAL DEVELOPMENT PROGRAM

MARTIN MARIETTA

Weak-field Transition

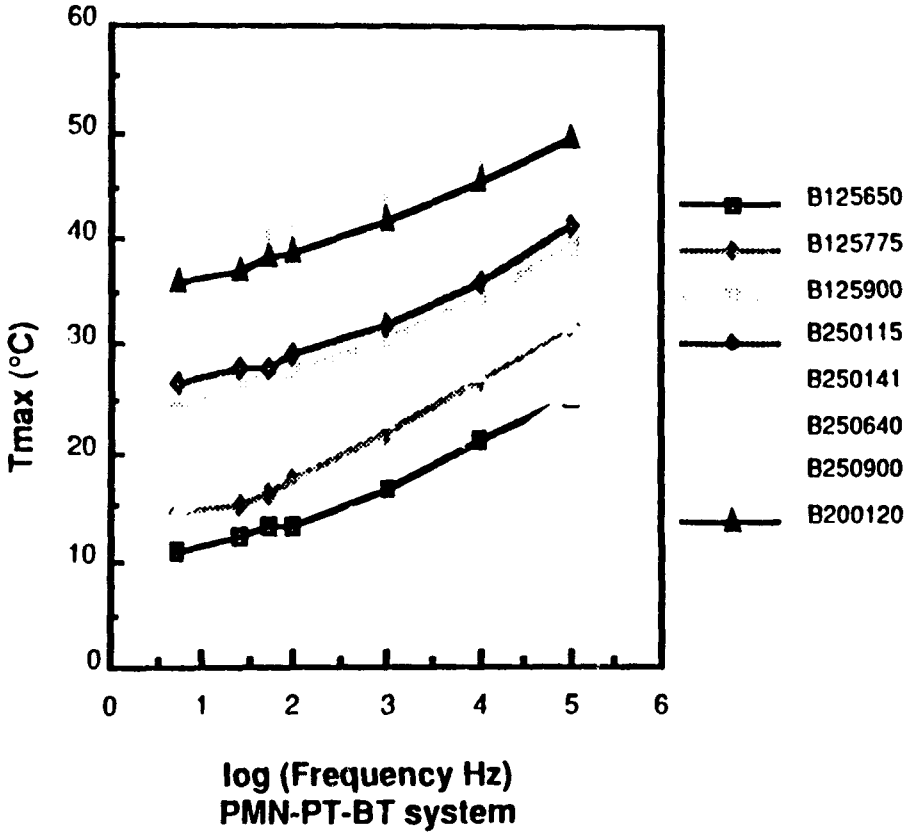

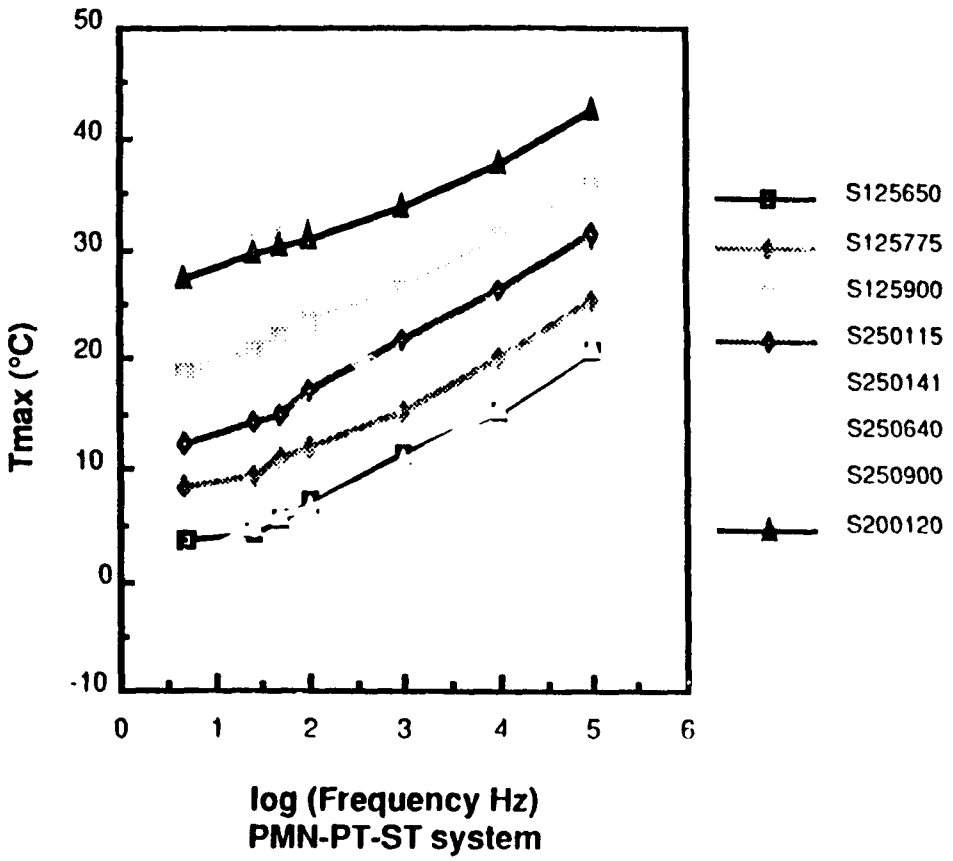

- T_{max} increases linearly with log frequency.
- Slope of frequency dependence increases with increasing PT content.

ELECTROSTRICTIVE ACTUATORS

MARTIN MARIETTA

Issues

	ISSUES
Electrostrictive Materials	Temperature dependence Field dependence Frequency dependence Phase transition Capacitance
Multilayer Actuators	Drive electronics Fabrication Cost Fatigue Accessibility Embeddability Compatibility

ACTUATOR FABRICATION

MARTIN MARIETTA

Low Voltage Operation

- Fabrication adapted from commercial multilayer capacitors
- Layer thicknesses to ~20 μm (operating voltages of 15-25 V)
- Conventional ceramic powder processing
- Tapecast layers and cofired stack

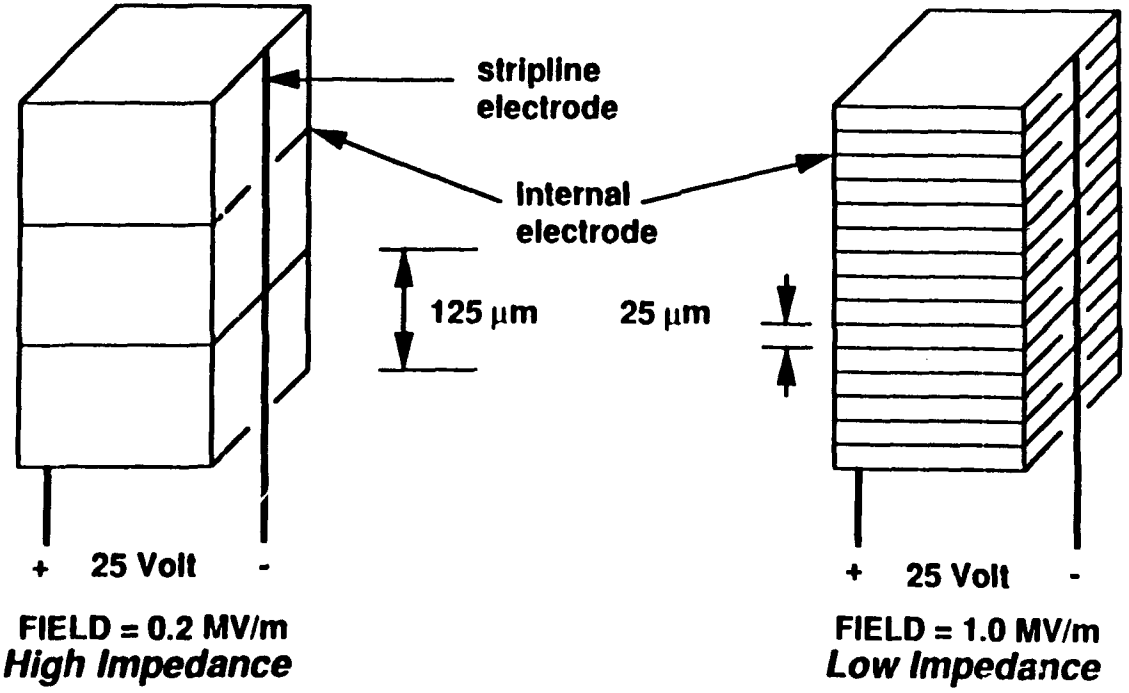

PAD APPROACH
- Square shapes
- Low investment
- High volume
- Lot uniformity

PUNCH APPROACH
- Simple shapes
- Complex shapes
- High volume
- Easy prototyping

ISSUES
- Stress concentrations
- Interconnections
- Fatigue
- High capacitance

INTEGRATED ACTUATOR AND SENSOR

MARTIN MARIETTA

Issue

- Smart, tunable actuators with feedback to control electronics.

Promise

- Sensor provides feedback of actuator output, environment, and secondary issues such as compliance, hysteresis, and non-linear effects.
- Ease of fabrication of actuator and sensor into a robust, cofired multilayer design
- Design and composition of both sections can be tailored to match impedence/capacitance/drive voltages with drive electronics and sensor signal amplifiers.
- PMN-X materials allow selection of piezoelectric or electrostrictive response in either section.

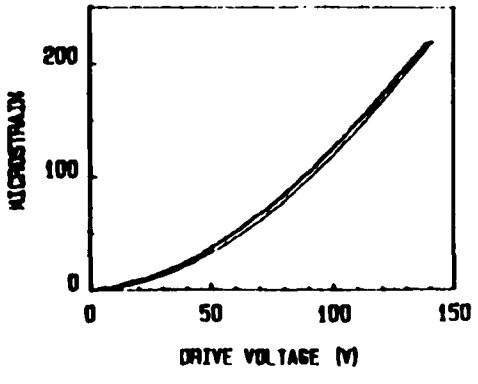

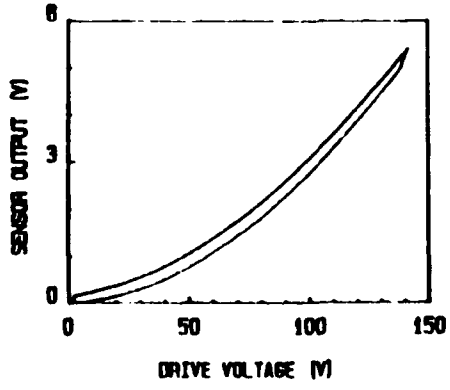

PROPORTIONAL VALVE ACTUATORS (FACT)

MARTIN MARIETTA

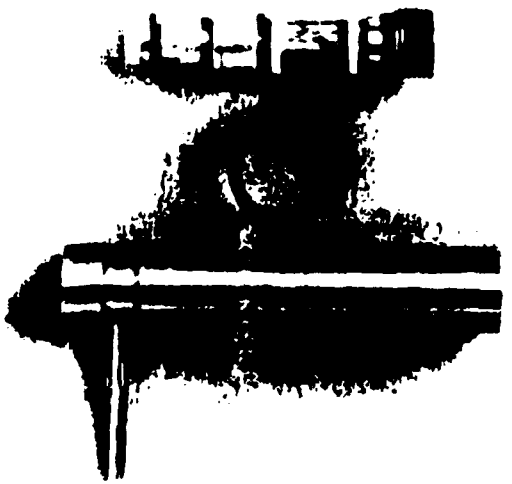

FACT valve

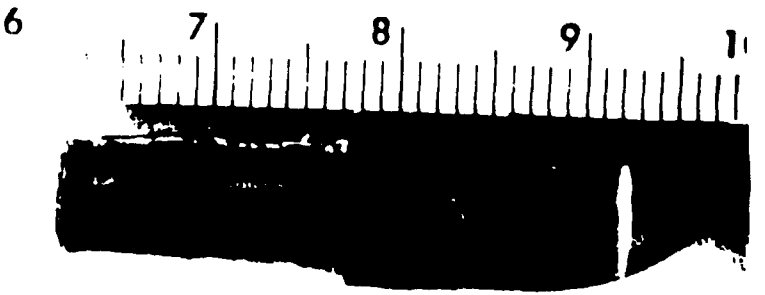

Electrostrictive actuator

Issue

- Design, fabrication, and characterization of linear piezoelectric and quadratic electrostrictive actuators.

Promise

- Low hysteresis, high strain electrostrictive materials
- Modelled, low-stress actuator designs
- High reliability processing

ELECTROSTRICTIVE ACTUATORS
Conclusions

MARTIN MARIETTA

Electrostrictive materials and actuators have a role to play in space-based systems.

Issues:

- **Temperature dependence of materials, how much control do we have?**
- **Field and frequency dependence of T_c, how much of a problem?**
- **Drive electronics (bias field control, power supplies) -- mineaturization.**
- **Fatigue / failure modes -- availability of large populations for statistical analysis.**

LIMITATIONS OF HIGH DRIVE PIEZOELECTRIC AND ELECTROSTRICTIVE MATERIALS

GENE H. HAERTLING

CLEMSON UNIVERSITY

PROPERTIES AND ASSOCIATED PHENOMENA OF PLZT FERROELECTRIC CERAMICS

PROPERTIES	PHENOMENA
✓DIELECTRIC	PHOTOCONDUCTIVE
PIEZOELECTRIC	PHOTOVOLTAIC
PYROELECTRIC	PHOTOCHROMIC
FERROELECTRIC	PHOTOREFRACTIVE
ELECTROSTRICTIVE	PHOTOSTRICTIVE
FERROELASTIC	PHOTO-ASSISTED DOMAIN SWITCHING
ELECTROOPTIC	ELECTROOPTIC SCATTERING
✓OPTICAL	SURFACE DEFORMATION
✓ELECTRICAL RESISTIVITY	SPACE CHARGE EFFECTS

✓singular properties

all others - interactive properties & phenomena

FACTORS LIMITING THE PERFORMANCE OF PIEZOELECTRIC AND ELECTROSTRICTIVE MATERIALS

1. COMPOSITION (ELEMENTS, PURITY, DOPANTS, ETC.)
2. MICROSTRUCTURE (DENSITY, GRAIN SIZE, PHASES)
3. PROPERTIES (VALUE, VOLTAGE DEPENDENCE)
4. TEMPERATURE (Tc vs.OPERATING TEMP., SELF HEATING)
5. HYSTERESIS (ELECTRICAL SWITCHING, DOMAIN WALL MOBILITY)
6. AGEING (TIME DEPENDENT PROPERTY CHANGES)
7. FATIGUE (OPERATIONAL DEGRADATION, CYCLIC EFFECTS)
8. CREEP (CYCLIC MECHANICAL INSTABILITY)
9. ELECTRICAL BREAKDOWN (MAXIMUM VOLTAGE CAPABILITY)
10. SPEED (ACTIVATION/RELAXATION PROCESSES)
11. SIZE (RESONANT/NON-RESONANT, FREQ. DAMPED EFFECTS)
12. STRESS (TENSILE, COMPRESSIVE, HYDROSTATIC, MISMATCH)
13. MECHANICAL STRENGTH (INTRINSIC, FLAWS, SURFACE FINISH)
14. FRACTURE TOUGHNESS (CRACK PROPAGATION, PRESTRESS)
15. ELECTRODES (TYPE, OHMIC CONTACTS, ELECT. MIGRATION)
16. STRUCTURES (MATERIALS, BONDING AGENTS, ENCAPSULANTS)
17. ENVIRONMENT (HERMITICITY, HUMIDITY, VACUUM, G-LOADING)
18. THERMAL HISTORY (MEMORY EFFECTS, POLED CONDITION)

TYPICAL RANGES OF PROPERTIES FOR PIEZOELECTRIC AND ELECTROSTRICTIVE MATERIALS

Material	K	Tan delta %	k_p	k_{33}^T	d_{33} pC/N	Q_{11} ($\times 10^{-16}$ m^4/C^2)	Q_{12} ($\times 10^{-16}$ m^4/C^2)
PZT	300-2000	.1-2.0	.2-.70	.3-.70	100-600	--	--
BT	500-3000	.2-1.0	.2-.40	.3-.50	100-300	--	--
PLZT	500-6000	2.0-8.0	.3-.72	.3-.80	150-700	--	--
PMN	10,000-25,000	2.0-8.0	--	--	--	.020	-.007
PN	200-600	.8-1.5	.1-.20	.4-.50	85	--	--
PZT 4	1300	.40	.58	.70	289	--	--
PZT 8	1000	.30	.51	.68	225	--	--
PZT 5A	1700	1.5	.60	.71	374	--	--
PZT 5H	3400	2.0	.65	.75	593	--	--
PLZT 7/65/35	1850	1.8	.62	.76	400	.022	-.012
PLZT 8/65/35	3400	3.0	.65	.78	682	.018	-.008
PLZT 9/65/35	5700	6.0	--	--	--	.020	-.010
PBZT 73/27	8000	7.0	--	--	--	.100	-.040

LIMITATING VALUES FOR SELECTED FACTORS AFFECTING THE PERFORMANCE OF PIEZOELECTRICS AND ELECTROSTRICTORS

COMPOSITIONAL REPRODUCIBILITY: ± 0.01%

SHRINKAGE REPRODUCIBILITY: ±0.1%

PROPERTY REPRODUCIBILITY: ±3%

USE TEMPERATURE:

PIEZOELECTRIC - $T < 1/2\ T_c$

ELECTROSTRICTOR - $T > T_t$ (T_t = T of stable polarization)

TYPICAL - $T <$ 100 degrees centigrade

SPEED:

BULK - > 1 usec

THIN FILM - > 1 nsec

STRAIN HYSTERESIS: >1%

AC OPERATING FIELD: <15 kV/cm

DC OPERATING FIELD: < 40 kV/cm

ELECTRIC FIELD BREAKDOWN:

BULK - 100 kV/cm (250 V/mil)

THIN FILM - 500 kV/cm (1250 V/mil)

MAXIMUM LOAD UNDER STRESS: VARIES (gms. to kgms.)

AGEING: -2%/DECADE OF TIME

MECHANICAL STRENGTH:

TENSILE - 70 MPa (10,000 psi) (ac - 4 ksi)

FLEXURE - 103 MPa (15,000 psi)

COMPRESSIVE - 350 MPa (40,000 psi)

REPRODUCIBILITY - +20 %

SMART CERAMICS

R.E. NEWNHAM

MATERIALS RES. LAB.

PENNSYLVANIA STATE U.

UNIVERSITY PARK, PA.

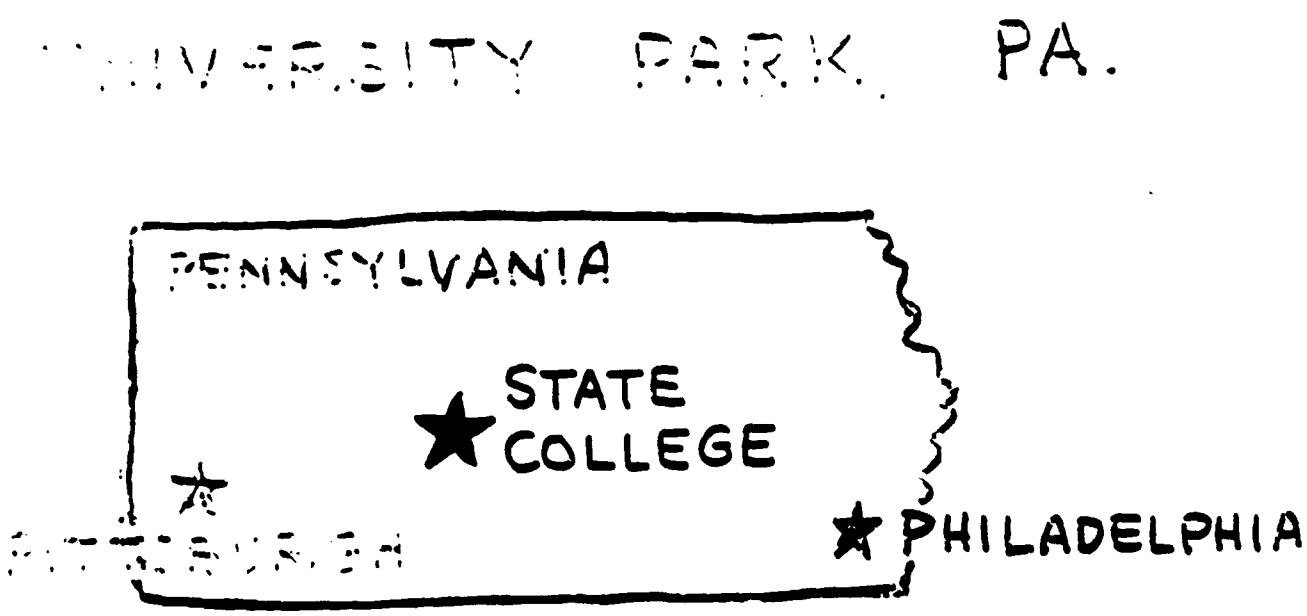

OFFICE OF NAVAL RESEARCH

ELECTROMECHANICAL TRANSDUCERS

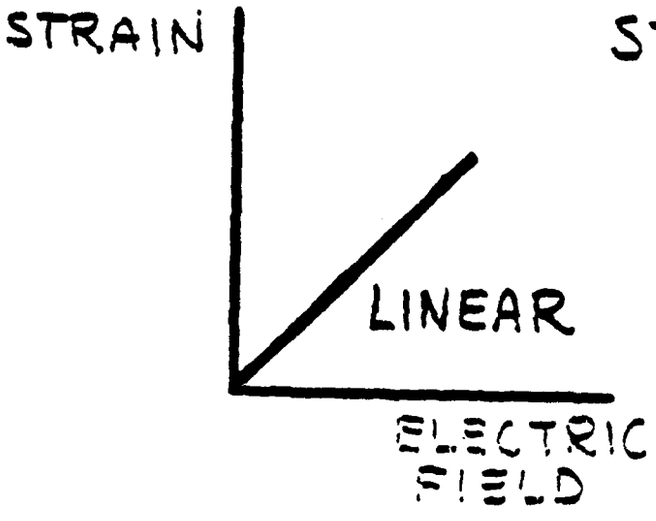

PIEZOELECTRICITY

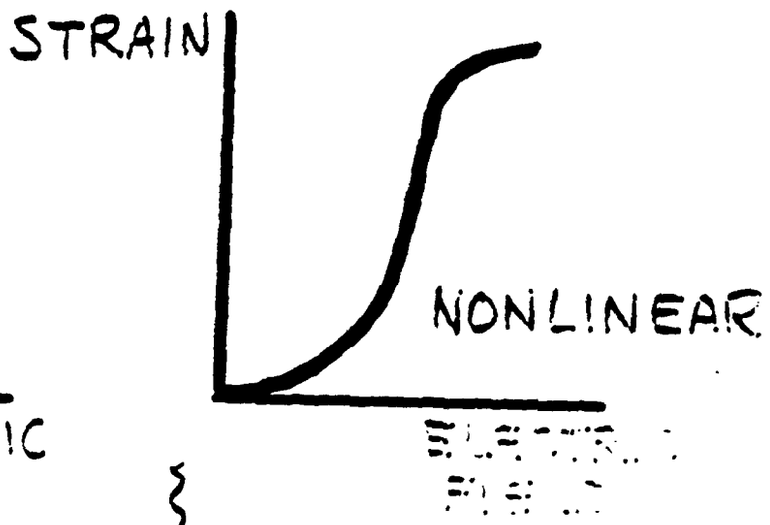

ELECTROSTRICTION

DOMAIN CHANGE

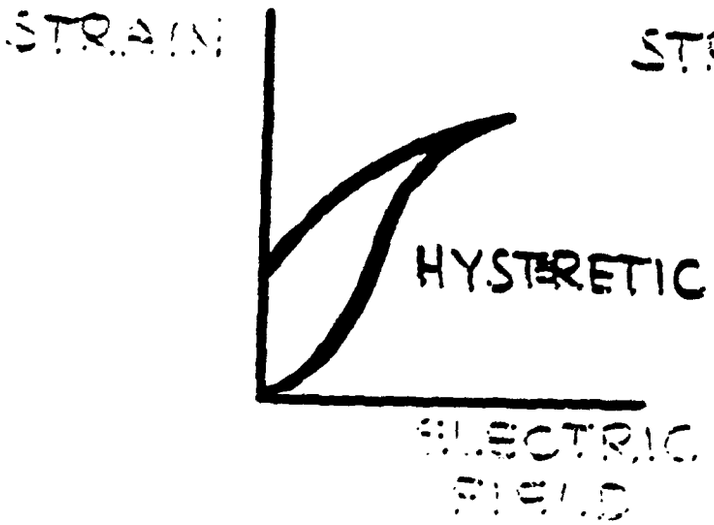

PHASE CHANGE

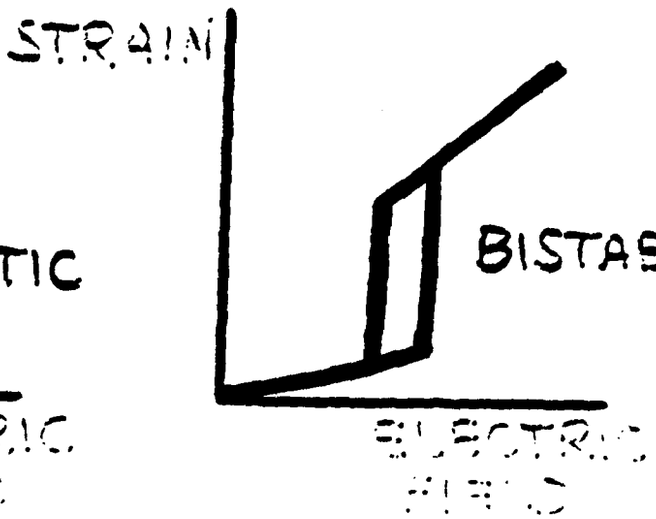

SMART COMPOSITE COMPONENTS

PIEZORESISTOR

CHEMICAL SENSOR

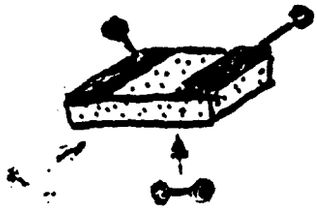

OPTICAL NANOCOMPOSITE

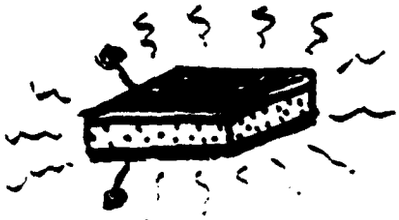

PTC THERMISTOR

MAGNETIC MEMORY

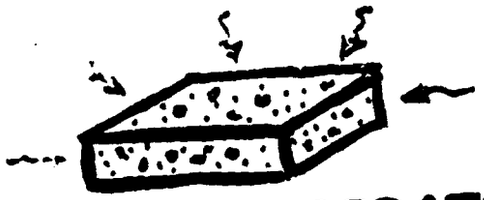

PCM TEMPERATURE STABILIZER

ELECTROLYTE

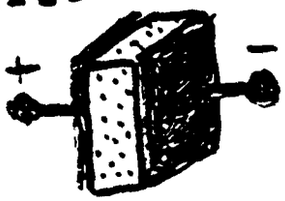

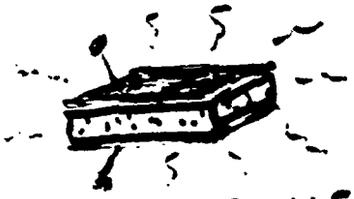

PTC THERMISTOR

VARISTOR

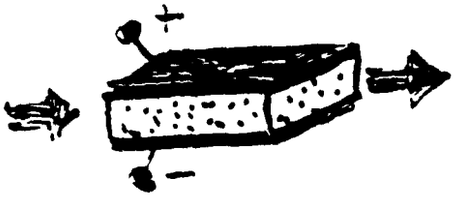

ELECTRORHEOLOGIC FLUID

PIEZOELECTRIC TRANSDUCER

PYROELECTRIC SENSOR

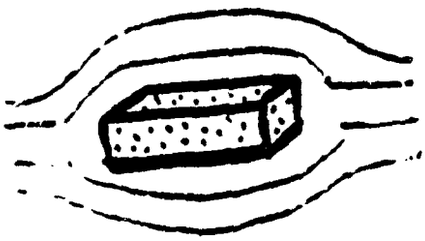

SUPER CONDUCTOR

SHAPE MEMORY

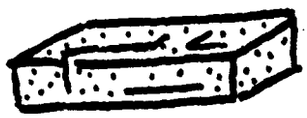

DIELECTRIC PACKAGE LOW K

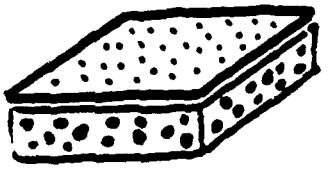

PARTICLES IN MATRIX 0-3

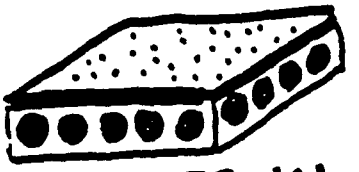

SPHERES IN MATRIX 0-3

1-3 RODS IN MATRIX

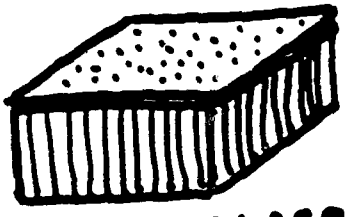

POLAR GLASS-CERAMIC 1-3

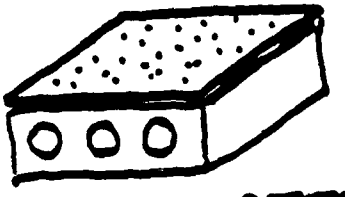

PERFORATED 3-1

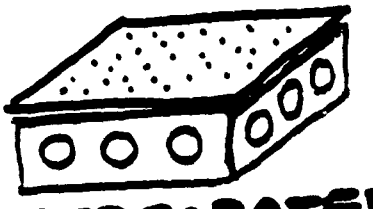

PERFORATED 3-2

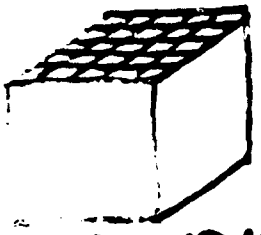

LONGITUDINAL HONEYCOMB 3-1

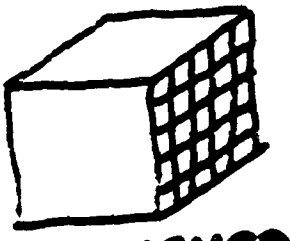

TRANSVERSE HONEYCOMB 3-1

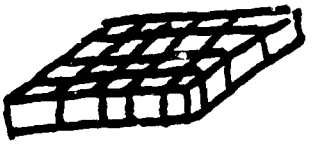

DICED CERAMIC 1-3

REPLAMINE 3-3

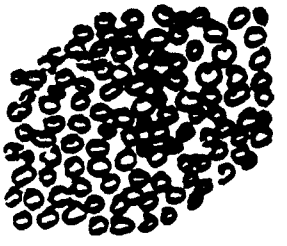

BURPS 3-3

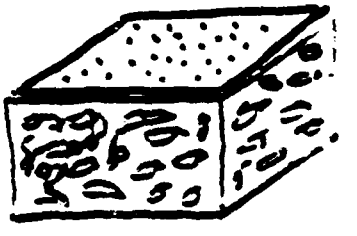

VYCOR 3-3

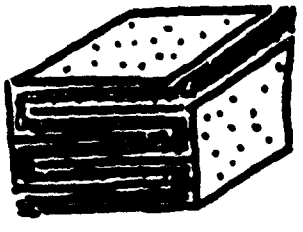

MULTILAYER 2-2

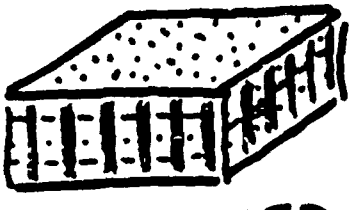

REINFORCED 1-2-3

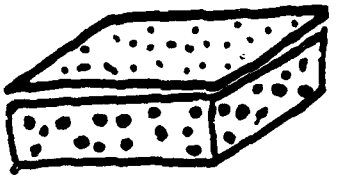

MIXED FILLER 0-0-3

CONTROLLED COMPLIANCE

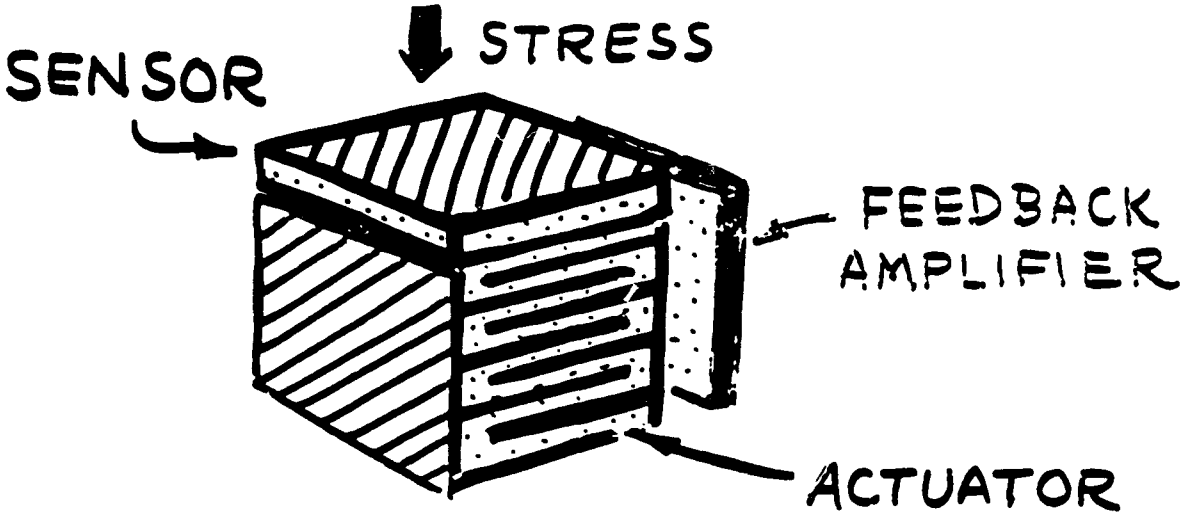

- ★ SENSOR DETECTS INCREASING STRESS
- ★ FEEDBACK AMPLIFIER REDUCES HEIGHT OF PIEZOELECTRIC ACTUATOR
- ★ COMBINATION MIMICS ULTRASOFT SOLID

TOYOTA ★ ELECTRONIC MODULATED ★ SUSPENSION ★

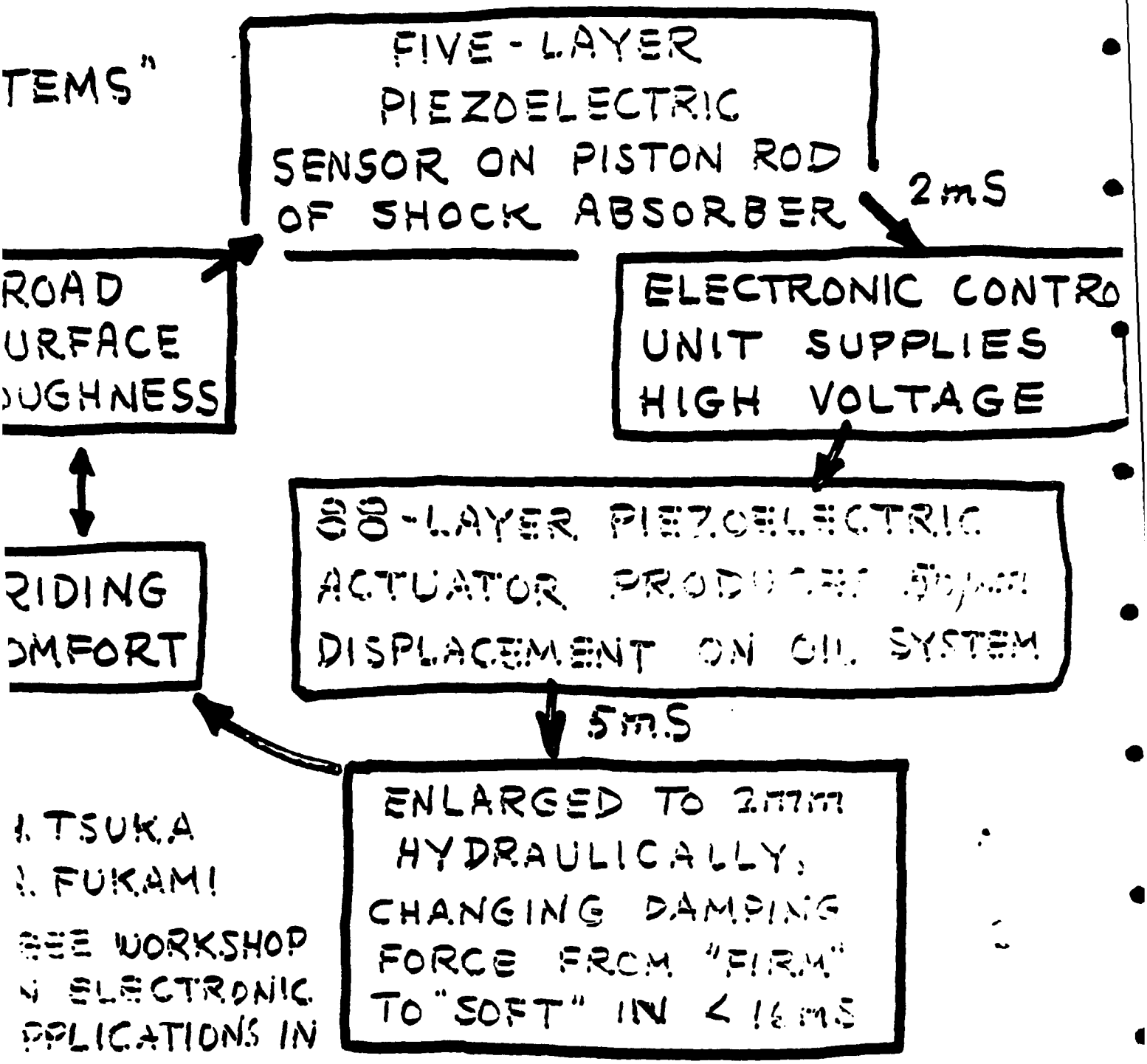

I. TSUKA
I. FUKAMI

EE WORKSHOP
N ELECTRONIC
PPLICATIONS IN
RANSPORTATION
1990

SMART SHOCK ABSORBER

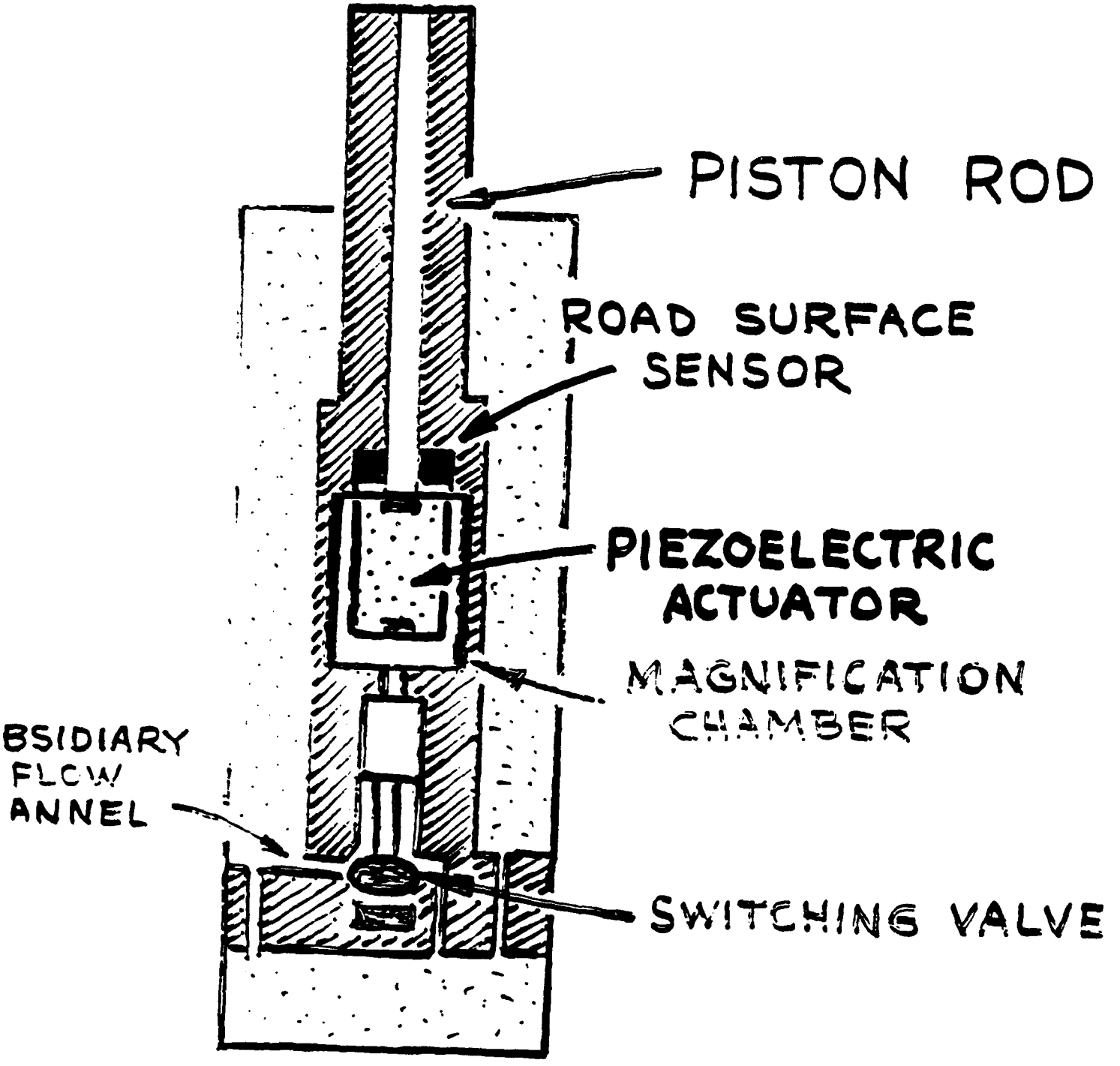

H. TSUKA, J. NAKOMO AND Y. YOKOYA
I.E.E.E. WORKSHOP, 1990.

ACTIVE VIBRATION CONTROL

ACTIVE SUSPENSIONS

- ★ RAILROAD CARS (OKAMOTO)
- ★ AUTOMOBILES (NAGAI)

FLEXIBLE STRUCTURES

- ★ ROBOTIC ARMS (FUKUDA)
- ★ SOLAR BATTERY ARRAYS (FUKUDA)
- ★ SPACE STRUCTURES (KASHIWASE)
- ★ CANTILEVERED PIPES (DOKI)
- ★ ANTENNAS (SETO)

VIBRATION & NOISE CONTROL

- ★ FORGING HAMMERS (TANAKA)
- ★ OFF-SHORE RIGS (YANG)
- ★ VIADUCTS & BRIDGES (YAHAGI)
- ★ ACTIVE BEARINGS (NONAMI)

REFERENCES IN J.J.S.M.E. 1985 ON

ACTUATOR DESIGNS

★ MULTILAYER STACK

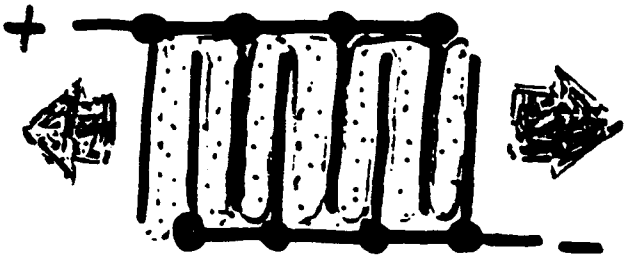

BIG FORCE
SMALL DISPLACEMEN

★ BIMORPH BENDER

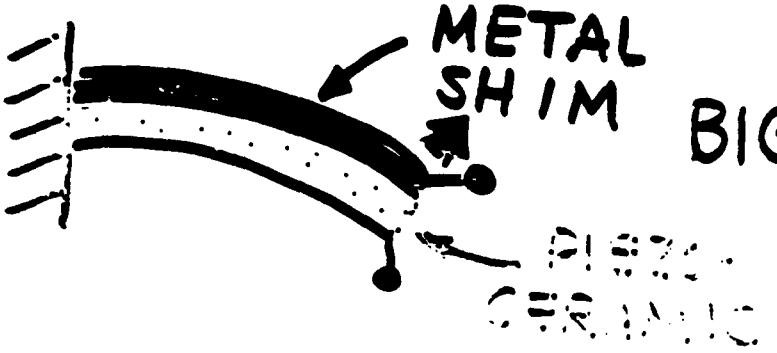

SMALL FORCE
BIG DISPLACEMENT

★ MOONIE DISK

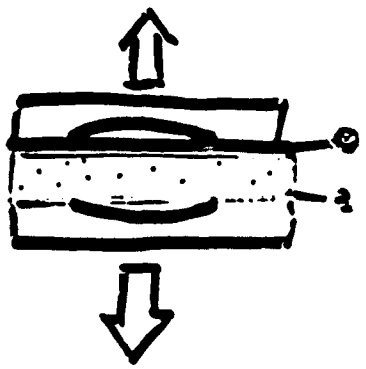

INTERMEDIATE
FORCES & DISPLACE-
MENTS

PIEZOELECTRIC MATRIX

DIRECT EFFECT

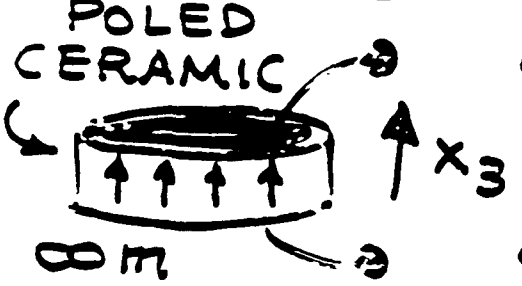

LARIZATION

$$\begin{pmatrix} P_1 \\ P_2 \\ P_3 \end{pmatrix} = \begin{pmatrix} 0 & 0 & 0 & 0 & d_{15} & 0 \\ 0 & 0 & 0 & d_{15} & 0 & 0 \\ d_{31} & d_{31} & d_{33} & 0 & 0 & 0 \end{pmatrix} \begin{pmatrix} \sigma_1 \\ \sigma_2 \\ \sigma_3 \\ \sigma_4 \\ \sigma_5 \\ \sigma_6 \end{pmatrix}$$

TENSILE STRESS

SHEAR STR...

CONVERSE EFFECT

ONGI-
DINAL
RAINS
...
HEAR
RAINS

$$\begin{pmatrix} \epsilon_1 \\ \epsilon_2 \\ \epsilon_3 \\ \epsilon_4 \\ \epsilon_5 \\ \epsilon_6 \end{pmatrix} = \begin{pmatrix} 0 & 0 & d_{31} \\ 0 & 0 & d_{31} \\ 0 & 0 & d_{33} \\ 0 & d_{15} & 0 \\ d_{15} & 0 & 0 \\ 0 & 0 & 0 \end{pmatrix} \begin{pmatrix} E_1 \\ E_2 \\ E_3 \end{pmatrix}$$

ELECTRIC FIELD

CRESCENT - SHAPED 2-0-2 HYDROPHONE (MOONIE)

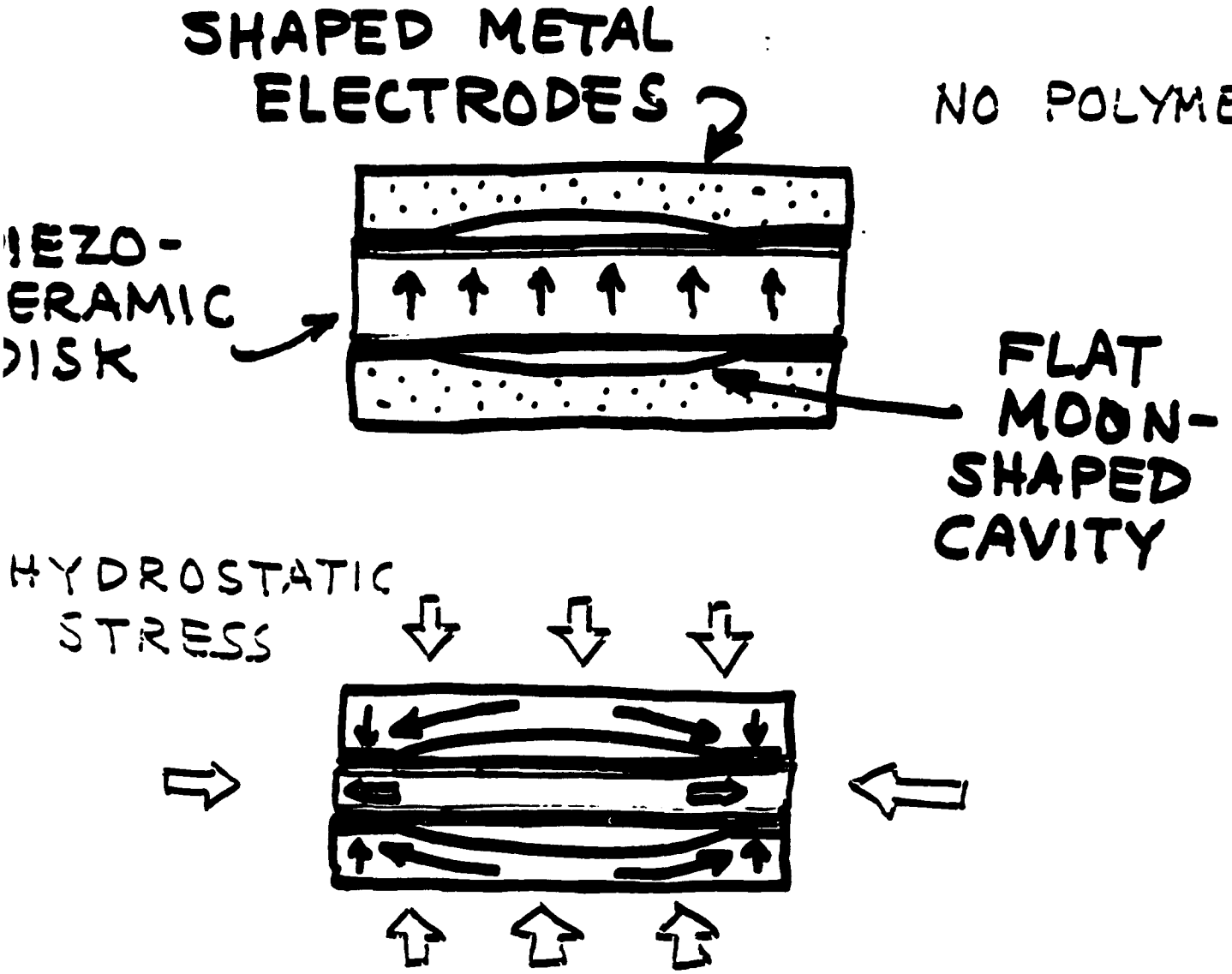

INTERNAL TENSILE STRESS ACTING ON PIEZOCERAMIC IN RADIAL DIRECTION

★CAVITY SIZE EFFECT

★ HYDROSTATIC PIEZOELECTRIC CHARGE COEFFICIENT

★ PRESSURE DEPENDENCE

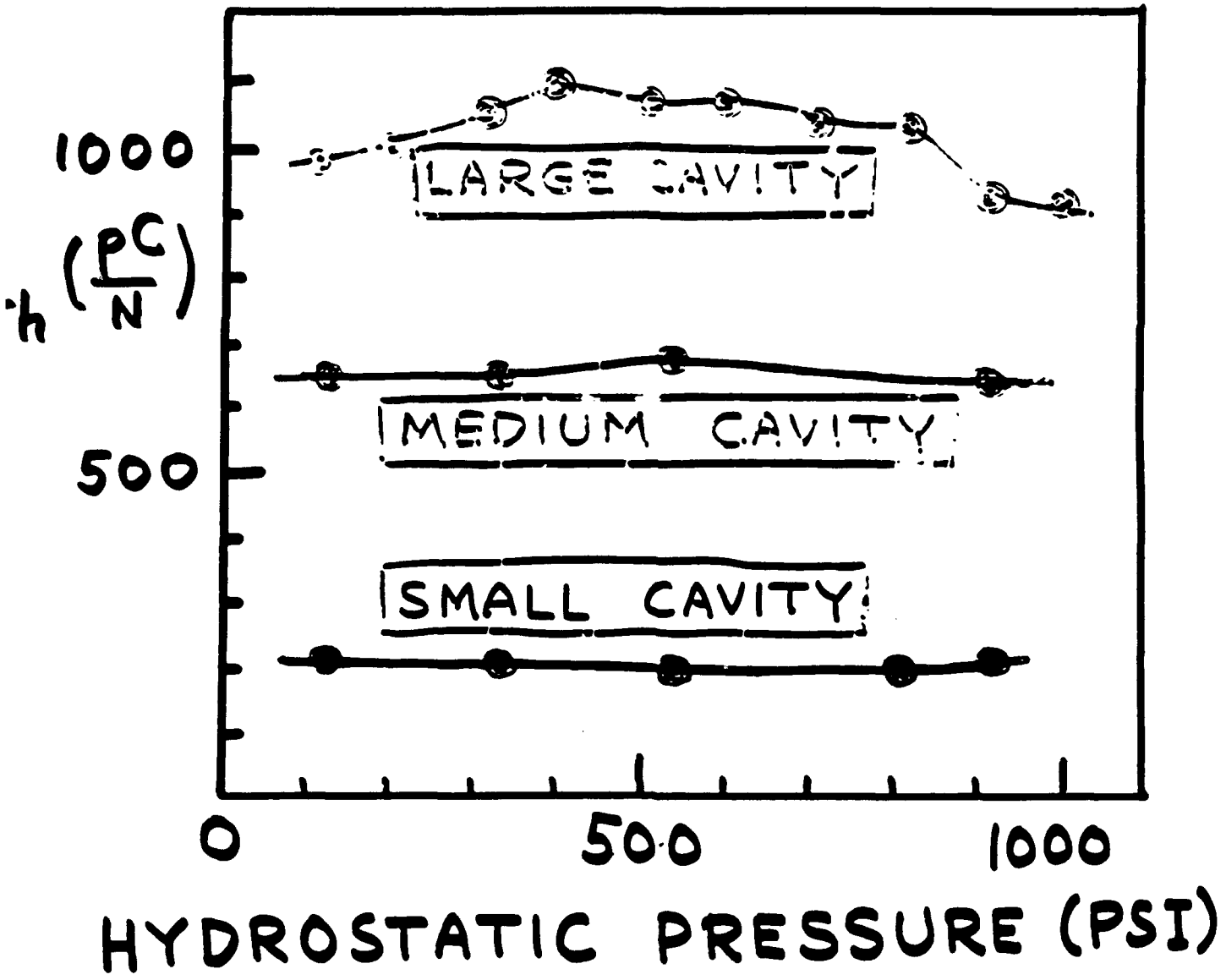

MOONIE ACTUATOR

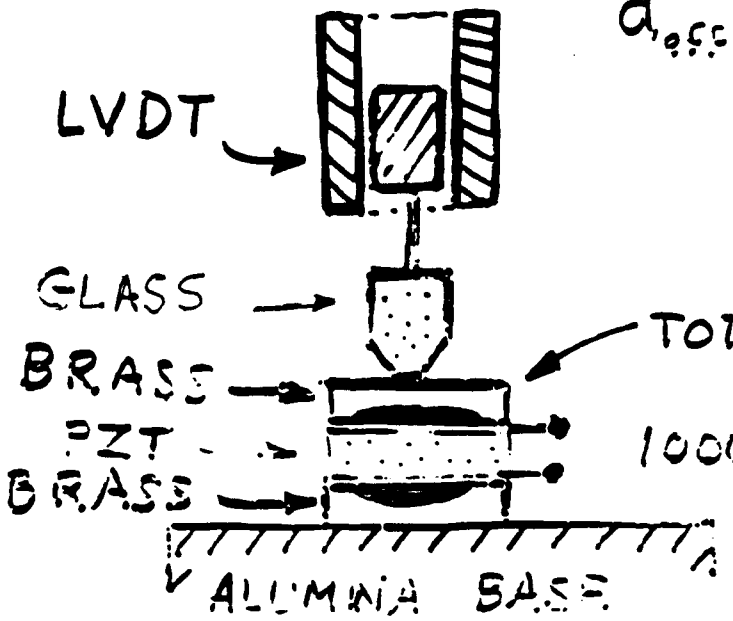

$$d_{eff} = \frac{\text{STRAIN}}{\text{FIELD}} = \frac{2.5 \times 10^{-3}}{10^6\ \text{V/m}}$$

$$= 2500\ \text{pm/V} \quad (6 \times \text{PZT})$$

MOONIE
TOTAL THICKNESS ~ 2 mm

1000 V/mm = E_{MAX}

Y. SUGAWARA

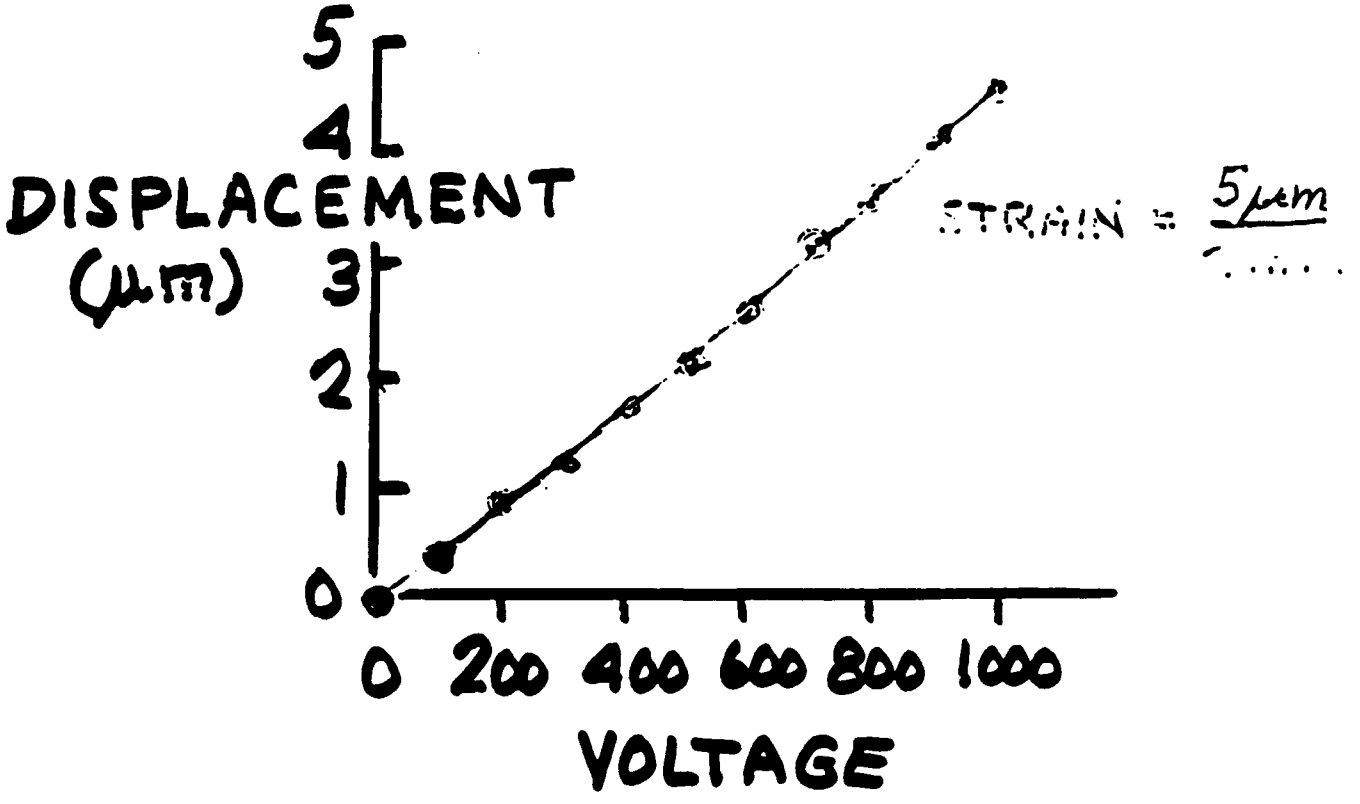

ELECTROSTRICTIVE MOONIE ACTUATOR

1 Cm MOONIE : 2mm THICK

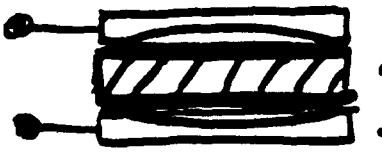

1mm PMN-PT CERAMIC

0.4mm BRASS END CAPS

SOLDER FOIL BONDING
NO POLING REQUIRED

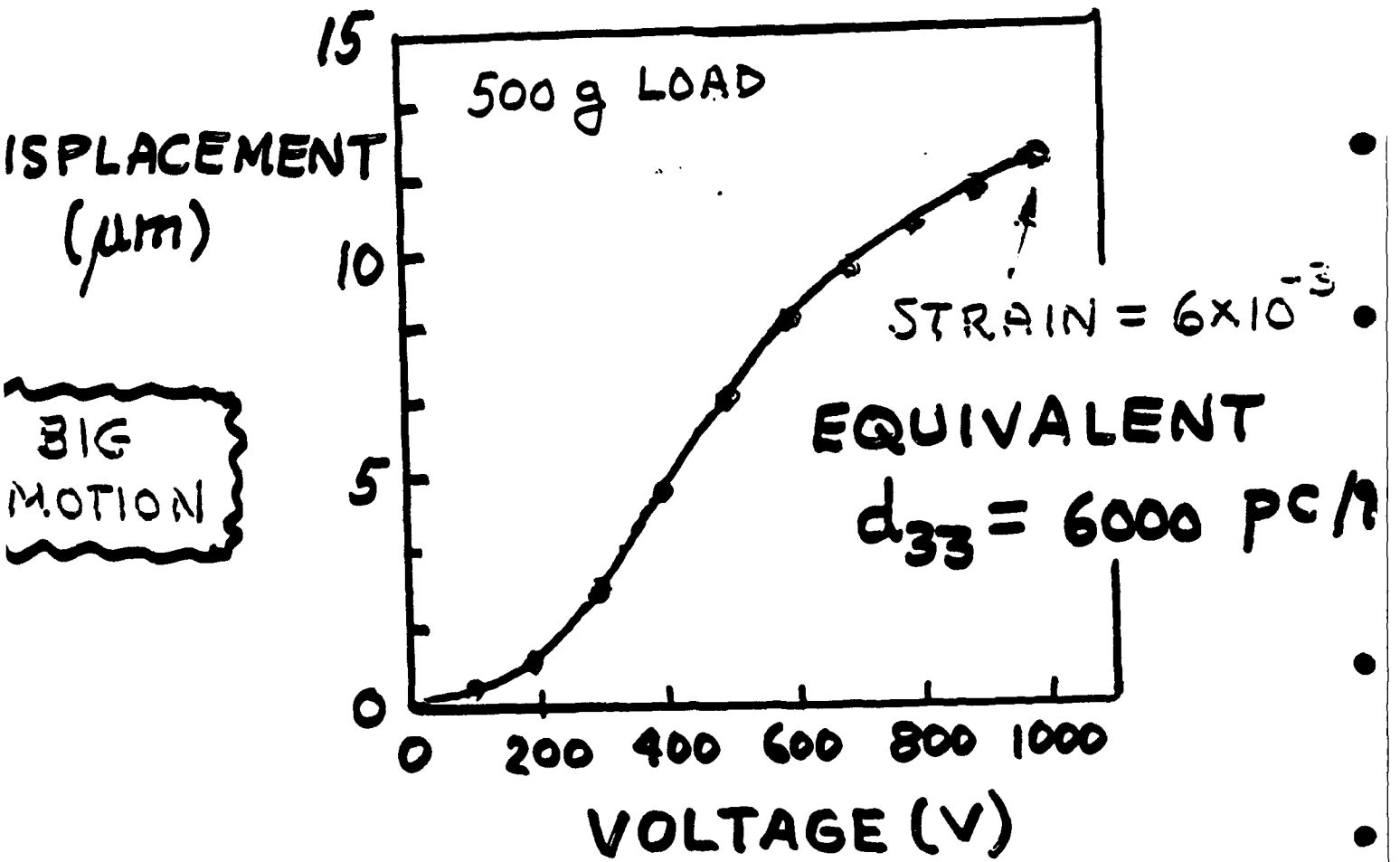

BIG MOTION

S. SUEAWARA, Q. C. XU, PENN STATE

MULTIMOONIE ACTUATOR

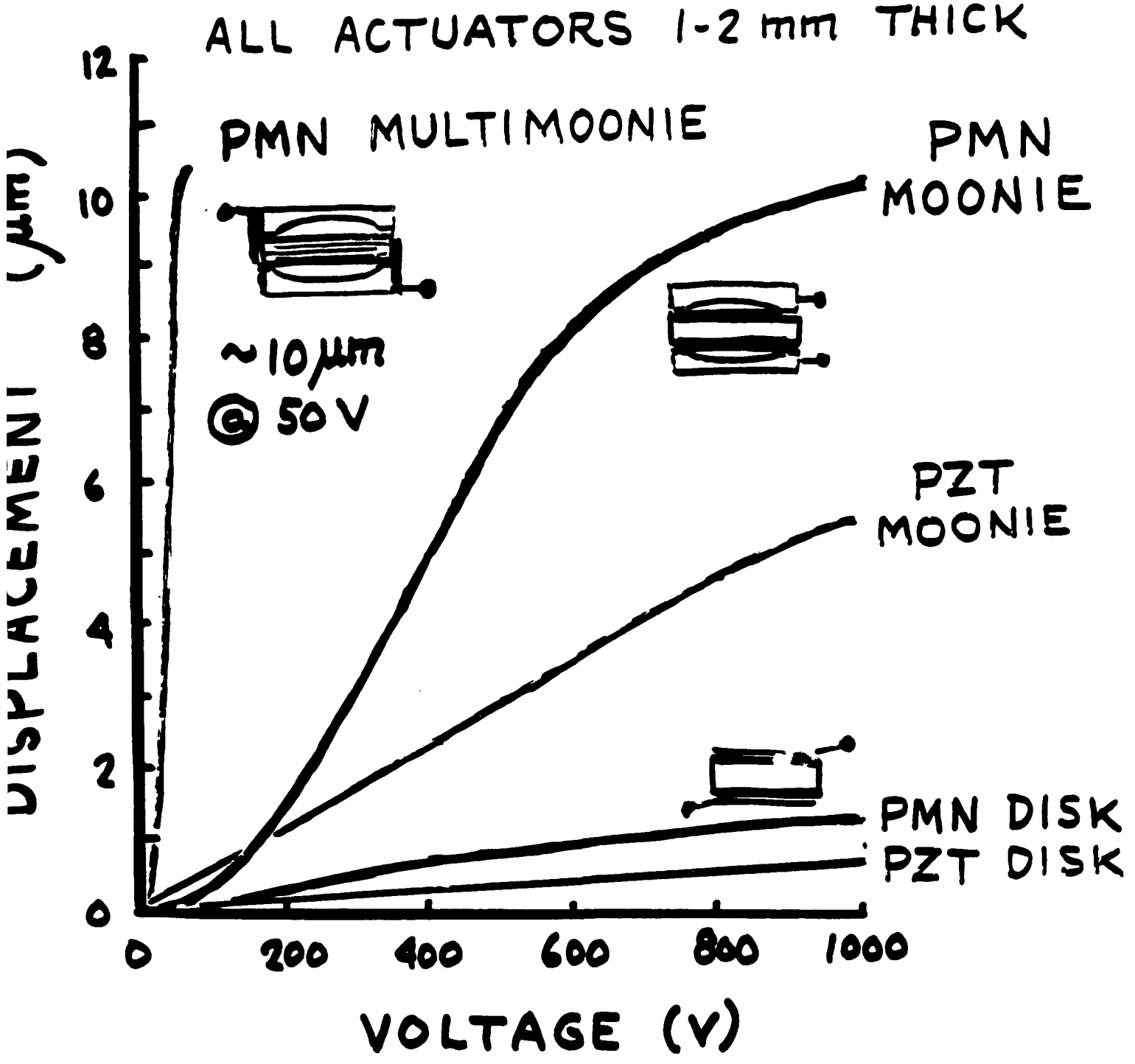

S. SUGUWARA (PENN STATE & SOPHIA)

PIEZOELECTRIC COEFFICIENTS

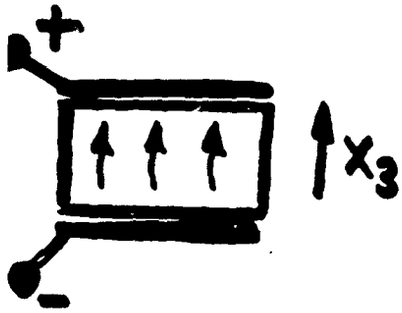

$$\epsilon_3 = \frac{\Delta t_3}{t_3} = d_{33} E_{33}$$

ϵ_3: LONGITUDINAL STRAIN

E_{33}: ELECTRIC FIELD

PIEZOELECTRIC CHARGE COEFFICIENT d_{33}

WEAK PIEZOELECTRIC (QUARTZ) — $d_{33} \sim 1\text{-}5$ pC/N

NORMAL PIEZOELECTRIC (PVDF) — $d_{33} \sim 10\text{-}50$ pC/N

STRONG PIEZOELECTRIC (PZT) — $d_{33} \sim 100\text{-}500$ pC/N

STRAIN AMPLIFIERS & TUNABLE PIEZOELECTRICS (MOONIES & RELAXORS) — $d_{33} \sim 1000\text{-}5000$ pC/

NUWC

PRESENTATION
TO THE
WORKSHOP ON ADVANCED PIEZOELECTRIC ACTUATOR MATERIALS FOR SPACE APPLICATIONS
AT THE
INSTITUTE FOR DEFENSE ANALYSIS

25 FEBRUARY 1992

REVIEW OF HIGH POWER TRANSDUCERS

FRANK A. TITO

NAVAL UNDERSEA WARFARE CENTER DETACHMENT
NEW LONDON, CONNECTICUT

RESTRICTIONS AND POWER LIMITATIONS ON SONAR PROJECTORS

- **MEDIA LIMITS, SUCH AS CAVITATION**
- **PHYSICAL LIMITS OF RADIATED SOUND THAT GOVERN THE REQUIRED PROJECTOR SIZE**
  - **RADIATING AREA**
  - **DISPLACEMENT**
- **INTERNAL PROJECTOR LIMITS**
  - **ELECTRICAL**
  - **MECHANICAL**
  - **THERMAL**

FLUID MEDIA LIMIT ** CAVITATION

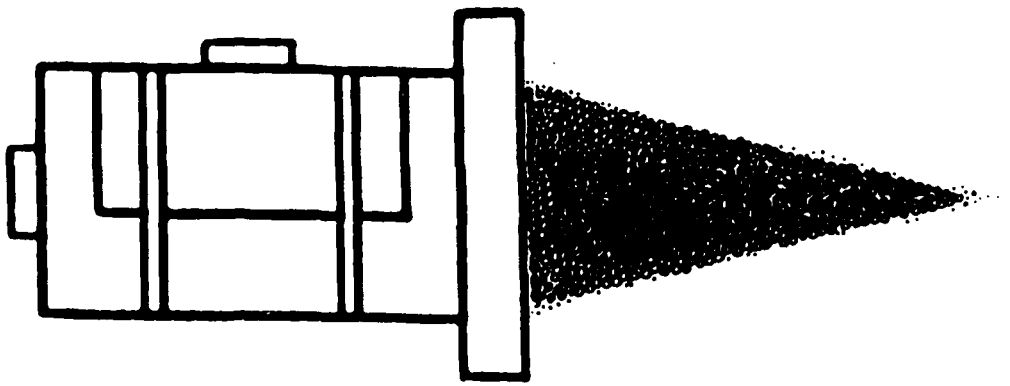

- **PROPERTY OF THE FLUID MEDIUM**
  - CAVITATION OCCURS WHEN ACOUSTIC PRESSURE EXCEEDS FLUID STATIC PRESSURE
- **CAVITATION THRESHOLD**
  - INCREASE WITH INCREASING DEPTH
  - INCREASE WITH HIGHER FREQUENCY (ESPECIALLY ABOVE 10 - 15 kHz)
  - INCREASE WITH SHORTER PULSE (< .005 SECONDS)
  - CAN OCCUR WITH NEAR FIELD LOCAL HIGH PRESSURE DISTRIBUTIONS

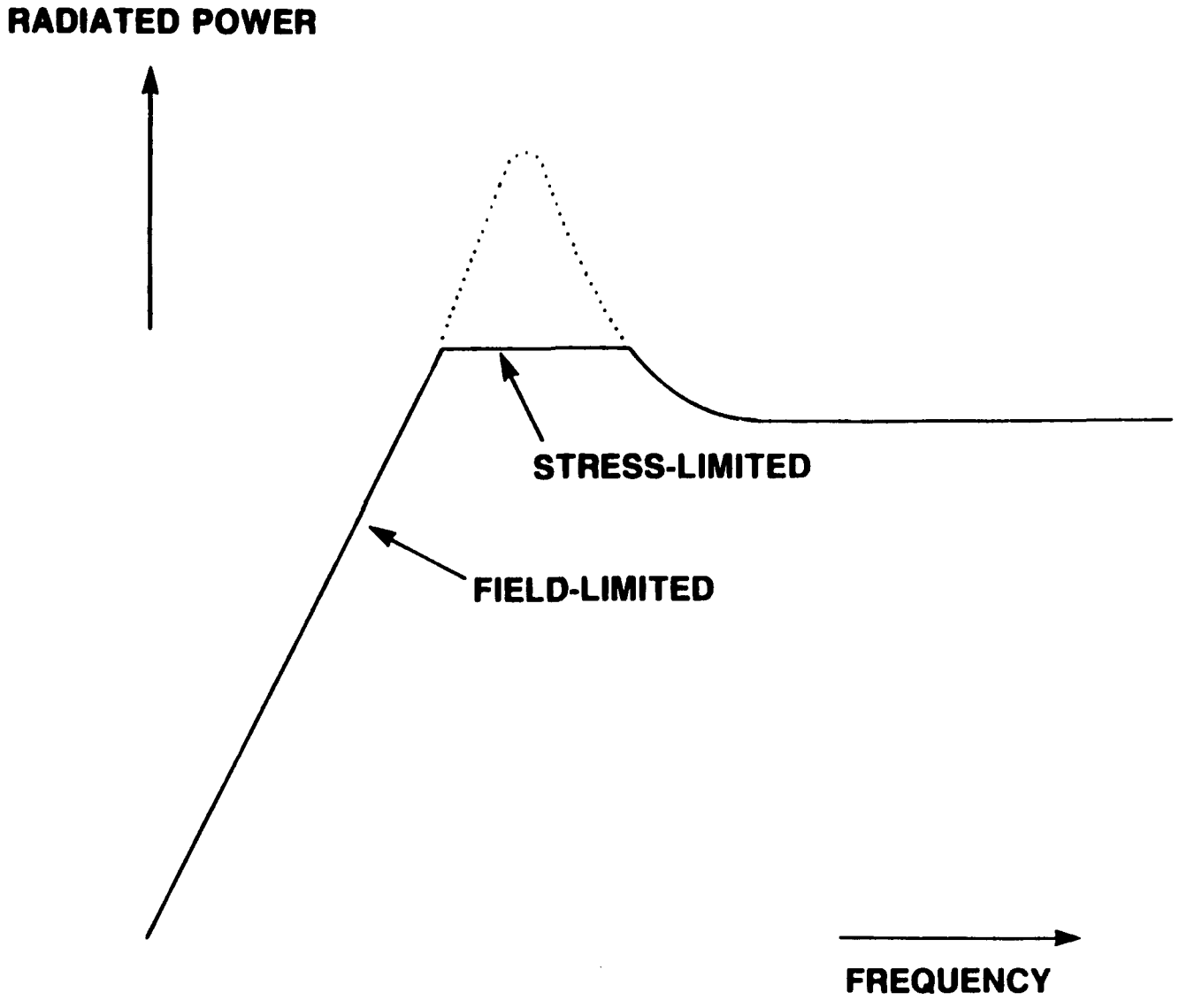
RADIATED POWER
STRESS-LIMITED
FIELD-LIMITED
FREQUENCY

POWER LIMITS AT RESONANCE

$$P_f = \eta \omega_o \, VQ \, k^2 \, u_f$$

$$P_s = \frac{\eta \omega_o \, VQ \, u_s}{1 + Q^2}$$

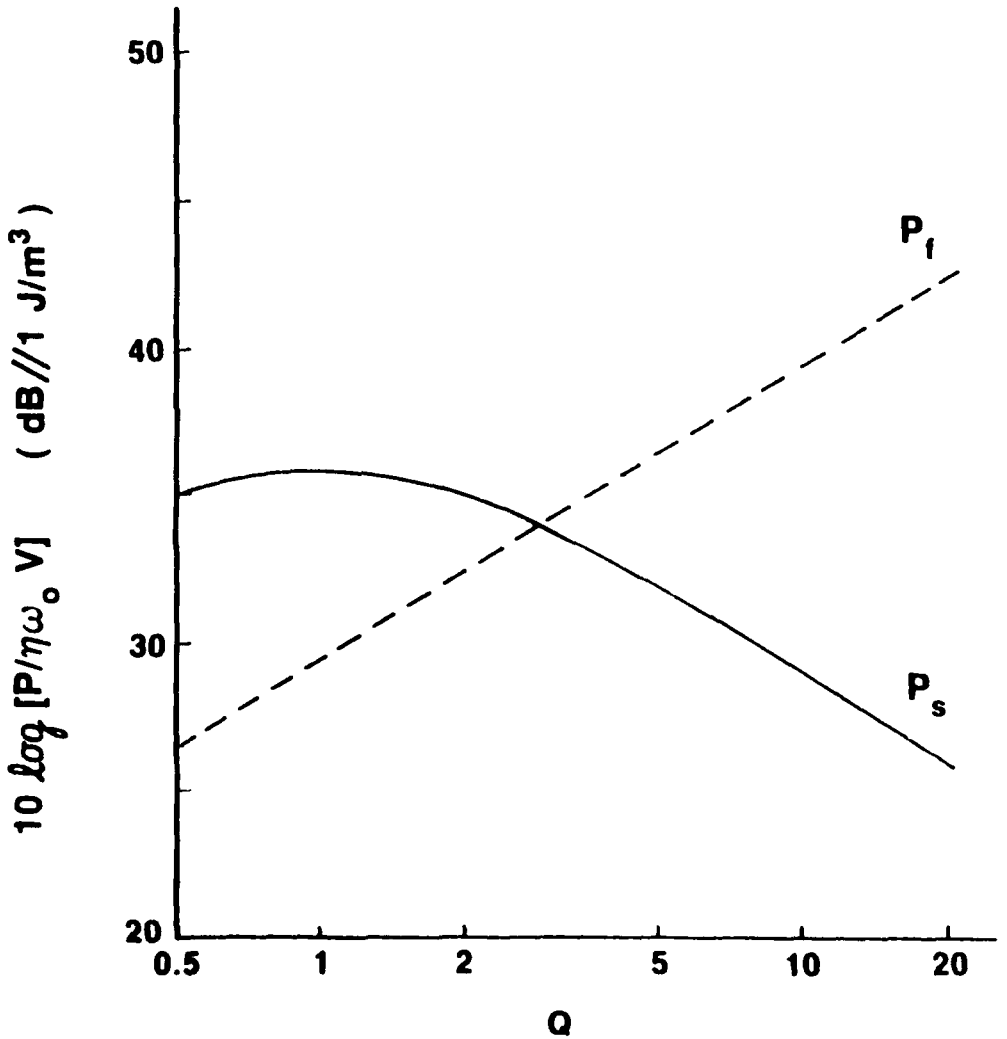

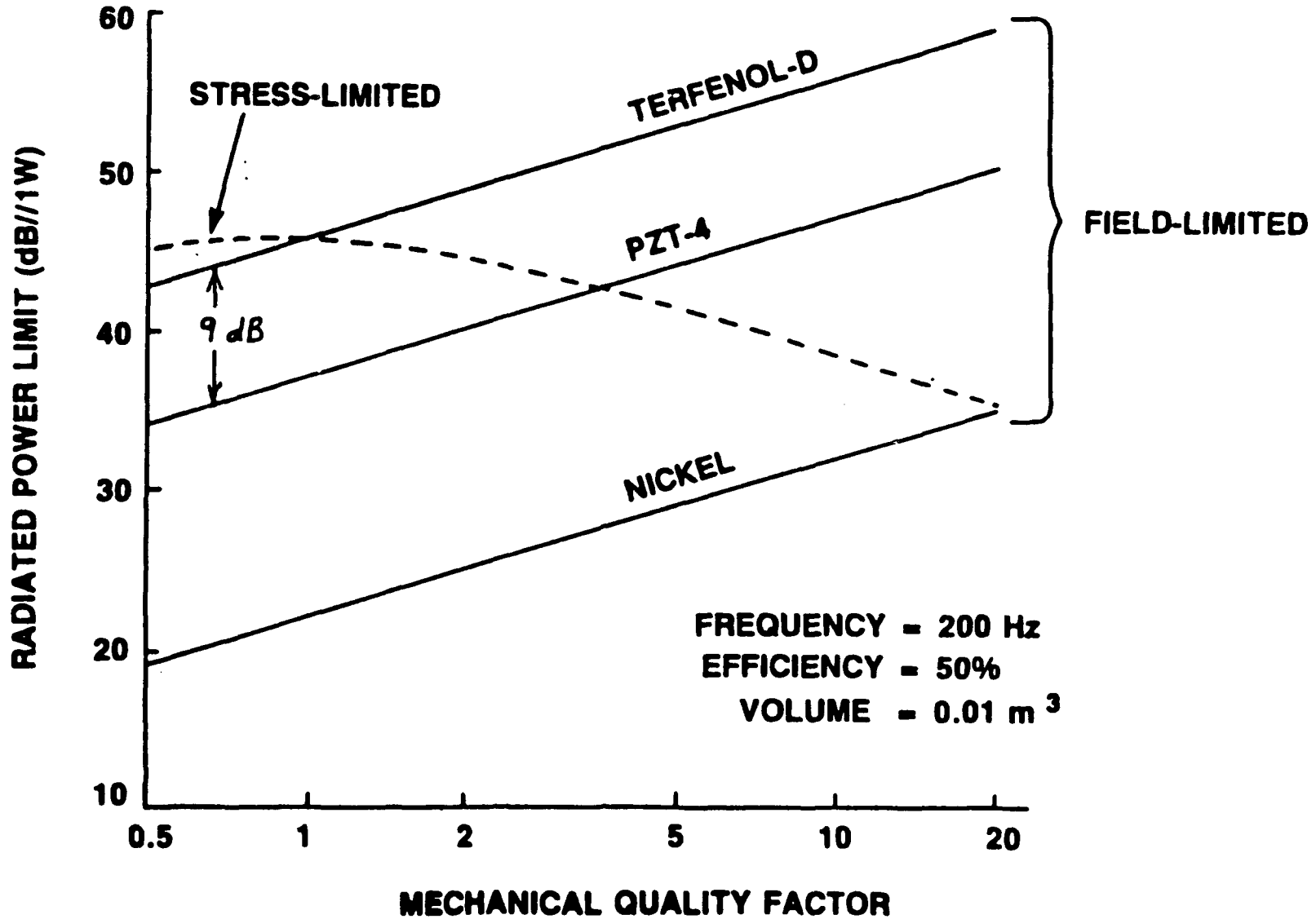
60
50
40
30
20
10
RADIATED POWER LIMIT (dB//1W)
STRESS-LIMITED
TERFENOL-D
PZT-4
NICKEL
9 dB
FIELD-LIMITED
FREQUENCY = 200 Hz
EFFICIENCY = 50%
VOLUME = 0.01 m 3
0.5
1
2
5
10
20
MECHANICAL QUALITY FACTOR

HYDROACOUSTIC TRANSDUCTION

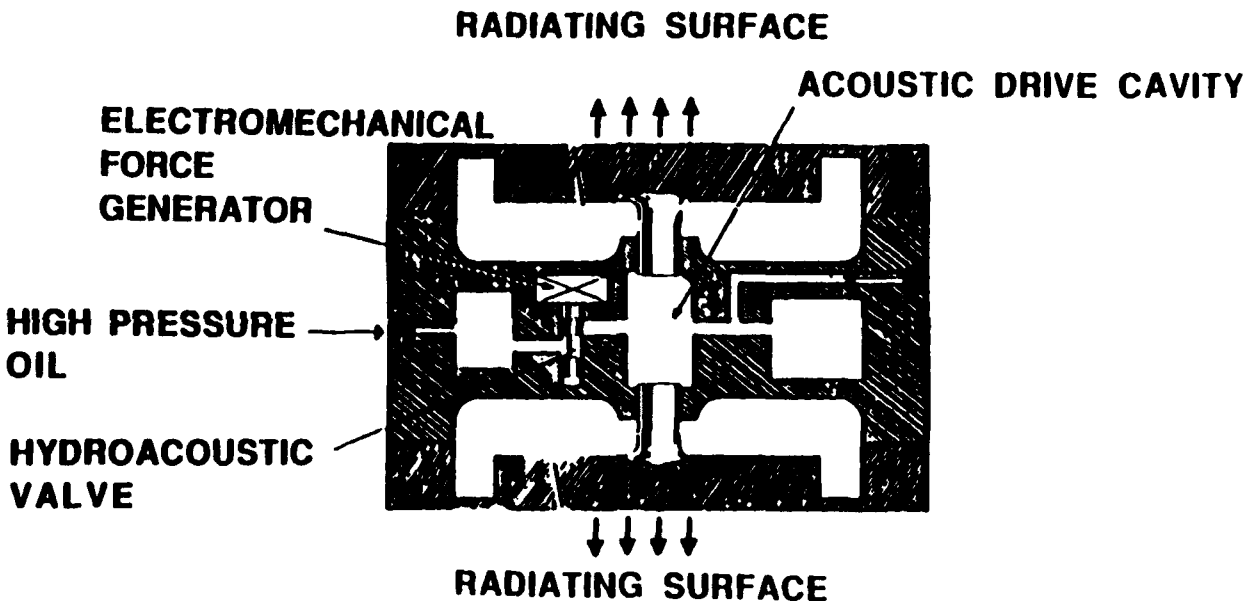

HIGH PRESSURE HYDRAULIC OIL MODULATED BY VALVE PRODUCES AC FLUCTUATIONS ON DRIVER

HYDROACOUSTIC PROJECTOR

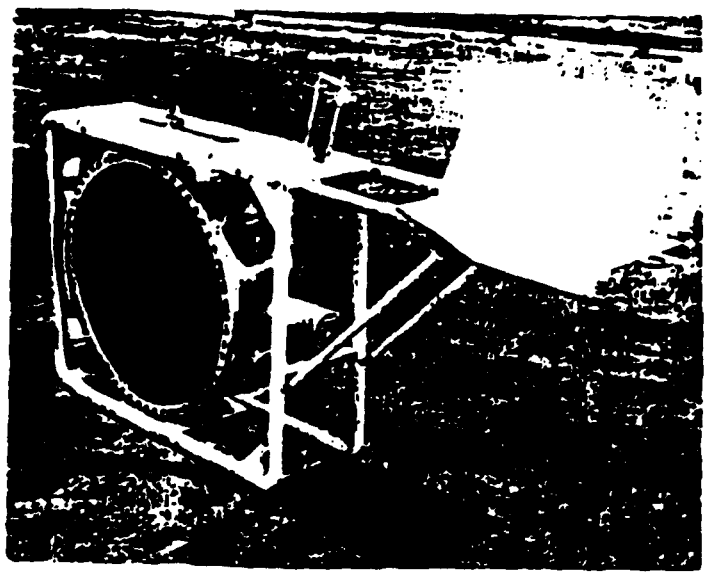

HVLF-1B

FREQUENCY RANGE	6 - 47 Hz
MAXIMUM SOURCE LEVEL	193 dB
WEIGHT	
AIR	2000 kg
WATER	950 kg
DIMENSIONS	1.5 m DIAMETER X 0.76 m THICK

MANUFACTURER:
HYDROACOUSTICS INC.

HYDROACOUSTIC PROJECTOR

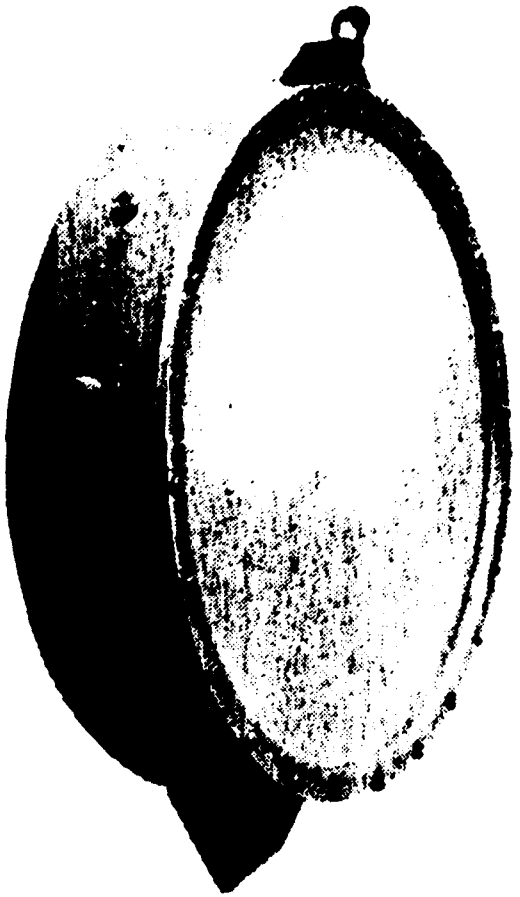

HLF-5

FREQUENCY RANGE	**200 - 300 Hz**
MAXIMUM SOURCE LEVEL	**194 dB**
WEIGHT	
AIR	**486 kg**
WATER	**141 kg**
DIMENSIONS	
	1.13 m DIAMETER X 0.43 m THICK

MANUFACTURER:
HYDROACOUSTICS INC.

MOVING COIL TRANSDUCTION

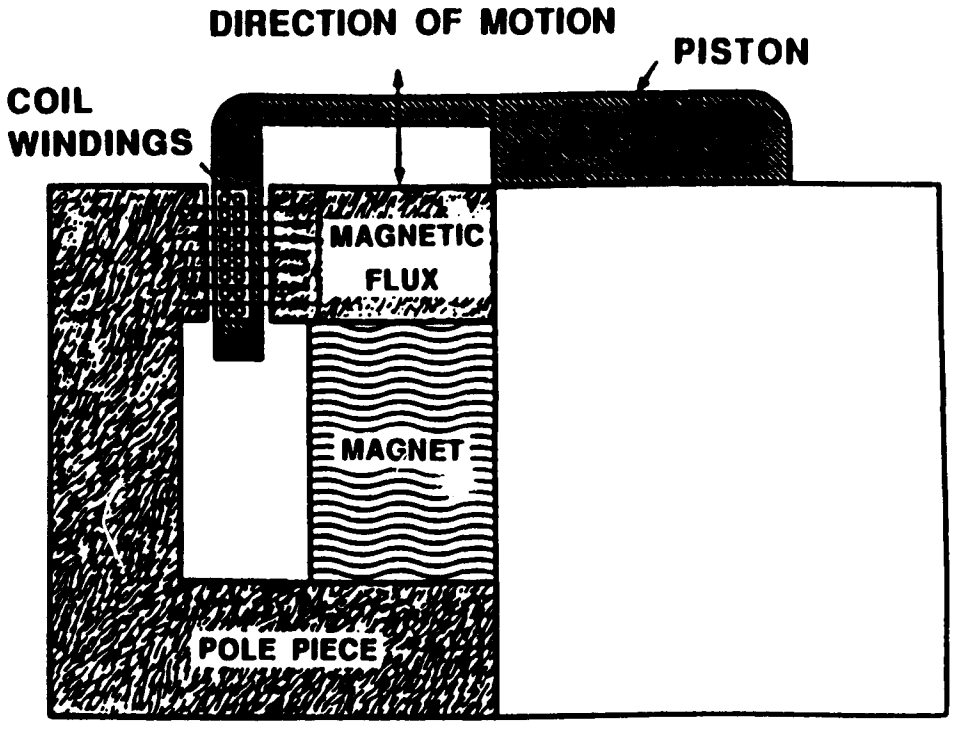

CYLINDRICAL COIL IS ELECTRICALLY DRIVEN IN A CONSTANT MAGNETIC FIELD WHICH IS PRODUCED BY EITHER DC WINDING OR PERMANENT MAGNET

MOVING COIL PROJECTOR

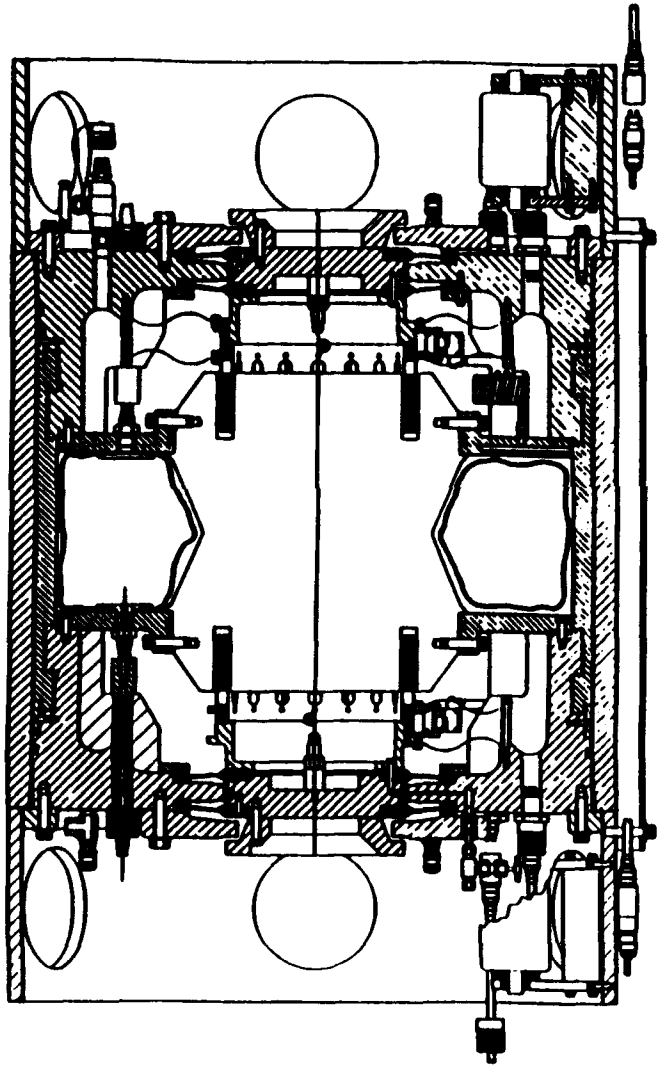

PB-1

FREQUENCY RANGE	35 - 100 Hz
MAXIMUM SOURCE LEVEL	175 dB
WEIGHT	
AIR	2500 LBS
WATER	1900 LBS
DIMENSIONS	32" DIAMETER X 51" HEIGHT

MANUFACTURER:
ARGOTEC, INC.

MOVING COIL PROJECTOR

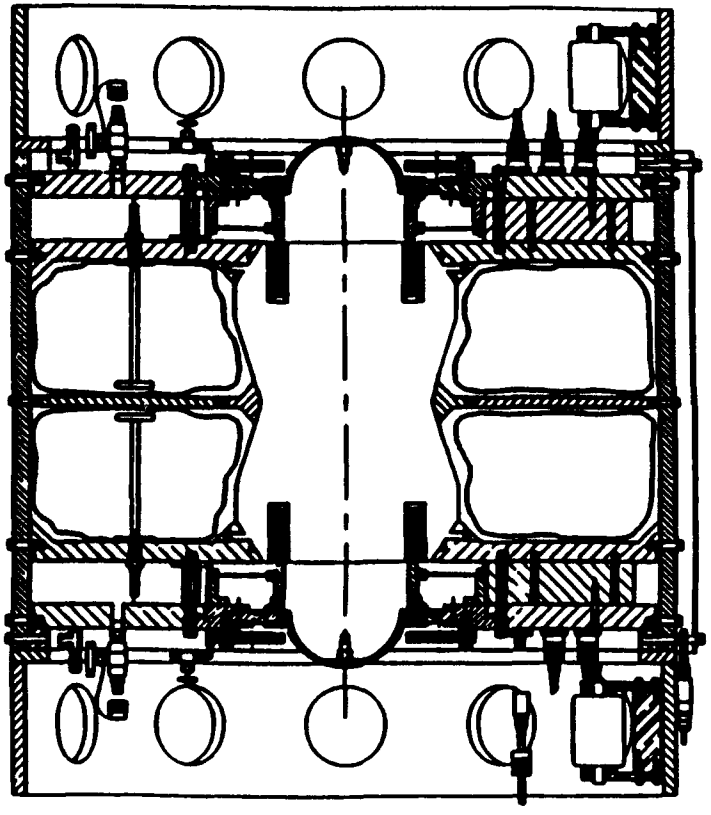

ALPHA

FREQUENCY RANGE	35 - 100 Hz
MAXIMUM SOURCE LEVEL	190 dB
WEIGHT	
AIR	4500 LBS
WATER	2100 LBS
DIMENSIONS	51" DIAMETER X 60" HEIGHT
MANUFACTURER: ARGOTEC, INC.	

FLEXURAL BENDER BAR TRANSDUCTION

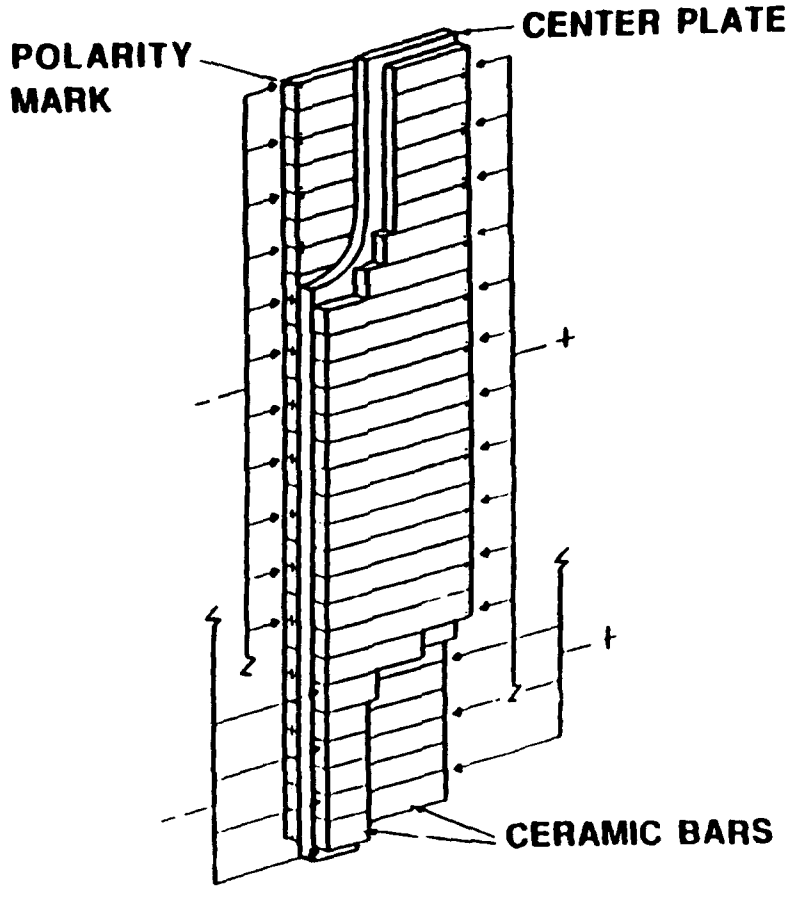

THE TWO CERAMIC STACKS ARE OPPOSITELY DRIVEN SUCH THAT ONE EXPANDS WHILE THE OTHER CONTRACTS CAUSING THE ENTIRE STRUCTURE TO FLEX

FLEXURAL BENDER BAR PROJECTOR

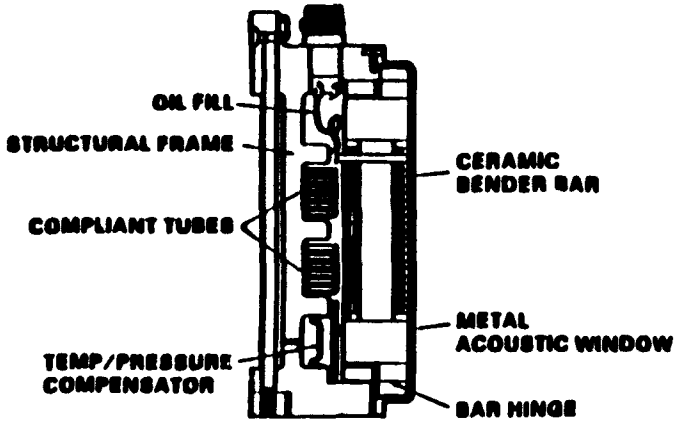

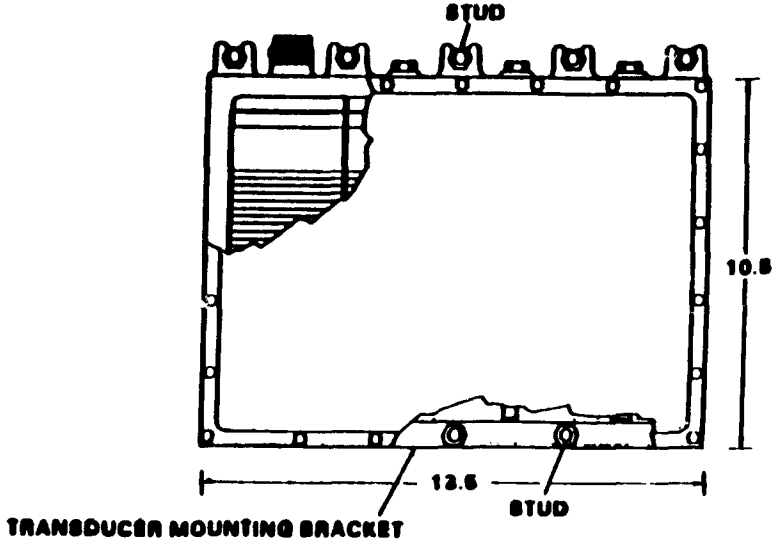

FLATPACK

FREQUENCY 1500 Hz

MAXIMUM SOURCE LEVEL 209 dB

DIMENSIONS

10.5 X 13.5 X 4.5 "

MANUFACTURER:

ALLIANT TECH SYSTEMS

FLEXURAL BENDER BAR PROJECTOR

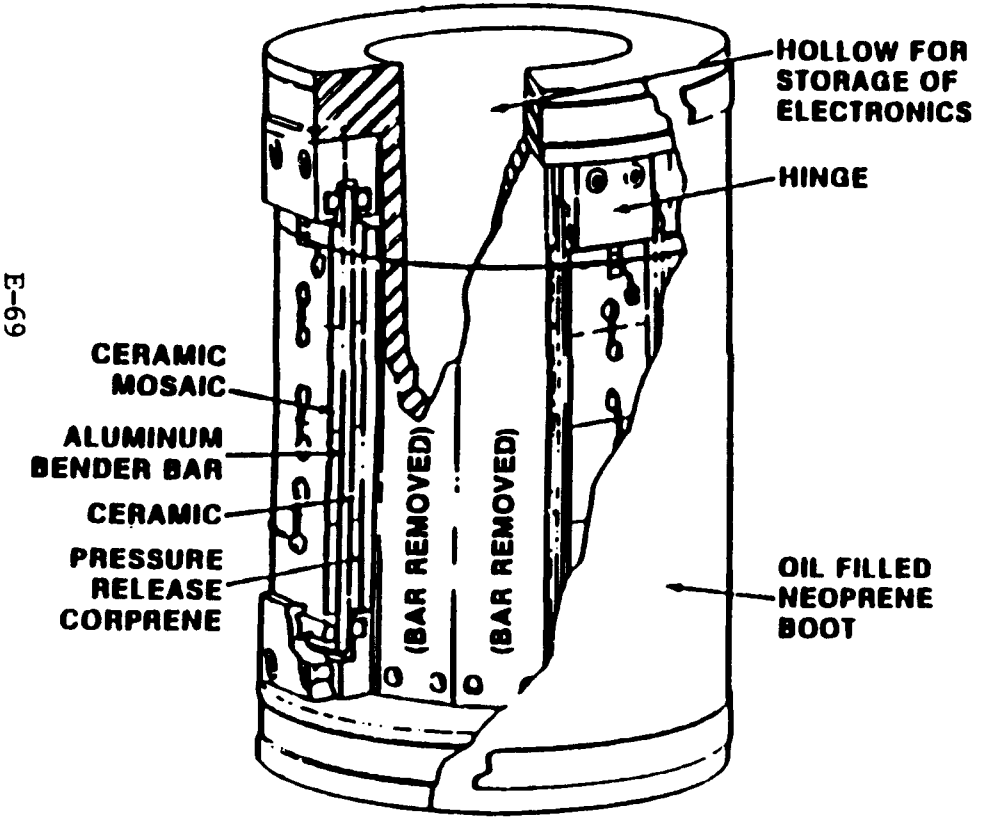

HX PROJECTOR

FREQUENCY RANGE	1300 - 1800 Hz
MAXIMUM SOURCE LEVEL	129 dB
WEIGHT	15 POUNDS
LENGTH	5.75 INCHES

MANUFACTURER:
ALLIANT TECH SYSTEMS

FLEXURAL DISK TRANSDUCTION

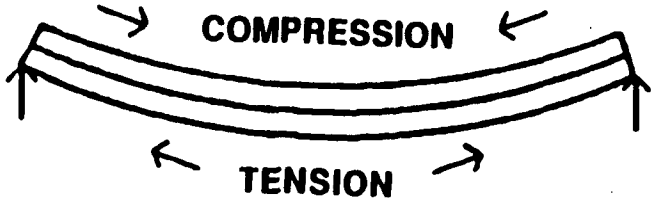

FLEXURAL BILAMINAR DISK ELEMENT

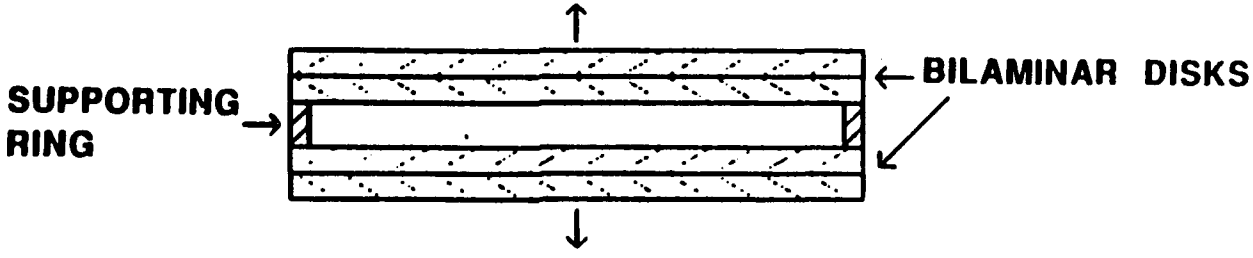

DOUBLE BILAMINAR DISK

ONE DISK IS DRIVEN INTO COMPRESSION AND THE OTHER INTO EXPANSION SUCH THAT THE PLATE IS MADE TO BEND

FLEXURAL DISK PROJECTOR

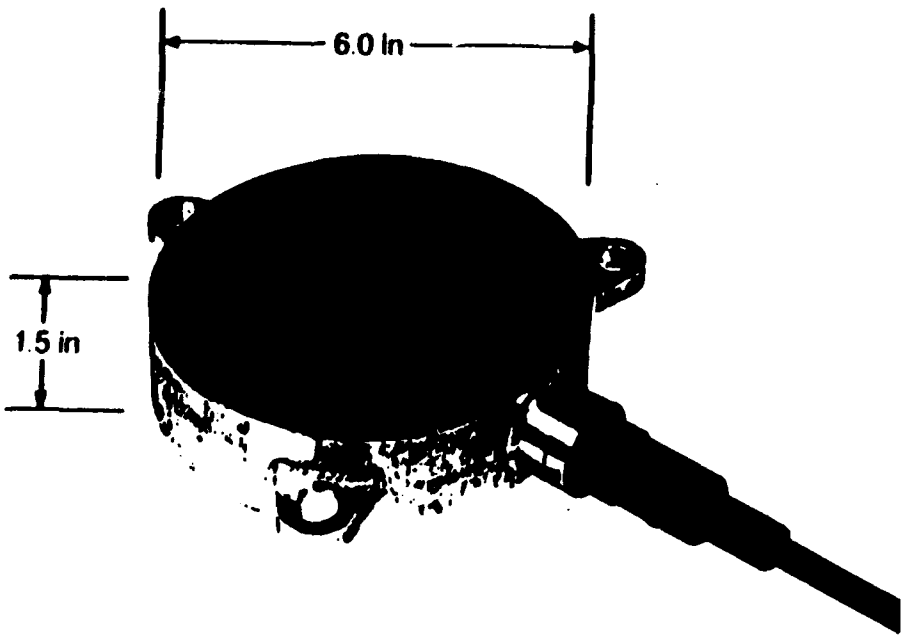

ITC-4004A

FREQUENCY RANGE	2 - 4 KHz
MAXIMUM SOURCE LEVEL	190 dB
WEIGHT	
AIR	6.8 LBS
WATER	4.6 LBS
DIMENSIONS	
	6.0 " DIAMETER X 1.5 " THICK

MANUFACTURER:
INTERNATIONAL TRANSDUCER CORPORATION

CLASS IV FLEXTENSIONAL TRANSDUCTION

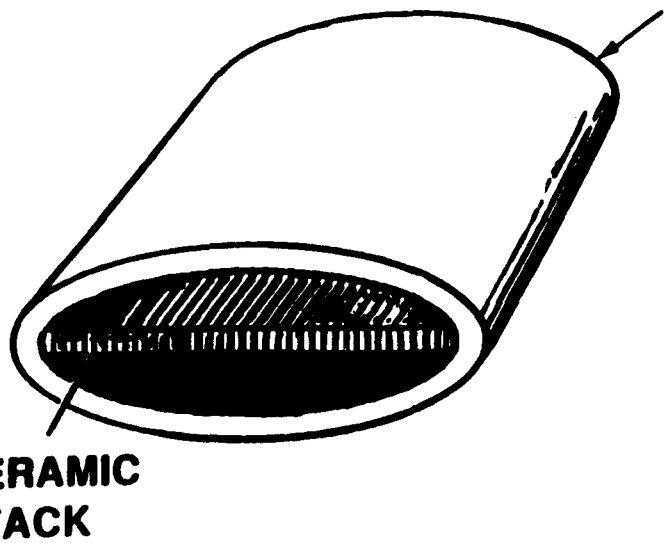

MODES

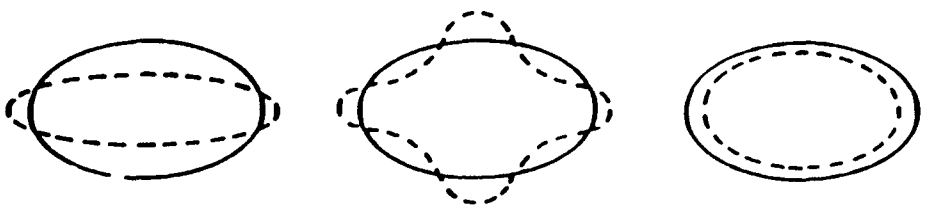

FIRST EVEN-EVEN (FUNDAMENTAL) ELLIPTICAL BENDING MODE

SECOND EVEN-EVEN ELLIPTICAL BENDING MODE

HOOP MODE

N = 3 ASYMMETRIC MODE

EXTENSIONAL MOTION IN STACK WORKING THROUGH MECHANICAL TRANSFORMER OF END OF SHELL PRODUCES FLEXURAL MOTION OF SHELL

CLASS IV FLEXTENSIONAL PROJECTOR

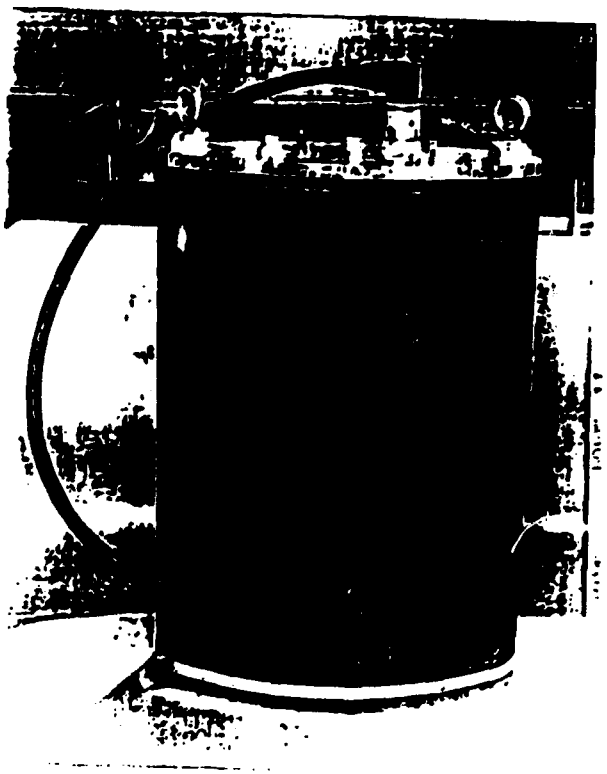

FREQUENCY RANGE	**450 - 600 Hz**
MAXIMUM SOURCE LEVEL	**220 dB**
WEIGHT	
AIR	**1150 LBS**
DIMENSIONS	
	24" MAJOR DIAMETER
	11" MINOR DIAMETER
	34" HEIGHT
MANUFACTURER:	
RAYTHEON	

CLASS IV FLEXTENSIONAL PROJECTOR

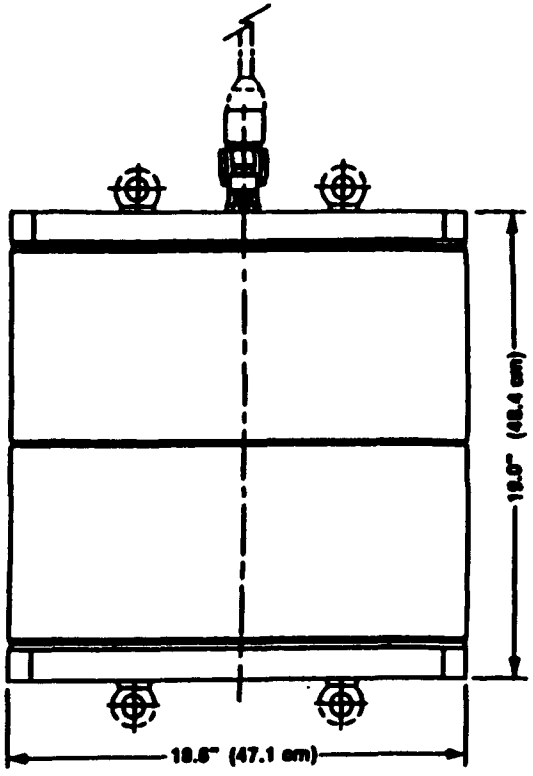

FREQUENCY RANGE	**800 Hz**
MAXIMUM SOURCE LEVEL	**206 dB**
WEIGHT	**198 LBS**
DIMENSIONS	**19 X 19 X 8.1"**

MANUFACTURER:
BRITISH AEROSPACE

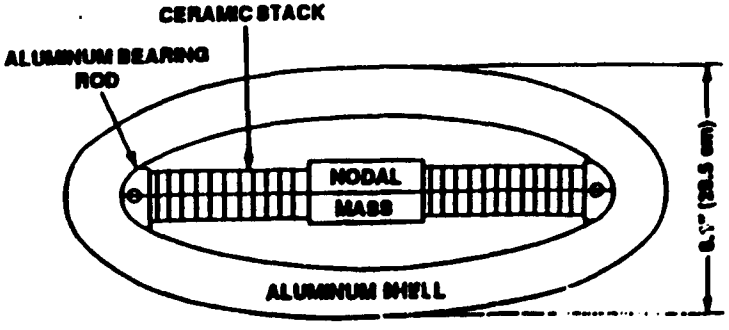

SHELL ASSEMBLY

RING TRANSDUCTION

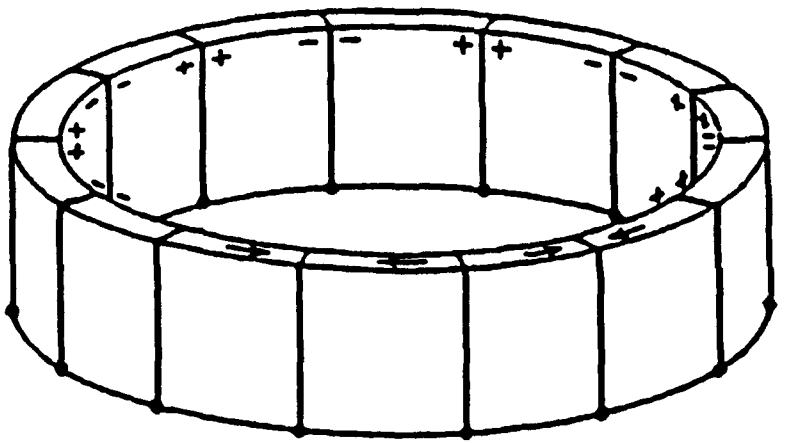

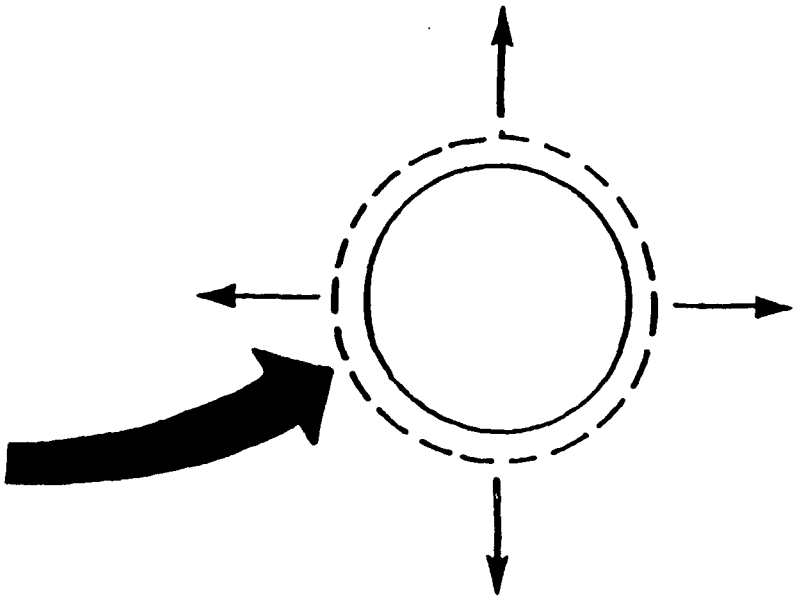

HOOP MODE MOTION

SEGMENTED PIEZOELECTRIC CERAMIC RING TRANSDUCER

RING IS DRIVEN CIRCUMFERENTIALLY

ACTIVE MATERIAL

- PIEZOELECTRIC CERAMIC
- MAGNETOSTRICTIVE

RING PROJECTOR

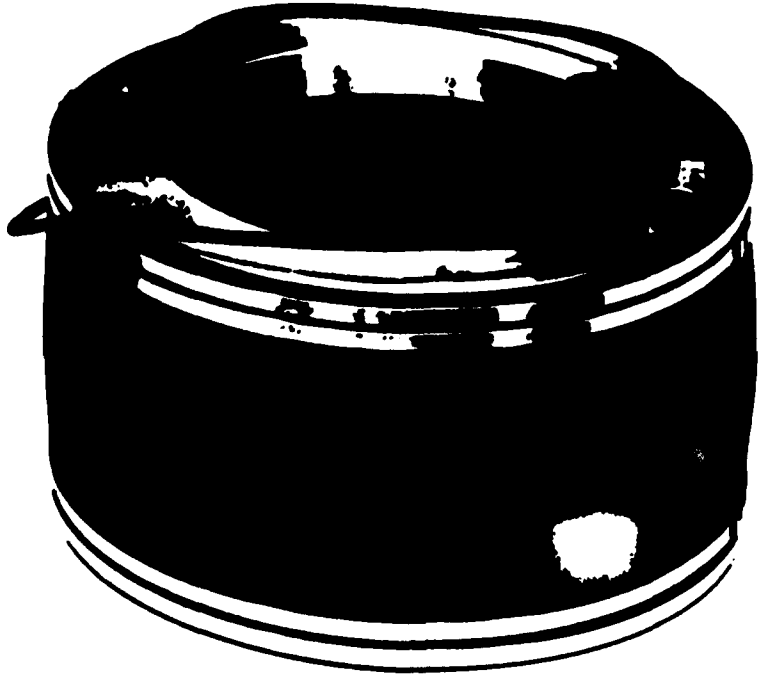

MODEL ITC-2015

FREQUENCY RANGE	**1800 - 400 Hz**
MAXIMUM SOURCE LEVEL	**212 dB**
WEIGHT	
AIR	**116 LBS**
WATER	**70 LBS**
DIMENSIONS	**15" DIAMETER X 7.8" HEIGHT**

MANUFACTURER:
INTERNATIONAL TRANSDUCER CORPORATION

RING PROJECTOR

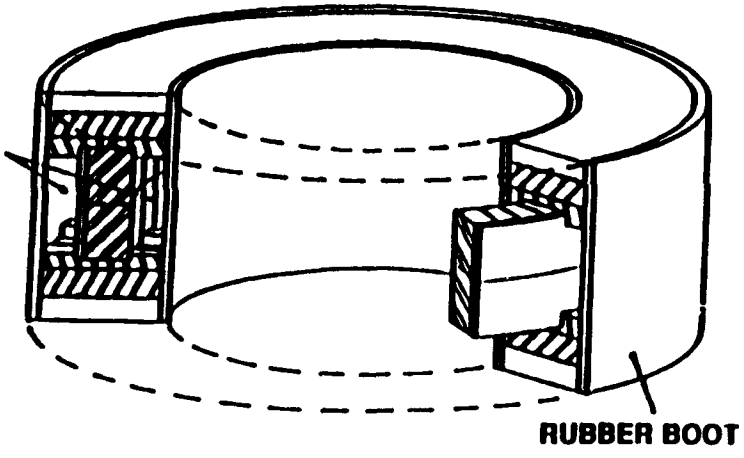

FREQUENCY RANGE	600 - 900 Hz
MAXIMUM SOURCE LEVEL	216 dB
WEIGHT	2000 LBS
DIMENSIONS	≈ 5' DIAMETER X ≈ 1' HEIGHT

MANUFACTURER:
GENERAL ELECTRIC

PROJECTOR MATERIALS

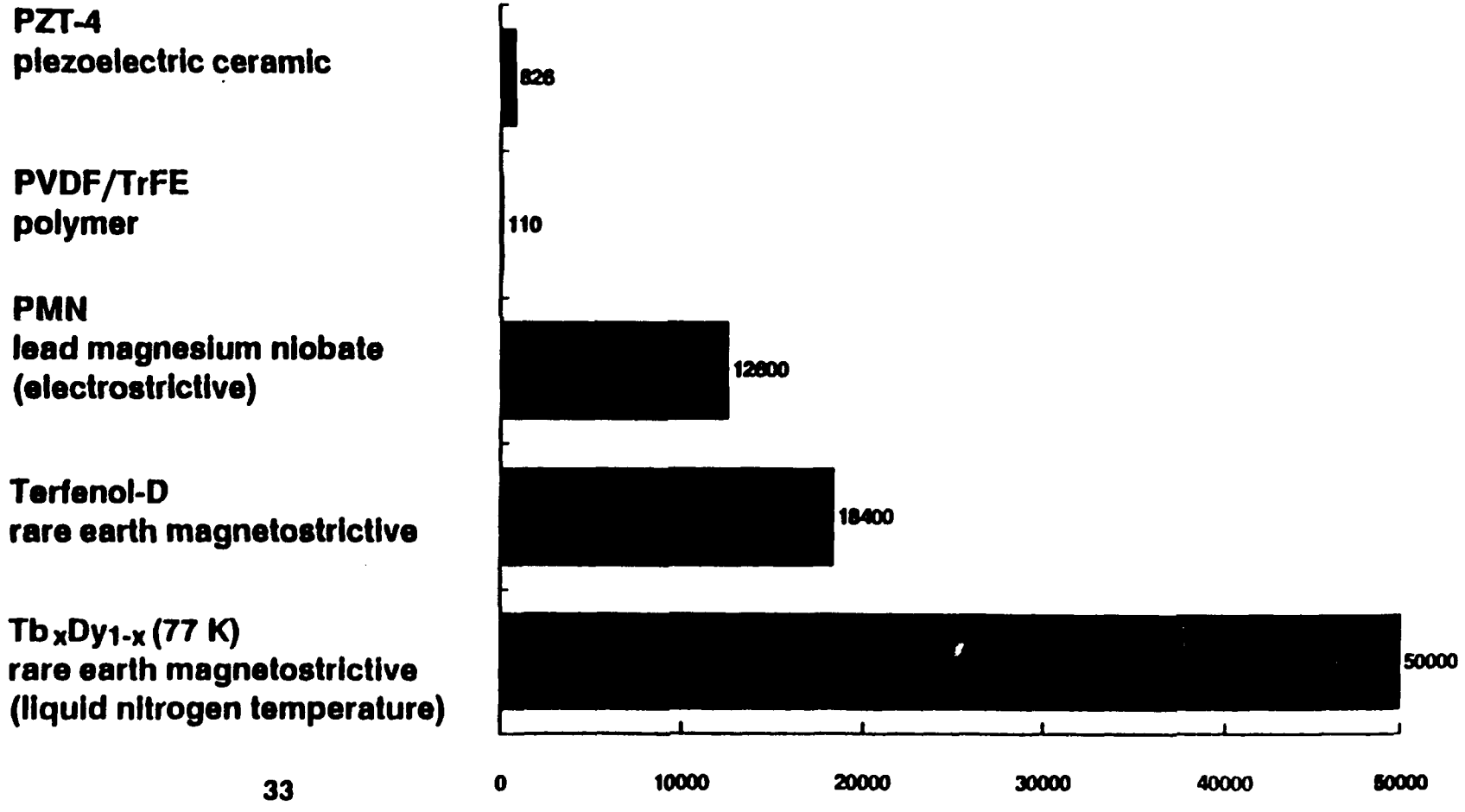

TERFENOL-D / CERAMIC PROJECTOR COMPARISON

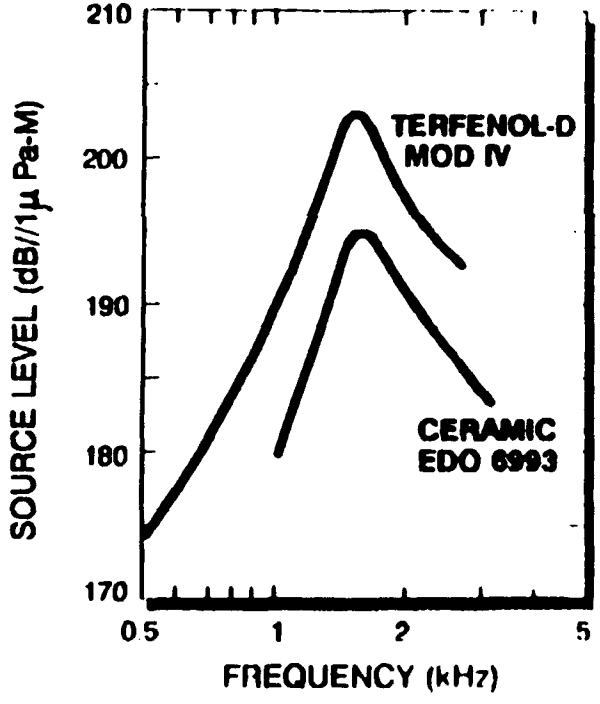

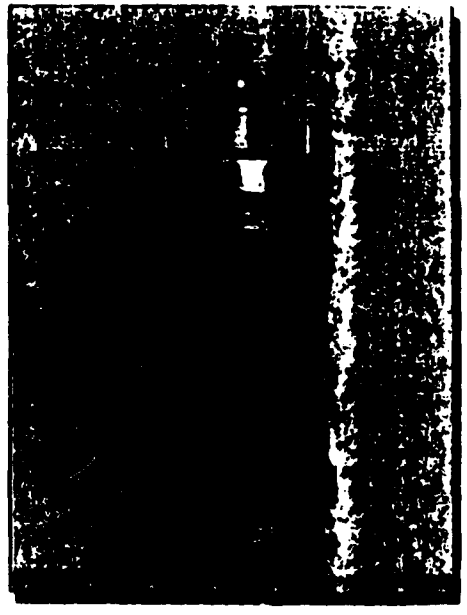

MOD IV TERFENOL-D BARREL-STAVE
FLEXTENSIONAL PROJECTOR

NUWC

SECTION A-A

RANGE OF OPERATING FREQUENCIES FOR VARIOUS TRANSDUCTION MECHANISMS

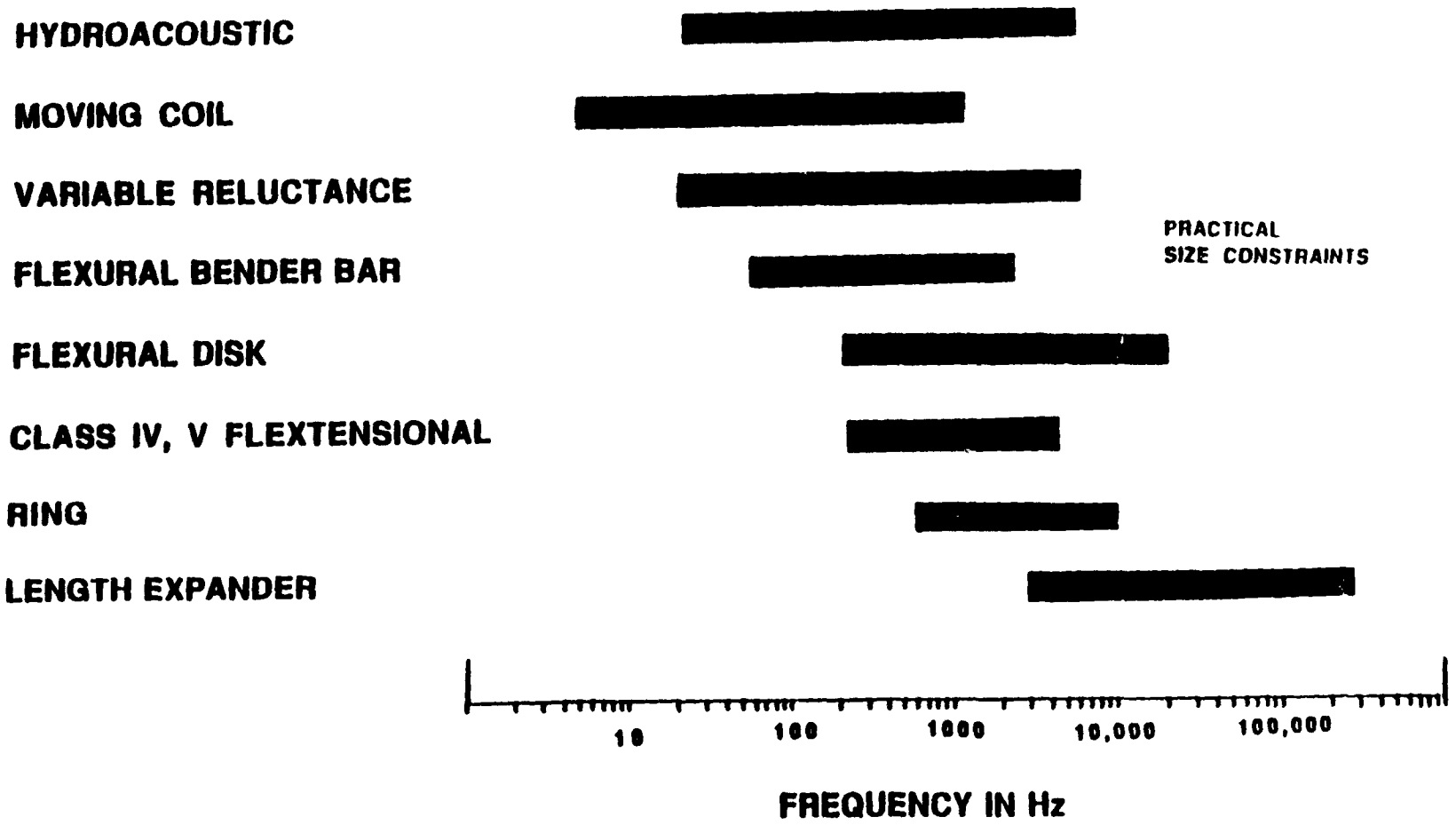

REFERENCES

T. MEYERS, "A REVIEW OF LOW FREQUENCY HIGH POWER REQUIREMENTS AND THE TRANSDUCERS AVAILABLE TO MEET THESE REQUIREMENTS," NUSC REPORT, APRIL 1989.

R. J. URICK, *PRINCIPLES OF UNDERWATER SOUND FOR ENGINEERS*, McGRAW-HILL, NEW YORK, SECOND EDITION, 1975.

D. STANSFIELD, *UNDERWATER ELECTROACOUSTIC TRANSDUCERS*, BATH UNIVERSITY PRESS, 1991.

J. DECARPIGNY, B. HAMONIC, AND O. B. WILSON, Jr., "THE DESIGN OF LOW-FREQUENCY UNDERWATER ACOUSTIC PROJECTORS: PRESENT STATUS AND FUTURE TRENDS," *IEEE JOURNAL OF OCEANIC ENGINEERING*, VOLUME 16, NUMBER 1, JANUARY 1991.

R. WOOLLETT, "POWER LIMITATIONS OF SONIC TRANSDUCERS," *IEEE TRANSDUCERS ON SONICS AND ULTRASONICS*, VOLUME SU-15, NUMBER 4, OCTOBER 1968.

APPENDIX F

IMPROVED PZT THROUGH CONTROLLED POWDER SYNTHESIS AND BULK POWDER PROCESSING

IMPROVED PZT THROUGH CONTROLLED POWDER SYNTHESIS AND BULK POWDER PROCESSING

by

Dr. Gerald Stranford — Alliant Techsystems (ATK)
Dr. Barry Koepke — Ceramics Center

and

Dr. Bruce Tuttle — Sandia National Laboratories

Goal

- Develop technique to manufacture PZT with improved and reproducible
  - electro-mechanical properties
  - microstructure
  - mechanical integrity

Process

- Adapt Haertling chemical precursor powder production technique currently used at ATK for transparent PLZT production to PZT fabrication.

Benefit

- Consistent, reproducible powder production
- Absolute control of powder chemistry
- Homogeneous green density, dopant distribution
- Superior sintered product

TYPICAL MIXED OXIDE POWDER PRODUCTION PROCESS

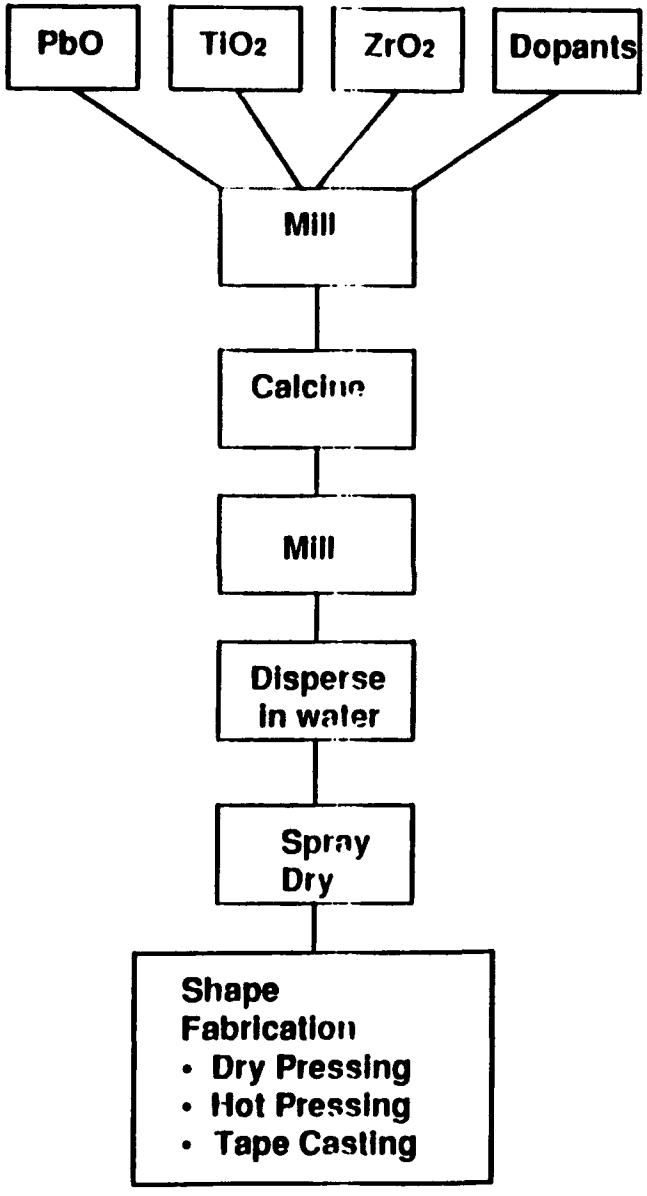

Technical Challenges

- Micron size starting powders can result in incomplete reaction and heterogeneous phase distribution.
- Difficult to homogeneously disperse low level dopants
- Formation of hard agglomerates due to high calcination temperatures
- High performance applications may require hot pressed material

Advantages

- Existing process for production of large quantities

ISSUES CONCERNED WITH OPTIMUM PROCESSING

Powder Characteristics

- Uniform chemistry with homogeneous dopant distribution
- Fine particle size to enhance rapid sintering to high density
- Narrow size distribution for uniform particle packing and densification
- Minimum agglomeration to eliminate differential shrinkage and resulting internal flaw formation

Organic Processing Additives

- Minimum binder content for better particle packing and easier burn out.
- Binders that burn cleanly.

Green Body Formation

- Uniform forming pressure to minimize microstructural texture in green body

CHEMICAL PREPARATION OF POWDER

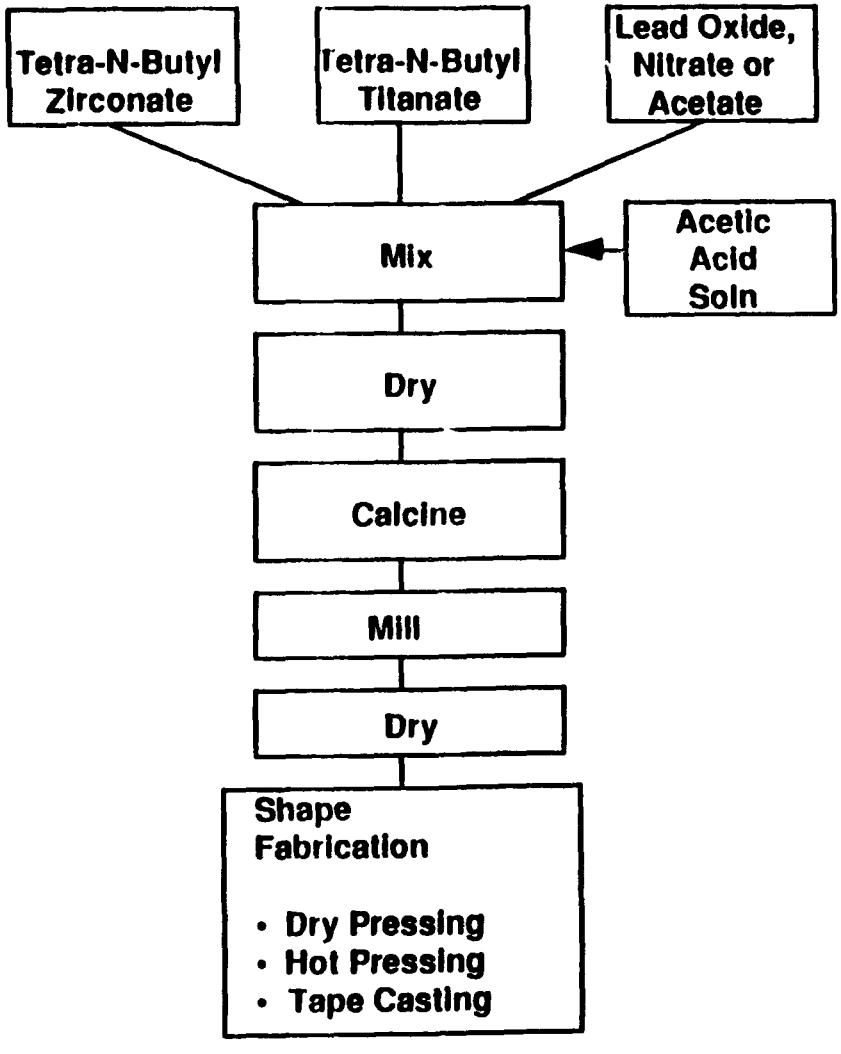

Advantages

- Uniform mixing of reactants
- Homogeneous distribution of dopants
- Lower calcination temperatures (weaker agglomerates)
- Finer particle sizes (g.s. control, lower temp. sintering, finer flaws)

Possible Modifications

- Freeze dry to minimize agglomeration

Current Capabilities

- Similar process used to prepare optical quality PLZT

PROPOSED JOINT ALLIANT TECHSYSTEMS/SANDIA NATIONAL LABORATORY PROGRAM

Objective

- Improve reproducibility and reliability in the manufacture of PZT through control of powder synthesis and bulk powder processing.

Approach

- Adopt Haertling PLZT chemical preparation process (presently used at ATK) to PZT.

Emphasis

- Powder preparation process
  - homogeneous overall/dopant chemistry
  - small particle size
  - narrow size distribution
  - weak agglomeration
- Green body characteristics
  - uniform density, pore size
  - minimum binder concentration

Goals

- Reproducible properties
- Improved sintering characteristics
- Reduced flaw populations
- Controlled dielectric aging

SUMMARY

- Actuator ceramics with repeatable (and controllable) properties, improved microstructures and enhanced mechanical integrity can be best produced from powders manufactured using chemical precursor techniques.

- Joint Alliant Techsystems/Sandia National Laboratory program is proposed to optimize this technology specifically for the production of PZT actuator ceramics.

- Necessary laboratory and production facilities are already in place.

MANUFACTURING ISSUES WITH HIGH PERFORMANCE PZT MATERIALS

by

Craig D. Near

Morgan Matroc Vernitron Division

February 1992

HIGH PERFORMANCE PZT MATERIALS

PROPERTIES

High Power Materials	K	kp	d33	Qm
▶ PZT-4S1	1500	0.640	360	300
▶ PZT-4S2	1350	0.625	330	350
▶ PZT-8M	1050	0.580	295	1000
High Strain Materials				
▶ PZT-5H	3286	0.654	664	68
▶ PZT-5K	6250	0.600	950	70

HIGH PERFORMANCE PZT MATERIALS

PERFORMANCE ISSUES

- High Performance
- High Reproducability
- High Reliability

HIGH PERFORMANCE PZT MATERIALS

MANUFACTURING ISSUES

- Compounding Interactive Multicomponent Systems
- Rheology Control of Mix, Mill, and Spray Dry
- ZrO2 Source
- Binder Materials
- Sintering Environment and Temperature Control

HIGH PERFORMANCE PZT MATERIALS

DEVELOPMENT ISSUES

- Formulation
- Chemical Processing
- Sintering Environment and Temperature Control
- Part/Actuator Manufacturing
- Real Environment Testing

HIGH PERFORMANCE PZT MATERIALS

MORGAN CHEMICAL PROCESSING R&D

	Estimated Powder Costs
▶ **Hydrothermal Synthesis**	$8/lb
▶ **Aqueous Coprecipitation**	$20 - 30/lb
▶ **Thermal Coprecipitation**	$15/lb
▶ **Sol Gel**	$18/lb
▶ **Emulsion Synthesis**	N/A

ADVANCED OXIDE POWDER PROCESSES

	Conventional	Sol-Gel	Co-Precip.	Hydrothermal
▶ **Cost**	Moderate	High	Moderate	Moderate
▶ **State of Development**	Commercial	R&D	Commercial	Commercial
▶ **Compositional Control**	Poor	Excellent	Good	Excellent
▶ **Morphology Control**	Poor	Moderate	Moderate	Good
▶ **Powder Reactivity**	Poor	Good	Good	Good
▶ **Purity**	<99.5%	>99.9%	>99.5%	>99.9%
▶ **Calcination**	Yes	Yes	Yes	No
▶ **Communition**	Yes	Yes	Yes	No

HIGH PERFORMANCE PZT MATERIALS

SINTERING CONDITIONS

PZT-4S1: Pb Atmosphere	K	kp	d33	dwt%
▶ Atm 1	1494	0.640	360	+.02
▶ Atm 2	1363	0.636	340	+.20
▶ Atm 3	1351	0.627	332	+.17
▶ Atm 4	1450	0.638	357	-.03
PZT-5K: Temperature				
▶ Temp 1	6193	0.581	910	-.38
▶ Temp 2	6284	0.582	948	-.64
▶ Temp 3	5967	0.560	872	-1.04
▶ Temp 4	5607	0.510	738	-.95

HIGH PERFORMANCE PZT MATERIALS

SPECIAL PROCESSING

PZT-5H	K	kp	d33	density
▶ **Standard**	3286	0.654	664	7.51
▶ **Special Powder Process**	3587	0.657	745	7.51
▶ **Special Firing**	3805	0.715	771	7.74

HIGH PERFORMANCE PZT MATERIALS

TESTING ISSUES

- **Real Environment: P, T, E, frequency**
- **Example: DOD-1376A High Field Testing**

PZT-8M High Field Testing (6.35 v/mil)

	dC%	DF
Specification	< 5%	<0.0200
MMVD	2.19%	0.0042
NUSC	1.11%	0.0037
Unilator	0.79%	0.0024

HIGH PERFORMANCE PZT MATERIALS

NEW FACILITY COSTS

▶ **Hydrothermal Plant**	$1.7M
▶ **Part Manufacturing**	
▶ **1:3 Fibers**	$500k
▶ **Stack Actuators**	$1M
▶ **Special Firing**	$250k
▶ **Testing**	$500k

EDO CORPORATION ELECTRO-CERAMIC DIVISION

DOD-STD-1376(A)SH Ceramics Types I, II, III and V at Cryogenic Temperatures

EDO CORPORATION ELECTRO-CERAMIC DIVISION

Agenda

- Introduction: EDO Capabilities
- DOD-STD-1376(A)SH Ceramics Types I, II, III and V at Cryogenic Temperatures
- Alternative Materials Warranting Development

Introduction

EDO Capabilities

- **Established, 1954 in Salt Lake City, Utah**
- **One of the Worlds Largest Piezoelectric Ceramic Suppliers**
- **Numerous Military and Commercial Products**
- **Capable of Production Rates of 10,000s per Month**
- **Strength: New Materials Development**
  - * Large Geometry Products
  - * High Volume Products
  - * Extending Performance Limits
    - Terfenol-D
    - Lead Zirconate Titanate
    - Lead Magnesium Niobate

EDO CORPORATION

Electro-Ceramic Division

Military Programs Using EDO Piezo-Ceramics

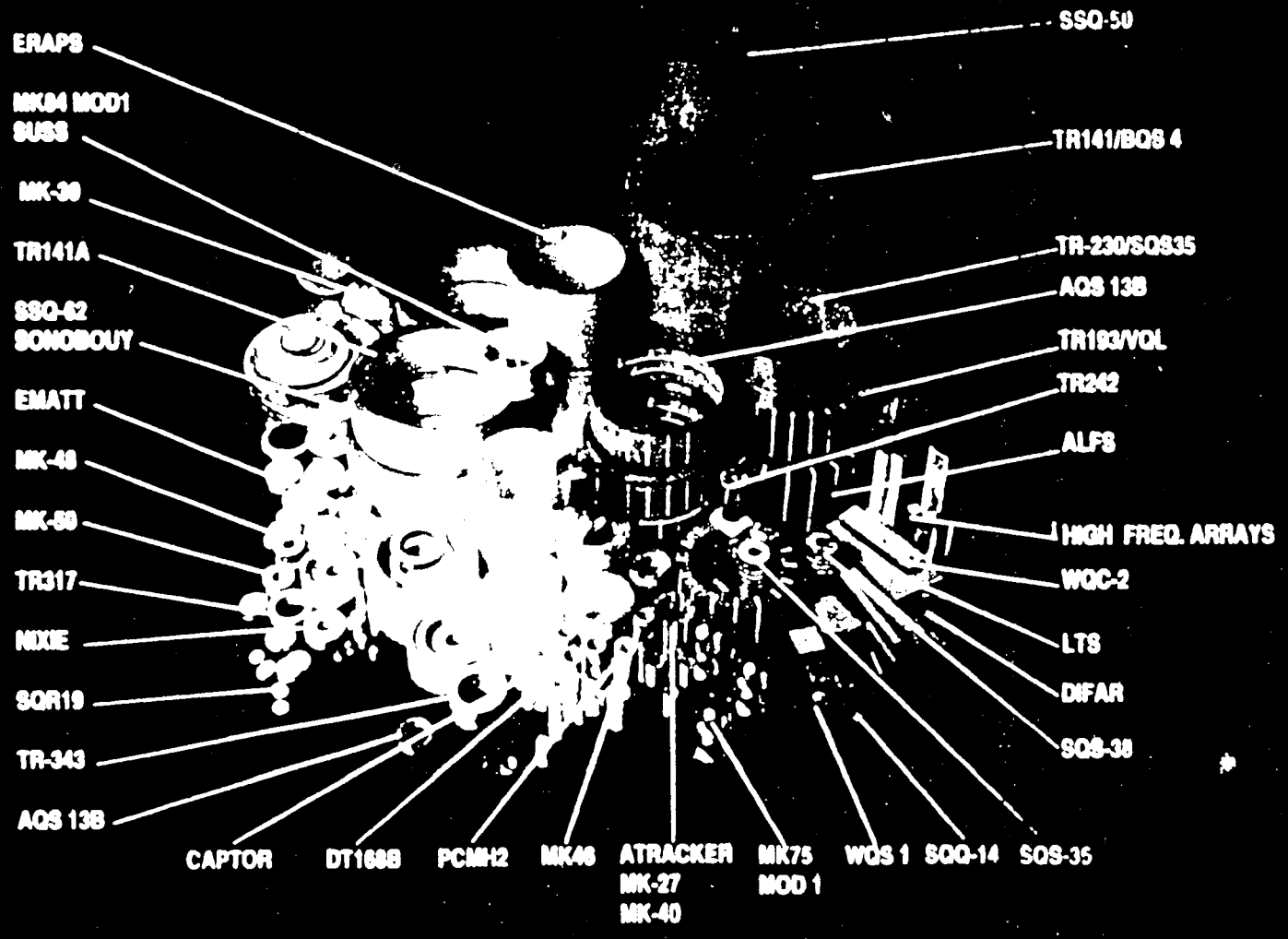

Electro-Ceramic Division

Military Piezo-Ceramic Applications

- SONOBUOY DICABS
- FLEXTENSIONALS
- ALPS HELICOPTER
- SQS-
- MK-
- MK-46 ADCAP
- WASHWHAM

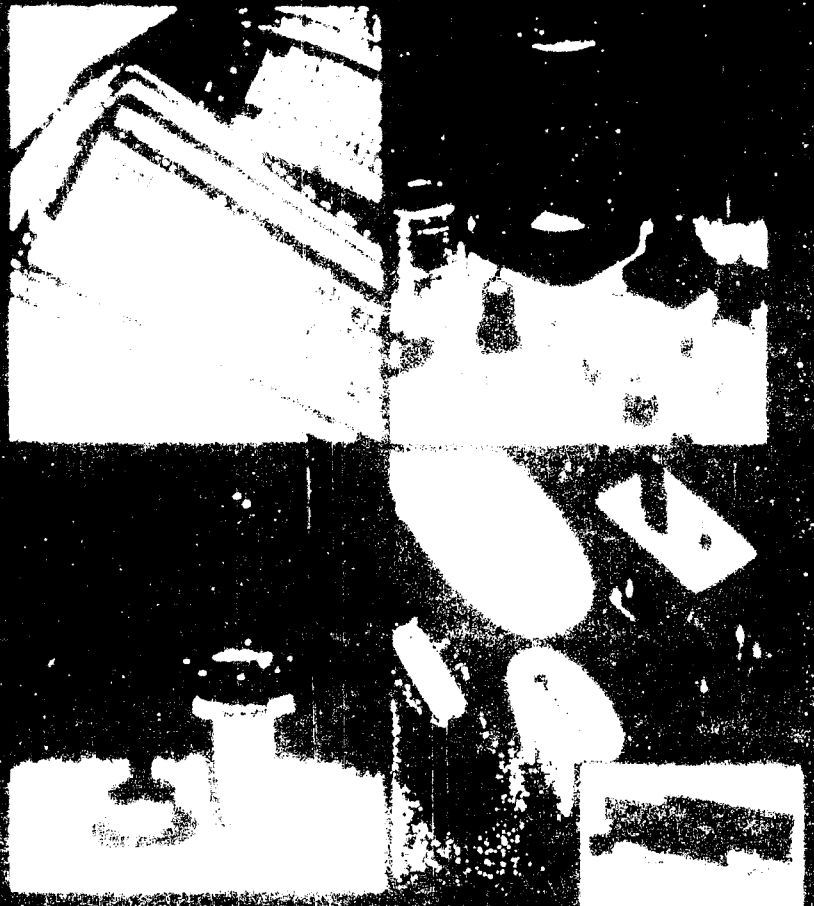

- TR-
- HIGH FREQUENCY ARRAYS
- A-
- MK-
- AN/

EDO CORPORATION

Electro-Ceramic Division

Commercial Piezo-Ceramic Applications

PRODUCTS USING EDO PIEZO-CERAMIC COMPONENTS

- MARINE SPEED AND DEPTH INDICATORS
- FISH FINDERS
- ACCELEROMETERS
- LASER ACTUATORS
- ULTRASONIC CLEANERS & WELDERS
- MEDICAL ULTRASONIC THERAPY
- INK JET PRINTERS

EDO CORPORATION ELECTRO-CERAMIC DIVISION

DOD-STD Ceramics at Cryogenic Temperatures

Problem and Objective

- How Will Piezo-Ceramic Devices Perform in Space (100 to 5°K)?
- Characterize Standard EDO Materials in a Space Environment

EDO CORPORATION ELECTRO-CERAMIC DIVISION

DOD-STD Ceramics at Cryogenic Temperatures

Approach

- **Test Standard Geometries Representing DOD-STD-1376(A)SH:**
  - * Type I (EC-64)
  - * Type II (EC-65)
  - * Type III (EC-67 or 69)
  - * Type V (EC-70)
- **Measured from 300 to 5°K: d_{33}, d_{31}, k_p, k_{33}, k_{31}, Q_m and K_{33}^T**
- **Measured per American National Standard C83.24-1962**
- **Measured by Penn State/MRL, Dr. E. Cross, during 1984**

EDO CORPORATION ELECTRO-CERAMIC DIVISION

DOD-STD Ceramics at Cryogenic Temperatures

Piezoelectric Constant, d_{33}

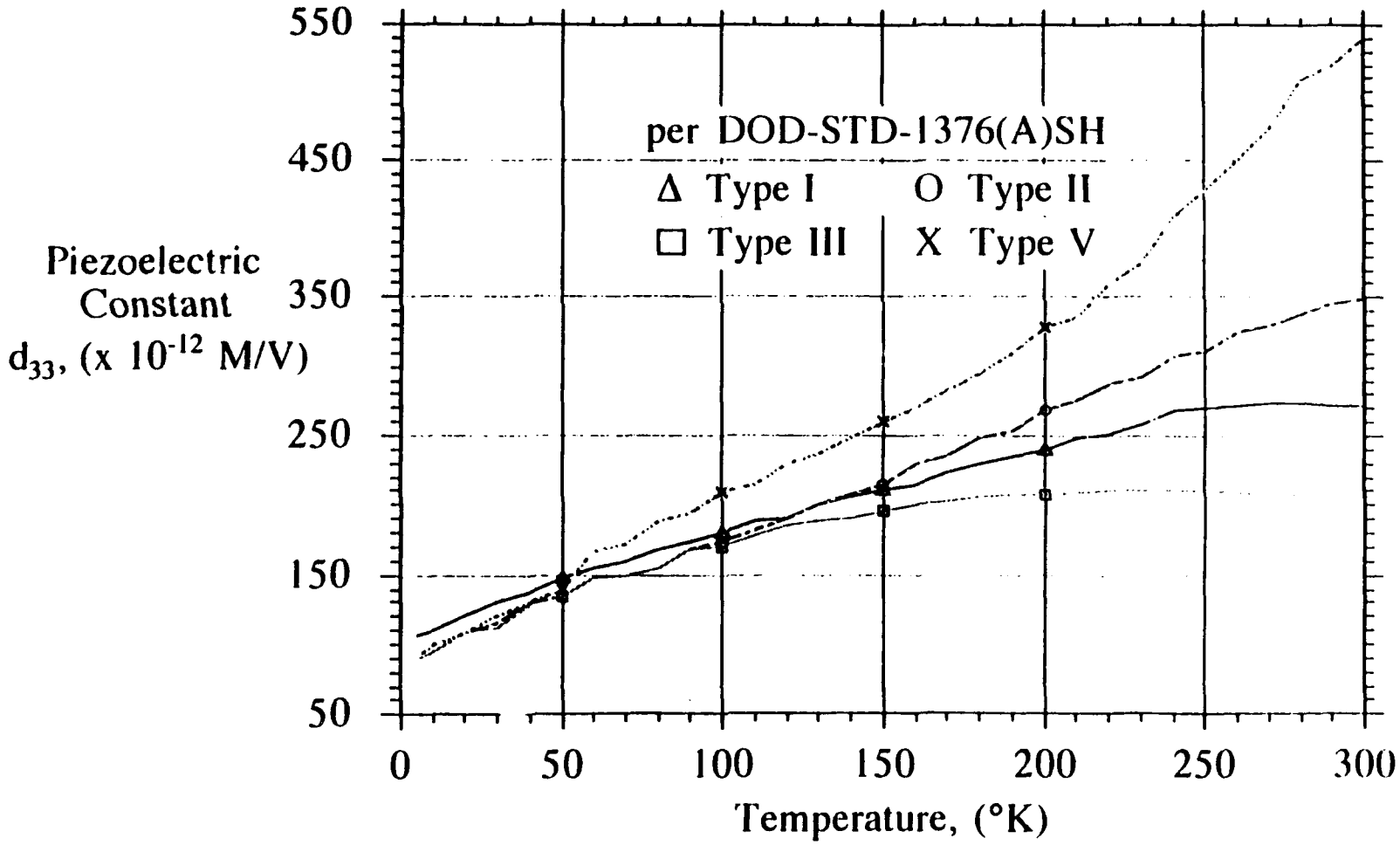

EDO CORPORATION ELECTRO-CERAMIC DIVISION

DOD-STD Ceramics at Cryogenic Temperatures

Piezoelectric Constant, d_{31}

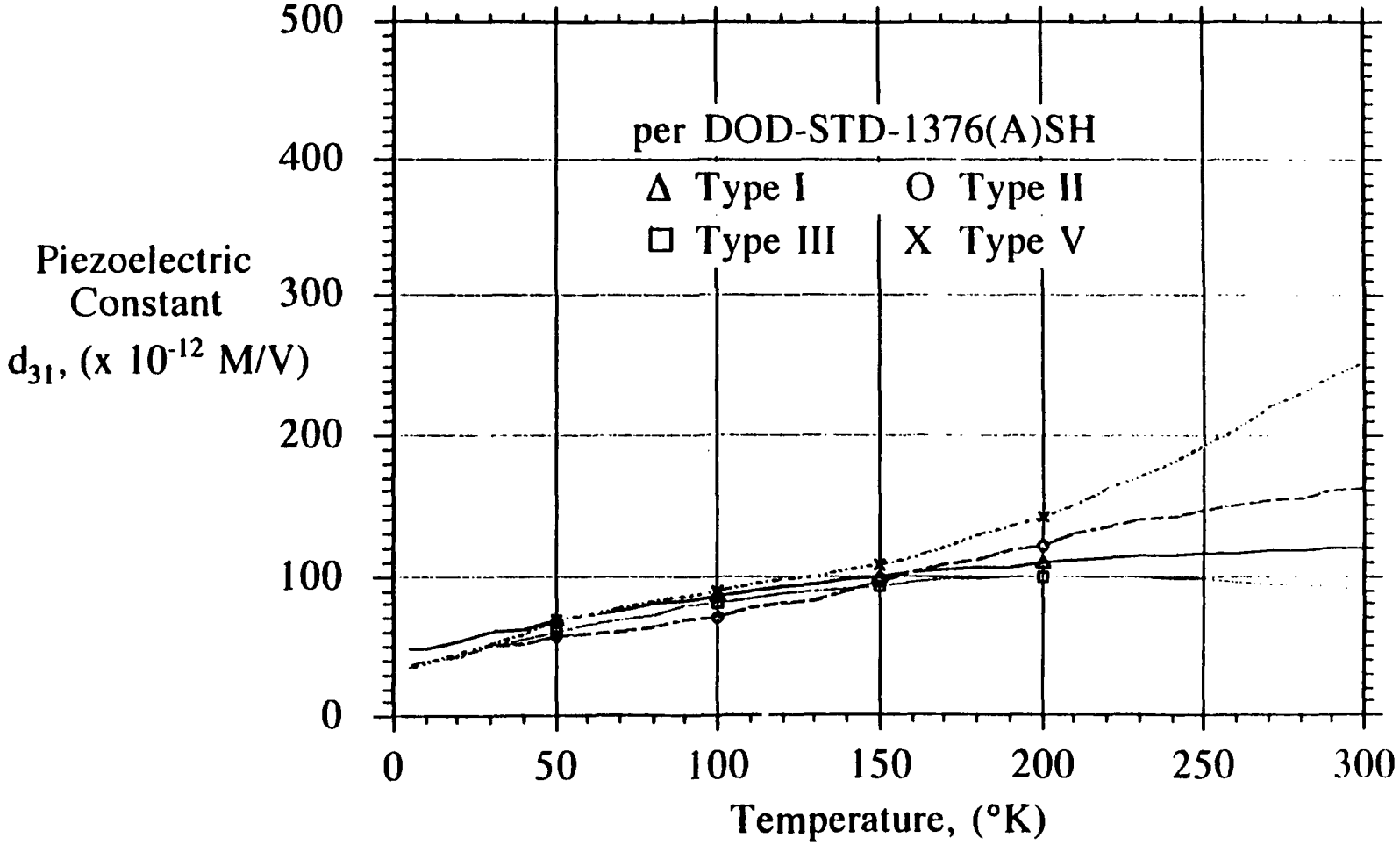

EDO CORPORATION ELECTRO-CERAMIC DIVISION

DOD-STD Ceramics at Cryogenic Temperatures

Coupling Factor, k_p

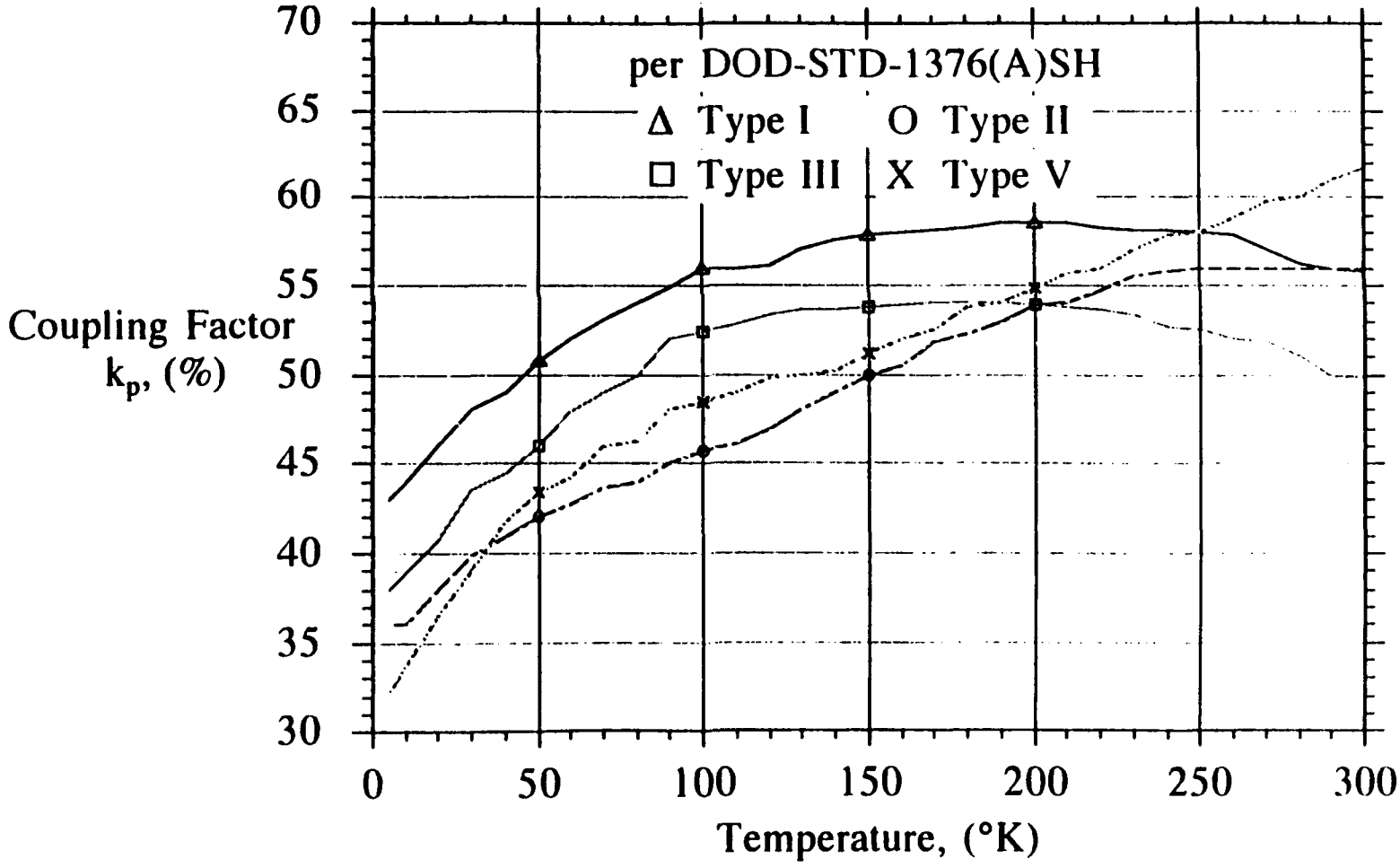

EDO CORPORATION ELECTRO-CERAMIC DIVISION

DOD-STD Ceramics at Cryogenic Temperatures

Coupling Factor, k_{33}

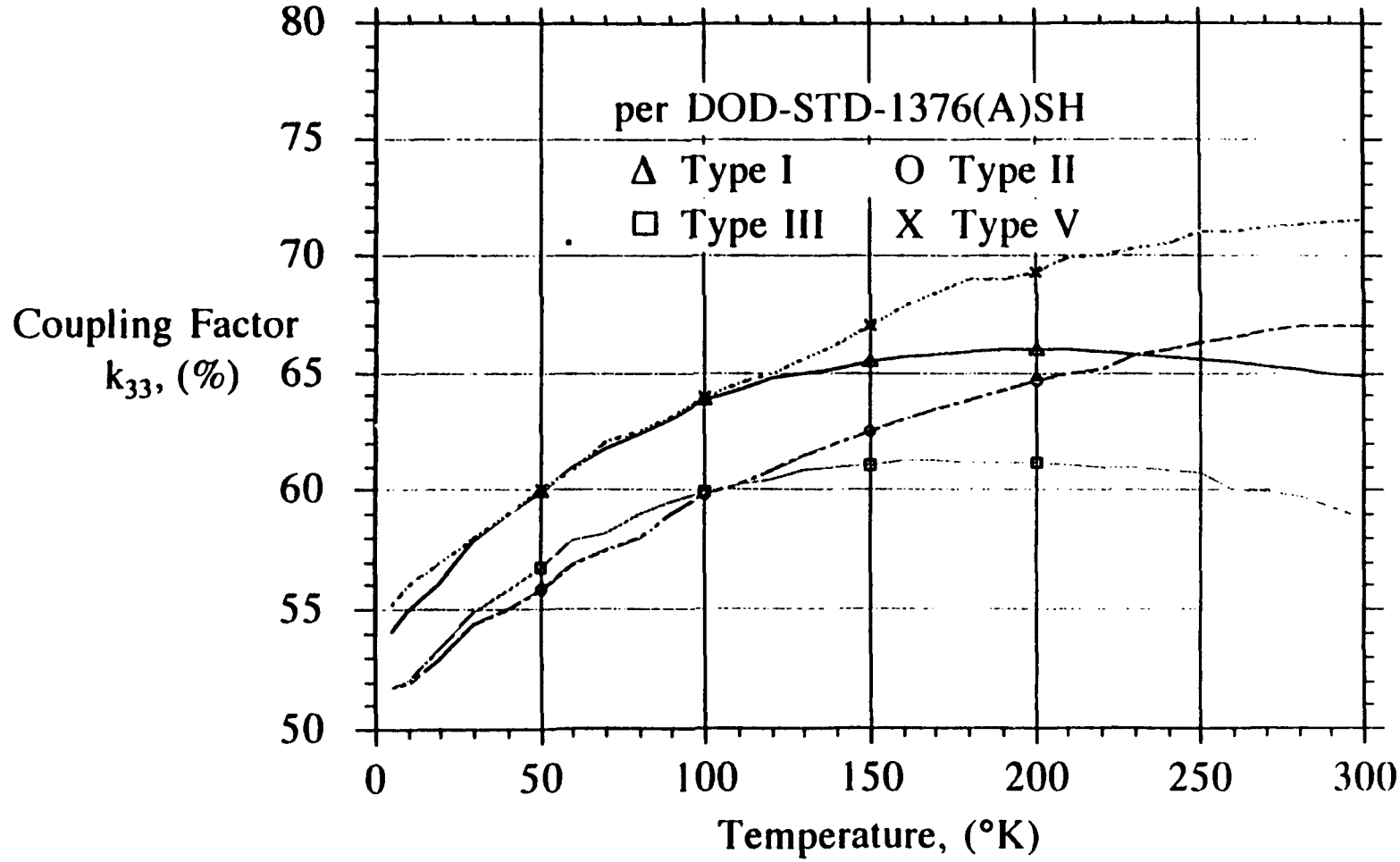

EDO CORPORATION ELECTRO-CERAMIC DIVISION

DOD-STD Ceramics at Cryogenic Temperatures

Coupling Factor, k_{31}

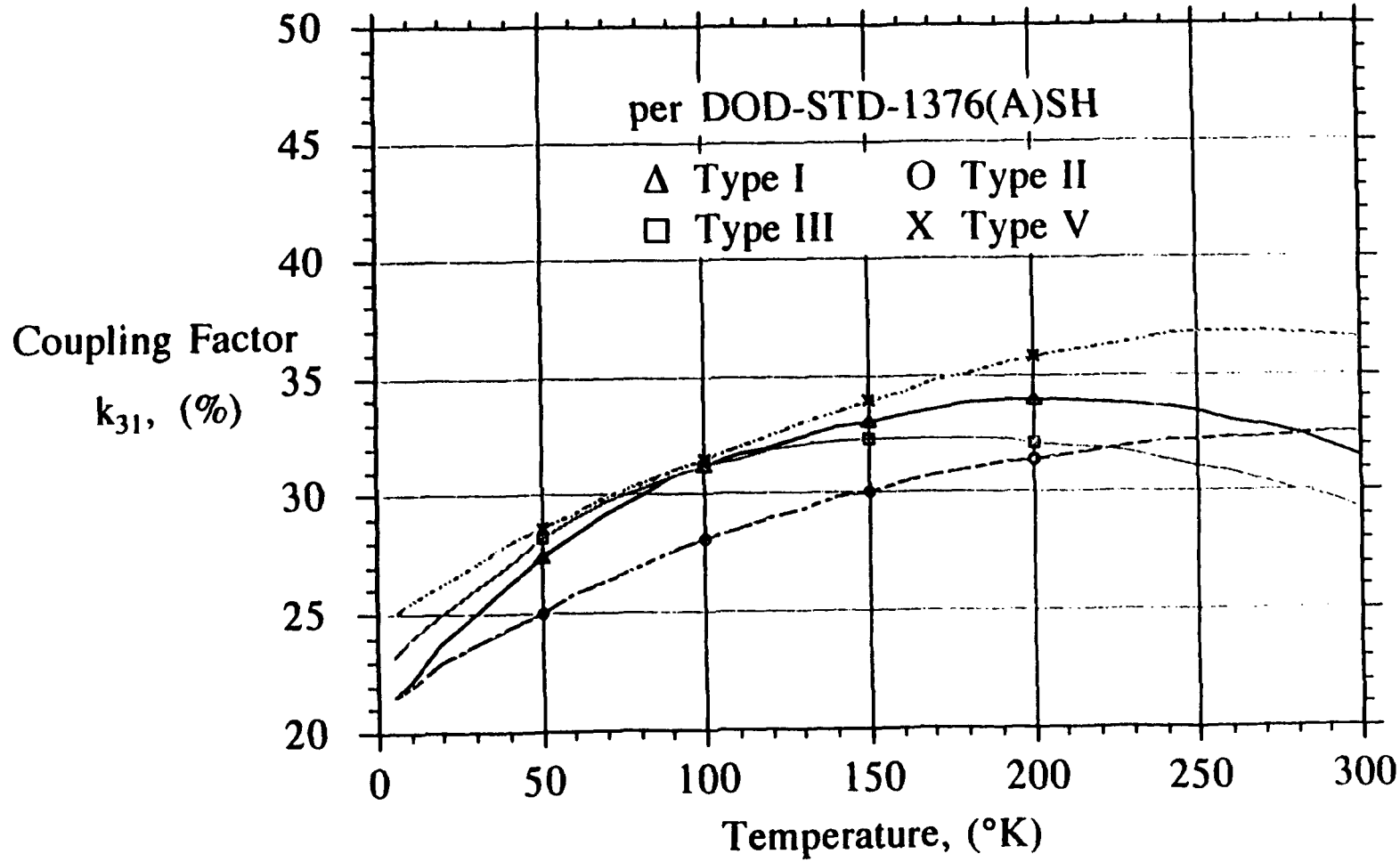

EDO CORPORATION ELECTRO-CERAMIC DIVISION

DOD-STD Ceramics at Cryogenic Temperatures

Mechanical Q_m

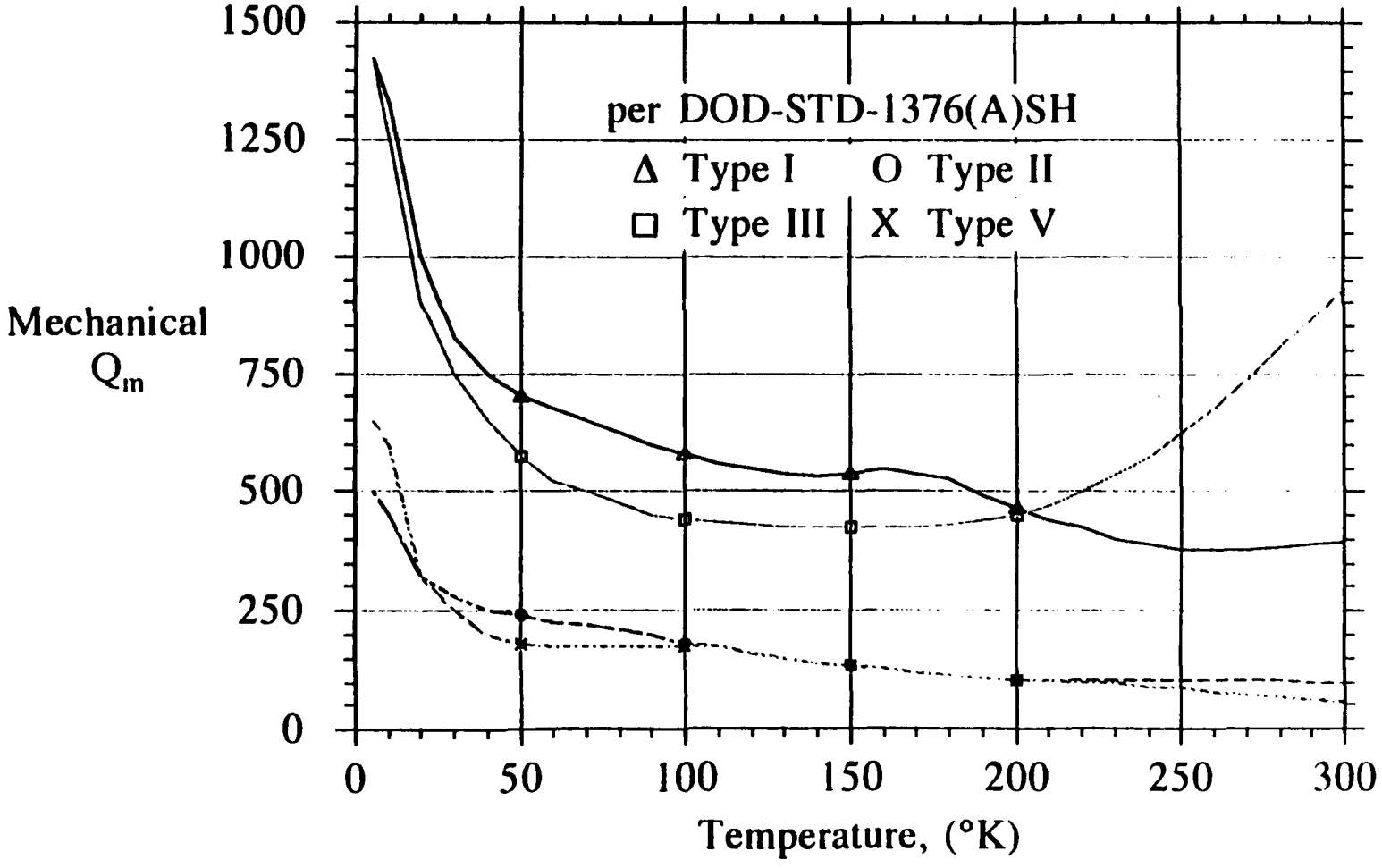

EDO CORPORATION ELECTRO-CERAMIC DIVISION

DOD-STD Ceramics at Cryogenic Temperatures

Dielectric Constant, K_{33}^T

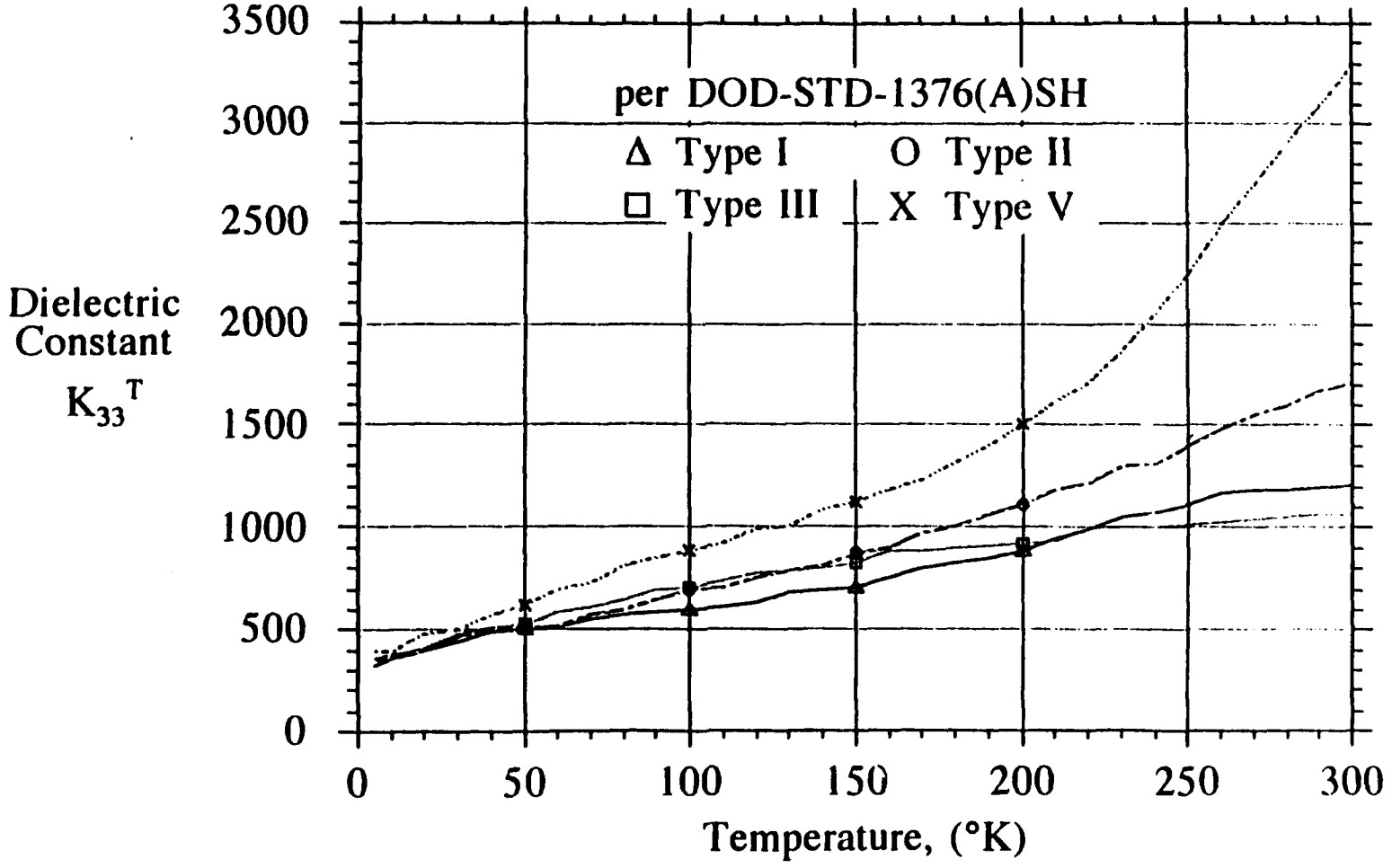

EDO CORPORATION ELECTRO-CERAMIC DIVISION

DOD-STD Ceramics at Cryogenic Temperatures

Summary of Results

	Type I				
	295°K Ambient	100°K	%Δ re Ambient	5°K	%Δ re Ambient
d_{33} x 10^{-12} M/V	273	180	-34%	106	-61%
d_{31} x 10^{-12} M/V	120	85	-29%	48	-60%
k_p %	56	56	0%	43	-23%
k_{33} %	65	64	-2%	54	-17%
k_{31} %	32	31	-3%	22	-31%
Q_m	393	580	46%	1425	262%
K_{33}^T	1205	600	-50%	320	-73%

	Type II				
	295°K Ambient	100°K	%Δ re Ambient	5°K	%Δ re Ambient
d_{33} x 10^{-12} M/V	347	173	-50%	90	-74%
d_{31} x 10^{-12} M/V	161	71	-56%	35	-78%
k_p %	56	46	-18%	36	-36%
k_{33} %	67	60	-10%	52	-22%
k_{31} %	32	28	-12%	22	-31%
Q_m	100	180	80%	500	400%
K_{33}^T	1690	690	-59%	350	-79%

EDO CORPORATION ELECTRO-CERAMIC DIVISION

DOD-STD Ceramics at Cryogenic Temperatures

Summary of Results (cont.)

	Type III				
	295°K Ambient	100°K	%Δ re Ambient	5°K	%Δ re Ambient
d_{33} x 10^{-12} M/V	206	170	-17%	90	-56%
d_{31} x 10^{-12} M/V	92	81	-12%	37	-60%
k_p %	50	52	4%	38	-24%
k_{33} %	59	59	0%	52	-12%
k_{31} %	29	31	7%	23	-21%
Q_m	895	440	-51%	1425	59%
K_{33}^T	1070	710	-34%	360	-66%

	Type V				
	295°K Ambient	100°K	%Δ re Ambient	5°K	%Δ re Ambient
d_{33} x 10^{-12} M/V	530	209	-60%	92	-83%
d_{31} x 10^{-12} M/V	247	90	-64%	36	-85%
k_p %	61	48	-21%	32	-48%
k_{33} %	71	64	-10%	55	-22%
k_{31} %	37	32	-14%	25	-32%
Q_m	60	175	192%	650	983%
K_{33}^T	3180	890	-72%	390	-88%

DOD-STD Ceramics at Cryogenic Temperatures

Conclusions

- **DOD-STD Ceramic Will Not Produce High Strain at Space Temperatures**
- **DOD-STD Ceramic Devices Will Perform Poorly in Space re Earth Ambient**
  - * Narrower Bandwidth
  - * Lower Strain
  - * Lower Efficiency

EDO CORPORATION ELECTRO-CERAMIC DIVISION

Alternative Materials Warranting Development

- Lead Lanthanum Zirconate Titanate
- Strontium Titanate

Actuator comparisons to Multi-layer Ceramic Capacitors

Area	ML Capacitors	ML Actuators
Dielectric	BT,Bi	PZT,PMN
Electrodes	Pd, Pd/Ag	Platinum
Design	40L/32A	500L/125A
Cer Thick	10-35 μ-m	150 μ-m
Overall sizes	< 3mm cubes	6 x 150 mm
Casting	50μ, water	200 μ-m, org
Printing	Thick Film	Same, 2X
Lamination	2 mm pad	25 mm pads
Dicing	Blades	Saw
Burnout	0/4 hrs	60/168 hrs
Firing	900/1300°C	1000°C
Termination	Silver/glass	Diff Comp
Leads	None	Ins. Wire
Coating	None	Si Varnish
Testing	Elect & Vis	& Mechan
Quantities	15 mil/day	100's/day
Cost	Pennies	10's dollars

Ceramic vs Electrode

Percent Firing Shrinkage

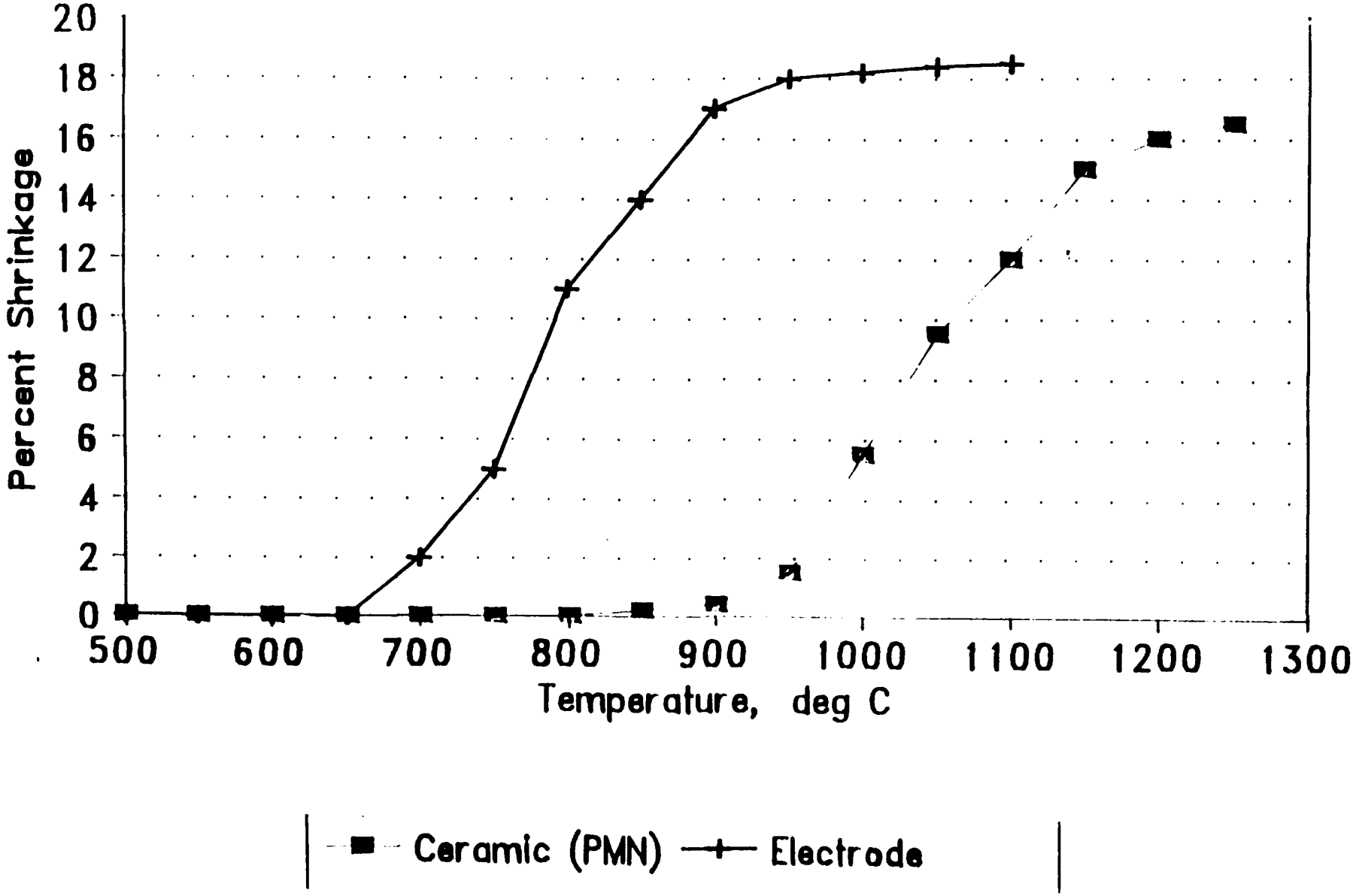

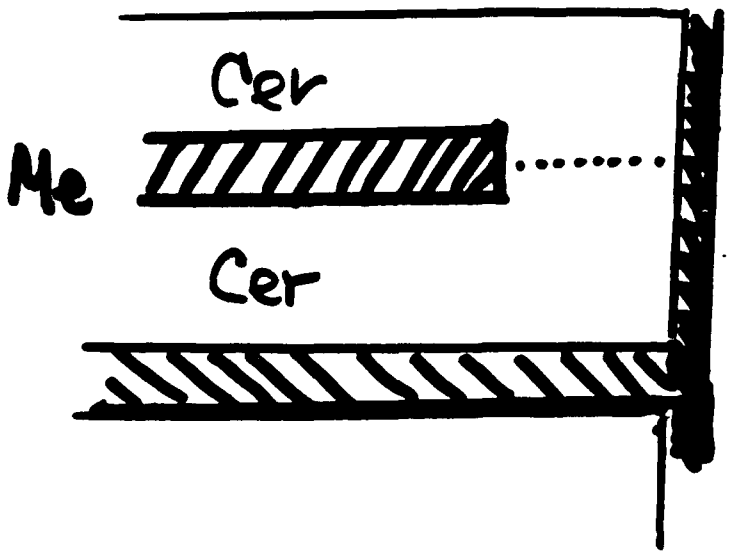

MLC

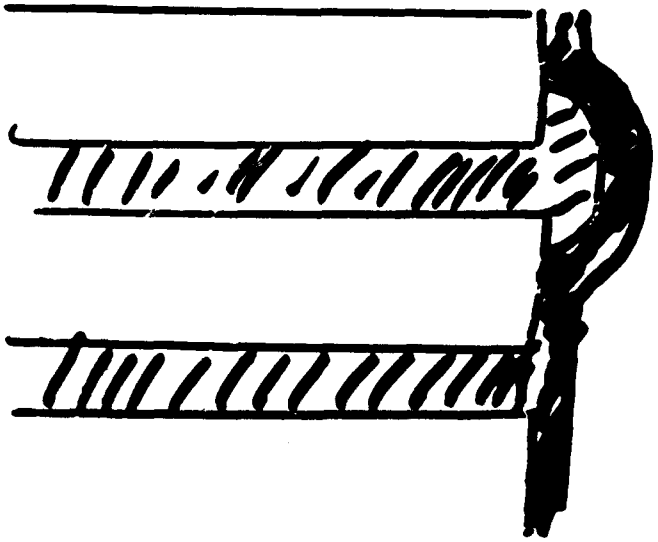

EP/GLASS

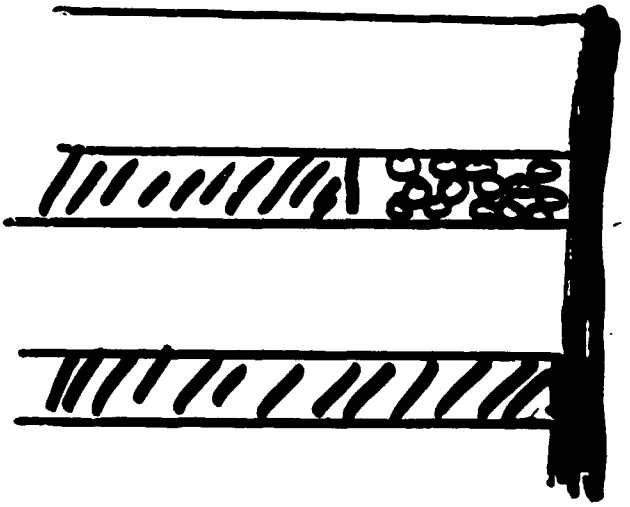

"LOOSE PACK"

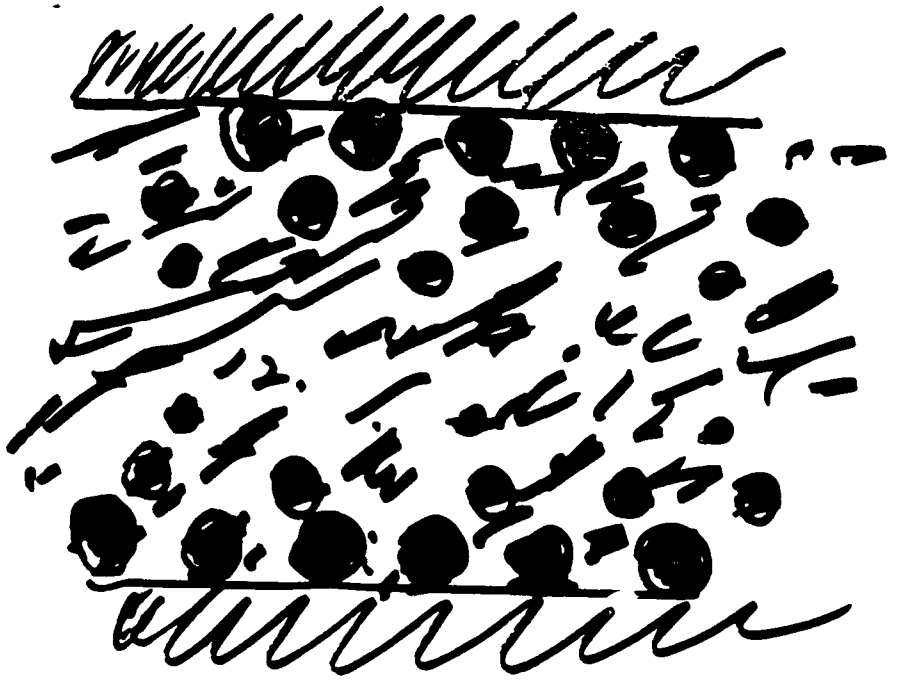

DIFFUSE ELECTRODE

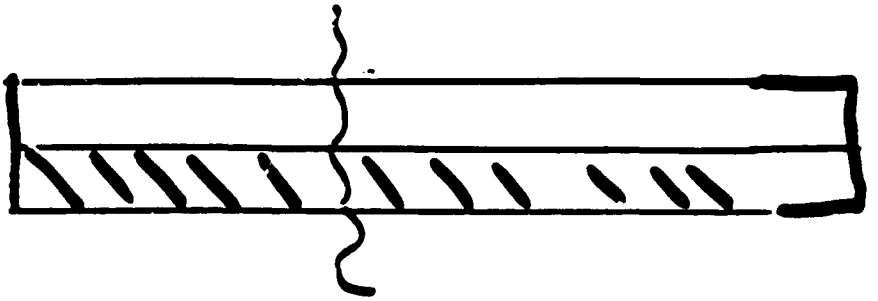

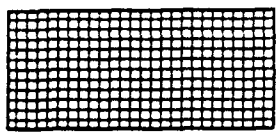

Materials Systems Inc.

INTRODUCTION

Develop and manufacture advanced piezoelectric materials and devices for defense and commercial transducer applications.

- Flexible Piezoelectric Composites
- Piezoelectric Composite Actuators
- Piezoelectric Actuator Assemblies
- Composite Transducers for Medical Ultrasound

TECHNOLOGY

o Process technology for ceramics and polymers:
  - Extrusion
  - Injection molding

o Near net-shape forming of complex ceramic shapes.

o Piezoelectric materials and composites expertise.

o Materials technology transfer and device prototyping.

INJECTION MOLDING PROCESS ROUTE

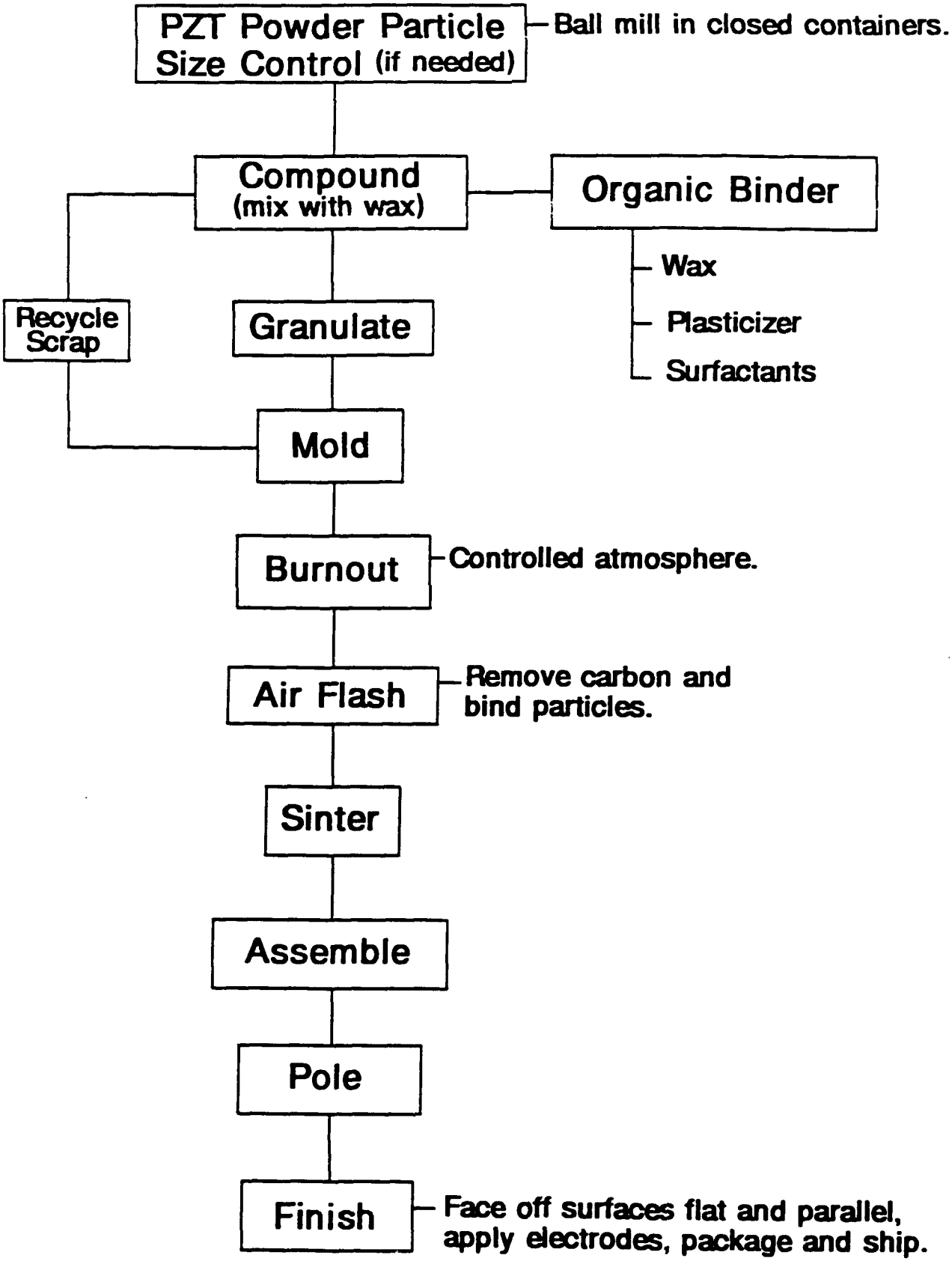

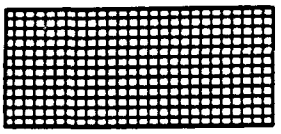

Materials Systems Inc.

PIEZOELECTRIC ACTUATORS

Observations

o Performance Characteristics:
- Fast response
- Large forces
- High voltages
- Small displacements

o Several routes to enhance displacement performance:
- High-strain piezoelectric materials
- Strain amplification using compound actuator designs
- Multiple actuator assemblies

o Displacement needs may require a combined approach.
- Compound actuator assemblies

o New high-strain materials and device designs are in the development stage.

o Need to integrate materials, design and manufacturing functions to best meet manufacturing requirements:
- Lab-stage materials
- Lab-stage designs
- Design with system goals, manufacturing viability and cost-effectiveness in mind.

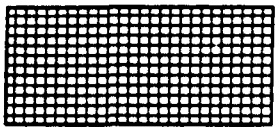

Materials Systems Inc.

ACTUATOR ASSEMBLIES

Focus: Actuators incorporating materials and designs at the limit of the current state-of-the-art:

- Compound actuator assemblies

Examples:
- Flextensional strain amplifiers
- Piezoelectric ceramic/polymer composites

Challenges: Materials/process issues:

- High-strain piezoelectric ceramics
- Ceramic/metal/polymer interfaces
- Complex shape fabrication

Assembly requirements:

- Alignment
- Joining
- Packaging
- Testing

PIEZOELECTRIC CERAMIC/POLYMER COMPOSITES

1-3 Composite

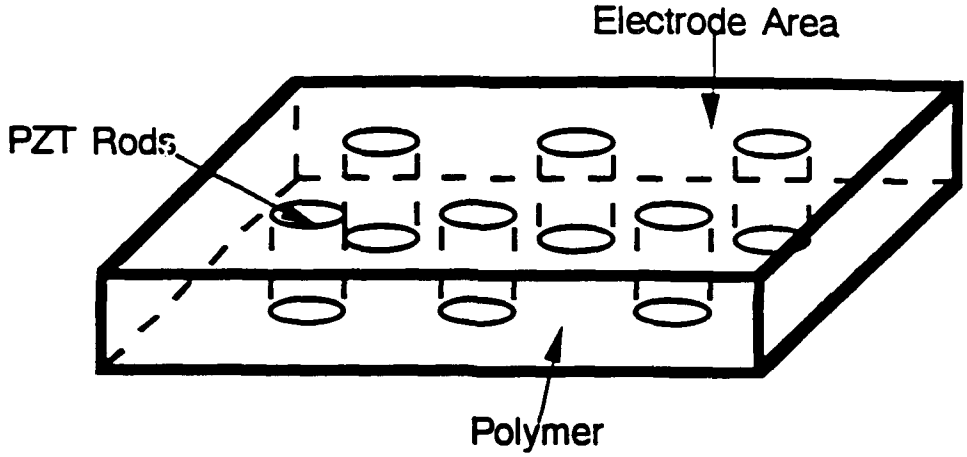

Production issues remaining to be solved:

- Handling large quantities of fibers.
- Composite assembly.
- Acceptable cost.
- Systems application and integration.

Manufacturing Approach:

- Use injection molding to form the ceramic elements to net-shape.

PZT CERAMIC PREFORM FABRICATION

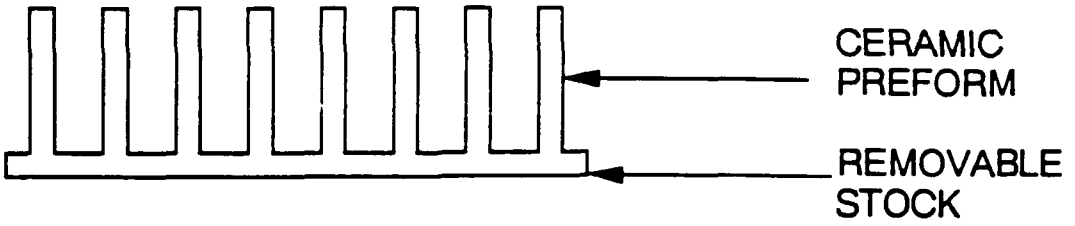

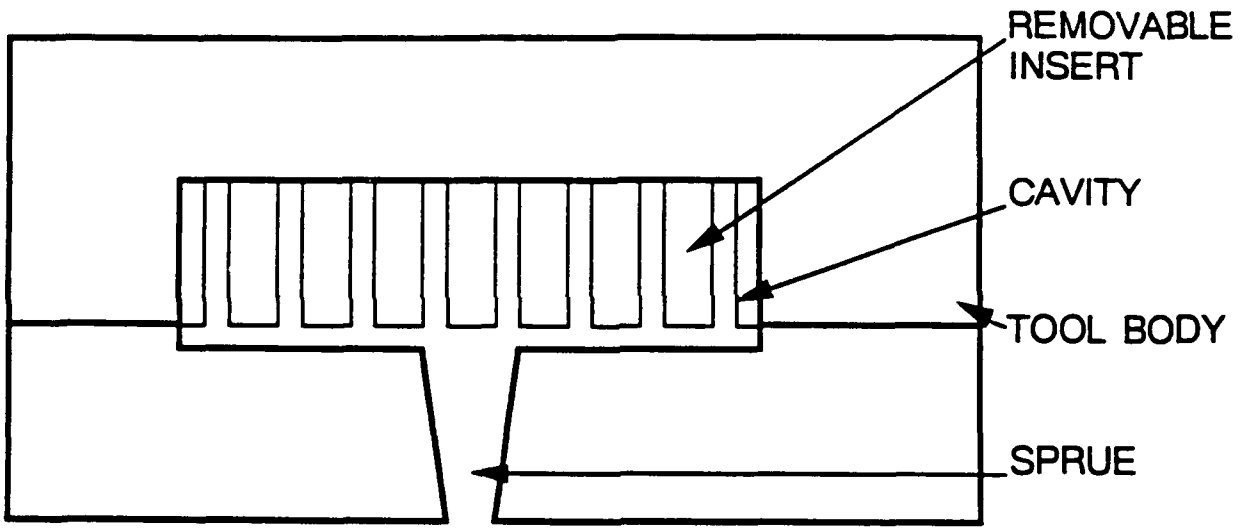

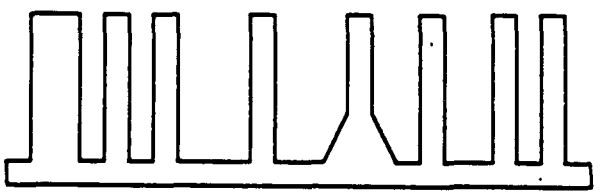

INSERT DEFINES
ELEMENT SHAPE
AND LAYOUT

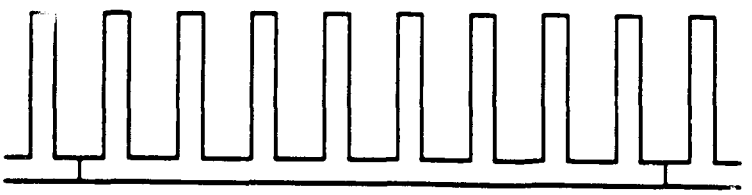

PREFORM LAY-UP
TO FORM LARGER
ARRAYS

FLEXTENSIONAL STRAIN AMPLIFIERS

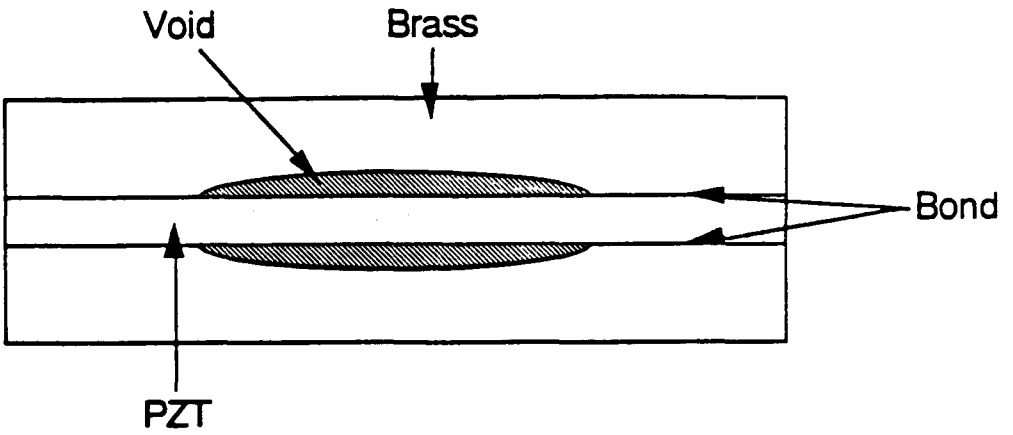

Production issues remaining to be solved:

- Alignment during assembly (reproducibility)
- Joining approach (device life)
- Design of multiple actuator assemblies (ruggedness)
- Acceptable cost
- Systems application and integration

Manufacturing Approach:

- Assemble prototype quantities manually: (needs tooling for alignment during joining and lay-up, and development of part dimensional specifications)

- Full-scale manufacturing would be facilitated by redesign to simplify joining and alignment

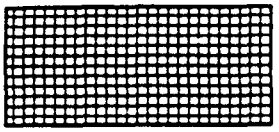

Materials Systems Inc.

SUMMARY

- Emerging actuator materials and designs hold promise for considerably improving strain performance over conventional piezoelectric ceramics.

- Pilot scale manufacturing of flextensional actuators for field evaluation is technically feasible now.

- Larger quantities would benefit from redesign for improved manufacturability and operating life.

- Cost-effective manufacturing of advanced actuator designs may require net-shape forming of complex ceramic shapes; injection molding is available for this purpose.